University of London

Imperial College of Science, Technology and Medicine

Tissue Engineering of Bone from Embryonic Stem Cells

Wesley Liam Randle BSc (Hons)

Submitted for a PhD degree in Pathology

This thesis is dedicated to my wife Rebecca, my parents and my fifth lumbar vertebra.

ABSTRACT

Our aim was to investigate embryonic stem cells (ESCs) as a source of material for bone tissue repair. The transition from the laboratory to the clinical setting and the large-scale production of tissue for effective treatment of patients is paramount. Serum-free media development, alginate encapsulation and bioreactors were employed in order to establish methods to manufacture 3D mineralised tissue using mESCs as a model. The transition from undifferentiated mESCs to bone tissue using traditional 2D culture protocols are fragmented, undefined, labour intensive, are difficult to sample, and are highly variable. 2D ESC culture involves three stages: a) ESC maintenance, b) Embryoid Body (EB) formation, and c) lineage-specific differentiation.

Three media formulations for each stage were developed and the transition from serum to serum-free media was found to be less deleterious at the maintenance phase. LIF (mESC pluripotency maintenance) BMP4 (Mesoderm induction) and PDGF-ββ / bFGF (osteogenic differentiation) were used during the three stages to induce osteogenic differentiation and 2D bone formation.

Bioreactors provide a dynamic cultivation system within a controlled environment that enables the expansion of cell populations. Suspension culture systems offer attractive advantages of scalability and relative simplicity that can improve the viability and turnover of specific stages and types of stem cells. However, 2D culture, in which normal 3D relationships with the extracellular matrix and other cells are distorted, may alter cellular behaviour.

To our knowledge, no current methodologies exist that allow the integrated maintenance, expansion and differentiation of ESCs towards the osteogenic lineage forming 3D mineralised tissue. This thesis presents a simplified, integrated, and reproducible bioprocess for the production of osteogenic cells from mESCs that would be amenable to automation and scale-up for the generation of clinically relevant numbers of high-quality bone cells and mineralised tissue. Specifically, we encapsulated mESCs in alginate hydrogels, cultured them in high aspect ratio vessels (HARV) and adapted our previously established protocols to induce osteogenic differentiation. In this one-step, integrated process, we differentiated mESCs into osteogenic cells capable of producing 3D mineralised tissue identified by demonstration of stained mineralised aggregates, the expression of markers such as osteocalcin, OB-cadherin and collagen type-I and micro-computed tomography.

The challenges to overcome before bone tissue engineering from ESCs reaches the clinic are providing a clinically acceptable hESC source, clinical grade homogeneous bone tissue manufacture, *in vivo* efficacy and safety trials, serum-free media formulation, negation of the immune response, ethical acceptance.

ACKNOWLEDGEMENTS

I would like to thank Sakis and Julia for their utmost attention and guidance throughout this thesis. My colleagues at the TERM centre and in Chemical Engineering (BSEL) have been great; providing friendship, advice, useful discussions and tremendous pub sessions. I would also like to thank the administrative staff and also Anne for their continued support during my thesis. Finally, I would like to thank the Chelsea and Westminster Hospital Trustees for their financial support and also the Imperial College Entrepreneurs centre for their guidance.

STATEMENT OF ORIGINALITY

I declare that this thesis was conducted and written by myself and that the work that it presents is my own except where stated otherwise.

Signed: 

Date: 07/SEP/06

ABBREVIATIONS

7-AAD	7-amino-actinomycin-D
AirSat	Air saturated
ALPase	Alkaline phosphatase
αMEM	Alpha-Modified Eagles Medium
ANOVA	Analysis of variance
ARS	Alizarin red S
ARSQ	Alizarin red S quantification
ASTM	American Society for Testing Materials
ATCC	American Type Culture Collection
ATP	Adenosine Tri-phosphate
βadex	L-ascorbate-2-phosphate, β-glycerophosphate and dexamethasone
Balb/c	Black or albino mice strain c
Bcl-2	B-cell CLL/lymphoma 2
bFGF	Basic fibroblast growth factor
BIO	6-bromoindirubin-3'-oxime
BMPs	Bone morphogenetic proteins
BRL	Buffalo rat liver
BSA	Bovine serum albumin
$Ca_{10}(PO_4)_6(OH)_2$	Hydroxyapatite
Calcein AM	3',6'-Di(O-acetyl)-2',7'-bis[N,N-bis(carboxymethyl)aminomethyl]fluorescein, tetraacetoxymethyl ester
Cbfa1	Core-binding factor alpha-1 also known as runx2
CCD	Charge coupled device
CD	Cluster of differentiation
CDL	Chemically defined lipids
CM	Conditioned medium
Coll I	Collagen type-I
Coll II	Collagen type-II
Collagen type-IIA	Collagen type-I splice variant A
Collagen type-IIB	Collagen type-I splice variant B
DAPI	4',6 diamidino-2-phenylindole
DDM	Doublet discrimination module
dEB	Disaggregated EBs
DMEM	Dulbecco's modified Eagles medium
DMEM-LG	DMEM-Low glucose
DMSO	Dimethylsulfoxide
dNTP	2'-deoxynucleoside 5'-triphosphate
DOE	Design of experiments
DTES	Department for device technology, evaluation and safety
E14Tg2a	E14 thioguanine resistance 2a mESC cell line
EB	Embryoid body
EC	Embryonic carcinoma
ECM	Extracellular matrix
EDTA	Ethylenediaminetetraacetic acid
EG	Embryonic germ
EGF	Epidermal growth factor
EPL	Primitive ectoderm like cells

ESCs	Embryonic stem cells
EthD-1	Ethidium homodimer-1
FACS	Fluorescence activated cell sorting
FCS	Foetal calf serum
FDA	Food and Drug Administration
FGF	Fibroblast growth factor
FGFR3	Fibroblast growth factor receptor 3
FITC	Fluorescein Isothiocyanate
FL	Fluorescence channel
Flk-1	Foetal liver kinase-1
FSC	Forward scatter
GapDH	Glyceraldehyde-3-phosphate dehydrogenase
GDF6	Growth and differentiation factor 6
GH	Growth hormone
GLU	Glutamate
Gluc	Glucose
GMP	Good manufacturing practice
GSK	Glycogen synthase kinase
GTPs	Good tissue practices
H&E	Haematoxylin & Eosin
HARV	High Aspect Ratio Vessel
HEPES	N-(2-hydroxyethyl) piperazine-N-(2-ethane sulfonic acid
HepG2	Hepatocarcinoma cell line (ATCC HB-8605)
hESCs	Human ESCs
HFEA	Human Fertilisation and Embryology Authority
hTERT	human telomerase reverse transcriptase
Hypo	Sodium thiosulfate
ICM	Inner cell mass
IDE	Investigational device exemption
IgA	Immunoglobulin A
IGFI	Insulin-like growth factor I
IGFs	Insulin-like growth factors
IgG	Immunoglobulin G
IgM	Immunoglobulin M
Ihh	Indian hedgehog
IND	Investigational new drug
IPA	Isopropyl alcohol
KOSR	Knock out serum replacement
LA-BSA	Linoleic acid-bovine serum albumin
Lac	Lactate
LIF	Leukaemia inhibitory factor
LPA	Lysophosphatidic acid
LWR	Lennon, Wiles, Randle
MEF-STO	Mouse embryonic fibroblasts cell line
mESCs	Mouse ESCs
MHC	Major histocompatibility complex
MHRA	Medicines & Healthcare Products Regulatory Agency
Micro-CT	Micro computed tomography
MIH	Muellerian inhibiting substance
mmHg	Millimetres of mercury
mOBs	Murine osteoblasts
MSCs	Mesenchymal stem cells

MTS	3-(4,5-dimethylthiazol-2-yl)-5-(3-carboxymethoxyphenyl)-2-(4-sulfophenyl)-2H-tetrazolium
NADH	Nicotinamide adenine dinucleotide
NADPH	Nicotinamide-adenine-dinucleotide-phosphate
NASA	National Aeronautics and Space Administration
NEAA	Non-essential amino acids
Neu5Gc	N-glycolylneuraminic acid
OB-cadherin	Osteoblast cadherin
OCN	Osteocalcin
OCT	Optimal cutting temperature
Oct-4	Octamer binding factor 4 also known as Oct-3 / Oct-3/4, Pou5f1
Osm	Osmolarity
OSX	Osterix
P CO_2	Partial pressure of carbon dioxide
P O_2	Partial pressure of oxygen
PBS	Phosphate buffered saline
PCR	Polymerase chain reaction
PD	Population doublings
PDGFRα	Platelet-derived growth factor alpha
PDGFs	Platelet-derived growth factors
PE	Phycoerythrin
PerCP	Peridinin-chlorophyll-protein complex
PES	Phenazine ethosulfate
PFA	Paraformaldehyde
PHEMA	Polyhydroxyethylmethacrylate
PHSA	Public Health Services Act
Pi	Inorganic phosphate
PLL	Poly-L-lysine
pNPP	p-nitrophenol phosphate
POU	Pit-Oct-Unc
PTFE	Polytetrafluoroethylene
PTHrP	Parathyroid hormone-related protein
PVA	Polyvinyl alcohol
PVC	Polyvinylchloride
Re	Reynolds number
RLT	Proprietary compound containing guanidinium thiocyanate
RPM	Revolutions per minute
RT-PCR	Reverse transcription PCR
SCID	Severe combined immunodeficient
SD	Standard deviation
SDS	Sodium dodecyl sulphate
SDS-PAGE	Sodium dodecylsulphate-polyacrylamide gel electrophoresis
SE	Standard error
SEM	Scanning electron microscopy
Shh	Sonic hedgehog
SRF	Serum response factor
SSC	Side scatter
SSEA-4	Stage-specific embryonic antigen-4
STAT	Signal transducers and activators of transcription
STLV	Slow turning lateral vessel

TE	Trypsin-ethylenediaminetetraacetic acid
TEMED	N,N,N',N'-tetramethylethylenediamine
TGFβ	Transforming growth factor-beta
TH	Thyroid hormones
Tra	Tumour rejection antigen
UV	Ultraviolet
WMDI	Windows multiple document interface

LIST OF FIGURES

Figure 1.1. Macroscopic bone diagram.
Figure 1.2. Schematic representation of bone architecture.
Figure 1.3. Ultrastructure of bone.
Figure 1.4. Schematic representation of the "egg-box" model in low and high $CaCl_2$ concentrations.
Figure 1.5. Schematic representation of the different gel network structures of a Ca-alginate gel bed.
Figure 2.1. HARV bioreactor photographs. Front and rear views.
Figure 2.2. Perfusion bioreactor photograph.
Figure 3.1. Media development flow chart.
Figure 3.2. mESCs cultured for 3 days in serum-free and serum-containing maintenance medium.
Figure 3.3. mESC seeding density affects colony morphology after 3 days culture.
Figure 3.4. mESC phenotypic characterisation and cell viability cultured in serum-containing and serum-free media.
Figure 3.5. Serum batch test.
Figure 3.6. Mesoderm flow data.
Figure 3.7. Phase contrast and confocal live/dead images of day 5 EBs in 3 different media.
Figure 3.8. Macroscopic images, bone nodules (Alizarin Red S).
Figure 3.9. Examples of alizarin red S and Cbfa1 staining.
Figure 3.10. Discrete bone nodule counts on day 21 of the bone nodule assay using 12 media combinations.
Figure 3.11. Examples of cell types formed.
Figure 4.1. Comparison of hypodermic needle gauges in relation to bead diameter before and after culture.
Figure 4.2. Bead diameter variations before and after culture.
Figure 4.3. SDS-PAGE gel indicating macro bead permeability.
Figure 4.4. Calcium distribution within an alginate bead.
Figure 4.5. High powered SEM of dehydrated alginate beads.
Figure 4.6. Macroscopic image of mESCs encapsulated and grown in alginate.
Figure 4.7. Undifferentiated mESC viability encapsulated and cultured within alginate beads.
Figure 4.8. 2D Confocal undifferentiated mESC colonies Oct-4 (Green) and CD9 (Red).
Figure 4.9. Single undifferentiated mESCs encapsulated and cultured within microbeads.
Figure 4.10. Single undifferentiated mESCs encapsulated and cultured within microbeads.
Figure 4.11. Undifferentiated mESCs encapsulated and cultured within macrobeads.
Figure 4.12. Undifferentiated mESCs immunostained for pluripotent markers after release from beads on day 10.
Figure 4.13. Morphological images of day 5 static cultures.
Figure 4.14. Morphological images of day 18 static cultures.
Figure 4.15. H&E images of day 29 static cultures.
Figure 4.16. Alizarin Red S images of day 29 static cultures.

Figure 5.1. Mean medium viscosity measurements vs. mean shear rate.
Figure 5.2. Images of 3D static, 3D stirred & 3D HARV vessels
Figure 5.3. Live / Dead images of 2D static, 3D static, 3D stirred, 3D HARV cultured for 29 days.
Figure 5.4. Morphology of encapsulated cells.
Figure 5.5. Day 3, 2D static, 3D static, 3D stirred and 3D HARV.
Figure 5.6. Day 7, 2D static, 3D static, 3D stirred and 3D HARV x4.
Figure 5.7. Day 7, 2D static, 3D static, 3D stirred and 3D HARV x10.
Figure 5.8. Day 21, 2D static, 3D static, 3D stirred and 3D HARV.
Figure 5.9. Day 21, 2D static, 3D static, 3D stirred and 3D HARV.
Figure 5.10. Day 29, 2D static, 3D static, 3D stirred and 3D HARV.
Figure 5.11. Disrupted beads and 2D replated tissue.
Figure 5.12. Day 3, paraffin embedded, sectioned, H&E stained alginate beads.
Figure 5.13. Day 8, paraffin embedded, sectioned, H&E stained alginate beads.
Figure 5.14. Day 15, paraffin embedded, sectioned, H&E stained alginate beads.
Figure 5.15. Day 22, paraffin embedded, sectioned, H&E stained alginate beads.
Figure 5.16. Day 29, paraffin embedded, sectioned, H&E stained alginate beads.
Figure 5.17. Day 29, paraffin embedded, sectioned, H&E stained controls.
Figure 5.18. 3D HARV bone aggregate characterisation.
Figure 5.19. Macroscopic comparison of bone quantity from 2D and 3D HARV culture.
Figure 5.20. Day 15, paraffin embedded, sectioned, Alizarin Red S stained alginate beads.
Figure 5.21. Day 22, paraffin embedded, sectioned, Alizarin Red S stained alginate beads.
Figure 5.22. Day 29, paraffin embedded, sectioned, Alizarin Red S stained alginate beads.
Figure 5.23. Day 29, paraffin embedded, sectioned, Alizarin Red S stained controls.
Figure 5.24. Day 15, 22 and 29, paraffin embedded, sectioned, von Kossa stained beads.
Figure 5.25. 3D tissue immunocytochemical characterisation, day 3 to 8.
Figure 5.26. Bone aggregate immunocytochemical characterisation.
Figure 5.27. Biochemical activity of 3D HARV: bone formation.
Figure 5.28. RT-PCR characterisation from day 0 to 8 in 2D and 3D HARV culture.
Figure 5.29. RT-PCR characterisation from day 15 to 29 in 3D HARV culture.
Figure 5.30. Ca++ 3D HARV medium analysis.
Figure 5.31. K+ 3D HARV medium analysis.
Figure 5.32. Na+ 3D HARV medium analysis
Figure 5.33. NH4+ 3D HARV medium analysis.
Figure 5.34. Glucose 3D HARV medium analysis.
Figure 5.35. Glutamate 3D HARV medium analysis.
Figure 5.36. Lactate 3D HARV medium analysis.
Figure 5.37. pH 3D HARV medium analysis.
Figure 5.38. P O_2 @ 37°C 3D HARV medium analysis.
Figure 5.39. 3D HARV micro-computed tomography.

Figure 5.40. Morphological 3D HARV, 3D HepG2 HARV and 2D EBs.
Figure 5.41. Morphological 3D HARV, 3D HepG2 HARV and 2D bone nodules day 29.
Figure 5.42. Alizarin Red S and von Kossa staining on 3D HARV and 3D HARV HepG2 cultures day 29
Figure 5.43. Alizarin Red S quantification, day 15 to day 29 comparing 3D HARV and 3D HARV HepG2 conditioned medium.
Figure 5.44. Morphological images of beads cultured in 3D HARV & 3D Perfusion cultured beads.
Figure 5.45. Micro-CT images of 3D HARV & 3D Perfusion cultured beads.

LIST OF TABLES

Table 1.1. Biomaterials and their usage.
Table 1.2. ESC characteristics.
Table 2.1. Antibody dilutions and blocking serums for immunostaining.
Table 2.2. RT-PCR primer table and conditions.
Table 5.1. Mean weight of water and culture medium.
Table 5.2. Basal analyte values from fresh media samples.
Table 5.3. 3D HARV feeding, analysis and bone aggregate formation.
Table 5.4. Phenotypic development of mESCs during 3D HARV culture.
Table 5.5. Efficiency of 2D versus 3D mESC osteogenic differentiation cultures.

TABLE OF CONTENTS

ABSTRACT **3**

ACKNOWLEDGEMENTS **4**

STATEMENT OF ORIGINALITY **5**

ABBREVIATIONS **6**

LIST OF FIGURES **10**

LIST OF TABLES **13**

1. INTRODUCTION **17**

1.1. PRINCIPLES OF TISSUE ENGINEERING 17
1.2. BONE 20
1.2.1. Macroscopic organisation *21*
1.2.2. Matrix and minerals *23*
1.2.3. Cellular components *25*
1.2.4. Development *29*
1.2.5. Macroscopic formation *31*
1.2.6. Molecular formation *33*
1.2.7. Diseases and defects *35*
1.2.8. Current repair and regeneration *36*
1.3. CELL SOURCES 36
1.3.1. Embryonic stem cells *38*
1.4. CLINICAL REQUIREMENTS 42
1.4.1. Serum-containing and serum-free media *43*
1.4.2. Bioreactors *46*
1.4.3. Encapsulation *51*
1.5. CRTICIAL INTERPRETATION OF THE LITERATURE AND GOAL FORMULATION 55
1.6. AIMS 57

2. MATERIALS AND METHODS **58**

2.1. MEDIA 58
2.1.1. Serum-containing media *58*
2.1.2. Serum-free media *59*
2.2. CELL CULTURE 60
2.2.1. 2D mESC maintenance and expansion *60*
2.2.2. 2D EB formation *61*
2.2.3. 2D bone nodule assay *62*
2.2.4. 3D Encapsulation *62*
2.2.5. Bioreactor descriptions *63*
2.2.6. Alginate bead dissolution *67*
2.2.7. Primary murine osteoblasts and MC-3T3-E1 culture *67*
2.2.8. Cryopreservation *68*
2.3. STAINING 69
2.3.1. Immunocytochemistry *69*
2.3.2. Histochemistry *71*

2.4. BIOCHEMICAL ASSAYS 72
2.4.1. Live/dead assay *72*
2.4.2. MTS assay *73*
2.4.3. DNA quantification *74*
2.4.4. Alizarin Red S (ARS) quantification *75*
2.4.5. Alkaline Phosphatase (ALPase) activity *75*
2.5. IMAGING 76
2.5.1. Light microscopy *76*
2.5.2. Micro-Computed Tomography (micro-CT) *76*
2.5.3. Confocal microscopy *76*
2.6. FLOW CYTOMETRIC ANALYSIS 77
2.6.1. Negative controls *77*
2.6.2. Calibration and suitable controls *78*
2.6.3. Two colour pluripotency analysis *78*
2.6.4. Two colour mesoderm analysis *79*
2.7. REVERSE TRANSCRIPTION-PCR 80
2.7.1. Primer design *80*
2.7.2. RNA isolation *82*
2.7.3. Reverse transcription *82*
2.7.4. PCR amplification *83*
2.7.5. Agarose gel electrophoresis *83*
2.8. MEDIA ANALYSIS 83
2.9. STATISTICAL ANALYSIS 84

3. ESTABLISHMENT AND CHARACTERISATION OF 2D BONE FORMATION FROM MESCS 87

3.1. INTRODUCTION 87
3.2. AIMS 89
3.3. MATERIALS AND METHODS 89
3.3.1. MESC maintenance *89*
3.3.2. Embryoid body formation *91*
3.4. RESULTS 92
3.4.1. MESC density studies and characterisation *92*
3.4.2. Flow cytometric analysis *96*
3.4.3. MESC media definition and optimisation *99*
3.4.4. Successful defined serum-free media *103*
3.5. DISCUSSION 109
3.6. CONCLUSION 116

4. ESTABLISHMENT AND CHARACTERISATION OF 3D CULTURE METHODOLOGY FOR MESCS 118

4.1. INTRODUCTION 118
4.2. AIM 120
4.3. MATERIALS AND METHODS 120
4.4. RESULTS 123
4.4.1. Encapsulation *123*
4.4.2. 3D cell culture *128*
4.4.3. 3D static prolonged culture (37 °C encapsulation temperature) *133*
4.5. DISCUSSION 136
4.6. CONCLUSION 140

5. 3D BONE FORMATION 142

5.1. INTRODUCTION 142
5.2. MATERIALS AND METHODS 145
5.2.1. Medium viscosity 145
5.3. AIMS 146
5.4. RESULTS 147
5.4.1. Medium viscosity 147
5.4.2. Bioreactor 3D bone formation 149
5.4.3. Development of mESCs to bone 195
5.4.4. Application of 3D HARV culture model 200
5.5. DISCUSSION 209
5.5.1. Maintenance and "EB formation" stages 210
5.5.2. Osteogenic differentiation stage 212
5.5.3. HepG2 conditioned medium 217
5.5.4. Perfusion bioreactor culture 218
5.5.5. Comparison to the literature and existing knowledge 218
5.6. CONCLUSION 220

6. DISCUSSION AND CONCLUSIONS 221

6.1. AIMS AND OBJECTIVES 221
6.2. SUMMARY OF MAJOR FINDINGS FROM THIS THESIS 221
6.3. FUTURE WORK AND CLINICAL IMPLICATIONS 222
6.3.1. Defined media 222
6.3.2. 3D culture 224
6.3.3. 3D bone formation 225
6.4. CONCLUDING REMARKS 227

7. REFERENCES 231

8. DERIVATIONS FROM THIS THESIS 250

9. APPENDICES 251

9.1. SERUM-FREE EXPERIMENTS 251
9.2. LWR1.1 SERUM-FREE MEDIUM 256
9.3. SERUM-FREE MEDIUM SURFACE COATINGS 256
9.4. LWR1.2 SERUM-FREE MEDIUM 257
9.5. DESIRABLE PARAMETERS FOR SERUM-FREE CULTURE 257
9.6. STATISTICS 258
9.7. DAY 3, BIOREACTOR IMMUNOSTAINING 271
9.8. DAY 8, BIOREACTOR IMMUNOSTAINING 272
9.9. NOVA BIOPROFILE 200 273
9.9.1. Measurement range 275
9.9.2. Principles of Measurement 275
9.10. MICROBEAD CELL MORPHOLOGY 277
9.11. CALIBRATION CURVES 278
9.12. MTS ASSAY 2D 278
9.13. MTS ASSAY 3D 278
9.14. DNA HOESCHT 279
9.15. ALKALINE PHOSPHATASE ACTIVITY 279
9.16. PUBMED SEARCHES 280

1. INTRODUCTION

1.1. Principles of Tissue Engineering

When asked what made an engineer, Isambard Kingdom Brunel (1806-1859) professed 'Engineers are extremely necessary for these purposes; wherefore it is requisite that, besides being ingenious, they should be brave in proportion.' (4). In short, calculated risks. In all engineering works, the safety of the public has to be uppermost, and engineers thus avoid taking unnecessary risks. Sometimes, the need to be sure gets in the way of the essential spark of engineering: the drive to innovate. Engineers must therefore retain this visionary drive.

When disease, injury or infection causes damage to an organ or tissue to the human body that is beyond the reparative capacity of its endogenous mechanisms, an alternative source is needed for regeneration. A recent classification defines tissue engineering as the implantation of *in vitro* seeded matrices in the form of bioactive, including bioresorbable, scaffolds that provide a biomechanical architecture enabling the seeded cells to produce an adequate extracellular matrix for further regeneration (5). This concept is distinct from guided tissue regeneration involving acellular matrices, which are repopulated by the host after implantation (6). The first accepted example of "tissue engineering" was thought to be published by Vincenzo Bisceglie (1933) who wrapped mouse tumour cells in a nitrocellulose, polymer membrane and successfully transplanted them into the peritoneum of a guinea pig in order to protect them from an immune response (7). The modern era began with the development of living skin for burn patients in the early 1980's (8;9).

Biomaterials were first conceived in the 1960's with the search for inert materials that combined suitable physical properties to match those of the replaced tissue with a minimal toxic response to the host (10). The second generation of biomaterials shifted from biologically inert materials to substances eliciting controlled bioactive responses in the local physiological environment (11).

Currently, there are many biomaterials in use (Table 1.1) but in bone tissue engineering, the materials under investigation are primarily polymers, hydroxyapatite and ceramics alongside emerging materials such as glasses, fabrics and hydrogels. The spectrum of biomaterials under investigation is wide, but few living tissue materials have been approved for clinical applications (Dermagraft® and TransCyte™).

Table 1.1. Biomaterials and their usage. Biomaterials in healthcare & tissue engineering

Material	Examples	Uses
Metals	Stainless Steel Titanium Alloy Cobalt-Chrome Alloy	Plates, Screws Femoral Stem, Dental implants Femoral Head
Polymers	Polyethylene Polytetrafluoroethylene (Teflon, PTFE) Polyvinylchloride (PVC) Polyurethanes Polypropylene, Silicone rubber	Acetabular sockets, catheters Gore-Tex blood vessel grafts Blood tubing Artificial heart, pacemaker leads, grafts Oxygenators (heart-lung machine)
Cements	Poly-methylmethacrylate (PMA)	Bone cement
Ceramics	Hydroxyapatite (HA)	Bone grafts, dental
Glasses	Bioglass®	Orthopaedic implants
Natural Materials	Collagen Cellulose	Porcine heart valve Haemostatic agents Burns Nerve regeneration Kidney dialysis membranes
Composites	Carbon fibre reinforced resins	Artificial ligaments
Fabrics	Polypropylene, Nylon Polytetrafluoroethylene (PTFE-Teflon)	Sutures, surgical drapes Blood vessel grafts
Coatings	Pyrolytic Carbon Silicone, Siloxane Polyethylene glycol Ceramic (Al_2O_3)	Heart valves Blood tubing Reduce protein adsorption Orthopaedic implants
Hydrogels	Polyhydroxyethylmethacrylate (PHEMA)	Contact Lenses, wound dressings, kidney dialysis membranes

Cell sources need to be in sufficient quantity and be free from pathogens and contamination. They can be autologous, allogeneic or xenogeneic and ideally should not cause an immune response in the patient. Mammalian stem cells are denoted based on their source: adult, foetal, embryonic and the mammalian umbilical cord [for review see (12)]. Mesenchymal stem cells (MSCs – or marrow stromal cells (13)] have been used, with some success, for autologous repair and regeneration of skeletal tissue as well as an allogeneic transplant to restore defective collagen type-I synthesis, in osteogenesis imperfecta patients (14). There are disadvantages with using MSCs; they are found in low numbers in the adult, with approximately 1 in 100,000 cells being a true stem cell (15;16) and their potential to proliferate and capacity to differentiate down specific cell lineages diminishes with patient age (15-17). Another possible source of cells for tissue engineering are embryonic stem cells (ESCs) which have the ability to differentiate to all cell types (18), including germ cells (19). Bishop (18) and others (20-24) have recently highlighted the potential of ESCs, as their inherent capacity for prolonged self-renewal, potentially negates cell expansion problems and provides tissue engineering with an unlimited pool of pluripotent cells.

Bone pathologies affect people of all ages, both sexes and range from osteogenesis imperfecta, caused by a single point mutation in the gene for collagen type-I (25) to osteoporosis, sports injuries, work-related injuries, adult trauma, cancer, microbial infection, developmental abnormalities and malnutrition (26). The tissue engineering approach to bone regeneration and repair has evolved in many guises. The key to success lies in providing the repair site with sufficient osteogenic progenitor cells in a suitable delivery vehicle to ensure osteogenic differentiation and optimal biosynthetic activity of

bone matrix and growth factors (27). Bone tissue engineering has developed from early bioactive glasswork with living tissues (28) to the use of murine (29-31) and human (32;33) ESCs in combination with resorbable bioactive gel-glasses to induce enhanced bone tissue formation.

Furthermore, 2D cultures suffer from being cumbersome, time-consuming and labour-intensive (34). These static cultures are also limited by the lack of mixing, lack of monitoring, and the need for frequent handling. Recent advances have seen the employment of 3D, perfused (35-39) bone culture systems such as encapsulated cells (40-42) in bioreactors to enhance and support the clinically driven models that currently exist. Bone tissue engineering therapies are still years from applications and there are a number of bridges to be crossed before these therapies reach the clinic, which will be discussed later (Section 1.4).

1.2. Bone

Galileo (43) suggested an association between the form and mechanical properties of bone and Weinmann and Sicher (44) eloquently described bone as a tissue and an organ. In the 19th century, surgeon Julius Wolff proposed that mechanical stress was responsible for determining the architecture of bone (45) and it was subsequently found that bone is deposited in sites subjected to stress and resorbed where there is little stress (46). The skeleton is multifunctional, providing a frame for protection and mechanical function, a metabolic regulator of body fluids and serves as a dynamic storage site for mineral ions and cytokines (47).

1.2.1. Macroscopic organisation

Macroscopically there are two types of bone: flat bones (skull bones) and long bones (tibia, femur) that are produced via intramembranous and endochondral ossification respectively. The key difference is the presence of a cartilaginous model, or anlagen, in endochondral bone formation. Long bones have two wider extremities (the epiphyses), a cylindrical hollow portion in the middle (the midshaft or diaphysis), and a transition zone between them (the metaphysis) (Figure 1.1). The epiphysis on the one hand and the metaphysis and diaphysis

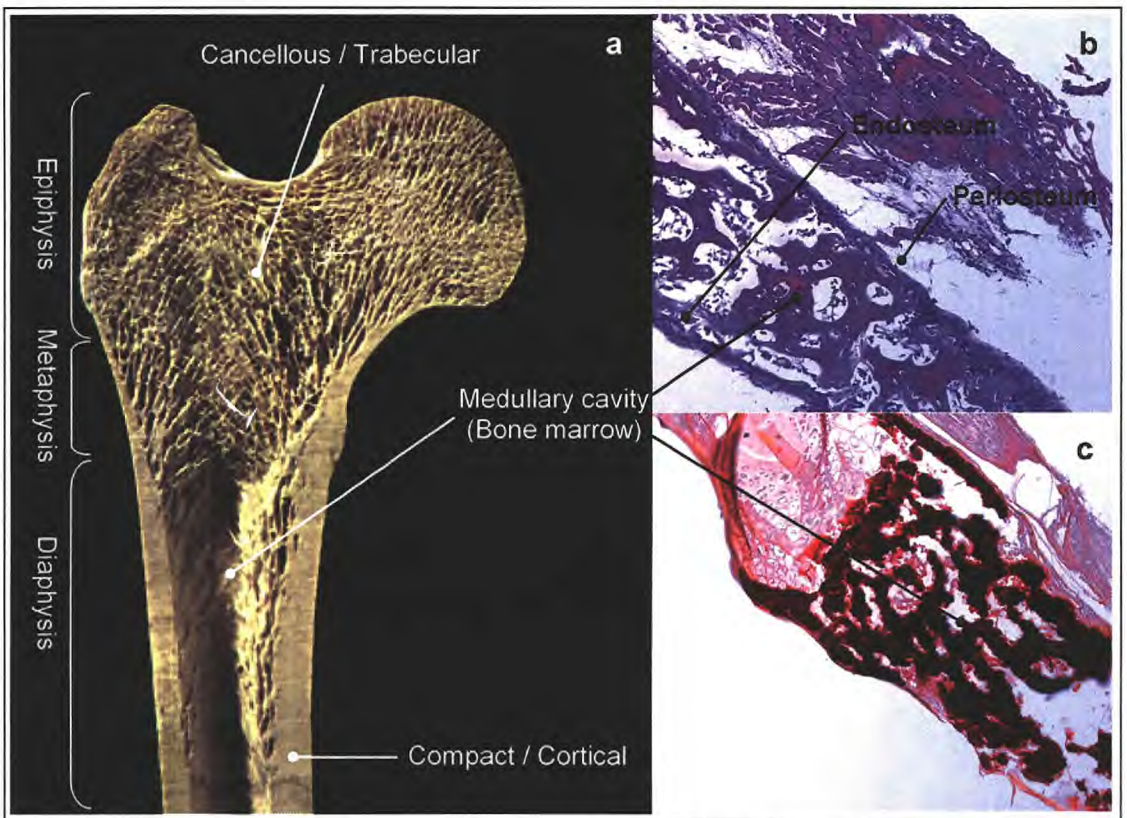


Figure 1.1. Macroscopic bone diagram. a. Portion of human femur. b. Portion of mouse femur, H&E stain. c. Portion of mouse femur, Alizarin Red S stain.

on the other hand originate from two independent ossification centres, and are separated by a layer of cartilage, the epiphyseal cartilage (which also

constitutes the growth plate) during the period of development and growth. This layer of proliferative cells and expanding cartilage matrix is responsible for the longitudinal growth of bones; it progressively mineralises and is later remodeled and replaced by bone tissue by the end of the growth period. The external part of the bones is formed by a thick and dense layer of calcified tissue, the cortex (compact bone) which, in the diaphysis, encloses the medullary cavity where the haematopoietic bone marrow is housed. Toward the metaphysis and the epiphysis, the cortex becomes progressively thinner and the internal space is filled with a network of thin, calcified trabeculae forming the cancellous or trabecular bone. The spaces enclosed by these thin trabeculae are also filled with haematopoietic bone marrow and are continuous with the diaphyseal medullary cavity. The outer cortical bone surfaces at the epiphyses are covered with a layer of articular cartilage that does not calcify. Bone is consequently in contact with the soft tissues along two surfaces: an external surface (the periosteal surface) and an internal surface (the endosteal surface) (Figures 1.1&2). Osteogenic cells line both the outer (periosteum) and inner (endosteum) surfaces. There are obvious structural and functional differences between cortical and trabecular but they are essentially composed of the same cells and matrix elements. The major structural difference is quantitative: 80% to 90% of the volume of compact bone is calcified, whereas only 15% to 25% of the trabecular volume is calcified (the remainder being occupied by bone marrow, blood vessels, and connective tissue). The result is that 70% to 85% of the interface with soft tissues is at the endosteal bone surface, including all trabecular surfaces, leading to the functional difference: the cortical bone fulfills mainly a mechanical and protective function and the trabecular bone mainly a

metabolic function, albeit trabeculae definitively participate in the biomechanical function of bones, particularly in bones like the vertebrae (48).

1.2.2. Matrix and minerals

Bone is composed of an organic matrix that is strengthened by deposits of calcium salts. Collagen type-I constitutes approximately 95% of the organic matrix; the remaining 5% is composed of proteoglycans and numerous non-collagenous proteins. Crystalline salts deposited in the organic matrix of bone under cellular control are primarily calcium and phosphate in the form of hydroxyapatite [$Ca_{10}(PO_4)_6(OH)_2$] (49). Hydroxyapatite is a plate-like crystal 20–80 nm in length and 2–5 nm thick. It is four times smaller than naturally occurring apatites and less perfect in structure, it is more reactive and soluble and facilitates chemical turnover. In other words, a more "perfect" crystal would be difficult to resorb, and thus repair of the matrix would be hindered (50).

Within lamellar bone, the collagen fibres form arches for optimal bone strength of aligned mineralised collagen fibrils (51). This fibre organisation allows the highest density of collagen per unit volume of tissue. The lamellae can be parallel to each other if deposited along a flat surface (trabecular bone and periosteum), or concentric if deposited on a surface surrounding a channel centered on a blood vessel (Figure 1.2, cortical bone Haversian system). Spindle or plate-shaped crystals of hydroxyapatite are found on the collagen fibres, within them, and in the matrix around. They tend to orientate in the same direction as the collagen fibers. When bone is formed very rapidly during development and fracture healing, or in tumours and some metabolic bone diseases, there is no preferential organisation of the collagen fibres. They are not as tightly packed and found in somewhat randomly oriented bundles; this

type of bone is called woven bone, as opposed to lamellar bone. Woven bone is characterised by irregular bundles of collagen fibres, large and numerous osteocytes, and delayed, disorderly calcification that occurs in irregularly distributed patches. Woven bone is progressively replaced by mature lamellar bone during the remodeling process (48).

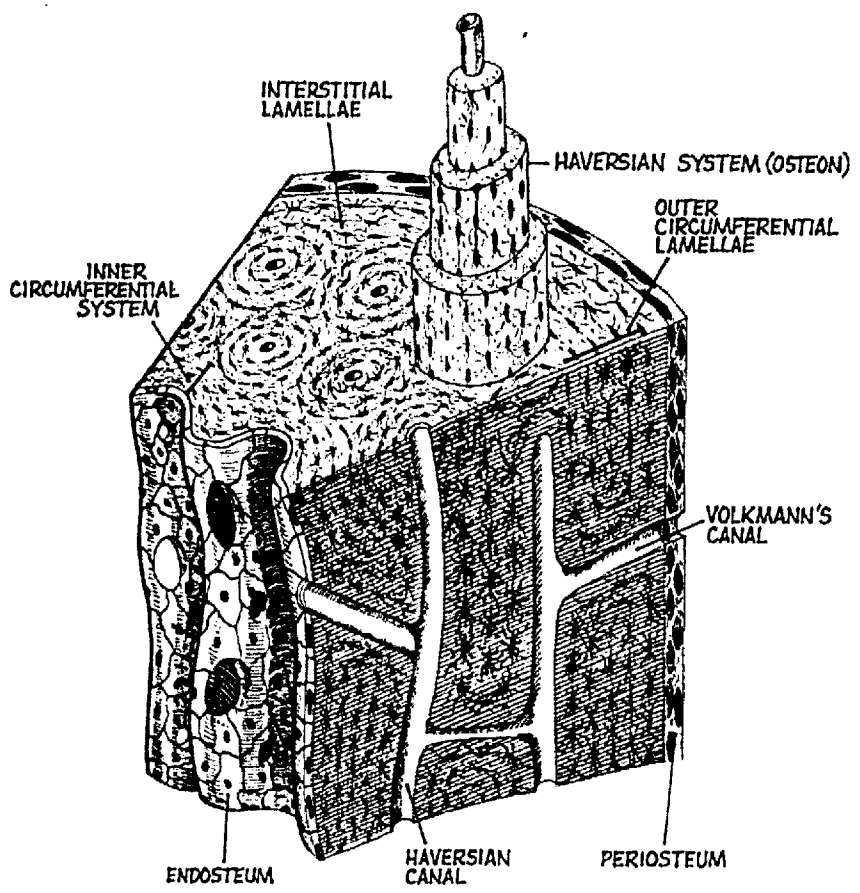


Figure 1.2. Schematic representation of bone architecture. Key characteristics of bone structure. Copyright permission received from JPMcGowan of www.jpmcgowandesign.com.

Calcified bone contains about 25% organic matrix, including cells (2–5%), 5% water, and 70% inorganic mineral (hydroxyapatite). Osteoid, the

freshly synthesized matrix prior to its mineralisation, consists primarily (approximately 94%) of collagen. Other proteins, some of them unique to bone, such as osteocalcin, are embedded in the extracellular matrix and may have important signaling functions (bone morphogenetic proteins, growth factors, cytokines, leukocytes, adhesion molecules) or play a role during the mineralisation process (osteopontin, osteonectin, matrix-gla protein) (52). Bone is composed of four different cell types: osteoblasts, osteoclasts, bone lining cells and osteocytes.

1.2.3. Cellular components

Functionally, osteoblasts are the cells within bone that lay down the extracellular matrix and regulate its mineralisation. Morphologically, these cells are cuboidal in shape and are located at the bone surface together with their precursors, where they form a tight layer of cells (52). Osteoblasts are highly anchorage dependent and rely on extensive cell-matrix and cell-cell contacts via a variety of transmembranous proteins (integrins, connexins, cadherins) and specific receptors (for cytokines, hormones, growth factors) to maintain cellular function and responsiveness to metabolic and mechanical stimuli (53;54). A human osteoblast lays down 0.5-1.5 μm of osteoid, per day and typically survives for up to 8 weeks (52). As the osteoblast may become trapped within its own matrix it is postulated that they differentiate to osteocytes and form connections throughout the overall network, acting as mechanosensors to aid new bone formation (55).

At the ultrastructural level, the osteoblast is characterised by the presence of an extremely well-developed rough endoplasmic reticulum with dilated cisternae and a dense granular content, and the presence of a large

circular Golgi complex comprising of multiple stacks (48). These organelles are involved in the major activity of the osteoblast: the production and secretion of collagenous and non-collagenous bone matrix proteins, including collagen type-I. Osteoblasts also produce a range of growth factors under a variety of stimuli, including the insulin-like growth factors (IGFs) (56), platelet-derived growth factors (PDGFs) (57), basic fibroblast growth factor (bFGF) (58), transforming growth factor-beta (TGFβ) (59), a range of cytokines (60), and the bone morphogenetic proteins (BMPs) (61). Osteoblast activity is regulated in an autocrine and paracrine manner by these growth factors, whose receptors can be found on osteoblasts, as well as receptors for a range of endocrine hormones. Classic endocrine receptors include receptors for parathyroid hormone / parathyroid hormone related protein receptor, thyroid hormone (62), growth hormone (63), insulin (64), progesterone (65) and prolactin (66). Osteoblastic nuclear steroid hormone receptors include receptors for oestrogens (67;68), androgens (69), vitamin D3 (70) and retinoids (71). Receptors for paracrine and autocrine effectors include those for epidermal growth factor (EGF) (72), IGFs (73;74), PDGF (75), TGFβ (76), interleukins (75;77;78), FGFs (79) and BMPs (80). Osteoblasts also have receptors for several adhesion molecules (integrins) (81) involved in cell attachment to the bone surface (48).

The calcified bone matrix is not metabolically inert, and cells (osteocytes) are found embedded deep within the bone in small lacunae. All osteocytes are derived from bone forming cells (osteoblasts) which have been trapped in the bone matrix that they produced and subsequently calcified. Even though the metabolic activity of the osteoblast decreases dramatically once it is fully encased in bone matrix, these cells still produce matrix proteins (48).

Osteocytes are trapped within the matrix and are responsible for maintenance in terms of synthesis and resorption. They are smaller in size than osteoblasts, contain fewer cell organelles such as ribosomes and endoplasmic reticulum and have an increased nucleus to cytoplasm ratio (52). Each osteocyte occupies a space (lacuna) within the matrix and extends filopodial processes through canaliculi in the matrix to contact processes of adjacent cells by means of gap junctions (Figure 1.3).

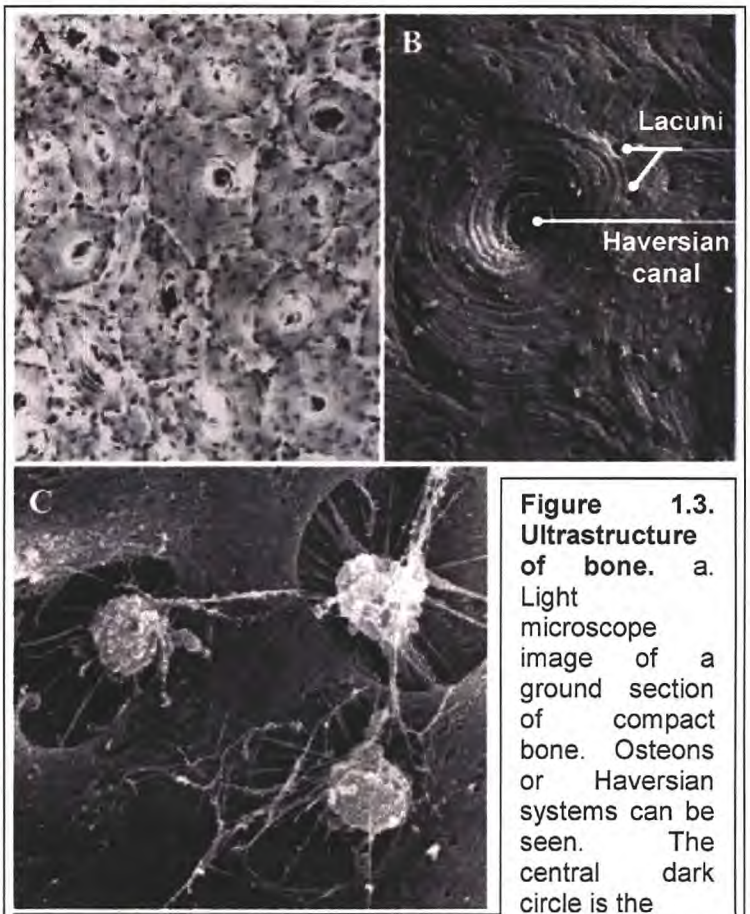


Figure 1.3. Ultrastructure of bone. a. Light microscope image of a ground section of compact bone. Osteons or Haversian systems can be seen. The central dark circle is the Haversian canal, which contains a nutrient artery *in vivo*. It is surrounded by concentric lamellae of calcified bone matrix. The dark spots are the lacuni in which osteocytes become entrapped. x350. b. Scanning electron micrograph (SEM) of a Haversian system. x800. c. SEM reveals individual osteocytes with cellular processes reaching out towards the lacunar wall and interconnecting cells. x1600. Copyright receiv from Glasgow University.

The network of connections (filopodia/gap junctions) permits communication between the internal and external surfaces of bone and with the blood system that supplies the immobilised structure. Matrix-producing osteocytes can be easily identified as they have similar organelles to osteoblasts, whereas osteolytic osteocytes contain lysosomal vacuoles and other features typical of phagocytic cells (49). Despite the complex organisation of the osteocytic network, and its location within the bone matrix, the exact function of these cells remains obscure. Given the structure of the network and the location of osteocytes within lacunae where extracellular fluid flow can be detected, it is likely that osteocytes respond to bone tissue strain and influence bone remodelling activity by recruiting osteoclasts to sites where bone remodelling is required (82). Osteocyte activity is increased after bone loading; studies in cell culture have demonstrated increased calcium influx and prostaglandin production by osteocytes after mechanical stimulation (83), but to date, there is no direct evidence for osteocytes signalling to cells on the bone surface in response to bone strain or microdamage (48).

Osteoclasts are large, multinucleated cells that have the role of resorption of fully mineralised bone at sites termed Howship's lacunae (52). Both macrophages and osteoclasts are derived from haematopoietic stem cells and, similar to macrophages, osteoclasts are highly migratory, polarised cells which carry an arsenal of lysosomal enzymes (84). When active, osteoclasts rest directly on the bone surface and have two plasma membrane specialisations: a ruffled border and a clear zone. The ruffled border (resorption bay) is typically highly folded, the point at which bone resorption takes place and where lytic enzymes are secreted. The clear zone (apical membrane) is a microfilament-rich, organelle-free area that surrounds the ruffled border and

forms a tight seal with the calcified matrix. The osteoclasts contain pleomorphic mitochondria, abundant lysosomal vesicles, multiple circumnuclear Golgi stacks and the nuclei are typically located in the parts of the cell most removed from the bone surface (49;52). An activated osteoclast is able to resorb 200,000 μm^3 of bone per day, which amounts to the manufacturing power of seven to ten generations of osteoblasts with an average lifespan of 15-20 days (85).

Bone lining cells are flat, elongated, inactive cells that cover bone surfaces and have few cytoplasmic organelles. It has been postulated that these cells could be precursors to osteoblasts (49) or in concert with osteocytes, constitute a functional syncytium involved in mineral homeostasis as well as in bone adaptation to mechanical loading (86).

1.2.4. Development

The vertebrate skeleton is divided into two main components: axial and appendicular. Skeletal cells are derived from three distinct embryonic cell lineages: neural crest cells, sclerotome cells and lateral plate mesoderm forming the craniofacial skeleton, somite-axial skeleton and appendicular components, respectively. The cells from these lineages participate in the process of skeletogenesis in four distinct phases:

1. Migration to the site of future skeletogenesis
2. Epithelial-mesenchymal interaction
3. Formation of condensations
4. Overt differentiation of chondroblasts and osteoblasts

Embryonic development of the vertebrate body plan is one of the most important, defining features of mammals. Upon gastrulation, paraxial

mesoderm cells segregate from axial and lateral mesoderm to form two identical strips of unsegmented tissue (referred to as presomitic mesoderm in the mouse embryo) on either side of the neural tube. Paraxial mesoderm in vertebrates gives rise to the axial skeleton, as well as all trunk and limb skeletal muscles and portions of the trunk dermis and vasculature. Somitogenesis sequentially proceeds from rostral (head) to caudal (tail) to form the somites and in turn the sclerotome. The cells involved differentiate into cartilage anlagen and migrate to the areas where the vertebral body and ribs will eventually form (47;52). Briefly, mesodermal tissue can be identified with markers such as platelet-derived growth factor alpha (PDGFRα), fetal liver kinase-1 (Flk-1) (87) and *Brachyury T* (88;89). In the postnatal state, cells with osteogenic potential persist in the bone marrow; namely MSCs.

Two mechanisms of bone formation can be observed during morphogenesis. One route involves MSCs differentiating directly into osteoblasts, which then proceed to form bone. Membranous or more precisely, intramembranous bone formation is found during skull development, but also in maxilla and mandibula morphogenesis. Progenitors migrate to the sites where bones are required to form. They condense, align, and secrete long strands of osteoid (collagenous material) while retaining the ability to proliferate throughout osteogenesis. Differentiated progenitors or osteoblasts deposit calcium salts that mineralise and form the bone matrix. The osteoids are now termed trabecula and consecutive growth rings (appositional growth) are added to increase thickness, which are termed lamellae.

If differentiation of MSCs proceed via chondrocytes, which then form cartilaginous templates (or anlagen) of the future bones, the process is termed endochondral ossification. Endochondral ossification begins with the migration

of progenitors (chondroblasts) to the site where the bones are required to form. In contrast to intramembranous ossification, chondroblasts are induced to form a dense mass of chondrocytes, which continue to proliferate and secrete a loose extracellular matrix (ECM) in the form of collagen type-I and complex polysaccharides. The ECM forces the chondrocytes apart (interstitial growth) resulting in complete cellular encapsulation and a decrease in proliferation. At this point the encapsulated chondrocytes apoptose, whereby bone cells invade in concert with vascularisation (90). At the periphery of this cartilage (the perichondrium), the mesenchymal cells continue to proliferate and differentiate which is called appositional growth (48).

Systemic and local mediators act upon the growth plate where endochondral ossification occurs and are important for linear skeletal growth in both animal and human studies. Systemic mediators found to act upon bone are growth hormone (GH), insulin-like growth factor I (IGFI), thyroid hormones (TH), oestrogens, glucocorticoids and vitamin D ($1,25(OH)_2$-vitamin D3). Local mediators found to act are cytokines, transforming growth factors β 1, 2 & 3 (TGFβ1,2,3), parathyroid hormone-related protein (PTHrP) and other factors such as Indian & Sonic hedgehog (I/Shh) and fibroblast growth factor receptor 3 (FGFR3) (47).

1.2.5. Macroscopic formation

Macroscopic bone formation occurs by three co-ordinated processes: production, maturation and subsequent mineralisation of the osteoid matrix. In normal adult bone, these processes occur at the same rate, so that the balance between matrix production and mineralisation is equal. Initially, osteoblasts deposit collagen rapidly, without mineralisation, producing a thickening osteoid

seam. This is followed by an increase in the mineralisation rate equal to the rate of collagen synthesis. In the final stage, the rate of collagen synthesis decreases, and mineralisation continues until the osteoid seam is fully mineralised. This time lag (termed the mineralisation lag time or osteoid maturation period) appears to be required for osteoid to be modified so it is able to support mineralisation. While this delay is not yet understood, it is likely that either collagen cross-linking occurs or an inhibitor of mineralisation, such as matrix gla protein (91) is removed during this time, thus allowing mineralisation to proceed. To initiate mineralisation in woven bone or in growth plate cartilage, high local concentrations of Ca^{2+} and PO_4^{3-} ions must be reached in order to induce their precipitation into amorphous calcium phosphate, leading to hydroxyapatite crystal formation. This is achieved by membrane-bound matrix vesicles, which originate by budding from the cytoplasmic processes of the chondrocyte or the osteoblast and are deposited within the matrix during its formation (92). These vesicles are the first structures wherein hydroxyapatite crystals are first observed. The membranes are rich in alkaline phosphatases and in acidic phospholipids, which hydrolyse inhibitors of calcification in the matrix [such as pyrophosphate and adenosine tri-phosphate (ATP)], and allow the condensation of apatite crystals. Once the crystals are in the matrix, they grow in clusters; later coalescing to completely calcify the matrix, filling the spaces between and within the collagen fibers. In adult lamellar bone, matrix vesicles are not present and mineralisation occurs in an orderly manner through progression of the mineralisation front into the osteoid tissue (48).

1.2.6. Molecular formation

The osteogenic differentiation pathway from totipotent stem cell in the fertilised egg, to mature bone tissue in the fully grown adult is regulated by a myriad of hormones, transcription factors and master control checkpoints that interact in a cross talking web. The most distinguished morphological feature specific to osteoblasts is located outside the cell in the form of a mineralised extracellular matrix. Based on bone nodule formation *in vitro* and macroscopic bone formation, the process has been subdivided into three stages: i) cell proliferation ii) ECM secretion/maturation, and iii) mineralisation (93). However, there is no evidence, to date, that bone matrix mineralisation is orchestrated by genes selectively expressed in osteoblasts. All genes expressed in fibroblasts are also expressed in osteoblasts, and, conversely, only two osteoblast-specific transcripts have been identified: one encoding core-binding factor alpha-1 (*Cbfa1*: now known as *runx2* - a transcription factor) and the other encoding osteocalcin (OCN), a secreted ECM protein that inhibits osteoblast function (94;95). For ease of nomenclature, cells can be artificially compartmentalised into a number of developmental stages: i) MSCs, ii) osteoprogenitor cells, iii) pre-osteoblasts, iv) osteoblasts, and v) mature osteocytes (96).

During embryonic development, *Cbfa1* expression precedes osteoblast differentiation and is restricted to mesenchymal cells destined to become either chondrocytes or osteoblasts (97). Subsequently, *Cbfa1* expression becomes limited to the osteoblasts with a lower level of expression in hypertrophic chondrocytes (98). *Cbfa1* is one of the earliest known markers of osteogenesis and can induce osteoblast-specific gene expression in fibroblasts and even myoblasts (97). More recently, an important transcription factor, *Osterix* (*Osx*) that is required for osteoblast differentiation, has been identified in the mouse.

It is a zinc-finger domain containing protein acting downstream of *Cbfa1* to drive differentiation of preosteoblasts towards a more mature end point (99). Finally, *AJ18* has also been identified as a novel gene that acts as a putative transcriptional repressor involved in the differentiation of osteogenic cells (100).

Expression of several osteoblast-associated genes such as those encoding *collagen type-I*, *alkaline phosphatase (ALPase)*, *osteopontin*, *OCN*, and *bone sialoprotein* are upregulated asynchronously, acquired and/or lost as the progenitor cells differentiate and the matrix matures and mineralises (101). Alongside gene expression analysis, osteoprogenitor proliferation and differentiation is regulated by many other transcription factors, hormones, growth factors and cytokines that will not be discussed here in detail (93).

The identification of the factors which regulate the proliferation and differentiation of cells of the osteoblast lineage remains one of the major challenges in the field of bone cell biology. The *in vitro* formation of mineralised nodules that exhibit the morphological, ultrastructural and biochemical characteristics of embryonic/woven bone formed *in vivo* represents the first evidence that the differentiation of functional osteoblasts can occur in cultures of isolated animal bone-derived cell populations. It is clear, however, that the culture conditions employed at present only permit a small number of cells to differentiate to the extent of being capable of organising their extracellular matrix into a structure that resembles that of bone (30;31;33). Briefly, serum, ascorbate (ascorbic acid) or the long acting ascorbate analogue (L-ascorbate-2-phosphate), β-glycerophosphate (organic phosphate not available *in vivo*) and dexamethasone (glucocorticoid) are known as *in vitro* inducers of osteogenic differentiation (102). Currently, serum with or without supplements [ascorbate, dexamethasone and simvastatin (103;104)] are absolute requirements for

nodule formation whereas β-glycerophosphate promotes or enhances mineralisation (105).

1.2.7. Diseases and defects

The United Nations declared the years 2000-2010 the "Bone and Joint Decade", to draw attention to the increasing impact that orthopaedic conditions will have on the world's health, as life expectancy increases and to the potential that current and future research have for eliminating these problems. The American Academy of Orthopaedic Surgeons reported that three million musculoskeletal orthopaedic procedures costing approximately $215 billion each year were performed in US hospitals in 1995 including fractures (15%), joint problems (22%) and spinal disorders (12%).

One of the first applications of tissue engineered bone may be for bone defects that are incapable of self fusion or renewal such as lumbar spondylolisthesis. This condition is common in elite athletes manifesting as back pain and is likely to originate as a stress fracture in the lumbar region of the spine. This condition usually affects between two thirds to a quarter of elite athletes that are under 20 years. It also affects around 4-6% of the UK population aged between 6 and 40 years (106;107). Nearly all patients require surgery, an autologous bone graft and / or pinning (108-111), complicating a painful surgical procedure. It is clear that younger adults can provide small amounts of suitable autologous material for a bone graft but older adults may not be able to provide grafts of suitable quality, which is where tissue engineered bone, would be useful.

1.2.8. Current repair and regeneration

Many of the current strategies to repair skeletal damage include the use of autogenic or allogeneic grafts, bone cements and metals (112), as well as various prosthetic implant devices and orthotic control of body segments (26). While successful, there are limitations; prosthetic devices fail and require replacement and bone tissue for grafting is often in limited supply. Joint replacement design has been forced to improve rapidly since the 1960's, mainly due to problems with infection, device breakage or loosening, general wear and tear, and wear debris-induced bone resorption (osteolysis) (113). Personalised healthcare for bone tissue engineering is the ultimate goal. The production of high quality tissue in sufficient numbers that does not pose immunogenic problems would be an ideal alternative to joint replacement.

1.3. Cell sources

The term "Stem Cell" has been used in the literature since 1896 (114) and defines cells that retain the capacity to self-renew indefinitely (which, is not a requirement *in vivo*) as well as to produce progeny that are more restricted (progenitors) in both mitotic potential and in the range of distinct subpopulations or cell lineages they can produce (115). Stem cells can be obtained from embryonic, foetal and adult tissue and are classified according to their ability to generate a number of tissue types. The totipotent (fertilised egg gives rise to embryonic and extraembryonic tissue) cells generate pluripotent cells (able to derive the three germ layers), which in turn give rise to multipotent cells (progenitors capable of generating multiple cell lineages) and finally unipotent cells (progenitors capable of generating only one cell lineage). To distinguish between progenitors and adult stem cells it is accepted that, when a stem cell

divides, one of the two new cells is often capable of replicating itself. In contrast, when a progenitor divides it can form two specialised cells, neither of which is capable of replicating itself (12). Division in human ESCs (hESCs) is exclusively symmetrical suggesting ESCs more closely resemble precursor or transit amplifying cells rather than adult stem cells (116).

Embryonic Germ (EG) cells are derived from foetal tissue and are isolated from the primordial germ cells of the gonadal ridge, which would normally develop into the testes or ovaries and were first described in 1991 (117). Embryonic carcinoma (EC) cells are cells derived from the undifferentiated component of teratocarcinomas, and are so-called due to their close resemblance to early embryonic tissue (118-120) and are known to be pluripotent (121). ESCs were first isolated from the inner cell mass (ICM) of the mouse preimplantation embryo over 20 years ago (122;123) and more recently in primates (124) and humans (125).

Adult stem cells have been discovered in a range of tissues, from umbilical cord blood (126) to more recent discoveries in teeth (127). However, these stem cells are thought to be more restricted in their differentiation potential than ESCs although reports of transdifferentiation and dedifferentiation to cell types other than the tissue of origin have been reported (128). A consensus has been reached providing some essential characteristics to define and characterise ESCs (Table 1.2) (12).

Table 1.2. ESC characteristics.
• [a]Derived from the ICM/epiblast of the blastocyst.
• [a]Capable of undergoing an unlimited number of symmetrical divisions without differentiating (long-term self-renewal).
• Exhibit and maintain a stable, full (diploid), normal complement of chromosomes (karyotype).
• Pluripotent ESCs can give rise to differentiated cell types that are derived from all three primary germ layers of the embryo (endoderm, mesoderm, and ectoderm).
• [a,b]Capable of integrating into all foetal tissues during development. (mESCs maintained in culture for long periods can still generate any tissue when they are reintroduced into an embryo to generate a chimaeric animal.)
• [a,b] Capable of colonising the germ line and giving rise to egg or sperm cells.
• [a] Clonogenic, that is a single ESC can give rise to a colony of genetically identical cells, or clones, which have the same properties as the original cell.
• Expresses the transcription factor Oct-4, which then activates or inhibits a host of target genes and maintains ESCs in a proliferative, non differentiating state.
• Can be induced to continue proliferating or to differentiate.
• Lacks the G1 checkpoint in the cell cycle. ESCs spend most of their time in the S phase of the cell cycle, during which they synthesise DNA. Unlike differentiated somatic cells, ESCs do not require any external stimulus to initiate DNA replication.
• Do not show X inactivation. In every somatic cell of a female mammal, one of the two X chromosomes becomes permanently inactivated. X inactivation does not occur in undifferentiated ESCs although some cell lines although it varies in some hESC lines (129).
[a] Not shown in human EG cells. [b] Not shown in human ESCs. All of the criteria have been met by mESCs.

1.3.1. Embryonic stem cells

ESCs differentiate and self-renew by symmetrical cell division (116). Relatively homogeneous undifferentiated populations (10^9 - 10^{10}) can be generated simply by observation of morphology, marker expression and efficient generation of equipotent subclones. ESCs appear to be immortal and, unlike primary cells, show no signs of senescence (130). However, constant monitoring and karyotyping must be performed if these cells are to be used in the clinic (131;132). The International Stem Cell Initiative Steering Committee was formed in London, January 2003 (Stem Cell Forum) and will discuss the results

of a global comparison of hESC lines (133) in August 2005 and publish the results in 2006.

Octamer binding factor 4 (also known as Oct-3, Oct-3/4, Pou5f1) is a Pit-Oct-Unc (POU) family transcriptional regulator restricted to early embryos, germ-line cells, and undifferentiated EC, EG, and ESCs (134). Oct-4 expression *in vivo* is required for the development of the pluripotent capacity of ICM cells (135) and *in vitro* it is chemostatically controlled for the maintenance of pluripotency (136). The complexity of Oct-4 function is highlighted by the fact that if ESC expression of these transcriptional regulators is altered slightly, then this provokes differentiation into endo/meso-derm in monolayer culture (136). A second homeodomain-containing protein, Nanog, is expressed in the ICM of a compacted morula and blastocyst (as well as early germ cells) and is down-regulated just prior to implantation. Nanog overexpression can maintain self-renewal of ESCs independently of the Leukaemia inhibitory factor (LIF)/glycoprotein (gp) 130 / Signal transducers and activators of transcription (STAT)3 pathway (137;138) (LIF/gp130/STAT3). CD9 is a surface marker that is present on pluripoptent mESCs and is lost after one or two days upon differentiation (139;140). CD9 was identified at the beginning of this thesis as a suitable marker for analysis as it was the only surface marker available at the beginning of this thesis suitable for immunocytochemical and flow cytometric analysis. It has subsequently been used by Geron, USA for hESC analysis as it is a good marker of pluripotent hESCs (Lebkowski – personal communication).

MESCs were originally isolated and co-cultured on a feeder layer and it was subsequently found that feeders can be substituted by conditioned media (141;142). LIF (a trophic factor) is secreted from the feeders, maintains mESC pluripotency and does so when supplied in a purified form (143), negating the

need for a feeder layer. Furthermore, overexpression of the anti-apoptotic protein B-cell CLL/lymphoma 2 (Bcl-2), in combination with LIF, removes the need for serum and feeders (144). For a full review of other extrinsic and intrinsic factors affecting ESCs see reference (145).

Differentiation can be initiated by the removal of feeders, LIF or feeder-conditioned media resulting in embryoid body (EB) formation or monolayer propagation. The EB suspension method developed for EC cells (146) leads to formation of multidifferentiated structures similar to post-implantation embryonic tissue by formation of all three germ layers (147). Spontaneous EB formation occurs in two phases (simple and cystic) and it is important to replenish serum-containing medium on day 3. Within 2 to 4 days in suspension culture, mESCs clump together and endoderm forms on the surface of the ICM, giving rise to structures termed "simple embryoid bodies." At around day 4 of differentiation a columnar epithelium with a basal lamina and central cavity forms. These "cystic embryoid bodies" bear similarities to egg cylinder-stage embryos and upon continuation of *in vitro* culture of EBs, endodermal and mesodermal cells appear (148).

The first report of the isolation of human ICM cells from human blastocysts was in 1994 (149) but these stem cells could only be maintained for two passages. Later Thomson, *et al.* (1998) successfully derived hESC lines that could be passaged indefinitely *in vitro* (125). More recently hESCs were maintained in serum-free, feeder independent conditions when grown in Matrigel™ (BD Biosciences, UK, Laminin major component) (150). Laminin receptors on the surface of hESCs - integrin heterodimers consisting of $\alpha 6$ & $\beta 1$ subunits - were found to be present on most cells (97-99%), which may form a dimer specific to laminin (150), aiding adhesion to laminin matrix. hESCs *in*

vitro are capable of long-term self-renewal of over 300 population doublings (21), while retaining a normal karyotype (125;151;152) and are probably immortal (Lebkowski – personal communication). HESCs (doubling time = 36hours) are more difficult to propagate than mESCs (doubling time = 12hours) (21;151). They form small, flat compact colonies the day after seeding, express high telomerase activity levels even after more than 300 population doublings and passage for more than a year in culture (125;151). HESCs also possess a normal karyotype, stable proliferation rates and stably express *Oct-4*, human telomerase reverse transcriptase (*hTERT*), *ALPase* and surface markers such as stage-specific embryonic antigen-4 (SSEA-4), tumour rejection antigen 1-60 (Tra 1-60) and Tra 1-81. In addition, they form teratomas in severe combined immunodeficient (SCID)/beige mice and differentiate *in vitro* into cells from all three germ layers demonstrating their pluripotency. As with mESCs, aggregation of hESCs into EBs causes spontaneous and random differentiation into multiple tissue types that represent endoderm, ectoderm, and mesoderm germ layers (153-157).

More recently, mouse and human ESCs have been maintained in feeder free conditions through the canonical Wnt signalling pathway by a glycogen synthase kinase-3 (GSK-3) specific inhibitor known as 6-bromoindirubin-3'-oxime (BIO) (158-161). In addition, it has been clearly shown that the addition of noggin and bFGF to unconditioned medium, in the absence of feeders, synergistically represses BMP signalling and sustains the proliferation of undifferentiated hESCs (162). The elimination of animal products is essential for clinical applications to avoid immune rejection and contamination with xenogeneic proteins. It has recently been found that animal proteins were present in hESCs lines cultured with animal feeder layers (163).

1.4. Clinical requirements

In the United Kingdom, human ESC lines can only be derived legally under licence from the Human Fertilisation and Embryology Authority (HFEA) and the lines must be placed in the Medical Research Council's Stem Cell Bank. The UK currently allows human ESC cloning but this is restricted to therapeutic nuclear transfer for the creation of autologous cells or the production of diseased cell lines for *in vitro* pathogenetic or drug discovery investigations. Reproductive cloning is illegal (164).

There are major obstacles to overcome before ESCs become useful in the clinic. These obstacles are: producing homogeneous tissue populations, providing sufficient cell numbers for treatment, proving *in vitro* and *in vivo* efficacy (animal model), testing for safety (teratoma formation) and negating the innate rejection mechanisms of the human body. There are a number of potential solutions to these problems and progress has been made on the issue of immune rejection using human ESCs generated by somatic cell nuclear transfer (165;166). An alternative strategy to overcome immunological rejection may be to generate a bank of ESCs with different major histocompatibility complex (MHC) genotypes, for matching donor to recipient. It may also be possible to downregulate the antigenicity of ESCs through suppression of MHC gene expression (167). ESCs could also be used to identify chromosomal abnormalities, monitor childhood tumour development, the toxicological assessment of new drugs (168), employed to screen toxins and used to develop genetic manipulation techniques for gene therapy (12).

The final hurdles, assuming that all these goals are achieved is, manufacturing these tissues under good manufacturing practice (GMP), using closed and controlled bioreactors (169) and supplying high quantities of tissue,

in order to conduct the four phases of clinical trials. Comparable regulations exist in different countries but the USA guidelines from the Food and Drug Administration (FDA) are clear and comprehensive. In February 1997, the FDA published two documents entitled "A Proposed Approach to the Regulation of Cellular and Tissue-Based Products" and "Reinventing the Regulation of Human Tissues" that established the current framework for the regulation of cell- and tissue engineered products. The intention of this FDA act was to: a) control the spread of infectious disease; b) prevent handling that may damage tissue products; and c) ensure safety and efficacy of such products [for a full review see (170)]. In the UK the Medicines & Healthcare Products Regulatory Agency (MHRA) also has guidelines and has a specific department for device technology, evaluation and safety (DTES) specifically dealing with tissue engineered and orthopaedic implants.

In light of these challenges, the first clinical application of stem-cell-engineered bone was the successful grafting of a new distal phalanx of the thumb. This graft comprised of periosteal-osteogenic cells from the distal radius and a calcium-alginate (Pronova Biopolymer, Norway) - porous coral scaffold (porous hydroxyapatite; 500-pore Pro Osteon, Interpore International, Irvine, USA) (171). However, the cells were grown using foetal calf serum (FCS) and could still cause complications through bovine protein contamination. To date however, the FDA have not approved any orthopaedic devices that incorporate tissue-derived components such as cells (170).

1.4.1. Serum-containing and serum-free media

Serum is an extremely complex biological cocktail that consists mainly of proteins (such as growth factors / cytokines), hormones, amino acids, glucose,

trypsin inhibitors and lipids. FCS has become the industry standard. Variations in quantity and quality of serum depend on age, health and nutrition of the animals used, supplier, country of origin, quality control measures and performance characteristics which forces the research community into continuous, laborious screening on virtually every batch of serum.

The most important factor in ESC culture is the control of differentiation. Consequently, serum offers the greatest variability and hence potential of uncontrollable, spontaneous differentiation. As discussed, serum plays a critical role in cell growth *in vitro* by providing amino acids, lipids, growth factors, vitamins, hormones, attachment factors, pH buffer and protease inhibitors (172-174). The addition of serum to a basal media changes the physiological properties such as viscosity, osmolarity, diffusion rates and provides protease inhibitors. Serum also provides cholesterol, albumin, transferrin, apolipoproteins, attachment factors (gelatin, collagen, fibrinogen, laminin, fibronectin, heparin, fibrin), growth factors (polypeptides with mitogenic activity including: EGF, fibroblast growth factor (FGF), PDGF, IGF and interferons), hormones (GH, insulin, oestrogen and hydrocortisone), helps nutrient solubility, provides detoxification proteins and aids the slow release of fatty acids which can be toxic at high levels. The list is almost endless and excludes the basic requirements of cells such as salts, vitamins, minerals, sugars, nucleic acid precursors and other metabolic factors obligatory for cell survival (175).

In a defined medium, each added component is identified and its precise concentration is known. A chemically defined medium is one in which each added component is not only specified and of known concentration but has a known chemical structure. Devising a well-defined medium formulation is imperative for generating repeatable and reliable data from a cell culture system

(1). The derivation of bone from ESCs essentially contains three stages: ESC maintenance, EB formation and osteogenic differentiation and the literature contains three medium formulations (89;176;177), related to these phases, to begin serum-free media development. Using these media and empirical evidence it appears that certain basal conditions are necessary [basal media, transferrin, insulin, a lipid source, an amino acid source, supplementary L-glutamine, polyvinyl alcohol (PVA)] and other cell culture parameters [avoidance of extremes; pH 7.2-7.4, light, heat, optimal cell densities and a medium buffer, minimal or no antibiotics, minimisation of mechanical forces, controlled adaptation (direct/sequential)] are requirements for successful cell culture. In addition, serum-free media also requires the use of trypsin inhibitors, for passage, which are normally found in serum to support cell viability and differentiation. Some researchers have published serum-free media formulations that could be used for either clinical applications or elucidating the mechanisms of stem cell biology (88;89;178;179).

The major problem with culturing stem cells under serum-free conditions is that cells generally tend to have a lower mitotic index, become apoptotic, and display poor adhesion in the absence of serum (180). To prevent transmission of pathogens, the patient's own serum could be used for the *in vitro* culture of stem cells. However, for clinical applications, there are a number of reasons that would make it preferable to eliminate serum from the *in vitro* culture milieu. First and foremost, the composition of serum is poorly defined, with a considerable degree of inter-batch variation, even when obtained from the same patient or manufacturer. This would impede good quality control in the laboratory. Serum is also not completely physiological, because it is essentially a pathological fluid formed in response to blood clotting. Additionally, it may

also contain uncharacterised growth and differentiation factors, which may result in the uncontrolled spontaneous differentiation of stem cells into divergent multiple lineages, other than the lineage of interest such as bone (170).

1.4.2. Bioreactors

The transition from an undifferentiated mESC to mineralised tissue/bone is fragmented, undefined, involves high maintenance, is difficult to sample, highly variable and limited to somewhat "unnatural" 2D conditions (181). By integrating the maintenance, EB formation and osteogenic differentiation phases into a simple, integrated and reproducible procedure it may be possible to scale up bone production from ESCs with a clinical application in mind. Static cultures, suffer several limitations: a) lack of mixing resulting in critical gradients for dissolved oxygen (low solubility) and cytokines (high molecular weight), and hence heterogeneity; b) lack of control options for dissolved oxygen and pH; and c) lack of support for frequent feeding (182).

Bioreactors are generally defined as devices in which biological and/or biochemical processes develop under closely monitored and tightly controlled environmental and operating conditions (e.g. pH, temperature, pressure, nutrient supply and waste removal). The high degree of reproducibility, control and automation introduced by bioreactors for specific experimental bioprocesses has been key for their transfer to large-scale applications (183). They enable the expansion of cells for transplantation and the growth of 3D tissues prior to transplantation. Their main function is to establish spatially uniform cell distributions using 3D scaffolds, maintain desired nutrient concentrations, provide efficient mass transfer of nutrients to those tissues and expose the tissues to physical stimuli to enhance differentiation. The general

design requirements for a bioreactor are the control of the physiological environment (P O_2, P CO_2, pH), aseptic feeding and sampling, simultaneous culture of multiple cell types, monitoring of cell and tissue function and structure, uniform cell and tissue quality leading to reproducibility (182-186). The generation of 3D tissues *ex vivo* not only requires the development of new biological models but also poses new technical challenges owing to the physicochemical requirements of large cell-masses (183).

It has long been known that the supply of oxygen and soluble nutrients becomes critically limiting for the *in vitro* culture of 3D tissues. The consequence of such a limitation is exemplified by early studies showing that cellular spheroids larger than 1 mm in diameter generally contain a hypoxic, necrotic centre, surrounded by a rim of viable cells (187). Stirred suspension culture systems offer attractive advantages of ready scalability and relative simplicity. Their relatively homogeneous nature makes them uniquely suited for investigations of different culture parameters (e.g. O_2 tension, cytokine concentration, serum components, media exchange rates, etcetera) that may influence the viability and turnover of specific stages and types of stem cells (13). In a flow perfusion system, there is continuous circulation of medium throughout the system. It provides enhanced delivery of nutrients by mitigating both external and internal diffusional limitations. It offers a convenient method of providing mechanical stimulation to the cells by way of rotating perfusion (bone cells are known to be stimulated by mechanical signals) (188;189) rather than turbulent mechanical stirring. A flow perfusion bioreactor thus extends the benefits offered by the stirred system by allowing external and internal media mixing without high shear forces. However, the effects of direct perfusion can be highly dependent on the medium flow-rate and the maturation stage of the

constructs, as recently demonstrated for 3D cultures of chondrocytes (190). Therefore, optimising a perfusion bioreactor for the engineering of a 3D tissue must address a careful balance between the mass transfer of nutrients and waste products to and from cells, the retention of newly synthesised ECM within the construct and the fluid induced shear stresses within the scaffold pores (183).

Bioreactors are required when a) a larger number of cells are required b) when accessory cells are used, or c) when high cell densities are desired (182). Cytokine concentrations appear to be of major importance and stem cell based culture systems will need to take into account the changing rates of depletion of each cytokine required. Thus, continuous monitoring of cytokine depletion may be essential for maintaining cytokine concentrations at levels that optimise the production of specific cell populations. In addition, the consequence of stimulating cells with high concentrations of cytokines is to temporally modulate their capacity to continue to respond to the same cytokines (e.g. through changes in cell surface receptor density) (13). To harness the full potential of bioreactors a perfusion (medium exchange with cell retention) system must be employed (182) as controlled medium replacement may also be necessary to optimise cytokine concentrations over time. These systems have the additional advantage that, depending on the medium exchange rate, changes in media formulations and the removal of inhibitory products can be performed online (182).

One of the major challenges in reaching this ambitious goal is to translate research-scale production models into clinically applicable manufacturing designs that are reproducible, clinically effective and economically acceptable while complying with GMP requirements (183).

Current FDA regulations address the extent of acceptable cell manipulation. Thus "minimally manipulated" tissue-engineered products (i.e., cryopreserved cells which are not otherwise processed, positive selected $CD34^+$ cells etcetera) are regulated solely by §361 of the Public Health Services Act (PHSA) regarding control of communicable diseases whereas "more than minimally manipulated" tissue-engineered products (i.e. preparations that involve either *ex vivo* expansion or genetic manipulations) must use either established Investigational New Drug (IND) or Investigational Device Exemption (IDE) mechanisms, and comply with both Good Tissue Practices (GTPs) and GMPs. Any cell product that contains *in vitro* expanded stem cells will, therefore, be considered as a "more than minimally manipulated" product and will require either IND or IDE clearance (170). Compliance with these regulations implies that the following excerpt from the regulations will be followed: experimental studies are primarily performed at a small-scale with cells cultured as monolayers and in open systems. This practice is not an optimal approach for obtaining the large quantities of cells generally needed for medical healthcare applications. Robust processes that protect both product and patient are necessary and require the use of clinical grade products, validated disposable devices, and development of high throughput closed-systems for obtaining safe and cost-effective products. In this respect, development of bioreactors, which allow automation and scale up in a GTP/GMP environment is most desirable [review see (183)]. Finally, since the risk/benefit ratio is never a life/death ratio in orthopaedics as in other medical specialties (e.g. cardiology), regulatory authorities will most probably emphasise biosafety and institute strict regulations for bioengineered bone.

In short, bioreactors provide a dynamic cultivation system within a controlled environment and enable the expansion of cells in 3D. Experiments in which cells are cultured in 2D, in which normal 3-dimensional relationships with the extracellular matrix and other cells are distorted, may not reflect the situation *in vivo*. Analysing cell interactions in more natural 3D settings, promises to provide a view that is closer to what actually happens in living organisms (181;191). In addition, the use of bioreactors for hESC culture has been documented and provided some preliminary evidence that dynamic, 3D conditions provide a suitable environment to culture ESCs (192). Currently no such procedure exists to take single cells or single cell suspensions of ESCs and culture them in dynamic, 3D conditions and induce osteogenesis in a simple integrated procedure. Moreover, the bone tissue engineering field is undergoing an evolutionary period whereby bioreactor designs are competing for prominence (36;37;193-195) but the most successful will not only be useful in the research laboratory but be suitable for clinical grade manufacture as well. The transition from laboratory- to industrial-scale will require a switch from highly flexible generic bioreactors to interchangeable, modular bioreactors, implementing defined bioprocesses in a standardised way.

1.4.3. Encapsulation

Alginate is a water-soluble linear polysaccharide extracted from brown seaweed and is composed of alternating blocks of 1-4 linked α-L-guluronic and β-D-mannuronic acid residues. Alginate forms gels with most di- and multivalent cations, although Ca^{2+} is most widely used. Calcium cations take part in the interchain binding between G-blocks and give rise to a 3-dimensional network in

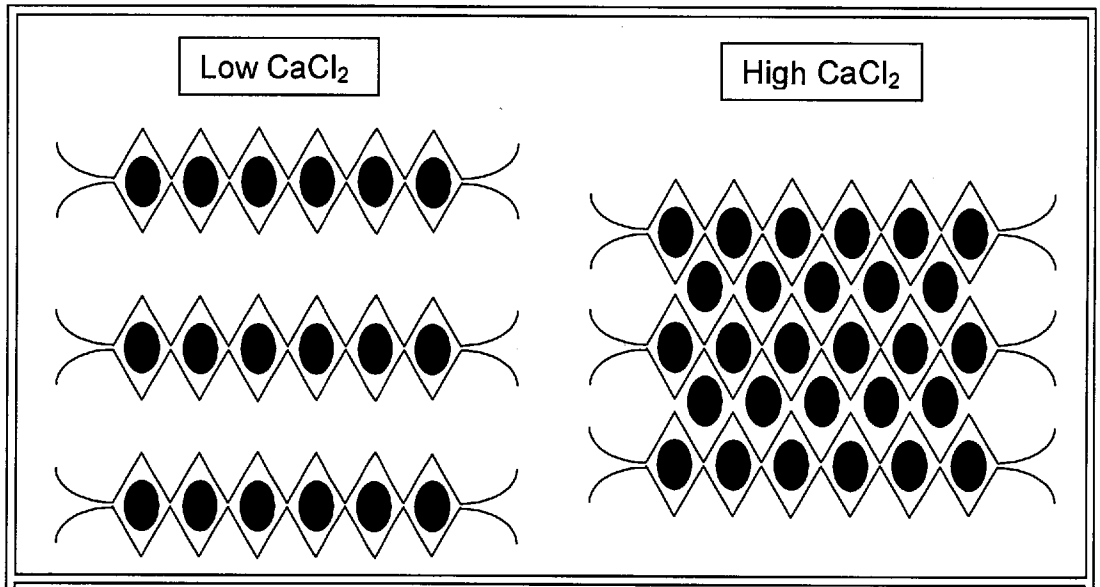


Figure 1.4. Schematic representation of the "egg-box" model in low and high $CaCl_2$ concentrations. The "egg-box" model is represented by solid blue ovals depicting calcium ions positioned between consecutive guluronic acid residues (red V-shaped structures), while consecutive mannuronic acid residues are depicted by the red curves at the end of the "egg-box" Adapted from (3).

the form of a hydrogel (Figure 1.4). The binding zone between the G-blocks is often described as the "egg-box model" (196). Alginates are widely used in industry such as food, pharmaceuticals and bioprocesses. As biomedical materials, purified alginates exhibit great biocompatibility (low undesirable immune response), significant mechanical resistance and functional

biodegradable properties. These characteristics make alginate a widely used choice for 3D cell culture (2). Implantation and the clinical use of alginate for tissue engineering has been explored with some adverse reactions in the early 1990's [review (197)] but recent examples have begun to provide more acceptable results (198-201).

Manipulating the strength of the alginate gel network can control the growth of encapsulated cells. Hydrogels with a weak gel network are advantageous in tissue engineered constructs or areas within a construct where cell growth and expansion are desired. Likewise, hydrogels with a strong gel network are recommended for constructs or parts of a construct where cell growth and expansion are not required (202-204).

Chang *et al.* (205) pioneered bioencapsulation in the 1960's and Lim *et al.* (40) eventually encapsulated xenograft islet cells for implantation into rats to correct diabetes. The use of alginate encapsulation has been mainly restricted to adult cells whereas Magyar *et al.* (41) encapsulated mESCs that were able to form "discoid" colonies, cystic EBs and smooth muscle cells upon release from the beads. Chondrogenic differentiation from MSCs encapsulated in alginate beads has been reported (206) and more recently alginate and gelatin have been considered to overcome the inert nature of alginate and increase bead integrity. Normally alginate hydrogels lose Ca^{2+} cations after prolonged culture but the incorporation of gelatin enables cell-mediated contraction and packing of the scaffold material (207). More recently, the use of alginate to enhance chondrogenesis from encapsulated EBs derived from mESCs has been attempted but yielded limited chondrogenic differentiation (208).

Alginate bead formation and the chemical interactions upon alginate encapsulation has been clearly described in detail by Bienaime *et al.* (2). First,

there is the formation of a superficial crust, acting as a spherical belt, progressively tightening the gel bead (this structure is a continuous, increasing obstacle to the diffusion of calcium within the forming gel bead). Second, there is a reduction of the gel bead volume, resulting from the reaction-diffusion process (alginate macromolecules and calcium cross-linking) with the tightening of the superficial crust with water expulsion (syneresis). Third, alginate molecules that have not yet reacted with calcium move progressively from the bead centre to the moving boundary of the reaction front, attracted by the accumulation of calcium ions at this interface. Fourth, all these phenomena produce a cascade of reaction-diffusion processes provoking the formation of micro fractures, shafts, shaft clusters and cavities. Surprisingly, bead production is highly reproducible when the same conditions and reagent concentrations are used.

In brief, the interactions between the alginate matrix and embedded cells plays a major role in their morphological and physiological behaviour. Despite the complexity of the gelation process and the apparent stochastic nature of this phenomenon, gel beads used to immobilise or encapsulate cells are well-structured macromolecular constructions (Figure 1.5). This architecture provides orientated and regular geometric structures throughout the gel network. Consequently, characteristics such as bead cohesion, bead porosity and gel density are closely linked to the gel molecular structures. The arrangements of polysaccharide blocks are very different between the peripheral layers and the bead centre. The distribution of calcium inside the gel bead is also quite heterogeneous (2).

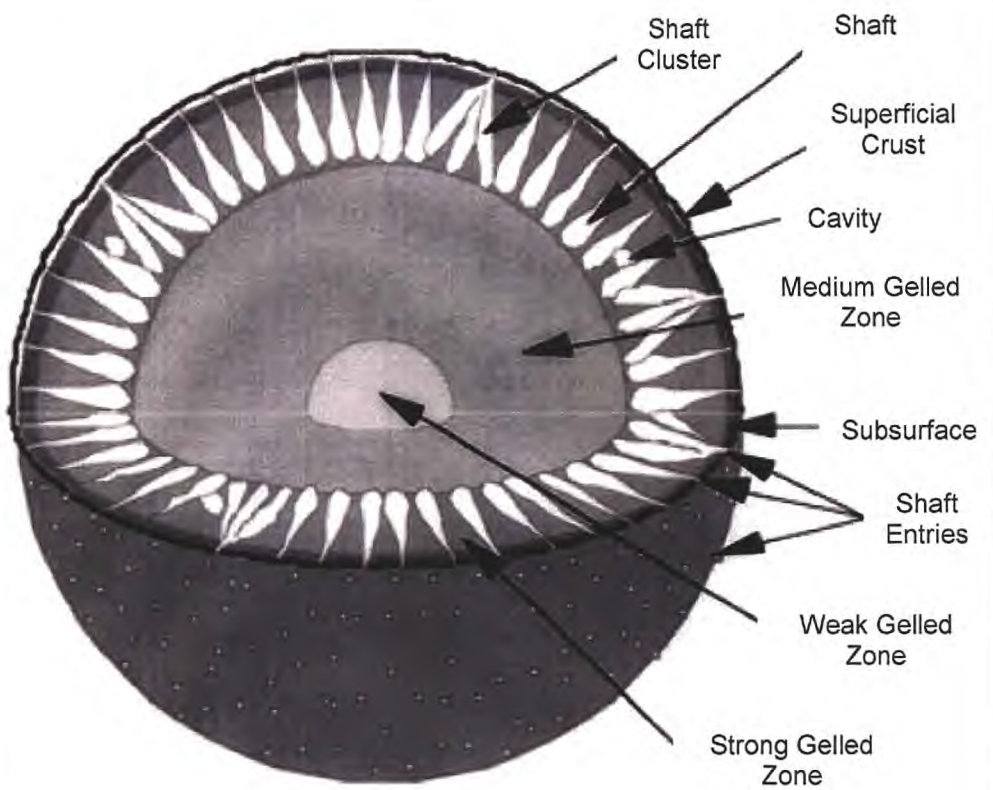


Figure 1.5. Schematic representation of the different gel network structures of a Ca-alginate gel bed. Copyright permission received from Global rights department, John Wiley & Sons, Inc. and adapted from (2).

1.5. Crticial interpretation of the literature and goal formulation There are three seminal publications that influence the thoughts behind this thesis. The first idealised that the credo of the next generation of tissue engineers would be '*secundum naturam*' (according to nature) not '*contra naturam*' (against nature) (209). This in my view is essential in order to produce clinical products that are suitable for implantation and short, medium and long-term repair and regeneration. The *secundum naturam* credo led me to developmental biology and the thought that *in vitro* differentiated ESCs need to be phenotypically and genotypically similar or identical to those formed via *in vivo* developmental pathways and also be capable of functionality in order to be clinically suitable. After reading Joseph Loebels seminal review on mESC differentiation (210) and through discussions with Jonathon Slack regarding *Xenopus* blastomeres and their homology to mouse development it was logical to follow an established *in vivo* development pathway. This initial thinking resulted in a credo that remained throughout the course of this thesis and begun with defined media development.

My goal was to take tissue engineering to another dimension, similar to organ printing, but something more accessible in the short to medium-term. A short review in *Nature* (181) solidified my thoughts that *in vitro* models and crucially tissue engineering should take on the challenge of re-creating the form and architecture of tissues that naturally develop within the human body. The initial challenge was to create a 3D micro-environment suitable for ESCs to grow in an undifferentiated state similar to that *in vivo;* namely the womb. It was clear that 3D tissue needs an adequate supply of nutrients and gaseous exchange in order to survive. Providing a protective vehicle for the cells to proliferate and a dynamic environment instead of relying on metabolite diffusion

were considered to be fundamental characteristics that should be incorporated within the 3D culture system.

Finally, the traditional nature of ESC culture lends itself to being time-consuming, laborious, subjective and fragmented. Inter and intra lab culture intracacies based on inherited protocols have resulted in a plethora of handling and differentiation techniques that deliver data but confuse a fragmented discipline. What was needed was a standardised, integrated protocol to culture ESCs in an undifferentiated state and also a simple, effective and robust means by which to differentiate into the tissue of interest. It was clear that the field had identified problems with EB formation (211) and the need for controlled 3D ESC culture (41) but had not combined them. The theory behind 3D tissue culture was that a platform technology such as alginate encapsulation could be utilised to provide a micro-environment for stable, robust culture of both undifferentiated ESCs and their derivatives without the need for extensive operator intervention throughout the entire culture process. It was conceived that an automated process with on-line sensors to monitor metabolite levels and tissue viability / integrity in real time would be the goal. For this to happen, tissue engineers need to consolidate the expertise from chemical engineering, developmental biology and materials science to provide tangible solutions to exisiting problems.

As stated in the first paragraph of this thesis, engineers, or more specifically tissue engineers should be brave in proportion. What I have tried to achieve in this thesis is to establish an effective solution by combining existing technologies in a novel manner that can be further optimised and perfected given more time and resources devoted to technology transfer.

1.6. Aims

The overall study goal was to investigate ESCs as a source of material for bone tissue repair using mESCs as a model.

Goal	Aims and Objectives
1. DEFINED MEDIA	• To formulate novel, defined serum-free media that allow cell viability, proliferation and transition throughout mESC maintenance, EB formation and osteogenic differentiation. • To define and optimise the components of serum-free media that maximises the efficiency of osteogenic differentiation from mESCs.
2. 3D CULTURE	• To form 3D tissue within characterised alginate beads suitable for scale-up and ultimately 3D bone formation. • The integration of traditional mESC culture through the encapsulation of undifferentiated mESCs and formation of 3D bone. • The production of clinically-relevant differentiated cells through culture in an integrated bioreactor culture system.

2. MATERIALS AND METHODS

2.1. Media

2.1.1. Serum-containing media

FCS was supplied by Invitrogen, UK and two similar batches were used throughout the thesis. Both were tested for mESC maintenance, EB formation and osteogenic differentiation (Batches 06G9130K & 3065946F).

2.1.1.1. Maintenance medium

Dulbecco's Modified Eagles Medium (DMEM; Invitrogen, UK) was supplemented with 10% (v/v) FCS, 100 iu/mL penicillin and 100 µg/mL streptomycin, 2 mM L-glutamine (all supplied by Invitrogen, UK), 0.1 mM 2-Mercaptoethanol (Sigma, UK) and 1000 U/mL Esgro™ LIF (Chemicon, UK) (143;212).

2.1.1.2. Differentiation or EB formation medium

Alpha-Modified Eagles Medium (αMEM; Invitrogen, UK), 10% (v/v) FCS, 100 units/mL penicillin and 100 µg/mL streptomycin (Invitrogen, UK).

2.1.1.3. Osteogenic medium

Differentiation medium was supplemented with 50 µg/mL L-ascorbate-2-phosphate, 10 mM β-glycerophosphate and 1 µM dexamethasone (All Sigma, UK).

2.1.2. Serum-free media

2.1.2.1. Lennon's medium

A serum-free maintenance medium developed by Lennon *et al.* (1995), initially to support the growth of rat marrow-derived MSCs and subsequently employed for ESC culture. 60% (v/v) DMEM-Low Glucose (LG) (Invitrogen, UK), 40% (v/v) MCDB-201 (Sigma, UK), 1.25 µL Phenol Red 1000X (Sigma, UK) per mL, 5 µg/mL bovine Insulin (Sigma, UK), 0.1% (v/v) linoleic acid-bovine serum albumin (LA-BSA) (Sigma, UK), 10 ng/mL human PDGF-ββ (Roche, UK), 1 ng/mL bFGF (Roche, UK) and 0.1% (v/v) or 10 iu/mL penicillin and 10 µg/mL streptomycin (Invitrogen, UK) (176).

2.1.2.2. Maintenance medium

DMEM high glucose / no sodium pyruvate (Invitrogen, UK) was supplemented with 12.5% (v/v) knock out serum replacement, 100 iu/mL penicillin and 100 µg/mL streptomycin, 2 mM L-glutamine (all supplied by Invitrogen, UK), 0.1 mM 2-Mercaptoethanol (Sigma, UK) and 1000 U/mL LIF (Chemicon, UK). This medium was previously used to culture mESCs upon a feeder layer (100-102) but not in a feeder-free system therefore proliferation rates and phenotyping were performed (Section 3.41&2). [Adapted from (143;212)].

2.1.2.3. Wiles' EB formation medium

Iscoves Modified DMEM & Nut Mix F-12 (HAM) 1:1 ratio (Invitrogen, UK) was supplemented with 0.1% (w/v) PVA (Sigma, UK), 1% (v/v) chemically defined synthetic lipids (Invitrogen, UK), 1 U/mL Esgro™ (LIF) (Chemicon, UK), 450 µM 1-monothioglycerol (Sigma, UK), 7 µg/mL bovine insulin (Sigma, UK), 150

µg/mL human apo-transferrin (Sigma, UK), sterile filter unit 0.2 µm (Nalgene, UK) and optional 2 ng/mL recombinant human BMP4 (Sigma, UK) (88;89).

2.1.2.4. LWR1.3 osteogenic medium (Lennon, Wiles, Randle1.3)

A "complete" medium that would enable mESC survival and proliferation after EB formation was developed. It consisted of 50% (v/v) DMEM-LG (Invitrogen, UK), 33% (v/v) MCDB-201 (Sigma, M6770), 1.25 µL Phenol Red (Sigma, UK) per mL, 0.1% (w/v) PVA (Sigma, UK), 15% (v/v) knock out serum replacement (KOSR; Invitrogen, UK), 2 mM L-glutamate, 1% (v/v) non essential amino acids (NEAA) (Invitrogen, UK), 1% (v/v) chemically defined synthetic lipids (Invitrogen, UK), 10 iu/mL penicillin and 10 µg/mL Streptomycin (Invitrogen, UK), 450 µM 1-monothioglycerol (Sigma, UK), 6 µg/mL bovine insulin (Sigma, UK), 10 ng/mL hPDGF-ββ (Roche, UK), 1 ng/mL bFGF (Roche, UK), 150 µg/mL human apo-transferrin (Sigma, UK) and NYL sterile filter unit 0.2 µm (Nalgene, UK).

2.2. Cell culture

2.2.1. 2D mESC maintenance and expansion

The E14Tg2a mESC line was routinely passaged on 0.1% gelatin (Sigma, UK) coated tissue culture plastic in a humidified incubator set at 37 °C and 5% CO_2. Undifferentiated mESCs (<p20) were passaged every 2 or 3 days and fed every day with fresh serum-containing maintenance medium. To detach the mESCs from the flasks, trypsin-ethylenediaminetetraacetic acid (TE; Invitrogen, UK) was administered to the mESCs for 3-5 minutes at 37 °C, after medium aspiration and a single wash with prewarmed phosphate buffered saline (PBS; Invitrogen, UK).

2.2.2. 2D EB formation

Embryoid body formation involved careful preparation of mESCs prior to suspension culture and is well documented (88;89;146;147;152;213). Nonetheless, empirical determination of the correct conditions before suspension was established with the E14Tg2a cell line. Briefly, cells in monolayer culture should be around 80% confluent, be either day 2 or 3 of culture and have a very high morphological, undifferentiated to differentiated ratio. MESCs were trypsinised as normal but clumps of 100-200 cells were used after 2-3 minutes instead of 5 minutes trypsinisation. The cells were then centrifuged at 300g for 3 minutes at room temperature (21°C). A confluent T75 flask after 2 or 3 days of growth in maintenance medium typically yielded around 5-7 x 10^6 cells which were resuspended in 30 mL of EB formation medium (serum-free or serum-containing) and distributed evenly between two 90 mm diameter bacteriological grade Petri dishes (Bibby Sterilin, UK). Clumps of 10-20 cells are essential for correct EB formation, as single cell suspensions or large clumps of thousands of cells will result in erroneous 3D aggregation. On day three of EB formation there was a medium change and on day 5 of culture the EBs were harvested by aspiration from the bacteriological plates and centrifuged at 66g for 4 minutes. The medium was aspirated and replaced with prewarmed PBS to wash away traces of serum. The cells were centrifuged again at 66g for four 4 minutes and the PBS was aspirated. After PBS washing, 1 mL of TE was added to the EBs, for 3-5 minutes at 37 °C. 1mL of prewarmed differentiation medium was then added to halt trypsinisation and the cells were resuspended in osteogenic differentiation medium as a single cell suspension to induce bone nodule formation.

2.2.3. 2D bone nodule assay

Standard bone nodule forming assays were performed using osteogenic differentiation medium from day 8 to day 29. Disaggregated EBs were cultured for 21 days at 37 °C with medium changes every 2 or 3 days on tissue culture plastic or glass slides. The plating density was 5.2 x 10^3 cells per cm^2 with 1 µL of medium for every 25 cells.

2.2.4. 3D Encapsulation

Undifferentiated, day 3, mESCs were trypsinised, counted, and resuspended at 1.6 x 10^6 cells / mL in 0.2µm sterile filtered, at room temperature (21°C), 1.1% (w/v) low viscosity alginic acid (This particular product is a straight-chain, hydrophilic, colloidal, polyuronic acid composed primarily of anhydro-β-D-mannuronic acid residues with 1→4 linkage; Sigma, UK) and 0.1% (v/v) porcine gelatin (Sigma, UK) (all dissolved in PBS, pH 7.4) solution. With a peristaltic pump (Model P-1, Amersham Biosciences, UK), a flow rate producing single droplets, a drop height of 30 mm (tubing autoclaved and then sterilised with 1M NaOH for 30 minutes and washed three times with sterile PBS) the cell-gel solution was passed through the peristaltic pump and dropped using a 25-gauge needle (Becton Dickinson, UK) into sterile, room temperature (21°C), 100 mM calcium chloride solution ($CaCl_2$; Sigma, UK) and 10 mM N-(2-hydroxyethyl) piperazine-N-(2-ethane sulfonic acid) (HEPES; Sigma, UK), in distilled water at pH 7.4. The cell-gel solution gelled immediately on contact with the $CaCl_2$ solution, forming spherical beads (2.3 mm diameter after swelling). The beads remained in gently stirred $CaCl_2$ solution for 6-10 minutes at room temperature (21°C). The beads were washed three times in PBS and placed into maintenance medium.

Undifferentiated mESCs encapsulated in alginate beads were cultured for 3 days in maintenance medium, as previously described in 50 mL, high aspect ratio vessel (Cellon, LUX) bioreactors with daily medium changes. Each reactor contained 600 beads and was rotated anticlockwise at 17.5 rpm from day 0-21 of culture and 20 rpm from day 22-29 of culture. To initiate differentiation, the maintenance medium was replaced in the HARV with EB differentiation medium on day 3 until day 8 of culture (replenished on day 6). On day 8 of culture, EB differentiation medium was replaced with osteogenic medium to induce bone nodule formation and changed every 2 or 3 days.

2.2.5. Bioreactor descriptions

2.2.5.1. Synthecon - High Aspect Ratio Vessel (HARV)

The high aspect ratio vessel (HARV) was developed in connection with the National Aeronautics and Space Administration (NASA) program to study tissue and cellular engineering in a low-shear, non-turbulent environment. It has a large radius-to-depth ratio (40 mm x 10 mm) providing a substantial surface area on the rear face for gas exchange through a gas-permeable membrane. The media volume is 50 mL and alginate beads, heavier than culture medium were used in this thesis, therefore culture was not under microgravity conditions. The culture vessel itself is a disposable, sterile, clear plastic circular unit with two sampling or injection Luer-lock ports and a half inch drain/fill port (Figure 2.1).

The vessels were "conditioned" overnight with serum containing media and this was then removed before cell culture. Input of media/beads was performed through the fill port and air bubble removal was undertaken through

the Leur valves. Bubble removal was performed daily. The HARV units were attached to a rotator base which sat in a humidified incubator and was controlled by an external electrical unit.

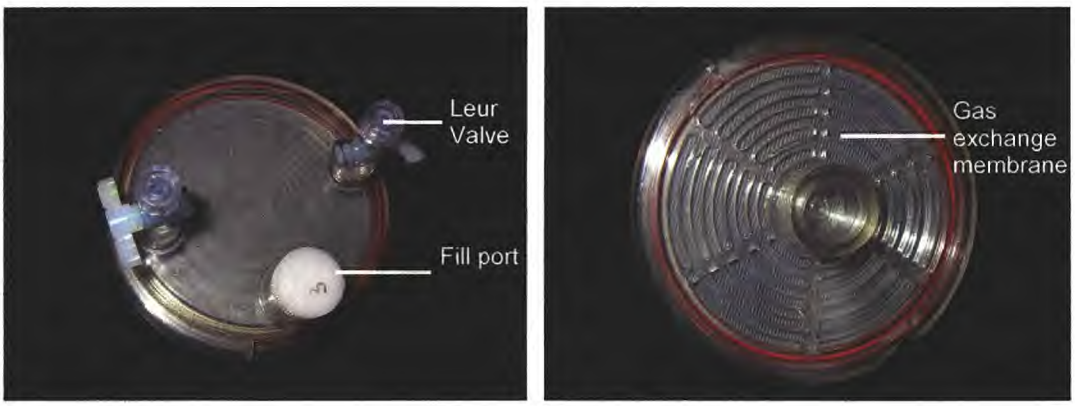


Figure 2.1. HARV bioreactor photographs. Front and rear views.

2.2.5.2. Synthecon – Perfusion reactor

The Rotating Cell Culture Max (RCMW™) continuously perfuses fresh nutrients and gas, and removes waste products while maintaining a low shear suspension environment. The large 500 ml media reservoir along with the 50 mL culture chamber provides extended culture time without the need for feeding. The media reservoir being outside the culture chamber essentially eliminates the need to remove the growth chamber from the incubator to replenish the medium. The key advantages of a perfused cell culture system include the ability for long-term un-interrupted cell culture, clear unobstructed viewing of the culture chamber environment and closed loop circulation of fluid, which reduces risk of contamination.

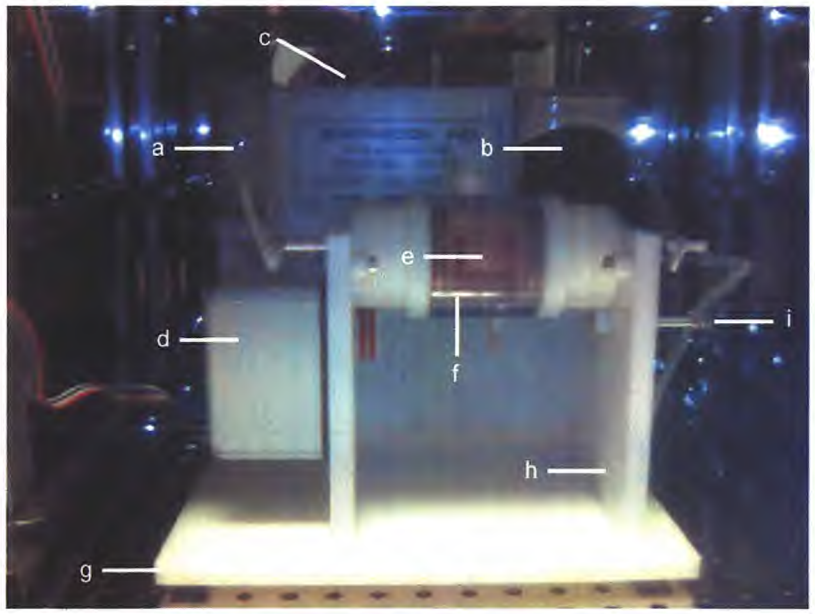


Figure 2.2. Perfusion bioreactor photograph. Front view. (a) Oxygenator. (b) Peristaltic pump. (c) Culture media reservoir. (d) Direct motor drive. (e) Perfusion Core. (f) Culture vessel. (g) Rotator Base/Assembly Support. (h) Upright roller cradle supports. (i) Silicone tubing standoff clips.

The perfusion bioreactor is composed of the following components (Figure 2.2).

(a) Oxygenator assembly - externally facilitates oxygenation/CO_2 exchange for cell and tissue cultures in the vessel

(b) Peristaltic pump - clockwise rotation provides the force to pump culture medium through the culture vessel. One rpm on the peristaltic pump is approximately equivalent to a flow rate through the circulation tubing of 0.5 ml/minute.

(c) Culture media reservoir - a 500 ml Pyrex glass bottle containing a long stainless steel media supply tube that extends to the bottom of the bottle, a short steel media return tube and a Whatman micro filter to vent the bottle.

(d) Direct motor drive – was used to rotate the culture vessel horizontally at 17.5 -21RPM. It is equipped with one extended service life stepper motor (no brushes or gear head).

(e) Perfusion Core - the plastic cylindrical core fits in the centre of the culture vessel. It is to be covered with a nitrocellulose dialysis membrane. Media flows through openings at either end of the core underneath the membrane. Media exchange with the cell compartment occurs through the pores of the dialysis membrane.

(f) Culture vessel - The 50 mL vessel is composed of two white polyacetyl endcaps. Affixed to the endcaps are white delrin luer fittings for attaching rotating fluid couplings. Assembled, the vessel is comprised of two white endcaps, a perfusion core, and a clear vessel wall. The vessel wall contains two sampling/injection Luer lock ports with rubber septums and drain/fill port with a Delrin plastic plug insert.

(g) Rotator Base/Assembly Support - serves to support and rotate the culture vessel. It is constructed of two rectangular white Delrin/Acetyl plastic plates (One horizontal and one vertical). Located on the vertical plate are the oxygenator assembly, peristaltic pump, and media bottle. The roller cradle assembly is attached to the horizontal base plate. It consists of two white Delrin uprights creating a roller cradle in which the vessel is naligned, supported and rotated.

(h) Upright roller cradle supports - vertical white Delrin plastic plates equipped with white Delrin direct-drive disk and roller support disk to maintain the culture vessel in proper alignment in the roller cradle assembly.

(i) Silicone tubing standoff clips - be sure tygon tubing is inserted through the clip and does not put strain on the rotating coupler. The rotating coupler must remain parallel with the central axis throughout system rotation.

The perfusion reactor was conditioned for 24 hours as per the HARV. The media was placed in the reservoir which was pumped by a peristaltic pump through the system. Firstly through the external oxygenation tubing and then through the core of the reactor (diffusion occurs into the main reactor chamber through a nitrocellulose membrane) and returns to the media reservoir for another cycle. Input of media/beads was performed through the fill port and air bubble removal was performed through the Leur septa. Media changes were performed by removal of the entire reactor into a laminar flow hood, PBS flushing and perfusion of fresh media before it was placed back into the humidified incubator.

2.2.6. Alginate bead dissolution

A sterile depolymerisation buffer was used to dissolve beads consisting of 50 mM tri-sodium citrate dihydrate (Fluka, UK), 77 mM sodium chloride (BDH Laboratory supplies, UK) and 10 mM HEPES (41). The dissolution buffer (Ca^{2+}-depletion) was added to PBS washed beads for 15-20 minutes while stirring gently. The solution was centrifuged at 400g for 10 minutes and the pellet was washed with PBS and centrifuged again, at 300g for 3 minutes.

2.2.7. Primary murine osteoblasts and MC-3T3-E1 culture

Positive control tissue was used as a benchmark to assess embryonic stem cell differentiation towards the osteogenic lineage. Primary osteoblasts obtained

from neonate mouse calvaria using sequential collagenase digestion (214) as well as MC-3T3-E1 (ATCC, USA) cells.

Primary osteoblasts (adherent cells) were maintained as monolayers in maintenance medium [in T75 flasks (Iwaki, UK). The cells were split once a week, or as required, to prevent full confluence, and the medium was changed every 2 or 3 days. Trypsinisation was similar to the mESC protocols with additional tapping of the tissue culture plates to detach firmly attached cells. Seeding densities differed with passage number. Briefly, 5 x 10^5, p3 cells seeded in a T75 flask (6.66 x 10^4 / cm^2) became confluent after 10 days and yielded around 1.2 x 10^6 cells. Low passage numbers typically proliferated faster than high passage cells (>p3) and also tended to lose their morphological phenotype. MC-3T3-E1 cells were cultured in an identical fashion but in osteogenic differentiation medium to induce mineralisation.

2.2.8. Cryopreservation

The standard cryopreservation method followed was to pellet 5 x 10^6, cells or a confluent T75 flask, resuspend them in 0.5 mL of FCS and then add 0.5 mL of 20% (v/v) dimethylsulfoxide (DMSO; Sigma, UK) and 80% (v/v) FCS solution to produce a final concentration of 10% (v/v) DMSO and 90% (v/v) FCS. The final solution of 1 mL was pipetted into a CryoTube™ (Nunclon, UK or Greiner, UK) and placed in a freezing container (Nalgene™, UK) filled with isopropyl alcohol (IPA) (BDH Laboratory supplies, UK) at -85 °C for 24 hours where a controlled drop in temperature of 1 °C per minute occurred. After 24 hours the cells were then transferred to liquid nitrogen for long-term storage.

2.3. Staining

2.3.1. Immunocytochemistry

2D cultured cells were washed once in PBS and fixed for 20 minutes at room temperature (21°C) in 4% (w/v) paraformaldehyde (PFA; BDH Laboratories, UK) whereas deparaffinised/hydrated 3D sections were pre-fixed for 30 minutes before embedding. Briefly, 2D slides or hydrated paraffin sections were treated with 0.2% (v/v) Triton-X-100 (BDH Laboratory Supplies) for 45 minutes at room temperature (21°C) and washed twice with PBS. The samples were then incubated with 3% (v/v) blocking goat or rabbit serum (Vector Laboratories) for 30 minutes at room temperature (21°C) in 0.05% (w/v) bovine serum albumin (BSA; Sigma), 0.01% (w/v) NaN_3 (Sigma) in PBS as primary diluent. The serum was removed and the samples were incubated with primary antibodies diluted in primary diluent at 4 °C overnight followed by two washes and incubation with secondary antibodies diluted in secondary diluent consisting of 0.05% (w/v) BSA in PBS for 1 hour at room temperature (21°C) in the dark. Subsequently, the samples were washed twice in PBS and mounted using Vectashield™ with 1.5 µg/mL 4',6 diamidino-2-phenylindole (DAPI) (Vector Laboratories). See table 2.1 for antibody dilutions.

Table 2.1. Antibody dilutions and blocking serums for immunostaining.

Antigen	Primary	Secondary	Blocking serum 1	Blocking serum 2
Oct-4	1:80 Rabbit polyclonal (Santa Cruz Biotech, Calne, UK)	1:80 goat anti-rabbit-FITC (Chemicon, Chandlers Ford, UK)	3% (v/v) Normal goat serum (Vector Laboratories, UK)	Not applicable
CD9	1:750 Rat monoclonal (Research Diagnostics, Concord, MA, USA)	1:80 goat anti-rat-rhodamine. (Chemicon)	3% (v/v) Normal goat serum (Vector Laboratories)	1.5% (v/v) Normal mouse serum (Serotec, Kidlington, UK)
Flk-1	1:200 Mouse monoclonal (Santa Cruz biotech)	1:80 Rabbit anti-mouse FITC (Dako, High Wycombe, UK)	3% (v/v) Normal rabbit serum (Vector Laboratories)	1.5% (v/v) Normal mouse serum (Serotec)
OB-Cadherin	1:50 Goat polyclonal (Santa Cruz Biotech)	1:100 Rabbit-anti goat FITC (Sigma)	3% (v/v) Normal rabbit serum (Vector Laboratories)	Not applicable
Osteocalcin	1:50 Goat polyclonal (Santa Cruz biotech)	1:100 Rabbit-anti goat FITC (Sigma)	3% (v/v) Normal rabbit serum (Vector Laboratories)	Not applicable
Type-I Collagen	1:50 Rabbit Polyclonal (Santa Cruz biotech)	1:100 Goat anti-rabbit-FITC (Chemicon)	3% (v/v) Normal goat serum (Vector Laboratories)	Not applicable

2.3.2. Histochemistry

2.3.2.1. Paraffin embedding beads

The alginate beads were fixed with 4% (w/v) PFA for 30 minutes at room temperature and then placed in PBS for 15 minutes prior to dehydration. The beads were taken through a sequential series of increasing ethanol concentrations to remove all the water. The ethanol was then completely replaced with neat xylene followed by incubation with paraffin saturated xylene at room temperature (21°C) overnight. The beads in paraffin saturated xylene were then placed in an oven (60 °C) for 20 minutes. The xylene was then completely replaced with liquid paraffin. The beads were then serially sectioned (4 µm) and left at room temperature (21°C) overnight to adhere to Vectabonded™ (Vector Laboratories, UK) glass slides. For Alizarin Red S, von Kossa and Haematoxylin and Eosin (H&E) staining the paraffin was removed from the sections by immersion in xylene, decreasing ethanol concentrations and then tap water. For immunocytochemistry, the sections were autoclaved while immersed in a 10 mM, pH 6.0 tri-sodium citrate, dihydrate buffer (Fluka, UK) and allowed to cool and dry in order to retrieve the antigens.

2.3.2.2. Haematoxylin & Eosin staining

2D cells were cultured on glass Flaskette slides (Nalgene, UK) and dipped in haematoxylin (Harris' solution; BDH Laboratory Supplies, UK) for 30 seconds following fixation. The slides were washed in running tap water for 2-3 minutes and examined for sufficient staining. Excess stain was removed by decolourising in 0.5-1% HCl in 70% ethanol for a few seconds and then washed in tap water for 5 minutes. The slides were finally dipped in 1% eosin (BDH Laboratory Supplies, UK) for 2 minutes and washed briefly in tap water. The

tissue was dehydrated by dipping in ethanol (70% (v/v) once and anhydrous or 100% twice), cleared in xylene and mounted in 1,3-diethyl-8-phenylxanthine mountant (DPX; BDH Laboratories, UK).

2.3.2.3. Alizarin Red S / von Kossa staining

Paraffin sections were deparaffinised and hydrated in a descending series of ethanols. The sections were immersed in a 2% (w/v) Alizarin Red S (ARS), (Sigma, UK) solution (pH4.2) for 5 minutes at room temperature (21°C), dipped in acetone 20 times and then in 1:1 acetone/xylene for 20 times, followed by clearing in xylene and mounting with DPX solution. Alternatively, the deparaffinised/hydrated sections were immersed in 5% (w/v) silver nitrate solution (BDH Laboratories, UK) and illuminated with a 60W lamp for 1 hour at room temperature (21°C). Rinsed 3 times in distilled water and immersed in 5% (w/v) hypo [(sodium thiosulfate), BDH Laboratories, UK] for 5 minutes. Washed in tap water, rinsed once in distilled water and immersed in nuclear fast red (Vector Laboratories, UK) for 5 minutes at room temperature (21°C). Dehydrated, cleared in xylene and mounted in DPX.

2.4. Biochemical assays

2.4.1. Live/dead assay

Membrane-permeant 3',6'-Di(O-acetyl)-2',7'-bis[N,N-bis(carboxymethyl) aminomethyl] fluorescein, tetraacetoxymethyl ester (calcein AM) is cleaved by esterases in live cells to yield cytoplasmic green fluorescence whereas membrane-impermeant ethidium homodimer-1 (EthD-1) labels nucleic acids of membrane-compromised cells with red fluorescence. A 4 μM EthD-1 and 2 μM calcein AM solution (Molecular Probes, UK) diluted in PBS was added to PBS

washed, live cells or alginate beads and incubated at room temperature (21°C) for 30 minutes, in the dark. A negative control was conducted using 100% (v/v) ethanol for 5 minutes in place of PBS. After incubation, the solution was aspirated and a small amount of PBS was added to the cells to prevent dehydration. The cells were then photographed, within 30 minutes using a Bio-Rad MRC600 confocal microscope (Bio-Rad, UK) to visualise the proportion of live and dead cells.

2.4.2. MTS assay

The CellTiter 96® AQueous One Solution Reagent MTS assay (Promega, UK) contains a novel tetrazolium compound [3-(4,5-dimethylthiazol-2-yl)-5-(3-carboxymethoxyphenyl)-2-(4-sulfophenyl)-2H-tetrazolium, inner salt; MTS] and an electron coupling reagent phenazine ethosulfate (PES). The MTS assay was used in order to assess the metabolic activity of an average bead throughout the culture period. Standard curves (Appendix 9.12&3) were produced using known numbers of cells in 2D and in 3D and related to absorbance measured at 450nm (MRX II plate reader; Dynex technologies, UK). Blanks (no cells or beads) were used in order to standardise the absorbance values at each time point.

2D cells were assayed in a 24 well plate and washed once with maintenance medium without phenol red (Invitrogen, UK) for 15 minutes at 37 °C. The medium was then replaced with 200 µL of phenol red free maintenance medium and 40 µL of MTS reagent followed by Incubation for 2 hours and halted with 50 µL of 10% (v/v) sodium dodecyl sulphate (SDS; Sigma, UK). Similarly, three beads were selected at random from different reactors at each time point and placed into separate 24 well plate wells. The culture medium

was replaced with phenol red free maintenance medium for 15 minutes at 37 °C, followed by an incubation step with 300 µL of phenol red free maintenance medium and 60 µL of MTS reagent for 4 hours at 37 °C. 100 µL of each well was then placed into a separate 96 well plate and read at 450 nm.

2.4.3. DNA quantification

Total DNA content of proteinase-K digested samples was measured using the DNA-specific dye, Hoechst 33258 (bis-benzimidazole; Sigma, UK). DNA content was used as an indirect method of evaluating the increase in cell number. Alginate beads were dissolved in depolymerisation buffer (41) for 20 minutes at room temperature (21°C) with gentle agitation. The solution was centrifuged at 400g for 10 minutes and the pellet was washed with PBS and centrifuged at 300g for 3 minutes. Cell pellets were snap frozen in liquid nitrogen and stored at -80 °C. Pellets were vortexed and digested overnight at 37 °C in 50 µg/mL proteinase-K (Sigma, UK) dissolved in 100 mM, dibasic potassium phosphate (K_2HPO_4; Sigma, UK). Proteinase-K was inactivated by heating the solutions to 90 °C for 10 minutes. The samples were then centrifuged at 12,000g for 10 minutes. 100 µL of the sample supernatant was placed in a DNA/RNA free eppendorf tube along with 100µL of Hoescht 33258 solution (2 µg/mL) and vortexed for 2-3 minutes. An aliquot (100 µL) of the solution was then read using a microtiter plate fluorometer (Dynex MFX, Finland) with the excitation wavelength being at 365 nm and the emission wavelength at 460 nm. A calibration curve (Appendix 9.14) was generated using highly polymerised calf-thymus DNA (Sigma, UK) and the amount of total DNA produced from routinely cultured mESCs was enumerated in order to

calculate the number of cells per sample based on DNA content. Samples were in duplicate on three separate occasions on day 0 and day 29.

2.4.4. Alizarin Red S (ARS) quantification

ARS quantification for 2D cells was performed as documented in Gregory *et al.* (215). A slight adaptation was used for the 3D beads in order to harvest the cells/tissue. Briefly, 100 beads were isolated, counted and washed in PBS and fixed with 10% (v/v) formaldehyde (BDH Laboratories, UK) for 30 minutes followed by washing twice in distilled water. The beads were then dissolved in depolymerisation buffer (41) for 20 minutes at room temperature (21°C) with gentle agitation. The solution was centrifuged at 400g for 10 minutes and the pellet was washed with distilled water and centrifuged at 300g for 3 minutes. The resulting pellet was then stained in an identical fashion to the 2D cultures.

2.4.5. Alkaline Phosphatase (ALPase) activity

Alkaline phosphatase activity was measured using ρ-nitrophenol phosphate (pNPP, Sigma, UK) as a substrate. Cellular ALPase was determined colorimetrically using pNPP according to the reaction. The assay was performed in the same format as the MTS assay in 2D and 3D using 24 well plates and 3 beads selected at random, in duplicate (n = 6). After washing, the cells/beads were placed in phenol red free maintenance medium for 15 minutes and incubated in 150 µL of ALPase buffer (Sigma, UK) and 150 µL of ρ-nitrophenol phosphate solution at 37 °C for 30 minutes in the dark. 100 µL of 0.5N sodium hydroxide (NaOH; BDH Laboratories, UK) solution was added to each well to stop the reaction and then 100 µL of the final solution was placed into a 96 well plate well and read at 410 nm (MRX II plate reader; Dynex technologies, UK). The amount of ALPase activity could then be calculated by

subtracting the control readings (no cells) from the samples and relating to a pre-determined standard curve. ALPase activity was then expressed as nPP µM / bead or well / minute.

2.5. Imaging

2.5.1. Light microscopy

Images were captured from a IX70 inverted microscope (Olympus, Southall, UK) equipped with a colour CoolPix 950 digital camera (Nikon, Kingston-upon-Thames, UK) or black and white F-View II, high resolution charge coupled device (CCD)-Camera (Soft Imaging Systems GmbH, Germany) or a BX60 upright (Olympus) microscope equipped with an axiocam (Zeiss).

2.5.2. Micro-Computed Tomography (micro-CT)

Micro-CT analysis was performed in order to reconstruct the mineralised bone formed within the alginate beads using a phoenix|x-ray v|tome|x computed tomography machine (Phoenix x-ray 3D Imaging System, UK), set at 70 kV, 160 µA and calibrated accordingly. Images were taken using one detector and rotated through 360°, each section being 6.75 µm apart. 3D reconstructions were generated using the Sixtos software, originally developed by Siemens, Germany. A negative control of alginate beads lacking encapsulated cells and a positive control using a Balb/c mouse bone chip were performed.

2.5.3. Confocal microscopy

Cells or EBs were imaged using a Bio-Rad MRC600 confocal microscope (Bio-Rad, UK) and processed using COMOS software (Bio-Rad, UK).

2.6. Flow cytometric analysis

The Becton Dickinson FACSCalibre was used for flow cytometric analysis using a Macintosh platform (CellQuest™ acquisition software) and Windows Multiple Document Interface (WINMDI, Freeware, Joe Trotter) software for post acquisition analysis.

The flow cytometric analysis in this study used three colours to identify surface antigens and assess cell viability simultaneously. The surface antigens of interest were CD9 (undifferentiated mESCs), platelet-derived growth factor receptor α (PDGFRα) and Flk-1 as mesodermal markers. CD9 was analysed along with viability (2 colour analysis) using undifferentiated mESCs and the two mesodermal markers were analysed along with viability (3 colour analysis) on day 5 EBs.

The FACSCalibre flow cytometer was equipped with a doublet discrimination module (DDM), where Fluorescence channel 1 (FL) was used for Fluorescein Isothiocyanate (FITC); FL2 for Phycoerythrin (PE); and FL3-H, FL3-A, and FL3-W for 7-amino-actinomycin-D (7-AAD). The appropriate emission filters were factory-installed. Data were collected using linear amplification for forward scatter (FSC) and side scatter (SSC), logarithmic (4-decade) amplification for FL1 and FL2, and linear amplification for FL3.

2.6.1. Negative controls

A negative control sample can be achieved by omitting the primary antibody to check for background fluorescence of the secondary antibody if used, as in indirect-2 layered fluorescent labelling. The positive sample can then be accurately interpreted with these data. The negative controls were used to position the markers on the fluorescence histograms to allow identification of

the exact position of the negative populations and to estimate the amount of non-specific binding of the monoclonal antibodies to cell surface antigens.

2.6.2. Calibration and suitable controls

Calibrite™3 beads (Becton Dickinson, UK) were used prior to analysis and are suitable for FITC/PE/ Peridinin-chlorophyll-protein complex (PerCP) and 7-AAD calibration. The calibration procedure adjusted the instrument settings, set the fluorescence compensation and checked the instrument sensitivity before analysis. Background auto-fluorescence occurs naturally in cells and can be accounted for by running a sample of cells without any staining and drawing a dot plot of FSC vs SSC (size vs granularity). A region termed R1 was drawn around the cell population of interest based upon size and granularity (gated). ESCs will typically have high granularity but vary in size. Compensation was required to counter spectral overlap in multicolour analysis. Cell control samples were stained separately in multi-colour analysis. The cells were analysed (acquired) and the two detectors for the unstained channels were electronically adjusted to be identical to that of an unstained sample.

2.6.3. Two colour pluripotency analysis

0.1% (v/v) BSA (Sigma, UK) in PBS was used for antibody dilution and washing steps and was kept at 4 °C throughout the staining procedure.

2.6.3.1. CD9 & 7-amino-actinomycin-D (7-AAD)

Antigen	Primary	Secondary	Blocking serum 1	Blocking serum 2
CD9 KMC8 clone	Rat anti mouse to (Research Diagnostics, USA)	Rabbit anti-rat FITC (Serotec, UK)	Normal rabbit serum (Vector Laboratories, UK)	Normal mouse serum (Chemicon, UK)

5×10^5 undifferentiated mESCs (>90% viable) were centrifuged at 300g for 3 minutes, resuspended in 100 µL of 3% (v/v) rabbit serum and incubated for 30 minutes at room temperature (21°C) to prevent non-specific binding. Subsequently, 1 mL of cold PBS was added to the cells which were centrifuged at 300g for 3 minutes at 4 °C followed by incubation with 0.5 µg of primary antibody (CD9) in 100 µL of diluent for 30 minutes at room temperature (21°C). The cells were washed with 1mL of cold PBS and centrifuged at 300g for 3 minutes at 4 °C. The secondary antibody was diluted according to the manufacturer's instructions in 100 µL with 1.5% (v/v) mouse serum. The cells were resuspended in this solution, vortexed gently for 10 seconds and left at 4 °C for 30 minutes in the dark. Subsequently, the cells were washed with 1 mL of cold PBS and centrifuged at 300g for 3 minutes at 4 °C. Finally, 2.5 µL of concentrated 7-AAD in 100 µL of cold PBS were added to the cells, which were incubated for 10 minutes in the dark. 100 µL of cold PBS wash was added to each tube and mixed thoroughly to ensure a single cell suspension just prior to analysis. The cells were kept at 4 °C and analysed 30-60 minutes after 7-AAD staining.

2.6.4. Two colour mesoderm analysis

Antigen	Primary	Secondary	Blocking serum 1	Blocking serum 2
PDGF Rα	Rat anti mouse (rat monoclonal) (Pharmingen, UK)	Rabbit anti rat FITC (Serotec, UK)	Normal rabbit serum (Vector Laboratories, UK)	Normal mouse serum (Chemicon, UK)
Flk-1	Mouse anti mouse (mouse monoclonal) (Santa Cruz Biotech, UK)	Goat anti rat RPE (Serotec, UK)	Normal goat serum (Vector Laboratories, UK)	Normal mouse serum (Chemicon, UK)

5×10^5 undifferentiated mESCs (>90% viable) were centrifuged at 300g for 3 minutes, resuspended in 100 µL of 3% (v/v) rabbit serum and incubated for 30 minutes at room temperature (21°C) to prevent non-specific binding. Subsequently, 1 mL of cold PBS was added to the cells which were centrifuged at 300g for 3 minutes at 4 °C followed by incubation with 0.5 µg of primary antibody (PDGFRα) in 100 µL of diluent for 30 minutes at room temperature (21°C). The cells were washed with 1mL of cold PBS and centrifuged at 300g for 3 minutes at 4 °C. The FITC secondary antibody was diluted according to the manufacturer's instructions in 100 µL with 1.5% (v/v) mouse serum. The cells were resuspended in this solution, vortexed gently for 10 seconds and left at 4 °C for 30 minutes in the dark. Subsequently, the cells were washed with 1 mL of cold PBS and centrifuged at 300g for 3 minutes at 4 °C. The same procedure was repeated for Flk-1 but goat serum was used instead. Finally, 2.5 µL of concentrated 7-AAD in 100 µL of cold PBS were added to the cells, which were incubated for 10 minutes in the dark. 100 µL of cold PBS wash was added to each tube and mixed thoroughly to ensure a single cell suspension just prior to analysis. The cells were kept at 4 °C and analysed 30-60 minutes after 7-AAD staining.

2.7. Reverse Transcription-PCR

2.7.1. Primer design

GeneTool Lite 1.0 (Advanced Bioinformatic Solutions, USA) was used to view and verify published primers (Table 2.2).

Table 2.2. RT-PCR primer table and conditions.

RT-PCR primers / conditions				
Gene	**FWD 5'-3'**	**RVS 5'-3'**	**Length (bp)**	**PCR conditions**
Gapdh	CATCACCATCTT CCAGGAGC	ATGCCAGTGAGCT TCCCGTC	474	10 min 94 °C, 35 cycles: 94 °C 30s, 60 °C 40s, 72 °C 60s & 10 min 72 °C
Cbfa-1	CAGTTCCCAAGC ATTTCATCC	TCAATATGGTCGC CAAACAG	444	10 min 94 °C, 36 cycles: 94 °C 60s, 45 °C 60s, 72 °C 60s & 10 min 72 °C
Collagen I	GAACGGTCCAC GATTGCATG	GGCATGTTGCTAG GCACGAAG	167	10 min 94 °C, 30 cycles: 94 °C 60s, 60 °C 60s, 72 °C 60s & 7 min 72 °C
Collagen II	CTGCTCATCGCC GCGGTCCTA	AGGGGTACCAGGT TCTCCATC	432 (Splice A, early development) 225 (Splice B, mature cartilage)	10 min 94 °C, 30 cycles: 94 °C 60s, 60 °C 60s, 72 °C 60s & 7 min 72 °C
Osteocalcin (OCN)	CGGCCCTGAGT CTGACAAA	ACCTTATTGCCCTC CTGCTT	193	10 min 94 °C, 30 cycles: 94 °C 60s, 60 °C 60s, 72 °C 60s & 7 min 72 °C
Oct-4	TGGAGACTTTGC AGCCTGAG	TGAATGCATGGGA GAGCCCA	800	10 min 94 °C, 30 cycles: 94 °C 60s, 55 °C 60s, 72 °C 60s & 7 min 72 °C
Bt	CTGGGAGCTCA GTTCTTTCG	TCACATAGATGGG GGTGACA	200	10 min 94 °C, 33 cycles: 94 °C 60s, 60 °C 60s, 72 °C 60s & 7 min 72 °C
Flk-1	CCTACCCCACAC ATTACATGG	TTTTCCTGGGCAC CTTCTATT	321	10 min 94 °C, 33 cycles: 94 °C 60s, 60 °C 60s, 72 °C 60s & 7 min 72 °C

2.7.2. RNA isolation

Pelleted cells were thawed from -80 °C, placed on ice and resuspended in Buffer RLT (guanidinium isothiocyanate; Qiagen, UK) and total RNA was isolated using the RNeasy Mini Kit (Qiagen, UK) according to the manufacturer's instructions. Following the lysis, homogenisation and washing steps, RNA was eluted from the silica-gel-based membranes in 30 µl of RNase-free water and the concentration and purity at 260/280 nm were determined using a spectrophotometer (Eppendorf BioPhotometer, Germany). Samples were stored at –80 °C until further use.

2.7.3. Reverse transcription

RNA was reversed transcribed into complementary DNA (cDNA) using the Reverse Transcription System (Promega, UK) according to the manufacturer's recommendations. Briefly, cDNA was prepared from 1 µg of RNA in the presence of 5 mM $MgCl_2$, 1 mM of dNTP mixture, 1 unit/µl recombinant RNasin ribonuclease inhibitor, 15 units/µl AMV reverse transcriptase and 0.5 µg/µl random primers in a total volume of 20 µl per reaction. Diluted RNA samples were heated at 70 °C for 10 minutes, briefly centrifuged and cooled on ice for 5 minutes. The mastermix+RNA was incubated at 22 °C for 10min, reverse transcription was performed at 42 °C for 40 minutes, followed by denaturation at 99 °C for 5 minutes and a cooling step at 4 °C for 5 minutes. Samples of cDNA were diluted 5-fold to a final volume of 100 µl and stored at -20 °C until further use.

2.7.4. PCR amplification

10 µl of the diluted cDNA samples were used for PCR amplification in 20 µl reactions. The cDNA samples were amplified in a thermocycler (Eppendorf Mastercycler, Germany) in the presence of 2 mM $MgCl_2$, 1X Gold buffer, 200 µM dNTPs, 1.25 U per reaction Amplitaq Gold Taq polymerase (all Applied Biosystems, UK), and 0.5 µM of each of 'forward' and 'reverse' primers (Invitrogen custom primers, UK). The number of amplification cycles used was optimised to ensure that product concentration was within the exponential part of the amplification reaction.

2.7.5. Agarose gel electrophoresis

Aliquots of 9.6 µl of amplified cDNA were mixed with 2.4 µl of 6x loading buffer and electrophoresed on a 1.5% (w/v) agarose gel (Made up with 10X TAE buffer from Sigma, UK; 0.4 M Tris acetate, 10 mM EDTA, pH 8.3), containing 0.001 µg/mL ethidium bromide, at 10 V/cm. When exposed to UV illumination, the gel showed a single band when the mRNA was expressed. Images of the gel were captured digitally using a BioRad Fluor-S multi-imager (BioRad/Zeiss, UK).

2.8. Media analysis

Media samples of 1.5 mL were taken at specific intervals (as specified in individual chapters) during the duration of cultures. Na^+, K^+, Ca^{2+}, NH_4^+, glucose, glutamate, lactate concentrations, P O_2 and pH were measured using a BioProfile Analyser 200 (Nova Biomedical, USA).

2.9. Statistical analysis

All statistical analysis was conducted using windows based software (Excel, Microsoft, USA and MINITAB® statistical software, USA). All the raw data are located in appendix 7.6. All graphical analyses are located within the main body of the thesis and are linked by reference to the corresponding raw data in the appendix and vice versa.

mESCs seeding densities and cell growth

This experiment was performed in triplicate on one occasion, using the same passage cells, five different seeding densities and two different media compositions. The data were normally distributed and a two-way ANOVA was used to find any significant differences between the media used and the seeding densities on the resulting cell numbers post culture (Appendix 9.6 - Page 258, Main body – Page 92).

Media optimisation data

Performed in duplicate on two separate occasions, three different media at EB formation stage and four different media at the osteogenic differentiation. The data were normally distributed and two and one-way ANOVA were used to find any significant differences on bone nodule formation with the 12 different media combinations (Appendix 9.6 - Page 259, Main body – Page 99).

1.1% alginate bead measurements before and after culture (No cells – varying needle size)

Fifty beads were created using the established equipment parameters and four different sized hypodermic needles. Five beads (10% of the population) were measured after one hour in DMEM to allow slight swelling and the same five beads were measured after 7 days culture. Horizontal and vertical diameters were measured for each bead and the horizontal / vertical diameter (H/V) ratios determined the sphericity. Beads were suspended in PBS and were not

allowed to clump as this would give inaccurate measurements. A graticule was photographed at the same time as the beads at all times and used for bead measurements. This was to ensure that the microscope software was calibrated accurately Using the analySISD* software (Oxford, UK) the horizontal and vertical diameters could be measured. An example of the graticule and a bead can be found in the appendix. (Appendix 9.6 - Page 261, Main body – Page 123).

1.1% alginate bead sizes before and after culture & 1.1% alginate + 0.1% gelatin bead sizes before and after culture (With cells – 25G needle)

One hundred beads of each cell cell density (10, 100, 1000 cells per bead) were created and gelatin was either included or not in the bead composition using only the 25G needle. Ten beads (10% of the population) were measured as described above in each category before and cafter culture and data were analysed with one and two-way ANOVA (Appendix 9.6 - Page 263, Main body – Page 124).

Alizarin Red S quantification

ARSQ was measured on days 0, 3, 8, 15, 22 and 29 in duplicate on three separate occasions. Measurements were relative to triplicate blanks conducted on each occasion and were adjusted to the amount of ARS per bead. Between 60 and 125 beads were used for a single measurement which represented 10% of the sample population of 600 beads per reactor. The data were normally distributed and one-way ANOVA was used to find any significant differences between the timepoints (Appendix 9.6 - Page 265, Main body – Page 178).

MTS activity

MTS activity was measured on days 0, 3, 8, 15, 22 and 29. Measurements were relative to quadruplicate blanks conducted on each occasion. Each

measurement consisted of three randomly selected beads from the two separate reactors, in quadruplicate and this measurement was averaged per bead. Therefore each data point represents three beads, in quadruplicate for readings, in duplicate on each occasion and on three separate occasions (72 beads per data point but n = 24 as the reading measured the metabolic activity of three beads). Data is represented as metabolic activity per bead. The data were normally distributed and one-way ANOVA was used to find any significant differences between the timepoints (Appendix 9.6 - Page 267, Main body – Page 178).

Alkaline Phosphatase activity

ALPase activity was measured on days 0, 3, 8, 15, 22 and 29. Measurements were relative to triplicate blanks conducted on each occasion. Each measurement consisted of three randomly selected beads from the two separate reactors, in triplicate and this measurement was averaged per bead. Therefore each data point represents three beads, in triplicate for readings, in duplicate on each occasion and on three separate occasions (54 beads per data point but n = 18 as the reading measured ALPase activity of three beads). Data is represented as ALPase activity per bead. The data were normally distributed and one-way ANOVA was used to find any significant differences between the timepoints (Appendix 9.6 - Page 269, Main body – Page 178).

3. ESTABLISHMENT AND CHARACTERISATION OF 2D BONE FORMATION FROM MESCS

3.1. Introduction

Devising a well-defined medium formulation is imperative for generating repeatable and reliable data from any cell culture system (1) with clinical applications in mind. The derivation of bone from ESCs essentially contains three stages: ESC maintenance, EB formation and osteogenic differentiation and the literature contains three medium formulations (89;176;177), related to these phases, to begin serum-free media development.

Defined media are designed by and large to either maintain/expand cells in a healthy state or cause some form of transition. In this thesis there were three stages to define: a) ESC maintenance, b) EB formation and c) osteogenic differentiation. Defining media is imperative in order to glean reliable and repeatable results, and more importantly, clinically acceptable, homogeneous tissue. A simple diagram (Figure 3.1) signifies the most logical approaches to

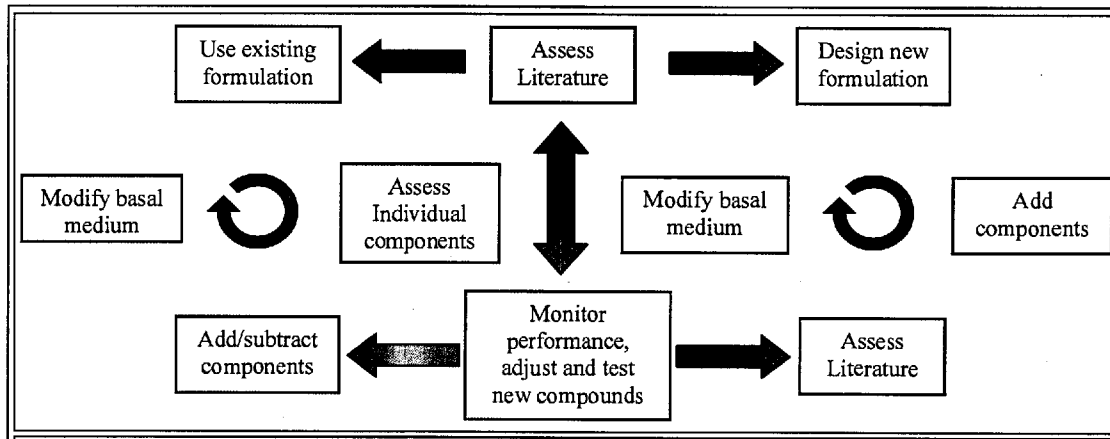


Figure 3.1. Media development flow chart. Illustrating pathways for devising defined media or adapting an existing media to suit one's intended cell culture system. Adapted from (1).

media development. In this thesis media development was considered either as a top-down or bottom-up process whereby a "complete" medium is selected and components removed, or, a minimalistic media is used and components added, respectively. It is clear that the former will provide short-term, working solutions but the latter will eventually provide an efficient, well-defined, cost-effective medium, albeit taking a long time to formulate.

The selection of successful cell culture media is an integral component of any cell culture system. Its importance can not be overlooked or easily disputed, because the growth, phenotype, health and stability of cultured cells are dependent upon the media in which they are maintained. Devising a defined medium formulation for a particular cell culture system may involve a considerable commitment of time and material resources. However, as the viability of cultured cells and the quality of data obtained from a cell culture system are contingent upon the cell culture media, its proper formulation is imperative and warrants making the necessary investment. Furthermore, once properly formulated, a defined medium may play a key role in the overall success of a particular research application (1).

Ultimately, defined, culture for the maintenance and differentiation of hESCs would be the goal. Human serum with human feeders has been considered but this still has obvious drawbacks such as availability, culture variability and it is cumbersome for large-scale production (216). The Geron corporation has recently formulated serum-free medium for maintenance of hESCs that would be suitable for therapeutic applications. The medium was completely defined, devoid of feeders and grown on human laminin (216) and was able to maintain the hESCs in an undifferentiated state, with a normal phenotype for over 30 passages.

3.2. Aims

- To formulate novel, defined serum-free media that allow cell viability, proliferation and transition throughout mESC maintenance, EB formation and osteogenic differentiation.
- To define and optimise the components of serum-free media that maximises the efficiency of osteogenic differentiation from mESCs.

3.3. Materials and methods

3.3.1. MESC maintenance

The E14Tg2a mESC line [(gift from Professor Austin Smith, Institute for Stem Cell Research, School of Biological Sciences, College of Science and Engineering, University of Edinburgh and from the American Type Culture Collection (ATCC), Rockville, MD)] was derived from strain 129/Ola mouse blastocysts by trypsinising immunosurgically isolated ICMs and culturing the dissociated cells on mouse embryonic fibroblasts (STO) in Buffalo Rat Liver (BRL)-conditioned medium. The subline E14Tg2a was selected with a modal chromosome number of 40, thioguanine resistance and identified as male (Y-chromosome detected) (213).

Firstly, a gelatin layer was formed on tissue culture treated plastic to enable mESC adherence. A 0.1% (w/v) solution of gelatin (Sigma, UK) was dissolved in sterile PBS and used to coat tissue culture treated-plates at 37 °C in a 5% CO_2 in a humidified incubator for at least 20 minutes. Serum-containing and serum-free maintenance media were used to handle and culture mESCs.

The exact details of feeder-free mESC culture are unique and have been investigated further, as described previously (Section 1.4.1). The lowest cell

seeding density for feeder-free mESCs was empirically determined (Section 1.4.1) and was 6.7 x 10^4 per cm^2, from a cryopreserved state and 3.3 x 10^4 per cm^2 when passaging. The concentration of LIF has a tendency to drop below the levels that maintain pluripotency after 24 hours in culture so medium changes were daily. Passaging normally took place every 2 to 3 days depending on the operator's opinion using morphological indications of the ratio of undifferentiated to differentiated cells and confluence. To passage the mESCs, 30 µL per cm^2 of TE (Invitrogen, UK) was administered to the mESCs for 10 minutes at 37 °C following a single wash with prewarmed PBS. A small amount of maintenance medium or trypsin inhibitor (if serum-free maintenance medium was used) was added to halt trypsinisation and the resulting cell suspension was then centrifuged at 200g for 3 minutes. The cells were then resuspended in prewarmed maintenance medium and manually counted using a haemocytometer and the trypan blue exclusion method to determine cell viability (Sigma, UK). The cells were then replated onto fresh gelatinised tissue culture plastic in prewarmed maintenance media.

The transition from serum-containing to serum-free media is too extreme for sensitive cells and direct or sequential adaptation is often necessary. Johansson and Wiles *et al.* (88;89) recommend passage in a chemically defined medium before EB formation but did stress that mESC phenotype would change if passaged for extended periods without serum. Therefore, the knock out serum-replacement medium (serum-free maintenance) was used to passage cells just prior to serum-free EB formation.

3.3.2. Embryoid body formation

Embryoid body formation involved careful preparation of mESCs prior to suspension culture and is well documented (88;89;146;147;152;213). However, empirical determination of the correct conditions before suspension was established here with the E14Tg2a cell line. Cells in monolayer culture should be around 80% confluent, be either day 2 or 3 of culture and have a very high morphological, undifferentiated to differentiated ratio. MESCs were trypsinised as normal but clumps of 100-200 cells were visible after 2-3 minutes instead of 5 minutes trypsinisation. The cells were then centrifuged at 300g for 3 minutes at room temperature (21°C). A confluent T75 flask after 2 or 3 days growth in maintenance medium typically yielded around 5-7 x 10^6 cells and was resuspended in 30 mL of differentiation medium and distributed evenly between two, 90 mm diameter bacteriological grade Petri dishes (Bibby Sterilin, UK). Clumps of 10-20 cells are essential for EB formation, as single cell suspensions or large clumps of thousands of cells will result in erroneous 3D aggregation. On day three of EB formation there was a medium change as essential growth factors become depleted (e.g. L-glutamine) and toxic metabolites accumulate (e.g. ammonia). On day 5 of culture the EBs were harvested by aspiration from the bacteriological plates and centrifuged at 66g for 4 minutes. The medium was aspirated and replaced with prewarmed PBS to wash away traces of serum. The cells were centrifuged again at 66g for 4 minutes and the PBS was aspirated. 1 mL of TE was added to the EBs, after washing, for 3-5 minutes at 37°C. 1 mL of prewarmed differentiation medium was then added to halt trypsinisation and the cells were resuspended in osteogenic differentiation medium as a single cell suspension to induce bone nodule formation.

Johansson and Wiles (88;89) developed a chemically defined, serum-free medium that would allow EB formation in suspension culture, which did not require a medium change on day 3. However, to obtain directed germ layer formation, exogenous growth factors should be added, at the required concentrations to serum-free medium, such as BMP4 to induce mesoderm formation. The protocols to form EBs in serum-free medium published by Johansson and Wiles were tested and not used in this project. Instead empirically determined protocols were defined for these experiments. For satisfactory serum-free EB formation, mESCs were first passaged in serum-containing maintenance medium that allowed a smooth transition from serum-containing to serum-free conditions.

3.4. Results

3.4.1. MESC density studies and characterisation

The undifferentiated mESCs were firstly phenotyped using immunocytochemistry and flow cytometry, their growth rates assessed, optimal seeding densities defined in serum-containing and serum-free media. A serum batch test was also performed to ensure that the ESCs could be maintained in a pluripotent state by assessing Oct-4 (134;217) and CD9 (139;140) expression and were capable of osteogenic differentiation.

Low passage (<p20) mESCs were cultured in maintenance medium, seeded in triplicate, in six well plates at five different cell densities ranging from 1.5 - 3.5 x 10^5 cells/well in a six well plate (1.5 - 3.5 x 10^4 cells/cm^2) in serum-containing and serum-free maintenance medium. Sequential adaptation from serum-containing to serum-free medium showed no advantage over direct

adaptation (data not shown). The media were changed daily and a trypan blue cell count was performed on day 3 (normal harvest day for mESCs).

Cell numbers increased in all cultures over three days but was significantly higher (Appendix 9.6, $p<0.05$) in serum-free medium cultures indicating that serum may inhibit as well as promote propagation (Figure 3.2).

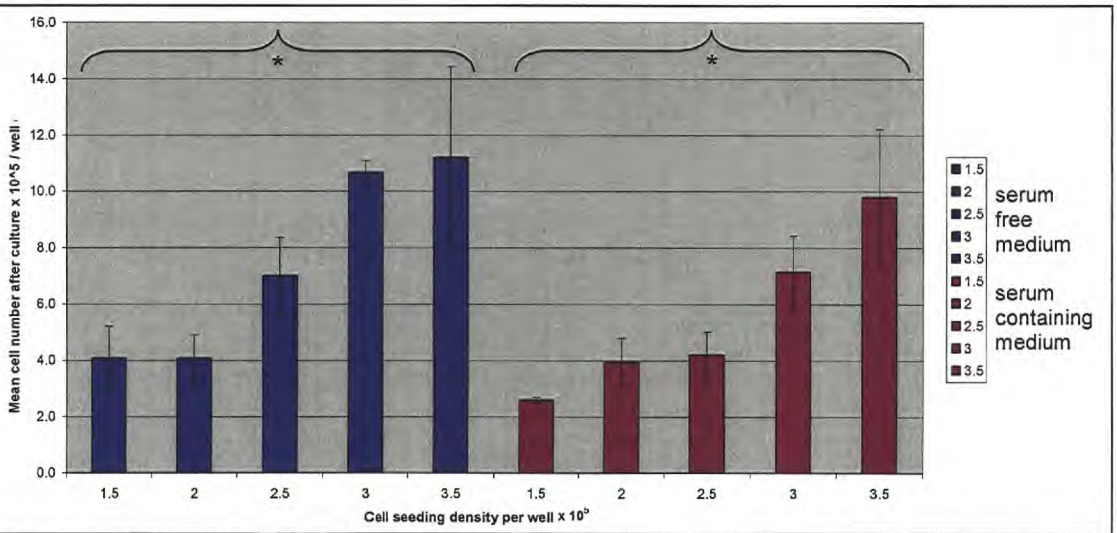


Figure 3.2. mESCs cultured for 3 days in serum-free and serum-containing maintenance medium. Cells were seeded at different densities Error bars represent Standard Error (n=3). ANOVA statistical analysis indicates that there is a significant difference between cell numbers grown in serum-free and serum-containing media ($p<0.05$)*.

Both serum-containing and serum-free media had optimal seeding densities of 3.5×10^5 cells per well (2.8-fold increase) and 3×10^5 cells per well (3.56-fold increase) respectively. However, cell morphology indicated that these seeding densities produced poor quality colonies that were not distinct from neighbouring colonies, which is essential for maintenance of pluripotency. Therefore, empirical judgement was used when selecting cells for differentiation, shown in Figure 3.3. Calculating the cell numbers needed for a T75 flask ranges between 2.25 -2.6 $\times 10^6$ cells per flask. However, in practice,

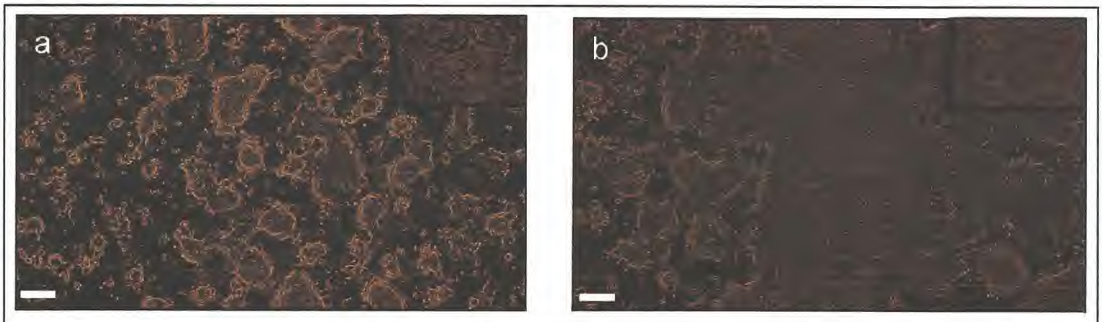


Figure 3.3. mESC seeding density affects colony morphology after 3 days culture. a. serum-free medium, seeding density = 2 x 10^5, day 3. b. Serum-free medium, seeding density = 3 x 10^5, day 3. Serum-containing medium similar (inset). x10 objective – scale bars 100 µm.

the larger area (75 cm^2) requires a cell density of around 3 x 10^6 cells per flask (or higher) from passage and 5 x 10^6 from frozen. This may be to due the larger volume of media and autocrine/paracrine differences. On day 3 of culture, colonies were also assessed with immunocytochemical markers and viability stains to qualitatively assess the cells that were to be used for differentiation studies (Figure 3.4). This indicates that the mESCs were viable and pluripotent when cultured in serum-containing or serum-free media for use in differentiation studies.

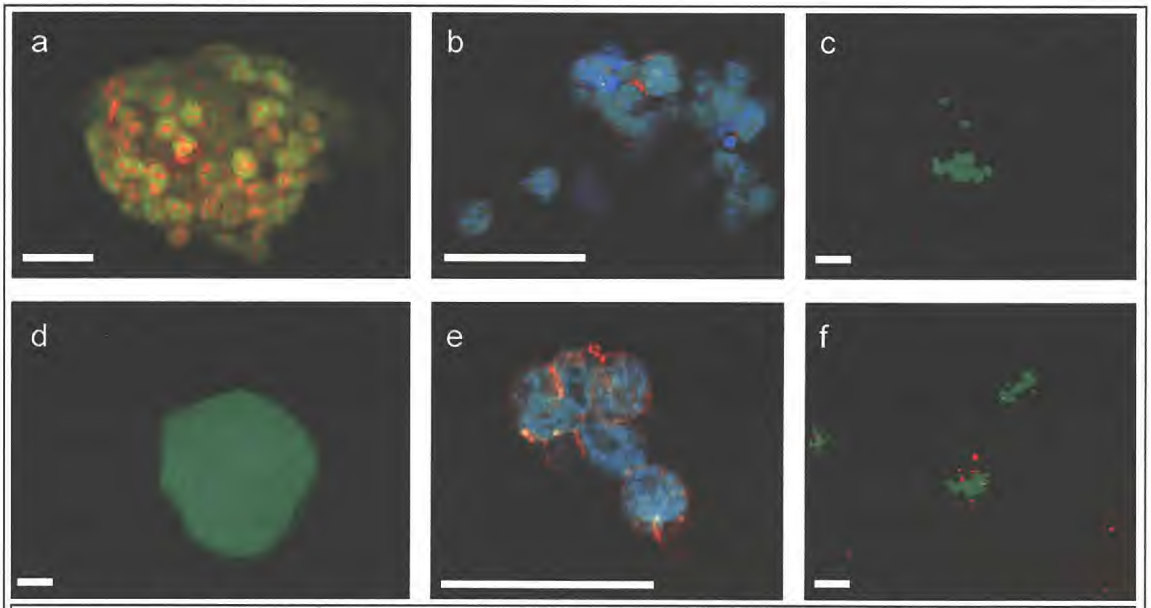
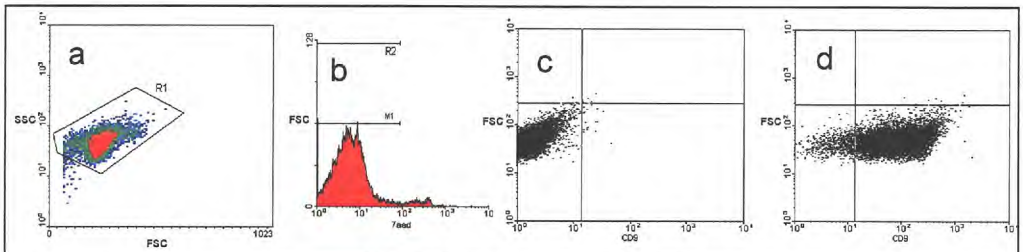


Figure 3.4. mESC phenotypic characterisation and cell viability cultured in serum-containing and serum-free media. On day 3 of culture mESCs were characterised with Oct4, CD9 and viability assessment (live/dead stain). a. Serum-containing Oct4 & PI x20 objective. b. Serum-containing CD9 & DAPI x40 objective. c. Serum-containing LIVE/DEAD x10 objective (confocal). d. Serum-free Oct4 x10 objective. e. Serum-free CD9 & DAPI x40 objective (x1.5 digital zoom). f. Serum-free LIVE/DEAD x10. Scale bars 100 μm.

3.4.2. Flow cytometric analysis

MESC pluripotency is optimally maintained in batch tested FCS although reports have identified that mESCs can be derived and maintained in defined serum-free medium using LIF/BMP4 to maintain pluripotency (218-220). Serum-containing maintenance medium was formed using three serum batches from different sources along with the existing batch (Invitrogen, UK, Batch: 3065946F). MESCs were seeded at 3 x 10^5 cells per six well plate in triplicate. The cells were maintained as previously described (Section 2.2.1) and cell counts were performed in duplicate on day 1, 2 and 3 along with morphological photographs. On day three, 5 x 10^5 cells per flow tube from each batch were analysed for CD9 marker expression and viability (7-AAD) by flow cytometry, with suitable controls in order to assess the amount of pluripotent cells and viability from each batch (Figure 3.5). Batch 06G9130K (Invitrogen, UK) was selected due to its similarities to the existing batch 3065946F (Invitrogen, UK) in terms of colony morphology and pluripotency. Batch tested (06G9130K), serum-formed, day 3, undifferentiated mESCs were around 95% viable and 95% of these viable cells possessed the pluripotent marker, CD9.



e

Serum Batch	Total Events	M1 (Viable cells)	Negative control				Positive sample			
			UL	UR	LL	LR	UL	UR	LL	LR
Supplier X	>10000	93.62	0.18	0.2	99.19	0.43	0.01	0.56	2.8	96.64
06G9130K	>10000	90.4	0.31	0.22	98.96	0.51	0.01	0.8	1.45	97.74
Supplier Y	>10000	93.67	0.16	0.31	99.1	0.43	0	0.48	0.96	98.56
3065946F	>10000	95.29	0.07	0.06	99.71	0.16	0	0.03	7.14	92.78
	Mean---->	93.25	0.18	0.20	99.24	0.38	0.01	0.47	3.09	96.43
	SD---->	2.05	0.10	0.10	0.33	0.15	0.01	0.32	2.81	2.56

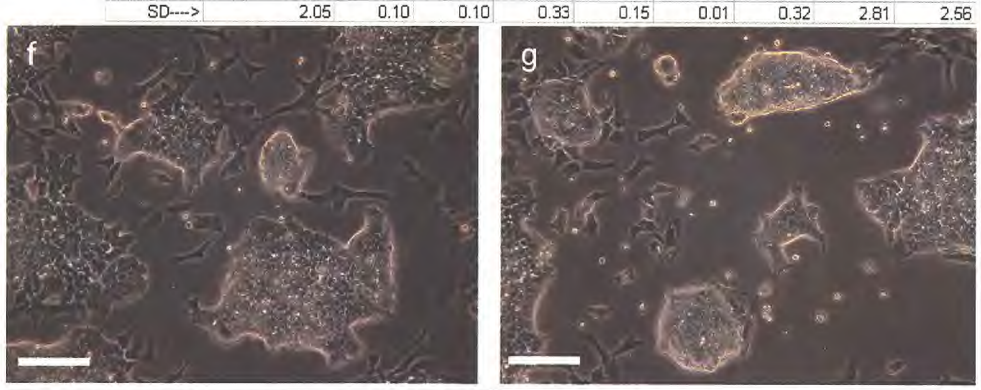
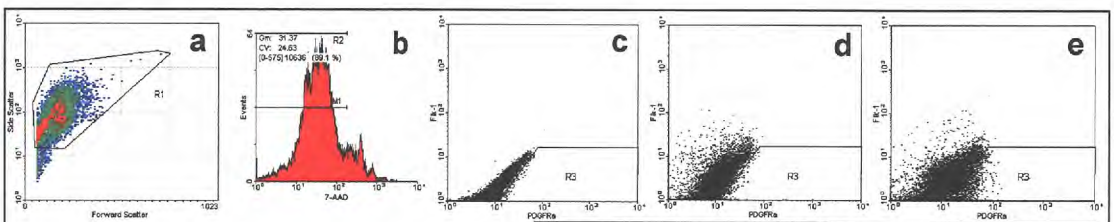


Figure 3.5. Serum batch test. Analysis shown using 3065946F to give an indication of the procedures followed. The cells were gated for R1 (debris removal), R2 (viable cells), quadrants set with 99% -ve LL. a. Density plot of FSC vs SSC, mESCs day 3 (R1 = no debris).b. Histogram of gate R1 of 7-AAD vs FSC (R2 = viable cells). c. Dot plot of gate R2 of CD9 vs FSC (negative control). d. Dot plot of gate R2 of CD9 vs FSC (positive sample). e. All flow analysis batch results A→D. f. Undifferentiated mESCs, day 3, serum-containing medium (06G9130K), x10 objective. g. Undifferentiated mESCs, day 3, serum-containing medium (3065946F), x10 objective. Scale bars 100 µm.

3.4.2.1. Mesoderm analysis

Although the markers used in the flow cytometric analysis may not identify all mesodermal cells or be completely specific, nonetheless the analysis provides valuable information and allows future cell sorting by FACS. EBs formed in serum-containing medium were cultured for 5 days and trypsinised lightly to form a single cell suspension. The cells were labelled with 7-AAD and two mesoderm markers, namely Flk-1 and PDGFRα (87). Flk-1 expression did not appear to be present, but the antibodies to Flk-1 had not been tested for flow cytometry. The results indicated that the negative controls functioned correctly (no positive staining) and that 9.29±2.57% of the viable cells analysed possessed PDGFRα (Figure 3.6).



f Gates	Mean (n=4)	SD
Events (R1)	11949	140
Viable Cells % (R2)	89.41	2.02
PDGFRa (R3)	9.29	2.57

Figure 3.6. Mesoderm flow data a. Density plot of Day 5 dEBs cultured in serum medium. FSC vs SSC (R1 = debris removed) b. Histogram of viable cells, R1 gate. 7-AAD vs Events (R2 = viable). c. Dot plot of PDGFRα vs Flk-1 gated using R2. No antibody staining -ve control, R3 = PDGFRα gate +ve cells). d. as c. but the cells were only stained with secondary antibodies (negative controls). e. as c. but all antibody layers used (positive sample). f. summary table of means for events (R1), viable cells (%) (R2) and viable cells (%) that were also tagged with PDGFRα for each of the four samples tested (R3).

However, for accurate mesoderm population analysis, the Flk-1 two-colour analysis should be conducted to identify double-positive, double-negative and single positive/negative populations. Some cells identified by these markers may not be mesodermal as the antibodies are not mesodermal specific. In summary, using serum-containing EB formation medium, 9.3±2.6% of the cells express the mesodermal marker PDGFRα and it would be expected that the osteoprogenitors are within this population. When EBs were formed in serum-containing medium, disrupted and plated into serum-containing osteogenic medium then 56±26 bone nodules formed as previously reported (30). The amount of mesoderm present on day 5 of EB formation gives an indication of the quantity of cells capable of forming bone nodules.

3.4.3. MESC media definition and optimisation

Serum-free media development was time consuming and the entire process including methodology development will not be described here but can be seen in Appendix 9.1 along with intermediate media formulations. The following section will highlight the rationale and the conclusions from the preliminary experiments 1-6, however experiment 7, the most promising result is shown in full.

Experiment 1	Comparison of serum-containing versus serum-free media.
Rationale	• Knock out serum replacement and Lennon's medium used as alternative to serum-containing medium for EB formation and the bone nodule assay • Comparison of previously established methods/media (30) and serum-free media
Conclusions	• EBs would not form in 15% (v/v) KOSR in contrast to serum • Lennon's serum-free, osteogenic media would not allow cell survival after EB disruption • Trace amounts of serum transferred from the serum-containing medium EB stage to the serum-free bone nodule medium allowed survival, adherence and proliferation for a limited time (less than 1 week). A soluble factor in serum may be absent from Lennon's medium that is present in serum

Experiment 2	Evaluation of Lennon's serum-free media using mouse osteoblasts.
Rationale	• Lennon's medium was tested on a similar cell line as reported in the literature (176) in order to evaluate the validity of results from Experiment 1.
Conclusions	• Mouse osteoblast cell line proliferated as expected in Lennon's media

Experiment 3	Improvement of Lennon's serum-free medium with a soluble factor present in serum.
Rationale	Lysophosphatidic acid (LPA), which is present in serum and is known to aid survival and adhesion, was added to serum-free osteogenic medium (221)
Conclusions	• LPA at concentrations found in serum did not allow disaggregated EBs (dEBs) to survive, adhere and proliferate • Day 5 dEB transition from serum-containing to osteogenic serum-free media was considered a critical stage for mESC survival

Experiment 4	Evaluation of serum-containing to serum-free media transition time.
Rationale	• mESCs were cultured in serum-free maintenance medium and were then placed into Wiles (89) serum-free medium to form EBs
Conclusions	• Transition from serum-containing maintenance medium to serum-free maintenance medium at maintenance stage proved successful • EB formation was suboptimal using Wiles' protocols/medium even when cell density was doubled

Experiment 5	Development of a novel "complete" osteogenic serum-free medium (LWR1.1) for bone nodule formation plated on various culture surfaces.
Rationale	• mESCs were cultured in serum-free maintenance medium and were then placed into serum-free EB formation medium in order to form EBs
Conclusions	• Using previously established EB formation techniques and LWR1.1 differentiation medium allowed dEBs to survive, adhere and proliferate

Experiment 6	Refinement of LWR1.1 serum-free differentiation medium to identify the major factors responsible for positive results.
Rationale	• LWR1.2 serum-free osteogenic differentiation medium was modified slightly and robust protocols for maintaining mESCs in serum-free maintenance medium and forming EBs in serum-free medium were followed
Conclusions	• LWR1.2 with knock out serum replacement is essential for dEB cell survival and allows bone-like nodule formation after 21 days culture compared to serum-containing media controls

The development of serum-free medium was time consuming and led to three different serum free media that permitted mESC maintenance, EB formation (mesoderm induction) and osteogenic differentiation (LWR1.3). The timing of transition from serum-containing to serum-free medium was critical and this transition was only successful at mESC maintenance stage as opposed to the EB disruption stage.

3.4.4. Successful defined serum-free media

Successful maintenance, EB formation and osteogenic differentiation media formulations allowed more detailed analysis to be performed.

Experiment 7	Evaluation of EB formation and osteogenic differentiation with serum-containing and serum-free medium.		
Media selection	Serum-containing then serum-free maintenance medium for 1 passage.	Serum-free EB formation medium (serum-free ± BMP4 2ng/mL) and serum containing EB formation medium control	LWR1.3 serum-free osteogenic medium and serum-containing osteogenic medium as a control
Cells	mESCs	EBs	dEBs
Methods	• Antibiotics were added at 0.1% from the EB stage onwards. • EBs were formed in serum-free EB formation medium, serum-free EB formation medium+BMP4 and serum-containing EB formation medium. • The EBs were disrupted and plated into 12 well-plates for 21 days in four different types of media: serum-containing differentiation medium, osteogenic serum-containing differentiation medium, LWR1.3 serum-free medium and LWR1.3 serum-free medium with osteogenic supplements. • Media was changed every 2 or 3 days and chamber slides were used in order to immunostain for Cbfa1. • Bone nodules were identified with Alizarin Red S staining. Repeated in duplicate on two separate occasions (n = 4). (Figure 3.8, 9&10).		
Conclusions	EB formation in serum-free medium with BMP4 allows bone nodule formation in LWR1.3, serum-free osteogenic medium without the need for the previously established osteogenic supplements (30).		

EB formation was assessed by morphology and confocal microscopy using the live/dead stain at day 5. Morphological images suggest EBs formed in serum-containing medium (Figure 3.7e/f) were normal (cystic EBs) and viable. Mesoderm analysis was conducted on these EBs and can be seen in Section 6.3. EBs formed in serum-free medium without the mesoderm inducer BMP4 appeared dense (Figure 3.7c) and contained more non-viable cells (Figure 3.7d) and did not appear cystic when compared to serum controls. EBs formed in serum-free medium with the mesoderm inducer BMP4 appeared cystic, similar to serum controls and viable (Figure 3.7a/b).

EBs were formed in three different media, disrupted and plated into a further four different media cocktails. After the EBs were disrupted on day 5 a

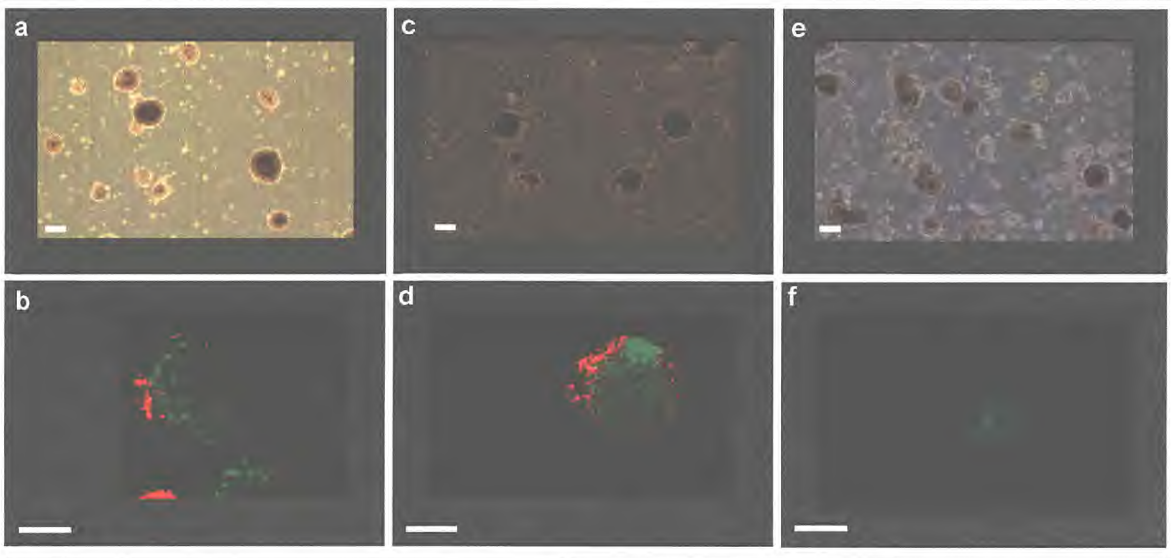


Figure 3.7. Phase contrast and confocal live/dead images of day 5 EBs in 3 different media. Normal EB formation is indicated by cavity formation and germ layer formation. Day 5 EBs resemble the egg cylinder stage *in vivo*. a. EBs day 5, serum-free medium + BMP4 (2ng/mL), x4. b. as a. but mid section LIVE/DEAD stain, x10. c. EBs day 5, serum-free medium, x4. d. as b. but mid section LIVE/DEAD stain x10 e. EBs day 5, serum-containing medium, x4. f. as e. but mid section LIVE/DEAD stain x10. Scale bars – 100 µm.

single cell suspension was placed into 12 well plates and cultured for 21 days. Tissue growth occurred in most cultures but bone nodule formation was limited

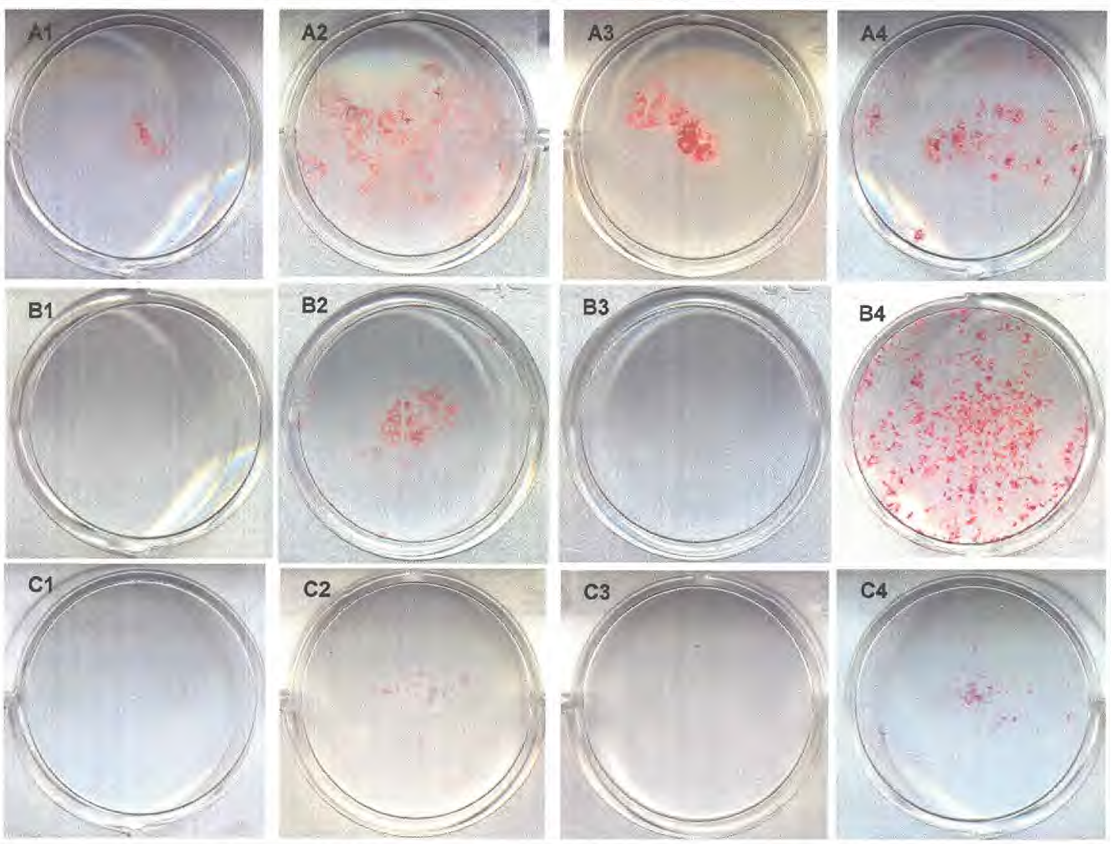


Figure 3.8. Macroscopic images, bone nodules (Alizarin Red S). dEBs were plated into 12 well plates and cultured for 21 days to assess osteogenic differentiation. A. EBs formed in serum- free + BMP4 (2ng/mL). B. EBs formed in serum-free. C. EBs formed in serum-containing then disrupted on day 5 and plated into 1 = LWR1.3 serum-free osteogenic medium. 2 = serum-containing differentiation medium. 3 = LWR1.3 serum-free osteogenic medium. 4 = serum-containing osteogenic medium. (n = 2)

to media combinations that allowed a smooth transition from serum-containing medium to serum-free (Figure 3.8).

Only discrete bone nodules that fluoresced under the fluorescence microscope were actually counted as opposed to nodules that did not fluoresce or were obviously a result of quenched staining (Figure 3.8&9, specifically B4).

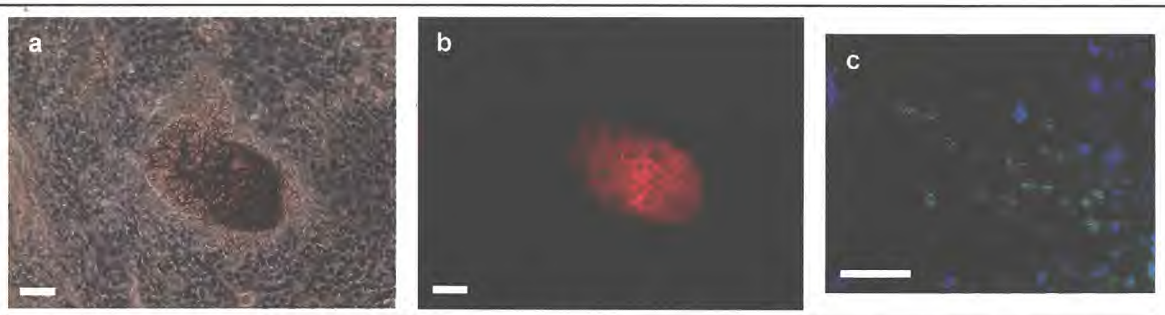


Figure 3.9. Examples of alizarin red S and Cbfa1 staining. a. Phase contrast image of a bone nodule stained with Alizarin Red S from media cocktail A1, x10. b. as 1 but nodule viewed with epiflourescence microscope excited between 530 to 560 nm and emitting at 580 nm which defines a true discrete bone nodule. c. Cbfa1-FITC immunostaining and DAPI from media cocktail A4, x20. Immunostaining was limited to 1 positive sample for Cbfa1 staining with a negative control. On both duplicates, all cells in the serum free wells tended to be washed off during the process of immunostaining. Scale bars – 100 µm.

A two-way ANOVA identified that there was a significant difference ($p<0.0001$) between the osteogenic media (Figure 3.10 & Appendix 9.6).

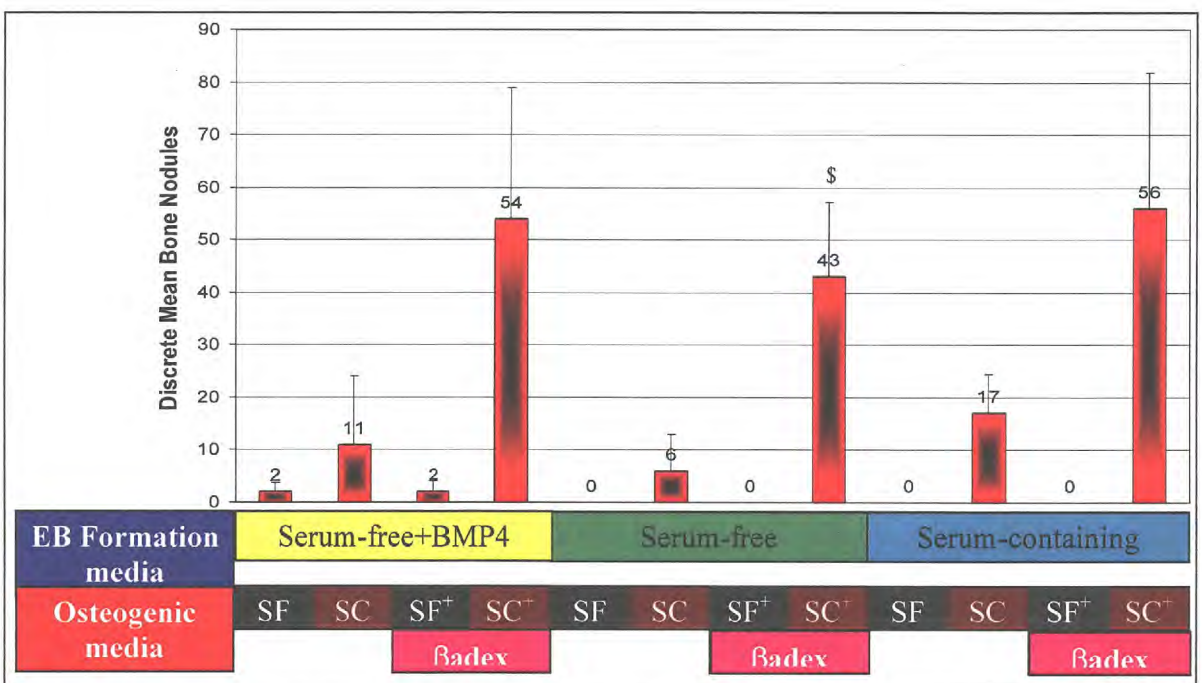


Figure 3.10. Discrete bone nodule counts on day 21 of the bone nodule assay using 12 media combinations. EBs formed in serum-free EB formation medium + BMP4 (2ng/mL). SF = Serum-free medium, SC = Serum-containing medium. Error bars indicate 1 standard deviation from the mean. (n = 4 except for $ = 2). βadex = osteogenic supplements.

Figure 3.9 shows the first evidence that osteogenic differentiation from undifferentiated mESCs to bone tissue can be achieved using a media combination that is completely free from serum and relies purely on growth factors to form bone nodules. EBs grown in serum-free EB formation medium with BMP4 mesoderm induction formed bone nodules when EBs were disaggregated and placed into serum-containing medium, serum-containing osteogenic medium, LWR1.3 serum-free osteogenic medium and LWR1.3 serum-free osteogenic medium with osteogenic supplements. Serum-free formed EBs without BMP4 mesoderm induction formed bone nodules when EBs were disaggregated and placed into serum-containing medium or serum-containing medium with osteogenic supplements. Serum formed EBs, only formed bone nodules when EBs were disaggregated and placed into serum-containing medium or serum-containing medium with osteogenic supplements. The addition of βadex osteogenic supplements (L-ascorbate-2-phosphate, β-glycerophosphate and dexamethasone) to the LWR1.3 serum-free osteogenic medium did not enhance the quantity of bone nodule formation.

Statistically, there was no significant difference in the number of bone nodules formed between the EB formation media regardless of the osteogenic medium used. However, there was a significant difference ($P<0.0001$) in bone nodule formation when using different osteogenic media within each EB formation media group. The formation of bone nodules exclusively using serum-free media (EB & osteogenic differentiation), in the presence of growth factors and in the absence of osteogenic supplements, was reproducible (3 out of 4 occasions) but was 5.5 fold less efficient than using serum alone during osteogenic differentiation, forming 2 as opposed to 11 mean bone nodules. What is important to note is that the use of serum-containing medium with

osteogenic supplements, after serum-free culture at the maintenance and EB formation stages implies that βadex has a negative effect on mesodermal progenitors, by reducing the number of bone nodules from 11 to 2.

Beating cardiomyocytes appeared in most cultures but were not quantitated. Smooth muscle contraction was also noted in 1 well from the A1 (serum-free) media combination but not elsewhere (Figure 3.11). It must be noted that Cbfa-1 immunostaining was performed on each separate occasion. Cbfa-1 nuclear staining was only achieved in media combinations that formed more than 40 bone nodules providing further evidence that bone formation and osteoblasts were present in the cultures. The remaining cultures did not yield enough tissue to perform immunostaining.

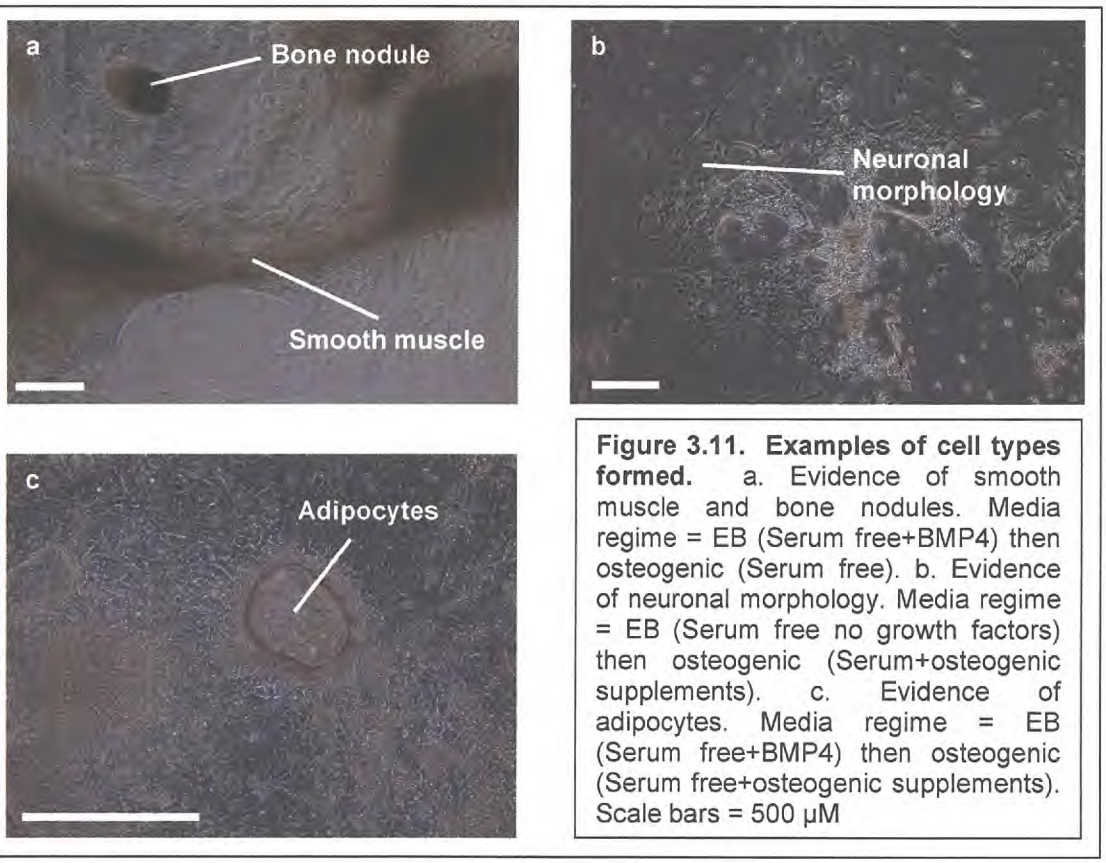


Figure 3.11. Examples of cell types formed. a. Evidence of smooth muscle and bone nodules. Media regime = EB (Serum free+BMP4) then osteogenic (Serum free). b. Evidence of neuronal morphology. Media regime = EB (Serum free no growth factors) then osteogenic (Serum+osteogenic supplements). c. Evidence of adipocytes. Media regime = EB (Serum free+BMP4) then osteogenic (Serum free+osteogenic supplements). Scale bars = 500 μM

3.5. Discussion

Cell culture in serum-containing and serum-free media indicates that the feeder-free cell line, E14Tg2a, expresses Oct-4 and CD9, which are markers of undifferentiated ESCs. When mESCs were cultured in serum-containing maintenance medium and passaged into serum-free maintenance medium, they retained their viability and pluripotency. This was a time point whereby transition from serum-containing to serum-free media can take place without cell death.

Flow cytometry results analysis for mesodermal progenitors were promising and highlighted that the protocols to identify progenitors will provide a high proportion of viable cells for future FACS purification. Positive cell selection using surface antigens is probably the easiest and most successful method of purification at present. However, the use of fluorescent antibodies used for FACS sorting may alter the cells' ability to respond, for example, to growth factors. PDGF-ββ (used in LWR1.3 serum-free osteogenic medium) normally interacts with PDGFRα (176) and this may be inhibited once the cells have been fluorescently labelled and sorted with PDGFRα antibodies. Mesodermal analysis was only conducted to identify the proportion of mesoderm present in day 5 EBs at this stage.

The proportion of mesoderm, or other cells that express PDGFRα such as the kidney (222) identified here, is promising being at 9.3% when mESCs were allowed to form EBs in serum-containing medium. During early mouse embryogenesis PDGFRα is essential for normal development of many mesodermal tissues, including the axial skeleton (223). These results give an indication to the potential that day 5 EBs have to undergo osteogenic differentiation.

In order to culture mESCs in serum-free medium for differentiation studies it was found that they need to be maintained in serum-containing maintenance medium and then passaged once into serum-free maintenance medium. A serum-free maintenance medium similar to that used here was reported in the literature using E14Tg2a (224) just after these results were generated, thus supporting the work described here. In serum-containing and serum-free maintenance media the cells possessed the ESC marker Oct-4, the pluripotency marker CD9 and were also viable. Day 3 undifferentiated mESC colonies, formed in serum-containing medium, were around 95% viable (after flow cytometric processing) and 95% of the viable cells also possessed the pluripotent marker CD9. The cell line E14Tg2a was therefore qualitatively and quantitatively viable for use in differentiation studies as 90.25% of day 3 cells were viable and pluripotent. Further characterisation using PCR, telomerase levels and karyotyping could have been undertaken but the constraining factor was time and these assays have already been addressed elsewhere (122;123;212).

The goal of differentiating mESCs to bone tissue using serum-free media has been achieved here, albeit to a limited extent. The three stages of culture: maintenance, EB formation and osteogenic differentiation are of great significance, as preparation of appropriate cell numbers, of sufficient quality for the subsequent stage is very important. The maintenance stage was the most successful stage for the transition of mESCs from serum-containing to serum-free medium. The cells were cultured in serum-containing maintenance medium and then placed directly into serum-free maintenance medium for one passage. However, it has been reported that more than one passage in Wiles' serum-free medium at the maintenance stage results in a loss of phenotype, as

reported in the literature (88;89). In contrast, undifferentiated mESCs in serum-free maintenance medium, recently used in the literature (224) did not appear to lose phenotype after one passage as indicated by expression of Oct-4 and CD9 although the karyotype could have changed, which was not evaluated.

The undifferentiated mESCs in serum-free maintenance medium were then placed into suspension culture to form EBs. Undifferentiated mESC clumps were placed in both serum-containing and also serum-free EB differentiation media; with or without the mesoderm inducer BMP4 (87;88;225-227). Our results indicate that only EBs that were formed in serum-free EB formation medium (with the addition of BMP4) or serum-containing medium, exhibited the normal cystic morphology and high cell viability as determined by confocal live/dead images. Serum-free EB formation medium without BMP4, resulted in EBs with a decrease in viability and did not appear to be cystic. In retrospect, propidium iodide staining and flow cytometric analysis of the cell cycle would highlight the stage at which the treated cells were. It would be interesting to investigate the proportions of serum-free formed EB cells that were at G_0 of the cell cycle. This would provide evidence of either cell quiescence or arrested development due to the lack of serum and / or mitogens.

The critical stage of mESC differentiation is day 5 of EB formation and disruption to a single cell suspension. EBs formed in serum-containing medium and plated as a single cell suspension into serum-containing, osteogenic medium survive and form bone nodules (30;31). Disrupting EBs and placing them into serum-free osteogenic medium is the most sensitive stage for ESCs and cell survival is low. Many factors could have affected cell survival but the essential factors identified from the literature that may increase cell survival are listed in Appendix 9.5. These factors and other supplements were used to

create the serum-free medium LWR1.3 (Lennon, Wiles, Randle 1.3), which combines survival factors, specific factors to culture ESCs and an optimised basal media with growth factors to promote osteogenic differentiation. The major problem was the survival and adherence of the disrupted EBs to the tissue culture plastic. Once this was achieved, then the cells could proliferate and differentiate freely. This major hurdle was achieved by adding 15% (v/v) knock out serum replacement and not by addition of any soluble factors, mitogens or other molecules. Knock out serum replacement appears to provide the serum-free medium with the correct osmolarity that ESCs are accustomed to. Knock out serum replacement is designed for use in place of serum for maintaining the pluripotency of ESCs and not used for differentiation. This suggests that it does not contain any mitogens or molecules known to differentiate ESCs. However, it may contain molecules and mitogens at the correct concentrations for undifferentiated ESC maintenance such as BMP4, growth and differentiation factor 6 (GDF6) or muellerian inhibiting substance (MIH) (218-220).

Examining in more detail the serum-formed EBs that were disrupted and placed into the four different media cocktails; on day 5, morphology appeared normal and the cells were approximately 90% viable after disruption, according to the 7-AAD flow cytometric analysis. The disrupted EBs did not form any bone nodules in LWR1.3 serum-free osteogenic medium or in LWR1.3 serum-free osteogenic medium with osteogenic supplements. However, serum-formed EBs did form bone nodules when plated into serum-containing media alone (17±7) or serum-containing medium with osteogenic supplements (56±26), which indicates that osteogenic supplements are capable of inducing a 3-fold increase in bone nodule formation when compared to serum alone to induce

osteogenic differentiation. The figures for bone nodule counts are identical to previous reports (30) when the amount of cells seeded are taken into account. The failure of bone nodule formation (and also high tissue growth) highlights the sensitivity of disrupted EBs when transferring from serum-containing to serum-free medium and justifies this move of this transition to the cell maintenance stage.

The serum-free medium formed EBs (without BMP4) appeared to contain a higher proportion of non-viable cells from confocal images (Figure 3.7). When EBs are formed in serum-free media without the addition of growth factors they are reported, to produce by default, some mesodermal tissue (88;89). When the EBs were disrupted and plated into serum-free medium they did not form any bone nodules. However, if they were plated into serum-containing media then bone nodule formation was similar to the serum controls. This would indicate that serum-containing medium is capable of inducing cells either in a state of quiescence (serum starved) to enter the cycle once again and begin the process of bone nodule formation in the presence or absence of osteogenic supplements.

Finally, our results indicate that EBs formed in serum-free EB formation medium (with BMP4 mesoderm induction) will form bone nodules when disrupted and placed in LWR1.3 serum-free osteogenic medium. These cells were disrupted on day 5 of EB formation and placed into the 4 different types of media for the bone nodule assay. Bone nodules formed in all 4 osteogenic media but to varying extents. The serum alone medium produced 11±13 bone nodules, which was 1.5 fold less than serum controls (serum formed EBs and serum with osteogenic supplements). Serum-containing medium with osteogenic supplements formed 54±25 bone nodules, which were equivalent to

serum-formed EB controls that were subsequently plated into serum-containing medium with osteogenic supplements. Therefore, we can assume that inducing mesoderm with BMP4 in serum-free EB formation medium is as efficient as mesoderm formation using serum-containing medium when comparing bone nodule counts.

The results shown here are the most encouraging and to my knowledge, represent the first report of bone formation using mESCs exclusively in serum-free media without the need for osteogenic supplements. Osteogenic differentiation in serum-free media can only be achieved by maintaining mESCs in serum-free maintenance medium, inducing mesoderm formation with BMP4 in serum-free EB formation medium and inducing osteogenic differentiation with LWR1.3 serum-free medium (2±2 bone nodules). The amount of bone nodule formation when using serum at all stages with or without osteogenic supplements was 5.5-fold and 27-fold less efficient, respectively. The addition of osteogenic supplements to LWR1.3 serum-free osteogenic medium did not increase bone nodule formation (2±2 bone nodules). This indicated that further optimisation of LWR1.3 serum-free osteogenic medium could be achieved by altering the concentration, timing and combinations of growth factors that have already been used or have been postulated in the literature to induce bone nodule formation [e.g. BMPs (228-230) and FGFs (231)]. This could be achieved by Design Of Experiments (DOE) but would be costly and time consuming.

Some other interesting observations were the appearance of other tissue types within the cultures (Figure 3.11). All cultures with bone nodule formation also contained cardiomyocytes, which were beating rhythmically. Their abundance was more noticeable in serum-containing than in serum-free media.

The occurrence of smooth muscle was also apparent when serum-free media was used at all three stages (maintenance, EB formation and osteogenic differentiation). There were also indications of adipocytes due to their size and morphology but further characterisation was not performed. When generating mesodermal tissue one would expect to induce progenitors for cardiac tissue, smooth muscle, fat and skin as well as bone. The growth factors in LWR1.3 have been reported to induce smooth muscle as well as other tissue of a mesodermal origin (210). The smooth muscle was noticeable only in the exclusively serum-free media combination suggesting that cultures with serum or osteogenic supplements may inhibit the progenitors for this tissue lineage. The heterogeneous nature of the culture, even when using the exclusively serum-free medium regime, identifies the need for full control over the differentiation process in order to produce tissue suitable for the clinic.

3.6. Conclusion

It is clear that the development of serum-free medium for mESC and human hESC maintenance and differentiation is a need. The complex nature of serum alters and conceals the effects of exogenous growth factors or inhibitory compounds. The three stages of osteogenic differentiation require slightly modified medium formulations in order to develop the mESCs in the desired manner and transition in the early stages; when the cells are more resilient to extreme changes, is a strategy that will provide successful culture systems.

The strategies used in this study to define medium were guided by previous formulations, findings from developmental biology and either a top-down or bottom-up approach. Previous formulations were useful as a starting point but are either optimised for the previous users' cells or are proprietary information. Using developmental biology as a guide is essential. Information was gleaned from researchers studying *Xenopus laevis* and mouse and human embryology. A top-down approach to medium development is similar to reverse engineering. Find a media formulation that works well (232), discover what is contained within it using differential proteomics (233-237) and deduction, then optimisation for the cell type of interest. This method is more suited to the academic field as intuition and informed decision making play a role. The bottom-up approach (additions to basal medium) relies on an attritional strategy whereby many factors are added in varying concentrations, combinations and with temporal differences. This strategy is both time-consuming and expensive and can provide excellent results, as in drug discovery, but will take time and almost unlimited resources. This strategy is more suited to the pharmaceutical or healthcare industries. However, modifying the bottom-up strategy slightly by

using factorial design decreases the time and effort needed to formulate a successful media.

In short, future ESC medium development in academia should be approached either using factorial design (bottom-up) or proteomics (top-down) because the goal of medium formulation is more likely to be commercial than scientific. A recent finding that the nonhuman sialic acid; N-glycolylneuraminic acid (Neu5Gc) can be incorporated by hESCs and EBs from both the murine feeder layer and medium (163) intensifies the need for chemically defined medium.

4. ESTABLISHMENT AND CHARACTERISATION OF 3D CULTURE METHODOLOGY FOR MESCS

4.1. Introduction

Analysing cell interactions in a more natural 3D environment promises to provide conditions that are closer to what actually occurs naturally, *in vivo* (181;191). Recently, the use of bioreactors for hESC culture has been documented and offered evidence that controlled conditions provide an advantageous environment for the culture of ESCs (192).

The need for improved cultivation methods is driven by the fact that many potential therapeutic applications are limited by the availability of stem cells or their derivatives. Cells in monolayer culture are not generally nutrient-limited. This is because passive diffusion is more than adequate to supply a 10 μm tissue thickness. In contrast, the supply of oxygen and soluble nutrients becomes critically limiting for the culture of tissues that are thicker than 100 – 200 μm (238). In the tissue engineering research community, culture volumes and the amount of tissue produced are typically low. Cell culture protocols and techniques are often fragmented and are not readily scaleable in terms of manufacturing. A major challenge is to translate these research-scale product designs into large-scale production of biologically based products that are reproducible, safe, clinically effective, and are economically acceptable and competitive. In addition, sophisticated technical skill in design and manufacture of the bioreactors and growth process are required, as is an understanding of

the specific challenges encountered in scale-up of the process, and storage and delivery of the final product (239).

Chang *et al.* (240) pioneered bioencapsulation in the 1960's and Lim *et al.* (40) eventually encapsulated xenograft islet cells for implantation into rats to correct diabetes. Alginate is a water-soluble linear polysaccharide extracted from brown seaweed and is composed of alternating blocks of 1-4 linked α-L-guluronic and β-D-mannuronic acid residues. Alginate forms gels with most di- and multivalent cations, although Ca^{2+} is most widely used. Calcium cations take part in the interchain binding between G-blocks and give rise to a three dimensional network in the form of a gel. The binding zone between the G-blocks is often described as the "egg-box model" (241).

Alginate encapsulation has been mainly restricted to adult cells whereas Magyar *et al.* (41) encapsulated mESCs that were able to form discoid colonies, cystic EBs and smooth muscle cells. Since this study, 3D ESC culture has become a topical issue and there are publications regarding 3D rhesus monkey ESCs (242), 3D hESC differentiation (243;244), osteogenic differentiation from mESC and then 3D culture (245), EB formation from mESCs leading to 3D chondrogenic culture (208;246) and shear controlled mESC expansion leading to EB differentiation (247). However, all these systems rely on fragmented, high maintenance, manual culture protocols to generate either the starting material or the endpoint tissue. Most of the protocols cite historical references for the choice of 3D scaffold or culture system but it appears that testing or exploration of these parameters has not been investigated to great length using ESCs.

Chondrogenic differentiation from MSCs encapsulated in alginate beads, has been reported (206) and, more recently, alginate with gelatin have been considered to provide a biodegradable delivery vehicle for tissue engineering

applications (248). Normally, alginate hydrogels lose Ca^{2+} cations after prolonged culture, but the incorporation of gelatin enables cell-mediated contraction and packing of the scaffold material (207).

4.2. Aim

- To form 3D tissue within characterised alginate beads suitable for scale-up and ultimately 3D bone formation.

4.3. Materials and methods

4.3.1.1. Calcium distribution staining

Beads were formed according to Section 2.2.4 and blotted on fibre-free paper (Whatman, UK) as excess water would cause ice crystal formation. A metal boat (5 x 5 mm) was formed from aluminium foil in order to hold the bead. Optimal cutting temperature (OCT; Tissue-Tek®, UK)-compound was then added to the boat to cover the bead. In a Pyrex vessel, isopentane (BDH Laboratories, UK) was frozen solid in liquid nitrogen, removed and allowed to warm at room temperature (21°C). Once the isopentane warmed to a liquid state, the metal boat was lowered into the isopentane (not immersed) and allowed to freeze. The bead was then sectioned (10 µm) using a cryostat, attached to poly-l-lysine coated slides (BDH Laboratories, UK) and allowed to dry for 30 minutes. The sections were then stained with ARS as previously described (Section 2.3.2.3).

4.3.1.2. Single cell encapsulation

Undifferentiated, day 3, mESCs were trypsinised, counted, and resuspended at 1 x 10^6 cells/mL in 0.2 µm sterile filtered, room temperature (21°C), 1.1% (w/v)

low viscosity alginic acid (Sigma, UK) and 0.1% (v/v) porcine gelatin (Sigma, UK) (in PBS at pH 7.4) solution. The suspension was transferred to the container of a commercially available, pump-action, atomiser and sprayed onto the surface of a sterile solution at room temperature (21°C), 100 mM calcium chloride solution ($CaCl_2$; Sigma, UK) and 10 mM N-(2-hydroxyethyl) piperazine-N-(2-ethane sulfonic acid) (HEPES; Sigma, UK), in distilled water at pH 7.4. Gelled microbeads, ranging in size between 40 and 200 µm were then quickly isolated using cell strainers and were washed twice in PBS. Single-cell containing microbeads were then selected under an inverted phase microscope and transferred to maintenance medium in 96-well plate wells. The same dissolution buffer in Section 2.2.5 was used but the microbeads were dissolved *in situ*, by transplantation into new chamber slides and cultured or stained accordingly.

4.3.1.3. SDS-PAGE

Sodium dodecylsulphate-polyacrylamide gel electrophoresis (SDS-PAGE) is used to assess the purity and molecular weight of proteins of interest. Migration distances of proteins within the gel is based on the electric current, the pore size of the gel and more importantly, the size (molecular weight) of the proteins of interest (smaller proteins migrate faster). This technique was used to assess the permeability of alginate beads. Essentially, the proteins are dissociated before use and those denatured polypeptides bind SDS and become negatively charged. The amount of SDS is proportional to the molecular weight, enabling efficient protein size separation.

Briefly, 500 alginate beads (without cells) were exposed to neat FCS (Invitrogen, UK) for 24 hours and washed once in PBS to remove any excess FCS from the outer surface of the alginate bead. The beads were then

dissolved in 5 mL of dissolution buffer and kept at 4 °C until needed. The FCS remaining within each bead would give an indication of the permeability of the alginate beads that were tested when compared to neat FCS and a broad range, molecular weight standard (Bio-Rad, UK). The molecular weight standard includes myosin (200 kDa), β-galactosidase (116.25 kDa), phosphorylase b (97.4 kDa), serum albumin (66.2 kDa) and ovalbumin (45 kDa).

A 6% (v/v) acrylamide resolving gel was chosen in order to separate proteins over a broad range, approximately between 45 and 170 kDa. 10 mL of resolving gel was made up according to standard protocols (249) and consisted of 5.3 mL of deionised water, 2 mL of 30% (w/v) acrylamide and N,N'-methylene-bis-acrylamide (Bio-Rad, UK), 2.5 mL of 1.5M Tris base (pH 8.8; Sigma, UK), 0.1 mL of 10% (w/v) sodium dodecylsulphate (SDS; Sigma, UK), 0.1 mL of 10% (w/v) ammonium persulfate (Sigma, UK) and 0.008 mL of N,N,N',N'-tetramethylethylenediamine (TEMED; Sigma, UK). This solution was mixed gently (by tipping 30 times) in a 15 mL centrifuge tube and then pipetted into a vertical electrophoresis tank (Bio-Rad, UK) and overlain with 0.1% (w/v) SDS at left to set for 30 minutes at room temperature (21°C). The SDS was then aspirated and washed 3 times with deionised water and all liquid was removed from the top of the gel. 3 mL of 5% (w/v) stacking gel, which was prepared using 2.1 mL of deionised water, 0.5 mL of 30% (w/v) acrylamide and N,N'-methylene-bis-acrylamide (Bio-Rad, UK), 0.38 mL of 1M Tris base (pH 6.8; Sigma, UK), 30 µL of 10% (w/v) SDS (Sigma, UK), 30 µL of 10% (w/v) ammonium persulfate (Sigma, UK) and 3 µL of TEMED was then added on top of the resolving gel and a Teflon comb inserted for 30 minutes. The tank was

filled with Tris-glycine electrophoresis buffer (25 mM Tris, 250 mM glycine at pH8 .3) and 0.1% (w/v) SDS.

Protein samples were diluted to the same concentrations and boiled for 3 minutes at 100 °C. 20 µL of each sample was added to 20 µL of Laemmeli sample buffer (Bio-Rad, UK) with 5% (v/v) β-mercaptoethanol (Sigma, UK) and 20 µL of this solution was loaded in the gel. The gel was run at 80V and then stained with 0.25% (w/v) Coomassie Blue R-250 (BDH, UK) in methanol:acetic acid solution, at room temperature (21°C) for 4 hours while gently rocking. The gel was then destained with the methanol:acetic acid solution for 4-8 hours (changing solution 3 times) and then stored and sealed in 20% (v/v) glycerol solution, until photographed.

4.4. Results

4.4.1. Encapsulation

4.4.1.1. Bead diameter

Hypodermic needle diameter determined bead size and 50 beads were created using the established equipment parameters. Five beads were measured after 1 hour in DMEM to allow slight swelling and the same five beads were measured after 7 days in static DMEM. Horizontal and vertical diameters were measured for each bead and the horizontal / vertical diameter (H/V) ratio determined the sphericity. The 25G needle produced beads that were 2402 ± 103 µm before culture and 2441 ± 84 µm after culture in DMEM for 7 days where swelling was only approximately 39 µm. The 25G mean bead sphericity (H/V) was very close to 1 before (0.97) and after (0.98) culture. Smaller beads provide better mass transfer due to the smaller distance from media to core

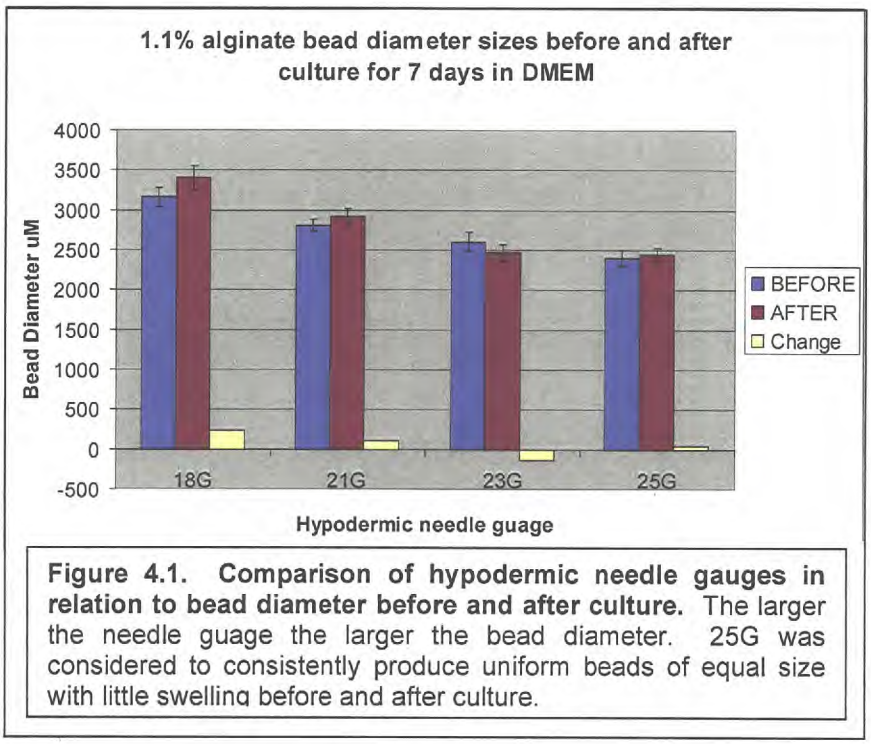


Figure 4.1. Comparison of hypodermic needle gauges in relation to bead diameter before and after culture. The larger the needle guage the larger the bead diameter. 25G was considered to consistently produce uniform beads of equal size with little swelling before and after culture.

therefore the 25G was selected for further experiments (Figure 4.1). It was now clear that the 25G needle would be used for further experiments.

4.4.1.2. Bead swelling/contraction

The average (alginate-gelatin) bead size after 1 hour in medium was 2303±70 µm in diameter (volume = 6.4 µL or 6.4 mm^3) using 1000 cells per bead and was almost identical using other cell densities (Figure 4.2). After 4 days of incubation, alginate-gelatine beads became significantly larger ($P<0.0001$) with a diameter of 2394±95 µm. (Appendix 9.6). In contrast, alginate beads without gelatin produced variable bead diameters before and after culture that were not suitable for future use (Figure 12a). A single bead (alginate+gelatin) was made up of 6.4 µL of cell-gel solution, which was confirmed using 1 mL of cell/gel

solution producing 154 beads (~6.49 µL/bead). The discrepancy between the calculated volume (6.4 µL/bead) and the measured volume (6.49 µL/bead) was acceptable because each bead appeared to possess a small "tail" that was an artefact of the drop process and was not taken into account in the calculated figure. Therefore, it was clear that cell/gel solution was not lost in the bead formation process and initial volume of cell/gel solution was a suitable means by which to estimate the number of beads formed.

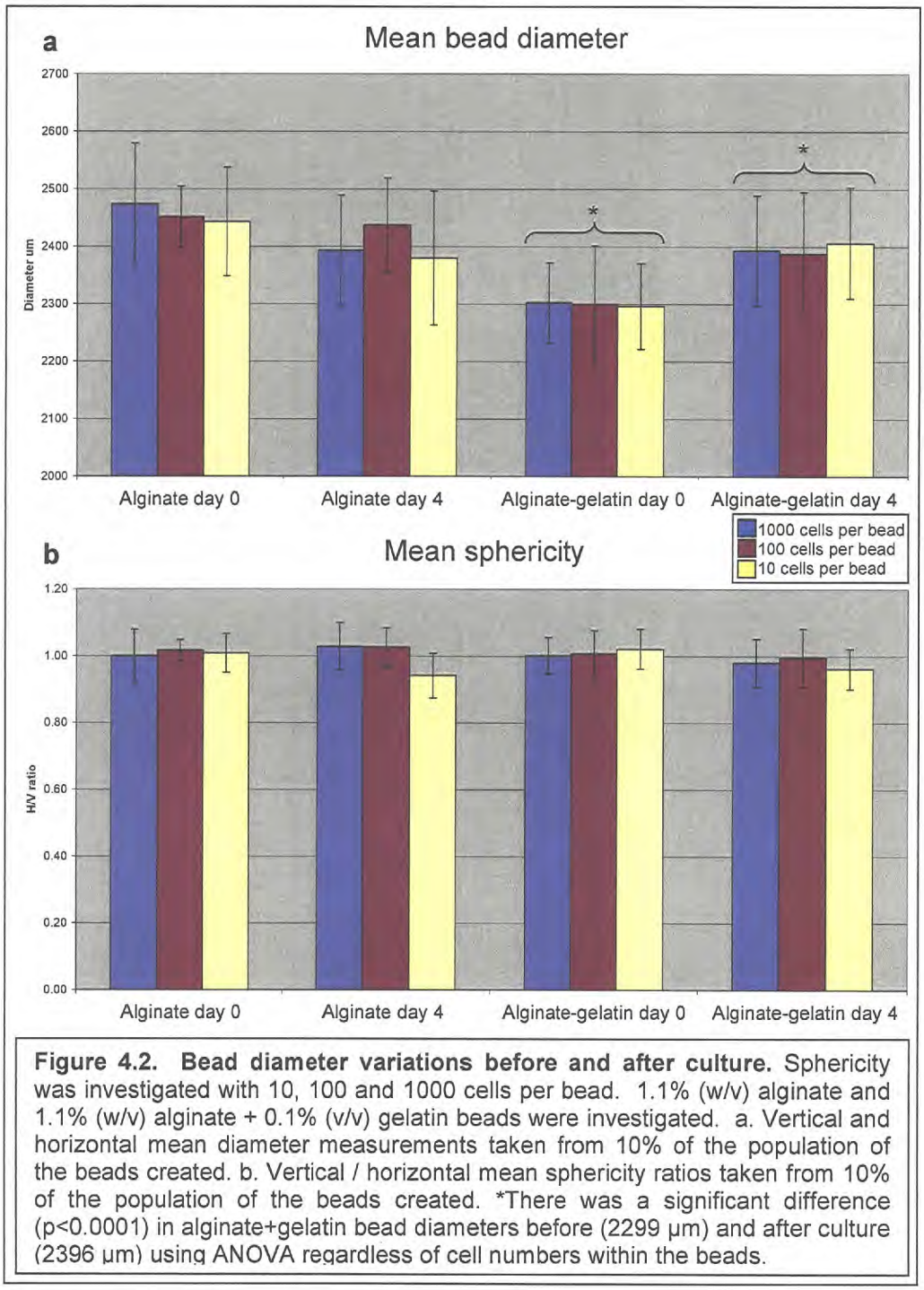


Figure 4.2. Bead diameter variations before and after culture. Sphericity was investigated with 10, 100 and 1000 cells per bead. 1.1% (w/v) alginate and 1.1% (w/v) alginate + 0.1% (v/v) gelatin beads were investigated. a. Vertical and horizontal mean diameter measurements taken from 10% of the population of the beads created. b. Vertical / horizontal mean sphericity ratios taken from 10% of the population of the beads created. *There was a significant difference ($p<0.0001$) in alginate+gelatin bead diameters before (2299 µm) and after culture (2396 µm) using ANOVA regardless of cell numbers within the beads.

4.4.1.3. Bead permeability

All beads were placed into 6 well plate wells and incubated at 37 °C overnight in neat FCS with or without shaking. Neat FCS was used as a control. The staining method used allows the detection of as little as 10 µg of protein. Beads incubated without shaking only contained proteins in one of the replicates which

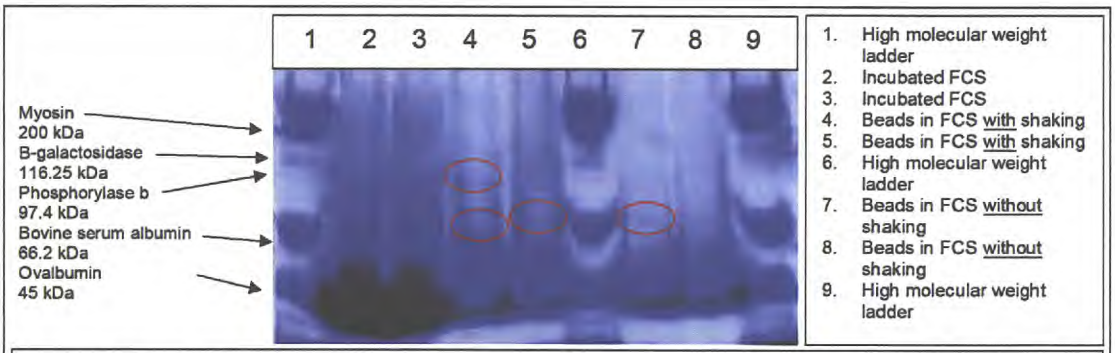


Figure 4.3. SDS-PAGE gel indicating macro bead permeability. Neat FCS shows a large amount of protein in the entire range whereas macro beads with shaking allow proteins up to 97.4 kDa.

had a molecular weight of 66.2 kDa (Figure 4.3). However, with shaking, the beads contained proteins with molecular weight of 66.2 kDa in both replicates and 97.4 kDa in one replicate. Therefore, with shaking or simply a dynamic environment, the beads allow proteins of at least 66.2 kDa in size, possibly up to 97.4 kDa to permeate. Bead heterogeneity is inherent during manufacture as beads remain in calcium chloride for 6-10 minutes which may affect porosity.

4.4.1.4. Bead morphology

The 25G needle size was selected and the protocol to manufacture these beads is listed in Section 2.2.4. This bead type was characterised further in order to assess the distribution of calcium throughout the bead along with the

architecture. From this point onwards all beads unless otherwise stated were manufactured according to Section 2.2.4.

4.4.1.5. Calcium distribution

Beads without cells were embedded, cryosectioned and stained with Alizarin Red S. Figure 4.4 is a section through the centre of a bead and illustrates the distribution of calcium within the bead which is predominantly around the periphery or superficial crust. These findings agree with the published literature and confirm the higher concentrations of alginate bound to calcium in the strong gelled zone (2).



Figure 4.4. Calcium distribution within an alginate bead. Visualised with Alizarin Red S stain, x4 objective, approximately 2.3 mm diameter

4.4.1.6. Scanning Electron Microscopy (SEM)

Beads were dehydrated and imaged in a similar manner found in the literature (250). The beads were completely dehydrated and reduced in size 4-fold. The high power SEM image was similar to a 1% (w/v) alginate bead created in the same manner (250) in terms of surface topography (Figure 4.5). The beads

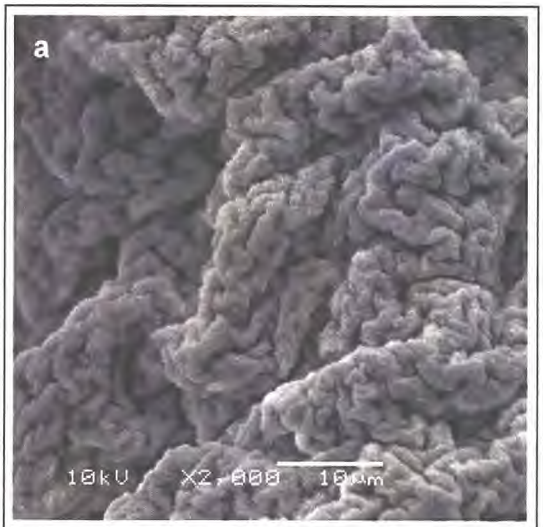


Figure 4.5. High powered SEM of dehydrated alginate beads. a. 1.1% (w/v) low viscosity alginate + 0.1% (v/v) porcine gelatin alginate bead.

almost completely collapsed under the vacuum of the SEM and pore size could not be established.

4.4.2. 3D cell culture

Encapsulating 5 x 10^6 cells per mL of 1.1% alginate solution, based on literature reports (41), gave an extremely high cell density per bead but did indicate that a single cell suspension would form cell clumps within the beads after 14 days of culture (Figure 4.6). The high number of cells per bead would limit colony expansion if cultured for up to 30 days for the bone nodule assay (30).



Figure 4.6. Macroscopic image of mESCs encapsulated and grown in alginate. mESCs cultured for 3 days in maintenance medium and then a further 11 days in differentiation medium (Static 14 days) x4.

4.4.2.1. Short term viability

It was clear from the bead measurements that alginate with gelatin inside the bead provided a bead that could be produced in a uniform manner. The incorporation of gelatin was initially added to provide an environment that would be conducive for mESCs survival and to maintain the undifferentiated phenotype (212). Alginate beads with or without gelatin were able to support the culture of viable mESCs for 3 days. Figure 4.7 gives an indication of the viability of cells from day 0 to day 3. Each bead contained approximately 1,000 uniformly distributed cells that were almost 100% viable, throughout the bead. By day 3, all beads had noticeable, viable colonies up to 50 μm in diameter.

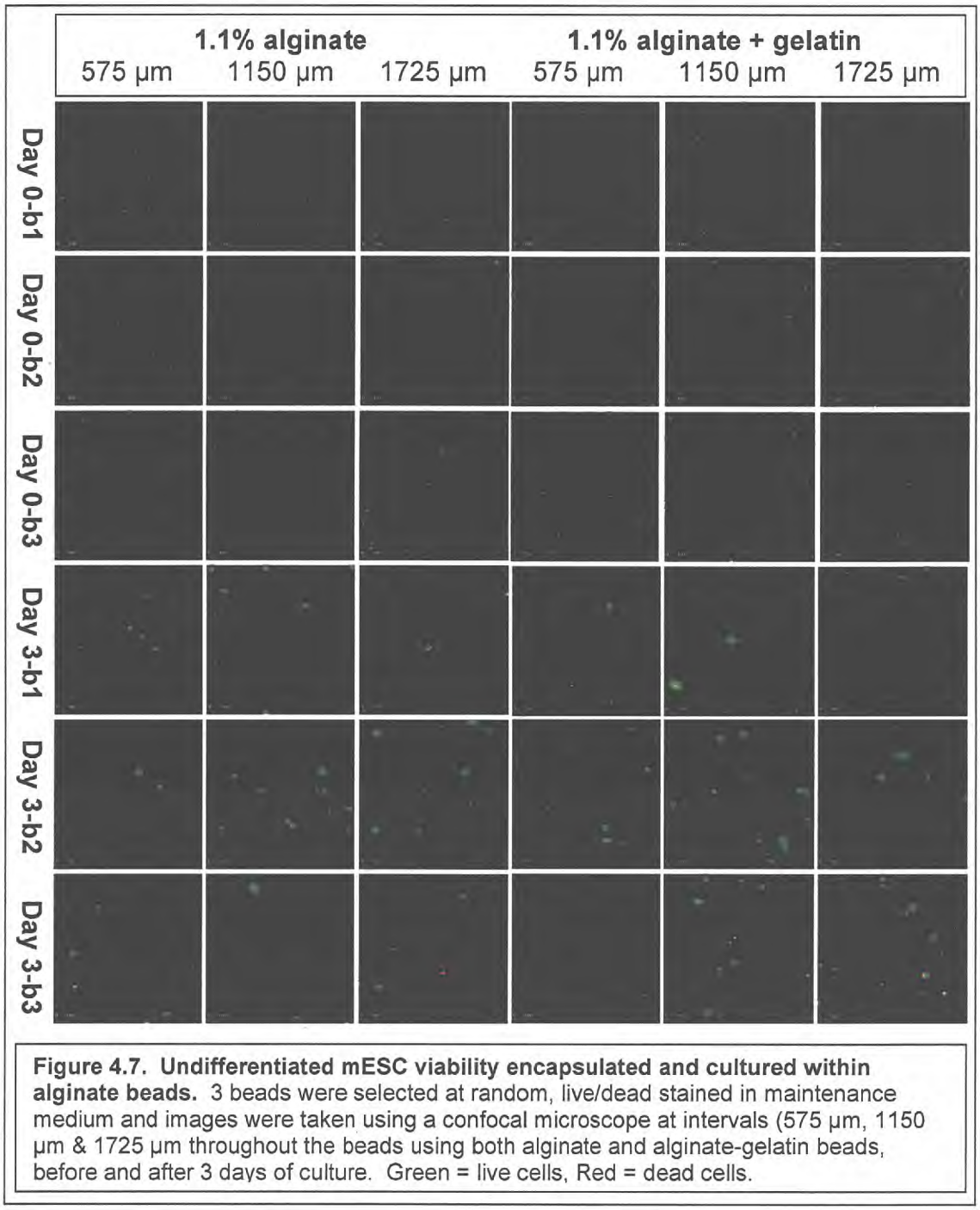


Figure 4.7. Undifferentiated mESC viability encapsulated and cultured within alginate beads. 3 beads were selected at random, live/dead stained in maintenance medium and images were taken using a confocal microscope at intervals (575 µm, 1150 µm & 1725 µm throughout the beads using both alginate and alginate-gelatin beads, before and after 3 days of culture. Green = live cells, Red = dead cells.

4.4.2.2. 3D culture and maintenance of pluripotency

Undifferentiated mESCs were trypsinised and placed into 2D gelatin (static) and 3D alginate-gelatin beads (static) at approximately 1000 cells per bead. Maintenance medium was changed every day and the cells were trypsinised or released from the beads on day 3. A viability stain was also performed to ensure cell viability was high within the beads on day 0 and day 3 (Figure 4.8). On day 3, 2D cultures were trypsinised and 3D beads were dissolved and the cells replated in 2D culture for a further 3 days in maintenance medium. On day 6 the mESC colonies were fixed and immunostained for CD9 and Oct-4 and imaged using confocal microscopy (Figure 4.8). In summary, mESCs encapsulated and maintained in alginate-gelatin beads retained almost 100% viability when cultured for 3 days in static culture (Figure 4.7). Upon release, tightly packed, 3D, spherical mESC colonies (approximate diameter of 70 μm) containing around 12 to 14 cells, formed undifferentiated 2D colonies when cultured for a further 3 days in maintenance medium upon gelatin-coated tissue culture plastic.

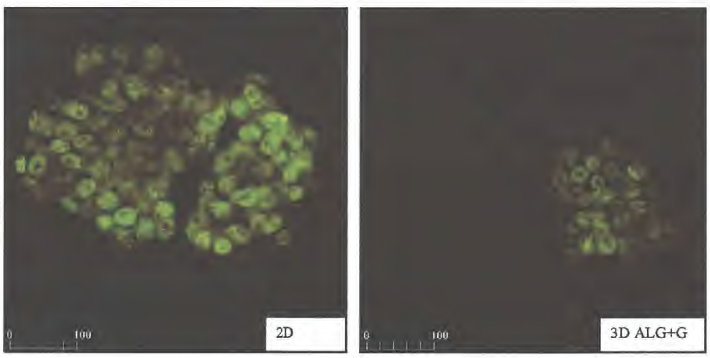


Figure 4.8. 2D Confocal undifferentiated mESC colonies Oct-4 (Green) and CD9 (Red). Cells from 3D culture were able to form undifferentiated 2D colonies after 3 days, identical to 2D controls. x25.

4.4.2.3. Single cell encapsulation: clonality

Micro beads were manufactured in collaboration with Dr Nick Evans (251). The overall aim was to study stem cell development and also develop a high-throughput screening platform. Single cells encapsulated within individual

beads survived for 10 days and formed colonies within these beads. The single cells that survived (23 out of 41) and remained viable formed similar colonies to that shown in Figure 4.9. Firstly forming a polar body (Day 2), and then dividing

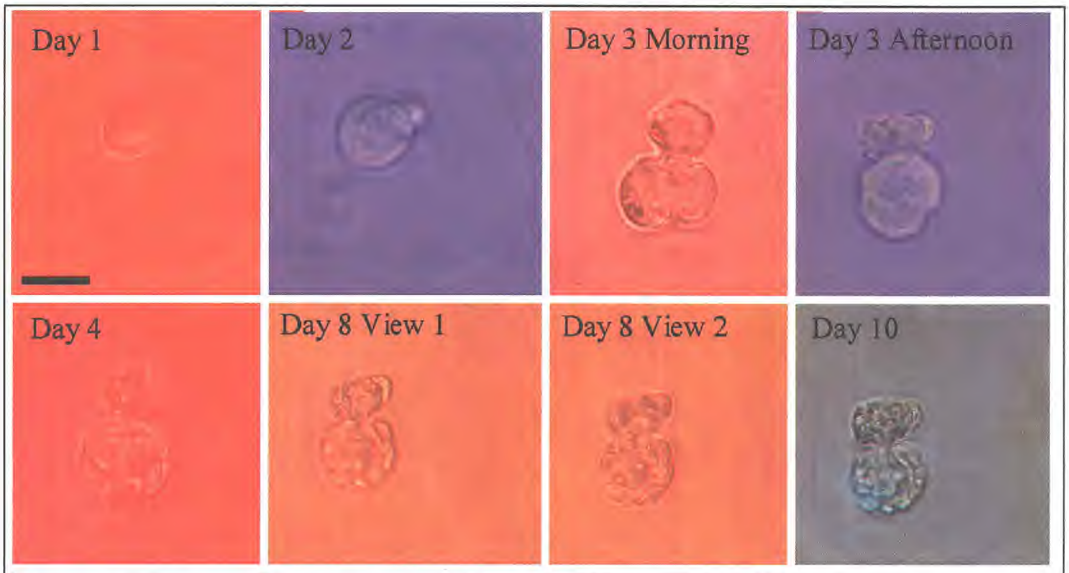


Figure 4.9. Single undifferentiated mESCs encapsulated and cultured within microbeads. A single cell was encapsulated within a microbead (~60 µm diameter) and cultured for 10 days in maintenance medium. Scale bar = 25 µm.

to form a structure of one to three cells (colony) that were intimately connected. Finally, the colony then appears to undergo compaction by day 4 until day 10. However, some single cells would form the intimately linked colonies and then form a structure such as that shown in Figure 4.10, day 8.

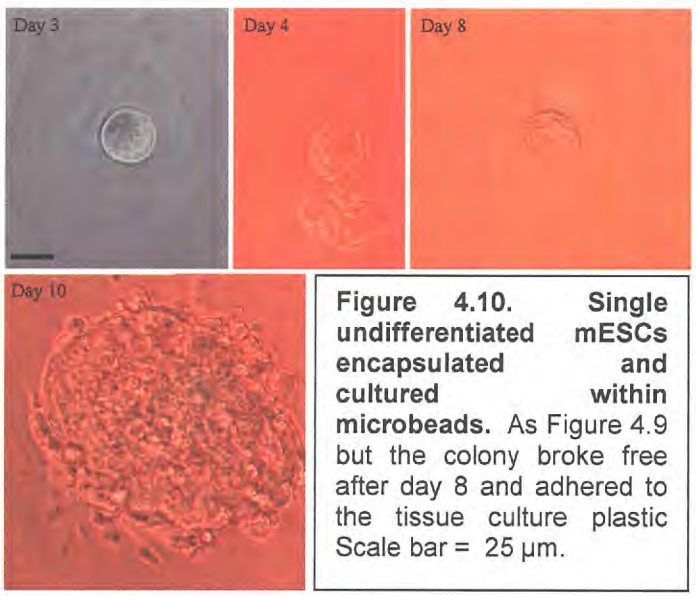


Figure 4.10. Single undifferentiated mESCs encapsulated and cultured within microbeads. As Figure 4.9 but the colony broke free after day 8 and adhered to the tissue culture plastic Scale bar = 25 µm.

Positive control macro beads were also cultured at the same cell density (Figure 4.11).



Figure 4.11. Undifferentiated mESCs encapsulated and cultured within macrobeads. Encapsulated at the same cell density as microbeads. Scale bar = 50 µm.

After 10 days, the individual beads were disrupted and plated for a further 3 days and exhibited markers of pluripotency (Figure 4.12). Therefore, undifferentiated single mESCs cultured in maintenance medium retained their characteristics once released from the beads, similar to the macro beads.

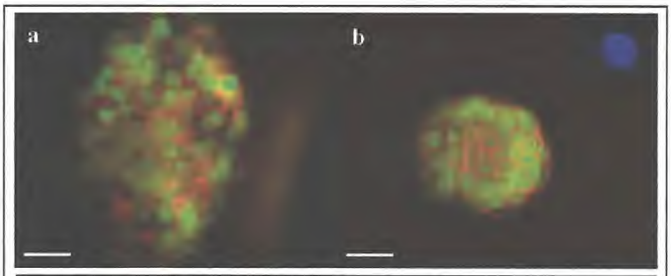


Figure 4.12. Undifferentiated mESCs immunostained for pluripotent markers after release from beads on day 10. DAPI, Oct4 (green) and CD9 (red) after 3 days of 2D culture. a. released from macrobeads. b. released from microbeads Scale bar = 50 µm.

4.4.3. 3D static prolonged culture (37 °C encapsulation temperature)

It was clear that prolonged culture was possible and the beads were robust enough to support long-term culture. Simple experiments using beads without cells in shaking culture remained intact for at least 30 days. However, it was considered beneficial for cell viability that the temperature at which the beads were formed should be changed from room temperature (21°C) to 37 °C. This was not based on any scientific evidence and published protocols do not specify the temperature of encapsulation. Both the alginate and the $CaCl_2$ were pre-warmed and beads were allowed to form. It is now clear that this small change, considered beneficial for cell viability upon encapsulation was detrimental to cell

viability in the long term. Cells were encapsulated as described previously (Section 2.2.4) with the temperature at encapsulation altered from room temperature (21°C) to 37 °C. The beads were cultured for 29 days to induce bone formation (30), in static conditions alongside 2D controls.

4.4.3.1. Tissue morphology

3D beads grown in static culture resulted in only around 10 out of 600 (~2%) beads that would permit limited cell expansion after the first 5 days, judging by morphology alone (Figure 4.13). After 18 days of culture 2D controls were growing as previously described whereas only 1 bead of out 600 formed a colony within it. The colony formed at the edge of the bead and eventually penetrated the surface (Figure 4.14&6). H&E and ARS staining showed that tissue had formed in 3D static conditions that was heterogeneous and that dark regions, deep within the tissue may have formed 3D mineralised aggregates (Figure 4.15&6). The temperature of encapsulation and its effects on cell viability were investigated further (data not shown). A 37 °C encapsulation temperature was therefore considered detrimental to cell survival within the first 3 days of culture, in any culture vessel and room temperature (21°C) encapsulation was re-instated for all further investigations from this point onwards as stated in Section 2.2.4.

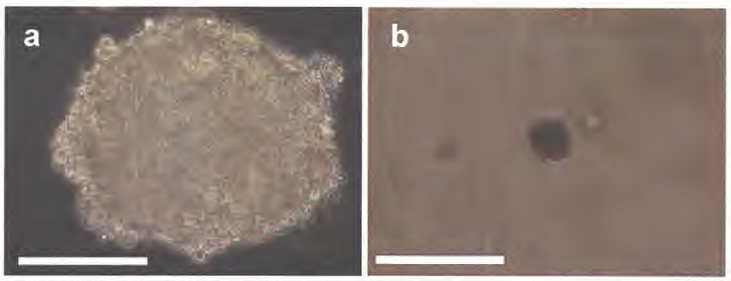


Figure 4.13. Morphological images of day 5 static cultures. a. 2D static (day 2 of EB formation) b. 3D static. Scale bar = 100 µm.

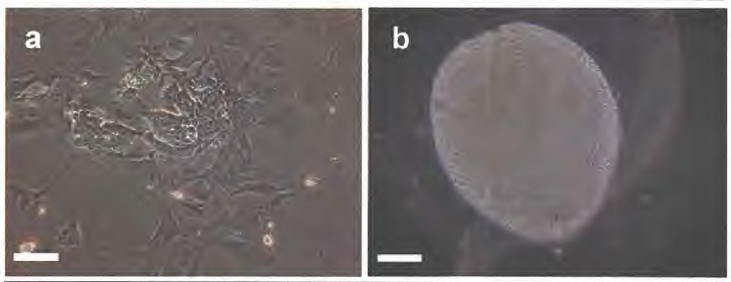


Figure 4.14. Morphological images of day 18 static cultures. a. 2D static (day 10 of bone nodule formation) b. 3D static. Scale bar = 100 µm.

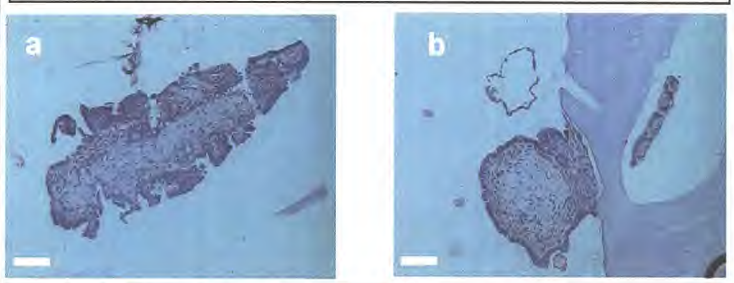


Figure 4.15. H&E images of day 29 static cultures. a. 3D static (day 21 of bone nodule formation) b. 3D static. Scale bar = 100 µm.

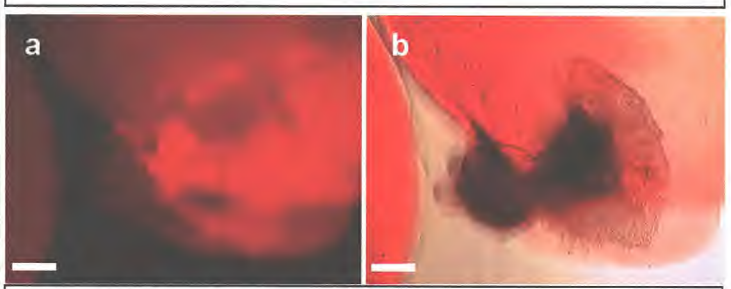


Figure 4.16. Alizarin Red S images of day 29 static cultures. a. 3D static red fluorescence and indication of bone formation b. 3D static phase contrast ARS image. Scale bar = 100 µm.

4.5. Discussion

The process of bead formation was adapted from various sources (40;41;252) to create a reliable and reproducible bead manufacturing process. These initial investigations were initiated in order to simplify and standardise mESC culture and osteogenic differentiation with scale-up in mind. Eventually, this would lead to a process suitable for 3D mineralised tissue / bone formation and online monitoring in order to define and optimise large-scale tissue production.

Firstly, the encapsulation process was empirically determined here in order to provide a simple, reproducible model for mESCs and long-term integrated culture to form bone tissue. Bead diameter was an important factor to consider in 3D culture as mass transfer of nutrients and metabolites would obviously be affected by this physical characteristic. As has been shown in bioreactor culture with hESCs without scaffolds or cellular vehicles, large tissue clumps necrose in their centres due to diffusion limitations (192). However, the only means by which to control bead diameter was to alter the gauge of the hypodermic needle; the higher the gauge, the smaller the bead diameter. This was successful and a 25G needle produced beads, without cells, that were 2402 ± 103 μm in diameter before culture and 2441 ± 84 μm after culture with almost perfect sphericity. Similar publications used varying needle sizes with no real discernable reasons for choice [22G, (252) and 16G, (206)] apart from that they actually allowed viable cell growth.

Gelatin was also used as a material to form beads due to its use in 2D cell culture of mESCs (212). The alginate-gelatin co-polymer beads were uniform in size and sphericity, before and after culture, regardless of the number of cells encapsulated within them. Cell density within the bead appeared too high using the recommendations from the literature (41) and a

range of cell numbers per bead was investigated to enable culture for extended periods of up to 30 days without causing overcrowding. With the addition of different cell densities and gelatin to the beads, the average bead diameters became increasingly uniform to manufacture and 2.3 mm diameter was considered an acceptable one to work with.

Of course, the limiting factor for smaller bead sizes was water surface tension and the hydrogen bonding that occurs between water molecules. Without the use of a harmonically vibrating nozzle (200;253-255), bead size was limited to droplet size from a hypodermic needle. However, a solution to this problem was investigated through a simple spraying technique (251) to produce micro beads.

The natural corollary to bead diameter and mass transfer considerations was bead permeability. Knowing the pore size and pore connectivity is necessary in order to ascertain whether cells encapsulated within the alginate beads have access to all the nutrients in the external medium and also whether toxic metabolites, produced by the cells, are able to perfuse through the bead. Permeability was investigated in a number of manners including light microscopy, micro-CT and SEM but these techniques have problems with visualisation, contrast and the use of a vacuum respectively. Environmental or wet SEM was considered but this was not available and the only other mechanism to determine permeability was with SDS-PAGE. Beads, similar to those manufactured in this thesis, were found to be permeable to molecules up to 68 kDa which would easily allow the diffusion of LIF (256) for example, which ranges in size from 20-60 kDa (257;258). The beads in this study allowed the passage of 66.2 kDa proteins and possibly as large as 97.4 kDa. The six most abundant proteins in serum are α1 – antitrypsin (52 kDa), albumin (66 kDa),

transferrin (80 kDa), IgG (150 kDa), IgA (180-500 kDa) and IgM (950 kDa) that represent more than 90% of total protein (259). This, of course is suitable for conventional cell culture and also restricts immunoglobulins entering the alginate beads upon implantation (201;208;260) in cell therapy.

Further characterisation of the beads was performed and revealed that high concentrations of calcium, detected by Alizarin Red S stain (detects calcium bound to an anion), were found in the periphery of the beads. This region is made up of the superficial crust and the strong gelled zone where most of the alginate and calcium are located. Where this zone ends, is the beginning of the sol-gel transition from gel in the strong gelled zone to a solution in the medium gelled zone (2).

The surface topography of the beads used in this study were similar to those produced in the literature (250). It is known that pore size in similar beads, on the external surface is approximately 0.5 - 1 μm in diameter (261), which relates to between 66.2 kDa and 97.4 kDa from the permeability analysis performed in this thesis. This, also indicates that mESCs (>20 μm in diameter) are not capable of leaving the beads when encapsulated unless they do so through growth and mechanical pressure. It has been noticed that small, finger-like projections form, from individually encapsulated cells and may be the result of small pores, unable to accommodate 3D growth (Appendix 9.10).

Undifferentiated mESCs that were encapsulated within the alginate-gelatin beads were 100% viable after around 1 hour from encapsulation in serum-containing maintenance medium. After three days in static culture the immobilised cells formed 3D colonies (consisting of approximately 12-14 cells) that were again almost 100% viable. 3D colonies were released from the beads and cultured for another 3 days (effectively a passage) on 2D gelatin coated

plates. The colonies that were generated exhibited the pluripotency markers, Oct-4 and CD9. Therefore, encapsulation did not affect the cells' ability to be maintained in an undifferentiated state.

Forming 2D bone nodules involves maintenance of the undifferentiated cells for three days, EB differentiation for 5 days and osteogenic differentiation for a further 21 days (29 days in total). These phases involve culture in tissue culture flasks, bacteriological grade plates and tissue culture plastic plates, respectively. A logical argument existed for the encapsulation of undifferentiated mESCs in alginate beads, in terms of the integration of ESC culture towards the formation of 3D bone. From the literature, traditional culture methods relied on the fact that EB formation was essential for osteogenic differentiation (30;31;262). However, traditional culture methods are not suitable for scale-up as they are fragmented, require operator judgement and are labour intensive. A simplified, integrated process capable of forming 3D mineralised tissue was needed. It was clear from our initial observations that culture of encapsulated undifferentiated mESCs, for 29 days was possible and that mineralised tissue could potentially be formed. However, the formation of beads at 37 °C instead of room temperature (21°C) and culture in static conditions for 29 days prevented high numbers of cells surviving. The increased temperature of 37 °C at encapsulation probably caused the reaction kinetics between alginate and calcium to increase significantly and form beads that were stronger and less porous. Room temperature (21°C) is recommended for the calcium-alginate gelation process to occur (2) but studies have not been conducted, to my knowledge, that have investigated this in detail. Commercial food manufacturing companies recommend altering the calcium concentration

to alter the reaction-diffusion process but do not discuss temperature as a major contributing factor (263).

Micro encapsulation was addressed using the spray technique with a view to studying stem cell development and the establishment of high-throughput assays. Micro encapsulation provided an incite into individual ESC division and the issue of clonality: whether single ESCs can form clones and whether it will form one or multiple 3D mineralised aggregates. Single mESCs have previously been isolated through dilution for experimentation (211) and hESCs have been discovered to exclusively divide through symmetric division by using time-lapse photography (116). These 3D methods, although useful, provide limited material to work with whereby limited characteristics can be assayed. The techniques developed in this body of work allow the user to monitor cell viability, division, without the need for sophisticated equipment and also allow the user to be sure that they start with a single cell, unlike dilutions. ESC populations are heterogeneous in terms of "stemness" and this technique may even provide a unique platform for the use of stem cells in high-throughput screening for drugs or toxic substances (168;251).

4.6. Conclusion

The most informative study on alginate bead characterisation concludes by informing us that: a multitude of microenvironments coexist inside a gel bead (gradient of matter, unequal cell distribution, evolving and dynamic characteristics of nutrients and metabolite diffusion, irregular residual electrostatic fields, etcetera), the consequence being a multiplicity of behavioural responses because of the inherent constraints generated around the confined cells (2). This view is tantamount to what occurs *in vivo* and will

allow us, with optimisation of bead manufacture techniques, to produce microenvironments in which complex, functional tissues can form.

The characterisation of any culture system is paramount before use and is an exhaustive process, similar to media formulation. However, within the constraints of a study such as this, one may halt characterisation in order to provide results with meaning. Further characterisation of this encapsulation system is vital before functionally and clinically acceptable methods of manufacture are acceptable to regulators. Simple bead characteristics were tested, based on literature examples and manipulated in order to provide a system that would be conducive for mESC maintenance, expansion, development and osteogenic differentiation. The macro and micro beads defined in this chapter provide useable models, as a platform for large-scale tissue manufacture and high throughput screening, respectively.

Macro bead model extension and 3D mineralised tissue formation is continued in chapter 5 but micro bead manufacture was not continued any further in this study but resulted in successful achievements (251). Extending micro encapsulation will rely on the invention of new or adapted techniques from conventional assays in order to monitor and analyse these culture systems. Tangible techniques are available such as time-lapse photography (116), single cell encapsulation (264;265), single cell RT-PCR (266-268), advances in electrophoresis such as the capillary method (269;270) and viability/protein assays (www.onecell.com).

5. 3D BONE FORMATION

5.1. Introduction

2D, traditional culture dishes are the most widely used vessels in use in tissue engineering. They provide sterility, are simple and easy to use and economical to manufacture. However, the culture dish requires individual manual handling for medium exchange, cell seeding, which ultimately limits its usefulness when large numbers are required. Scale-up of the culture dish would involve creating many culture dishes and not increasing the size of each dish (239). In contrast, the spinner-flask bioreactor is a simple cylindrical glass container with a stirring element located at the bottom of the tank that ensures the mixing of the liquid culture medium. Despite its simple geometry, this culture system generates a complex flow environment. Moreover, spinner flasks may be fitted with ports and filters for gas exchange, and hence may constitute a more "closed system" than conventional dishes and flasks. However, they suffer from similar drawbacks in terms of requirements for individual handling and difficulty of scale-up (239). The flow environment within such bioreactors is not only unsteady but also turbulent. Turbulent flow has been verified by the experiments discussed later. In order to measure the amount of mixing and turbulence in the spinner flask the Reynolds number was used as a means by which to quantify mixing.

A rotating wall bioreactor known as a high aspect ratio vessel (HARV) was developed by NASA to study tissue and cellular engineering in a low-shear, non-turbulent, simulated microgravity environment. This rotating wall bioreactor has a large radius-to-depth ratio providing a substantial surface area on the rear face for gas exchange through a gas-permeable membrane (271). Previous

analysis (272) proposed that the simultaneous gravitational, buoyant, centrifugal, coriolis, and drag forces combine to produce a "near static" condition or constant freefall. The direction of the gravitational force changes cyclically in the rotating frame and, over one revolution of the reactor, the cells experience an average gravitational force of near zero, thereby leading to what has been described as the simulated microgravity environment (271).

Currently there exists no procedure that allows the integrated culture, expansion and differentiation of ESCs under dynamic, 3D conditions towards the osteogenic lineage. Chaudhury *et al.* (273) showed that mESCs induced to differentiate to form osteogenic precursors were capable of forming 3D mineralised tissue when seeded on to scaffolds and cultured in osteogenic medium. However, this did not provide a means by which to integrate the entire developmental transformation from undifferentiated mESCs to 3D mineralised tissue. In addition, a more recent study has investigated the use of single-step mESC expansion and EB-based differentiation but still did not utilise an integrated approach (247).

Bone is a complex highly structured mechanically active 3D tissue composed of cellular and matrix elements. The true biological environment of a bone cell is thus derived from a dynamic interaction between responsively active cells experiencing mechanical forces and a continuously changing 3D matrix architecture. Flow perfusion culture of marrow-stromal osteoblasts permits the generation and study of 3D, actively modelled, mineralised matrix and can therefore be a valuable tool for both bone biology and tissue engineering (39). Moreover, it has also been shown that flow perfusion culture alone induces osteogenic differentiation of rat MSCs and that there is a

synergistic effect of enhanced osteogenic differentiation when both dexamethasone and flow perfusion culture are used (36).

Botchwey *et al.* (193) have shown that the combination of appropriately designed 3D microcarrier scaffolds and fluid flow through and around the scaffolds during HARV rotation enhances the elaboration of 3D mineralised bone matrix by osteoblast-like cells. They have also shown through theoretical and experimental methods that osteoblast-like cells grew extensively in the interior regions of their scaffolds and retained their osteoblastic phenotype as measured by ALPase activity. In addition, flow cytometric analysis of the overall cell population showed that cells constitutively expressed integrin α3β1 during 3D hydrodynamic culture (274). Finally, another research group has shown that medium perfusion had beneficial effects on the proliferation and biosynthetic activity of an osteosarcoma cell line and the system mimicked the 3D geometry of bone tissue (38).

It is also known that weightlessness induces bone loss in humans and animal models which is a concern when using a "simulated microgravity" HARV reactor to culture bone tissue. However, a study has identified that osteoblast-like cells grown in a rotating wall vessel (RWV) bioreactor exhibit high levels of ALPase expression and activity, and elevated expression of osteopontin, osteocalcin and BMP4 albeit with reduced proliferation (275). Modelling of the HARV reactor used in this thesis has been performed and validated using macro carriers with density greater than the surrounding fluid medium (alginate beads have this characteristic). They follow a circular motion relative to the culture medium combined with a persistent migration and eventual collision with the outer wall of the reactor (271). Therefore, it is logical to assume that they

are not in simulated microgravity but still remain in a low shear/low turbulence environment.

5.2. Materials and methods

5.2.1. Medium viscosity

The medium viscosity was required in order to calculate the Reynolds number for the spinner vessel reactor. Distilled water, serum-containing maintenance and differentiation media at 37 °C were measured in triplicate using an AR1000 Rheolyst rheometer (TA Instruments, UK) with 50 shear rate data points between 0 and 1000 (1/s).

Reynolds number calculations.

$$Re(Spinner) = \frac{\rho * U * D}{\mu}$$

The density (ρ) (kg/m^3) and viscosity (μ) (Pa s) of the cell culture medium were measured to be identical to water (Section 5.5.1) and the values were set at 993.34 kg/m^3 and viscosity 0.0006835 Pa s, respectively. The impellor diameter in the spinner flask diameter (D) was measured at 0.024 m. The impellor velocities (U) were calculated by converting their speed (RPM) to radians and multiplying this by the impellor or vessel radius. The Reynolds number and therefore mixing could therefore be calculated.

5.3. Aims

- The integration of traditional mESC culture through the encapsulation of undifferentiated mESCs and formation of 3D bone.
- The production of clinically-relevant differentiated cells through culture in an integrated bioreactor culture system.

5.4. Results

Tissue engineering of bone from embryonic stem cells in *in vitro* culture is artificially divided into three stages based on traditional protocols (Maintenance: day 0 – 3, EB formation: day 3 – 8 and Osteogenic differentiation: day 8 – 29) (30). In the 3D system used in this chapter these stages are represented only by media changes at the relevant time points in order to induce lineage specific differentiation. The results are presented in this chapter with headings for each type of analysis and described from day 0 to day 29 as a continuous process; undifferentiated mESCs to bone tissue. At the end of these results there is a brief section (5.4.3) that interprets all these results together as a continuous process.

5.4.1. Medium viscosity

This work was conducted in collaboration with Sandeep Chandarana in Chemical Engineering, Imperial College, London. The weight (g) [converted later to density (ρ) (kg/m^3)] and viscosity (μ) (Pa s) of the cell culture medium at

Liquid type	Water		
Replicate	Weight of Bijou g	Weight of Bijou + liquid g	Weight of liquid g
1	4.4422	5.4429	1.0007
2	4.4477	5.4475	0.9998
3	4.4567	5.4575	1.0008
		Mean	1.0004
		SD	0.0004
Liquid type	Maintenance medium		
Replicate	Weight of Bijou g	Weight of Bijou + liquid g	Weight of liquid g
1	4.5035	5.4913	0.9878
2	4.441	5.441	1
3	4.4625	5.4661	1.0036
		Mean	0.9971
		SD	0.0068
Liquid type	Differentiation medium		
Replicate	Weight of Bijou g	Weight of Bijou + liquid g	Weight of liquid g
1	4.425	5.4056	0.9806
2	4.5104	5.4977	0.9873
3	4.4387	5.434	0.9953
		Mean	0.9877
		SD	0.0060

Table 5.1. Mean weight of water and culture medium. 1 mL of each liquid was heated to 37°C and measured in triplicate.

37 °C were measured to be identical to distilled water (Table 5.1 & Figure 5.1) and the values were set at 993 kg/m^3 and viscosity 0.0007 Pa s, respectively based on published values (276). The spinner flask impellor diameter (D) was measured at 0.024 m. The spinner velocity was set at its lowest speed (166 RPM) resulting in a Reynolds number of 7276 providing an incredibly high amount of turbulence in the spinner flask. Turbulent flow is indicated by a Reynolds number over 4000.

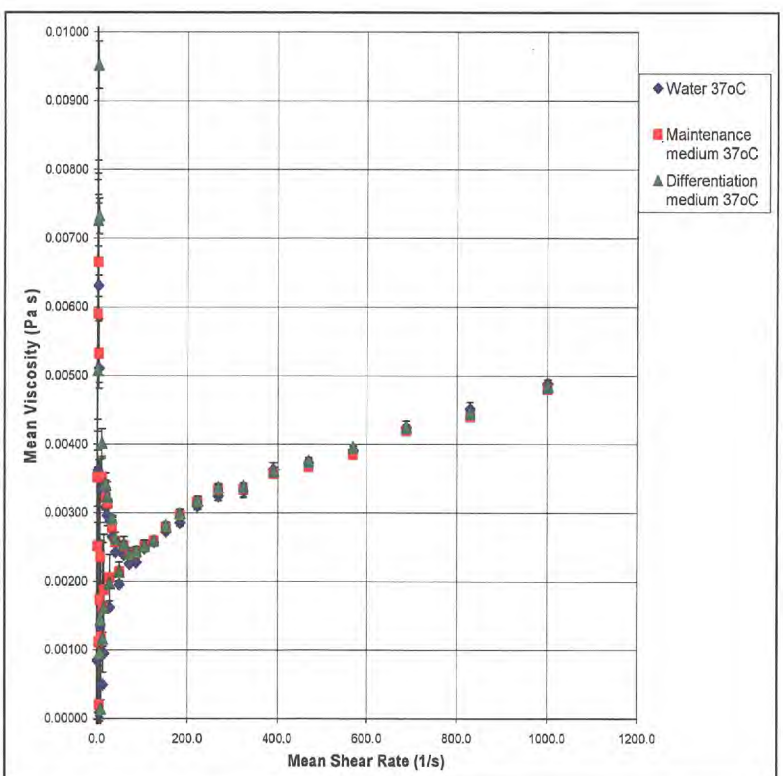


Figure 5.1. Mean medium viscosity measurements vs. mean shear rate. 50 Shear rate data points between 0 and 1000 (1/s). Each liquid measured in triplicate.

5.4.2. Bioreactor 3D bone formation

Undifferentiated mESCs were encapsulated and placed in 2D (control for osteogenic differentiation), 3D static, 3D stirred (166RPM) or 3D HARV (17.5RPM) cultures for 29 days in order to form 3D mineralised tissue (Figure 5.2). The cells were cultured for 3 days in maintenance medium, a further 5 days in differentiation medium and a further 21 days in osteogenic differentiation medium. Multiple experiments were conducted in order to characterise the developmental process and 3D mineralised tissue formation. The 3D HARV culture was the most successful as growth and 3D mineralised tissue formation was observed. 2D, 3D static and stirred results are in the appendices where stated. The biochemical assays for 3D HARV culture are shown in full but is not shown for 2D static, 3D static and 3D stirred. In retrospect, the culture protocols for 2D static were not directly comparable as the culture system was fragmented and the 3D static/stirred cultures did not provide adequate cellular material for analysis. However, other analyses such as immunostaining, RT-PCR and viability / histochemical / mineralisation staining are shown.



Figure 5.2. Images of 3D static, 3D stirred & 3D HARV vessels. All 3D systems contained 50 mL of medium at all times and 600 beads from day 0.

5.4.2.1. Cell viability

Cell viability was monitored throughout culture in order to maintain a visual representation of all cultures, including the replicates to identify discrepancies in batches of beads (Figure 5.3). It is clear that on day 0, all 3D cultures were

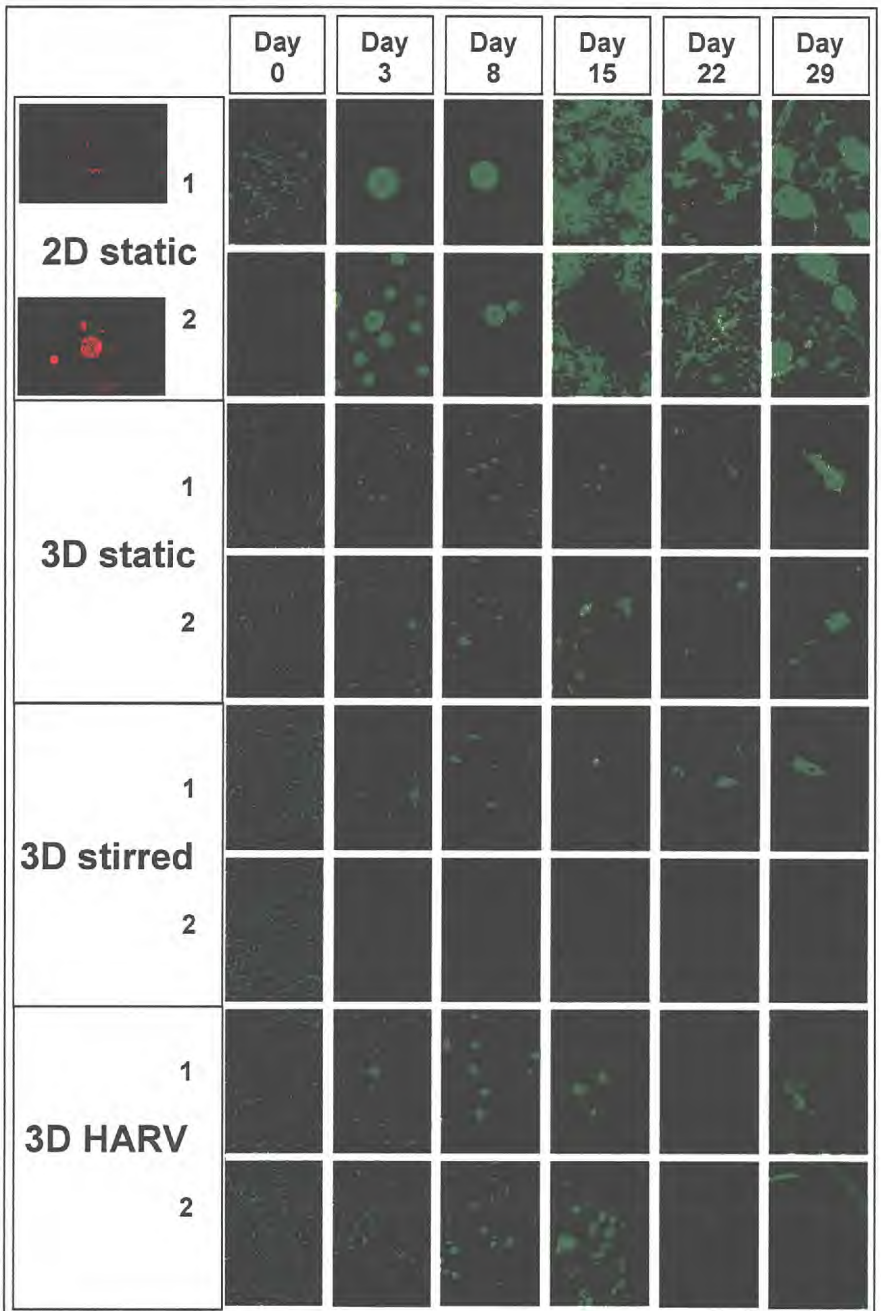


Figure 5.3. Live / Dead images of 2D static, 3D static, 3D stirred, 3D HARV cultured for 29 days. Image dimensions = 12367 x 845 µm. x10 objective. Red negative controls, day 0 and day 3, neat ethanol treatment for 5 minutes.

viable and appear to be uniformly distributed throughout the bead. By day 3, discrete viable 2D colonies formed and appear, in general, larger in diameter than the 3D colonies. In general, 3D stirred had an overall decrease in viable cells although non-viable cells were not visible. 3D static and 3D HARV did exhibit signs of non-viable cells on day 3 with 3D static having the greater numbers of dead cells (red cells Figure 5.3). There was little evidence of cell death, but the majority of cells had begun to form discrete, live colonies. It is not clear whether cell numbers increased in 3D or whether the existing, single cells formed colonies by attraction to each other. It was not clear whether single cells formed colonies from clonality or whether they migrated to each other and then formed colonies. However, it appears the uniformly distributed cells on day 0 migrated to each other through the sol-gel alginate hydrogel and formed colonies. Visually, there were virtually no single cells remaining at day 3 and most viable cells were in colonies.

By day 8, 2D EBs had formed and indicated signs of non-viable cells on their periphery. All 3D cultures have begun to form larger colonies, at the same abundance as day 3. 3D HARV cultures appear to be visually larger at around 50 μm, larger in diameter than other 3D cultures. Between days 8 and 29, 2D EBs were disrupted and plated onto tissue culture plastic in order to form bone nodules on tissue culture plastic, in osteogenic medium. At day 15, a viable monolayer had formed and by day 22, discrete nodules with some signs of cell death was occurring. However, by day 29, these nodules increased in size but also showed some signs of cell death. In 3D static culture, colony size and viability did not alter until day 29 when the number of small colonies has decreased and the only remnants of viable tissue are single, large pieces of tissue that have numerous necrotic areas. In 3D stirred culture, only one single

colony, albeit viable was detected in replicate 1. In contrast, 3D HARV viable colonies were more numerous on day 15 but almost disappeared by day 22. Non-viable cells were not visible which would only indicate a drop in esterase activity to process the green fluorescent stain. By day 29, viable colonies had re-appeared, were numerous and larger than the colonies seen on both days 15 and 22. Negative controls were performed throughout the culture periods and day 0 and 3 (2D) are shown as an example.

5.4.2.2. Morphology & Histology

For convenience, the beads that were cultured in the 3D HARV bioreactor are shown in Figure 5.4, both morphology and histology and a description of the HARV culture follows. A comprehensive library of morphological and histological images of the other cultures: 2D static, 3D static and 3D stirred can be found following the description of the 3D HARV bioreactor for direct comparisons (Figures 5.5-17).

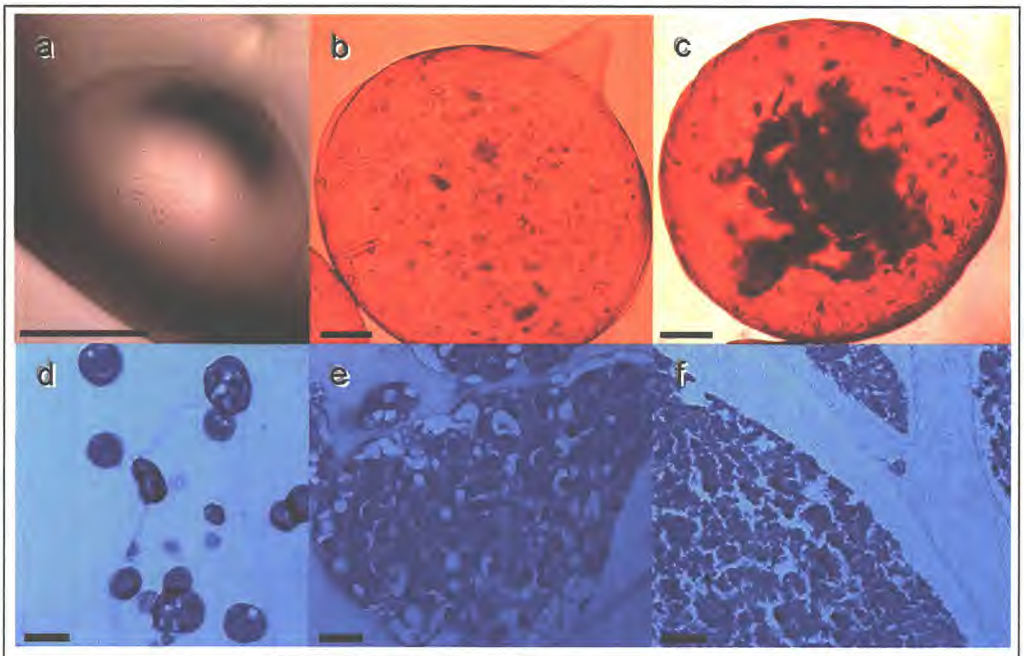


Figure 5.4. Morphology of encapsulated cells. a. Day 3, *1000μm* b. Day 7, *500μm* c. Day 21, *500μm* d. Day 3, H&E Light Balanced Daylight (LBD), *20μm* e. Day 8, H&E (LBD), *20μm* f. Day 22, H&E (LBD), *20μm*. (*Scale bar lengths*).

Dispersed mESCs were encapsulated (approximately 10,000 cells per bead) within alginate hydrogel beads of a diameter of 2.3 mm. After 3 days of culture in maintenance medium, the initially dispersed mESCs formed 3D colonies of between 4-10 cells (Figure 5.4ad and Figure 5.4abc) between 20 and 50 μm in diameter. Colonies were spherical, discoid or fusiform and distributed evenly around the beads but rarely located near the immediate outer surface of the bead (Figure 5.4a). Following removal of LIF and culture in the EB formation medium for 5 days, most colonies presented a uniform appearance and appeared to be increasing in cell number and overall size in discrete "pockets" within the alginate matrix (Figure 5.4be and Figure 5.4d), with the size of the colonies ranging from 50 to 400 μm in diameter. By day 22 of culture, the colonies were very tightly packed. Most of the large colonies were located towards the centre of the bead (Figure 5.4cf) and a zone that did not contain any cellular material was clearly visible on the periphery of the beads. After 29 days of culture, colonies were up to 500 μm in diameter (Figure 5.4e).

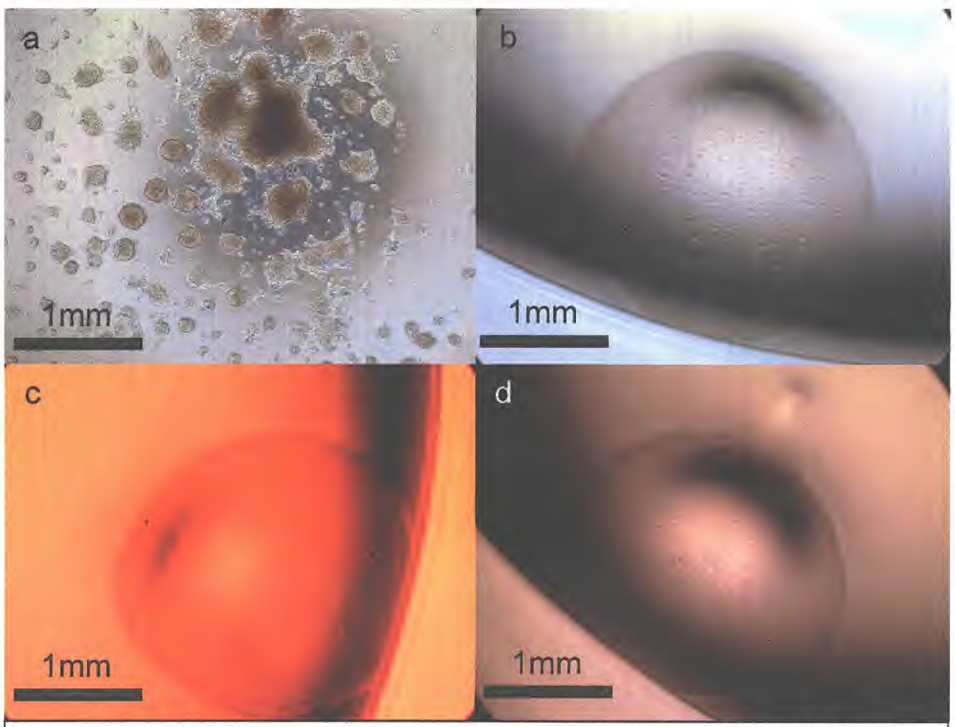


Figure 5.5. Day 3, 2D static, 3D static, 3D stirred and 3D HARV. Phase contrast images of cultures. a. 2D static b. 3D static c. 3D stirred d. 3D HARV. x4 objective.

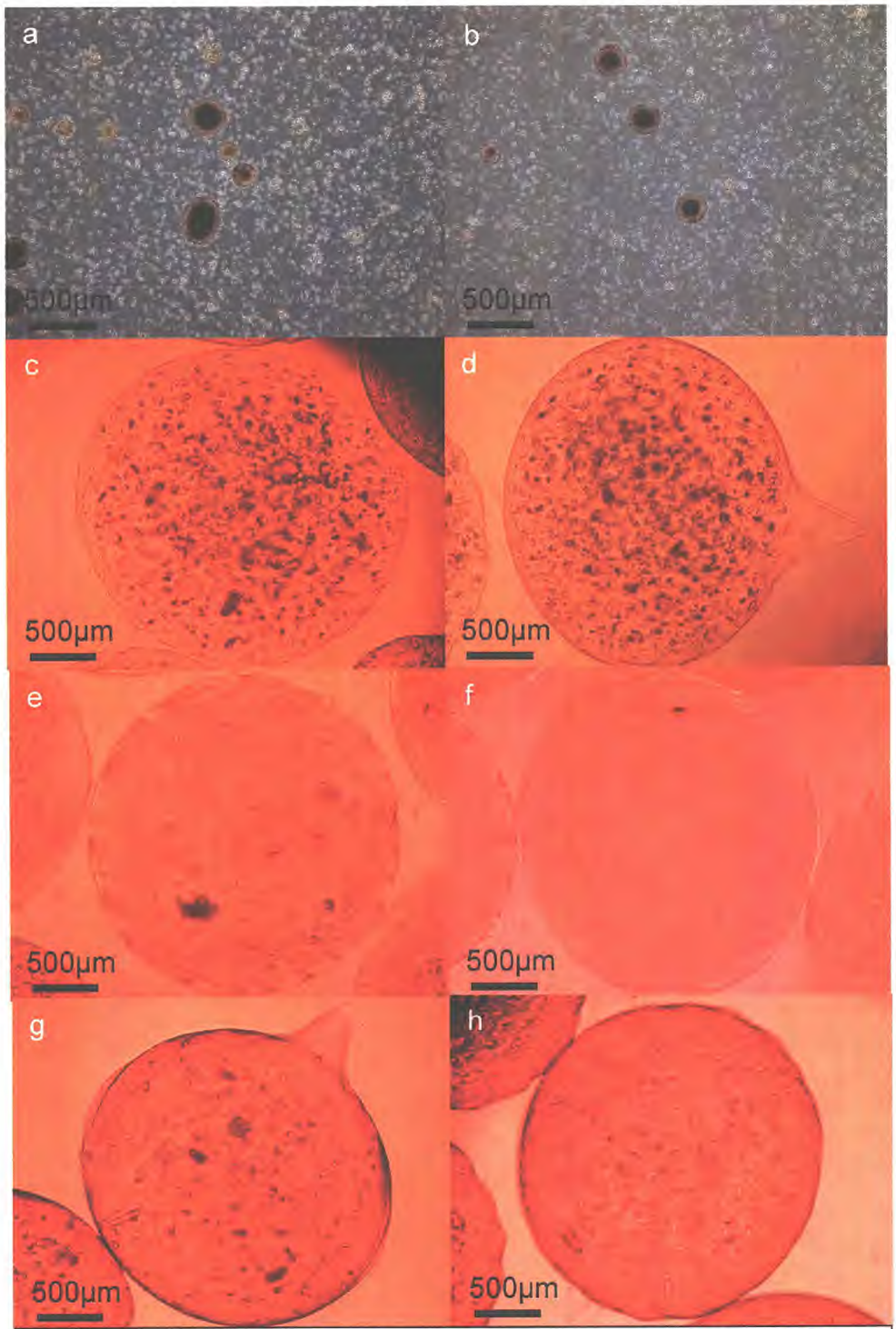


Figure 5.6. Day 7, 2D static, 3D static, 3D stirred and 3D HARV. Phase contrast images of cultures. a. 2D (1) b. 2D (2) c. 3D static (1) d.3Dstatic (2) e. 3D stirred (1) f. 3D stirred (2) g. 3D HARV (1) h. 3D HARV (2). x4 objective.

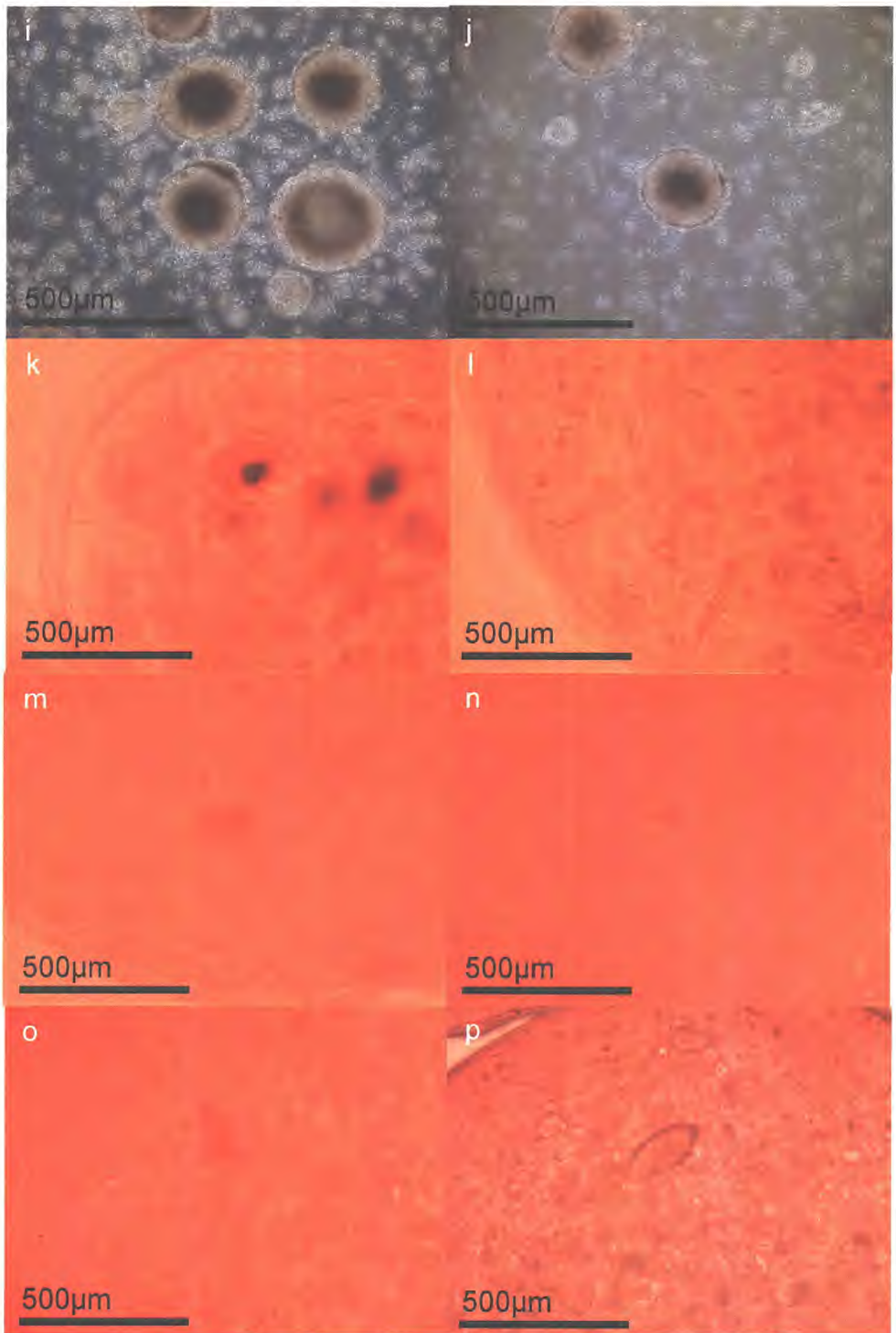


Figure 5.7. Day 7, 2D static, 3D static, 3D stirred and 3D HARV. Phase contrast images of cultures. i. 2D (1) j. 2D (2) k. 3D static (1) l.3Dstatic (2) m. 3D stirred (1) n. 3D stirred (2) o. 3D HARV (1) p. 3D HARV (2). X10 objective.

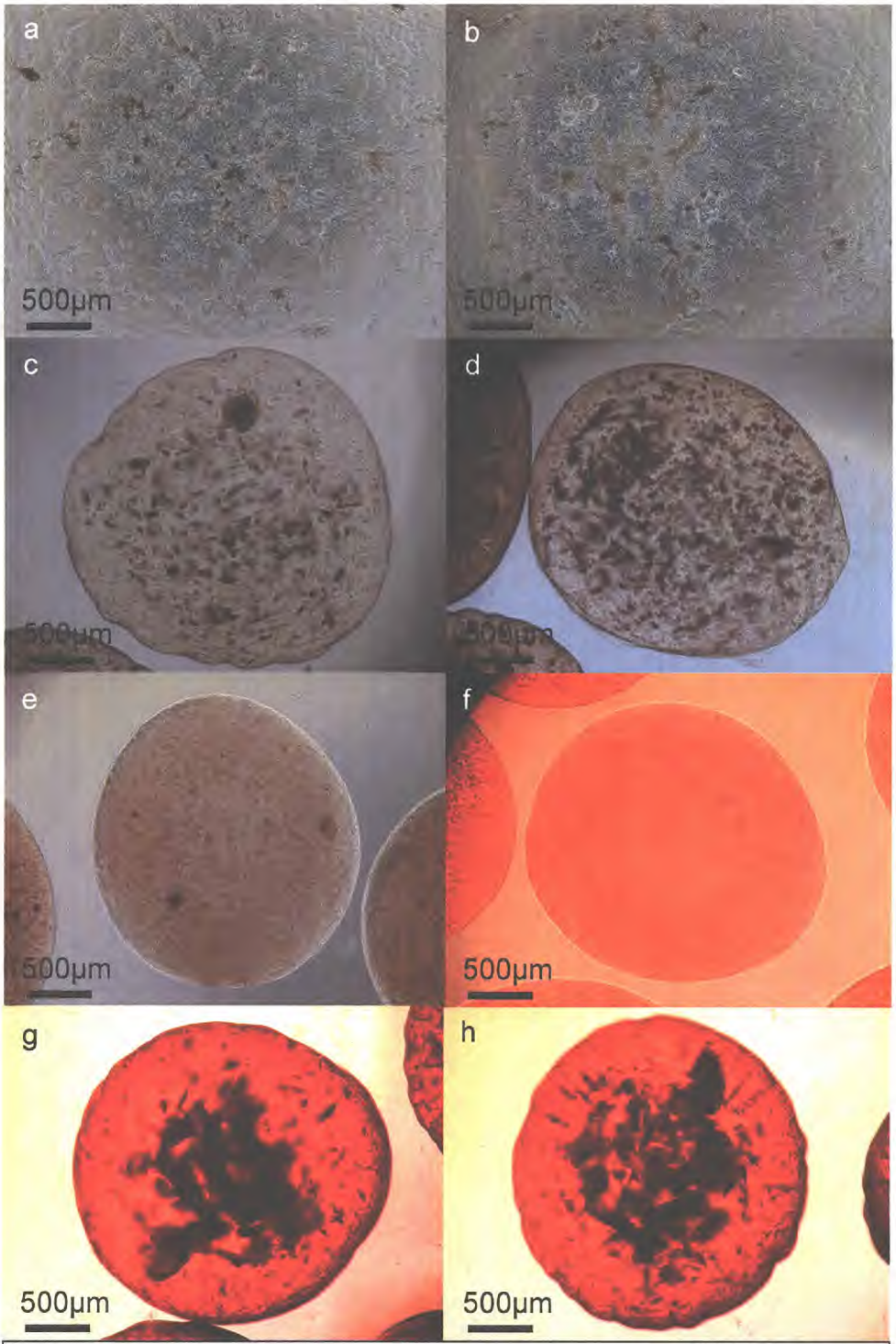


Figure 5.8. Day 21, 2D static, 3D static, 3D stirred and 3D HARV. Phase contrast images of cultures. a. 2D (1) b. 2D (2) c. 3D static (1) d.3Dstatic (2) e. 3D stirred (1) f. 3D stirred (2) g. 3D HARV (1) h. 3D HARV (2). x4 objective.

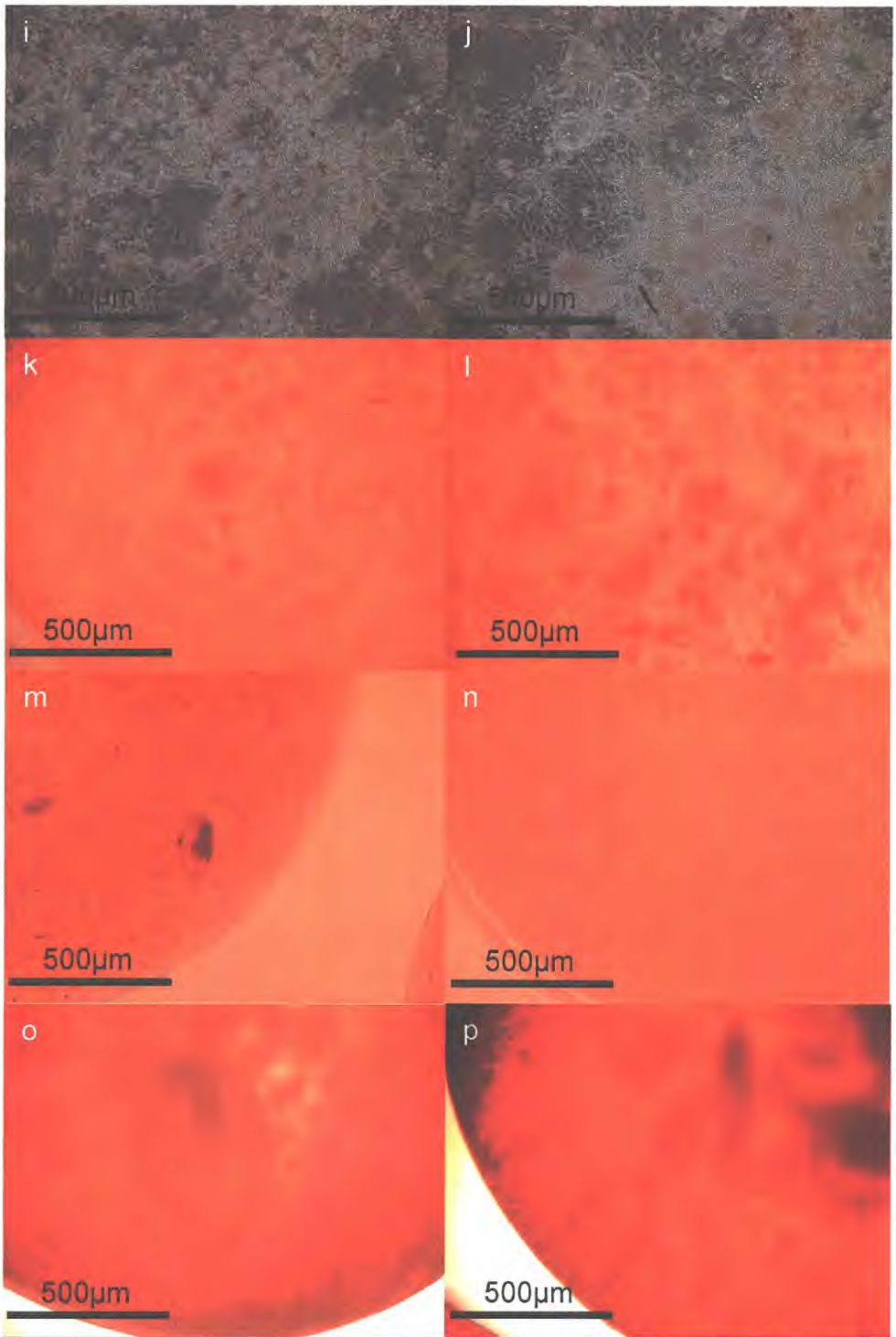


Figure 5.9. Day 21, 2D static, 3D static, 3D stirred and 3D HARV. Phase contrast images of cultures. i. 2D (1) j. 2D (2) k. 3D static (1) l.3Dstatic (2) m. 3D stirred (1) n. 3D stirred (2) o. 3D HARV (1) p. 3D HARV (2). X10 objective.

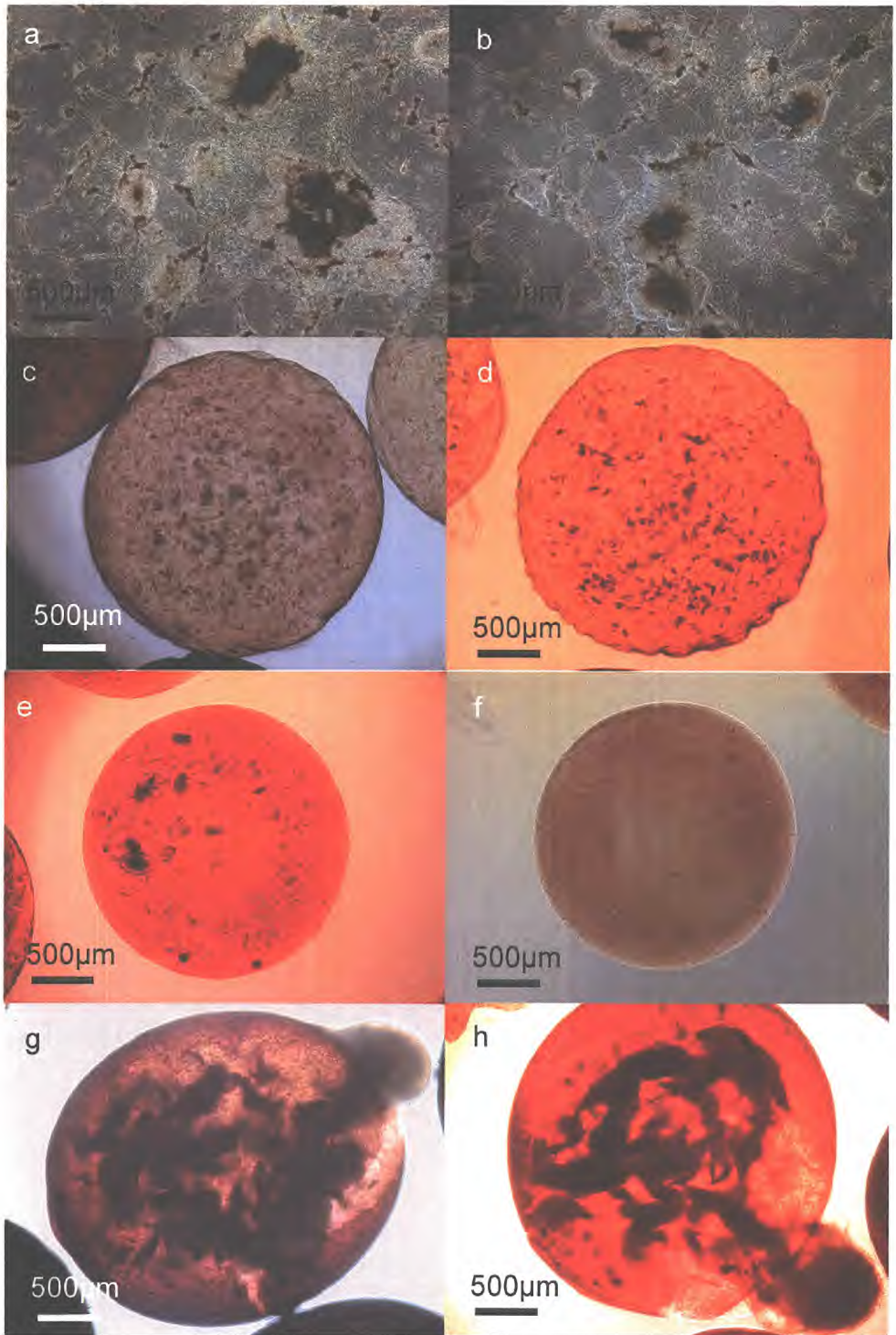


Figure 5.10. Day 29, 2D static, 3D static, 3D stirred and 3D HARV. Phase contrast images of cultures. a. 2D (1) b. 2D (2) c. 3D static (1) d.3Dstatic (2) e. 3D stirred (1) f. 3D stirred (2) g. 3D HARV (1) h. 3D HARV (2). x4 objective.

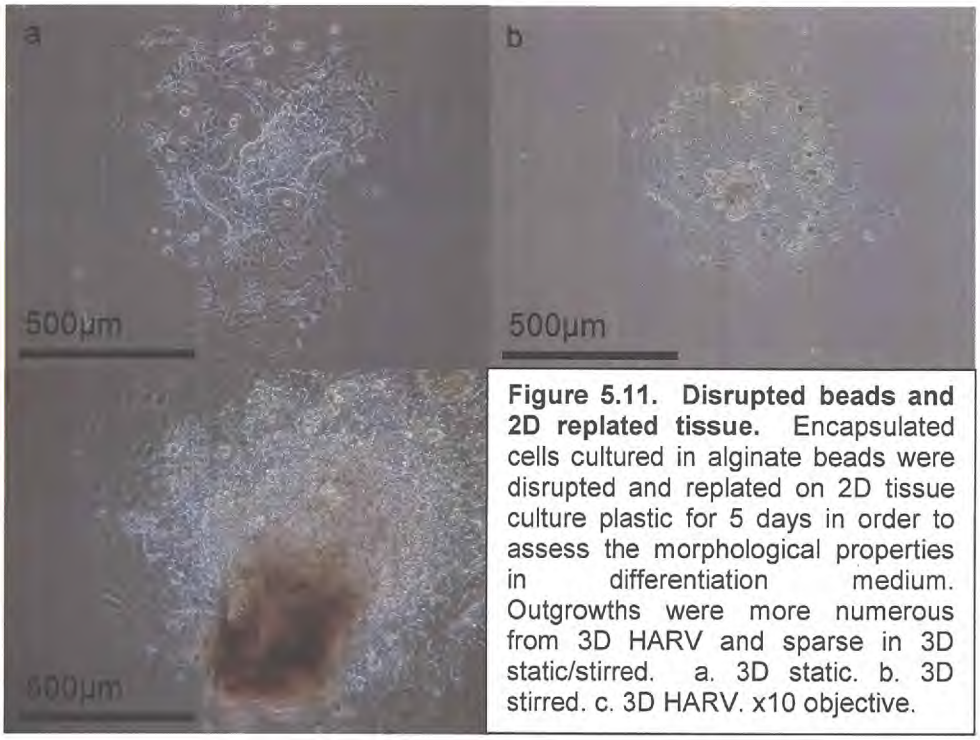


Figure 5.11. Disrupted beads and 2D replated tissue. Encapsulated cells cultured in alginate beads were disrupted and replated on 2D tissue culture plastic for 5 days in order to assess the morphological properties in differentiation medium. Outgrowths were more numerous from 3D HARV and sparse in 3D static/stirred. a. 3D static. b. 3D stirred. c. 3D HARV. x10 objective.

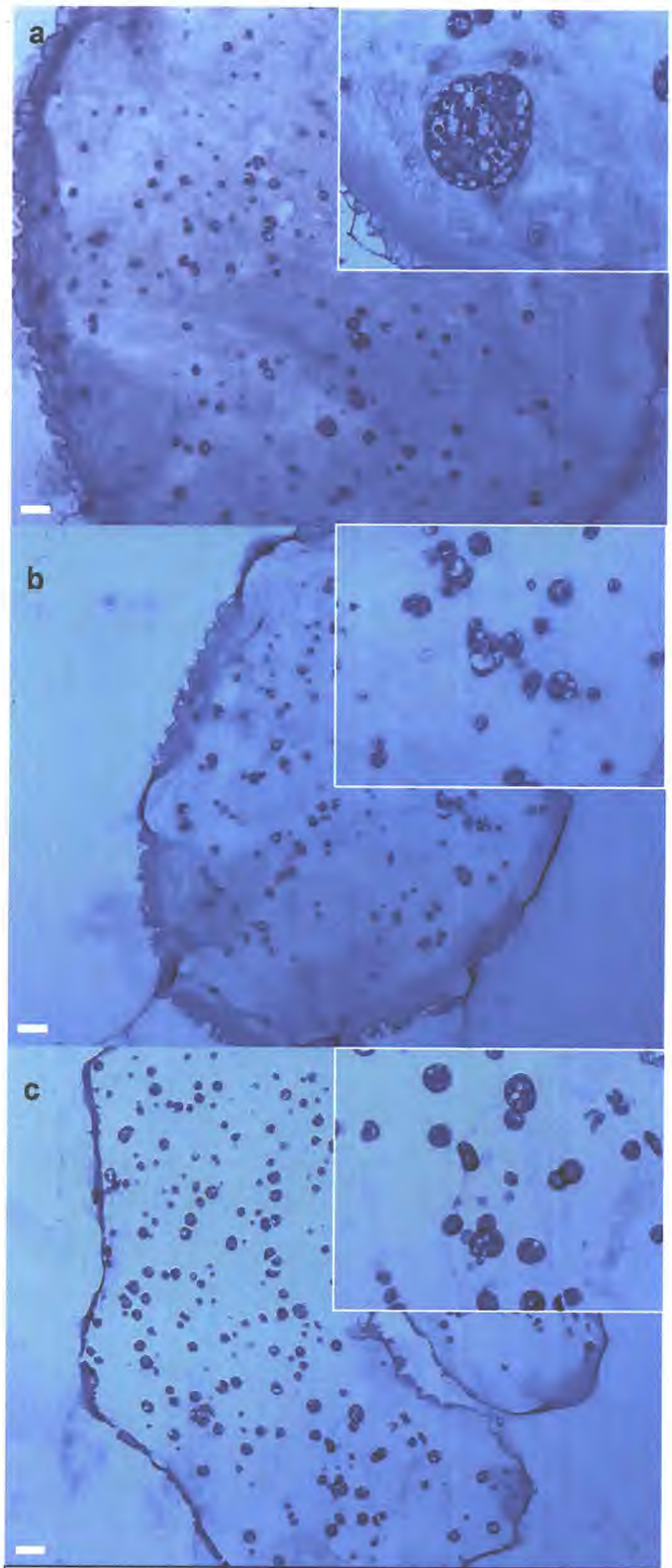


Figure 5.12. Day 3, paraffin embedded, sectioned, H&E stained alginate beads. a. 3D static. b. 3D stirred. c. 3D HARV. Scale bars = 100 µm. Inset high mag.

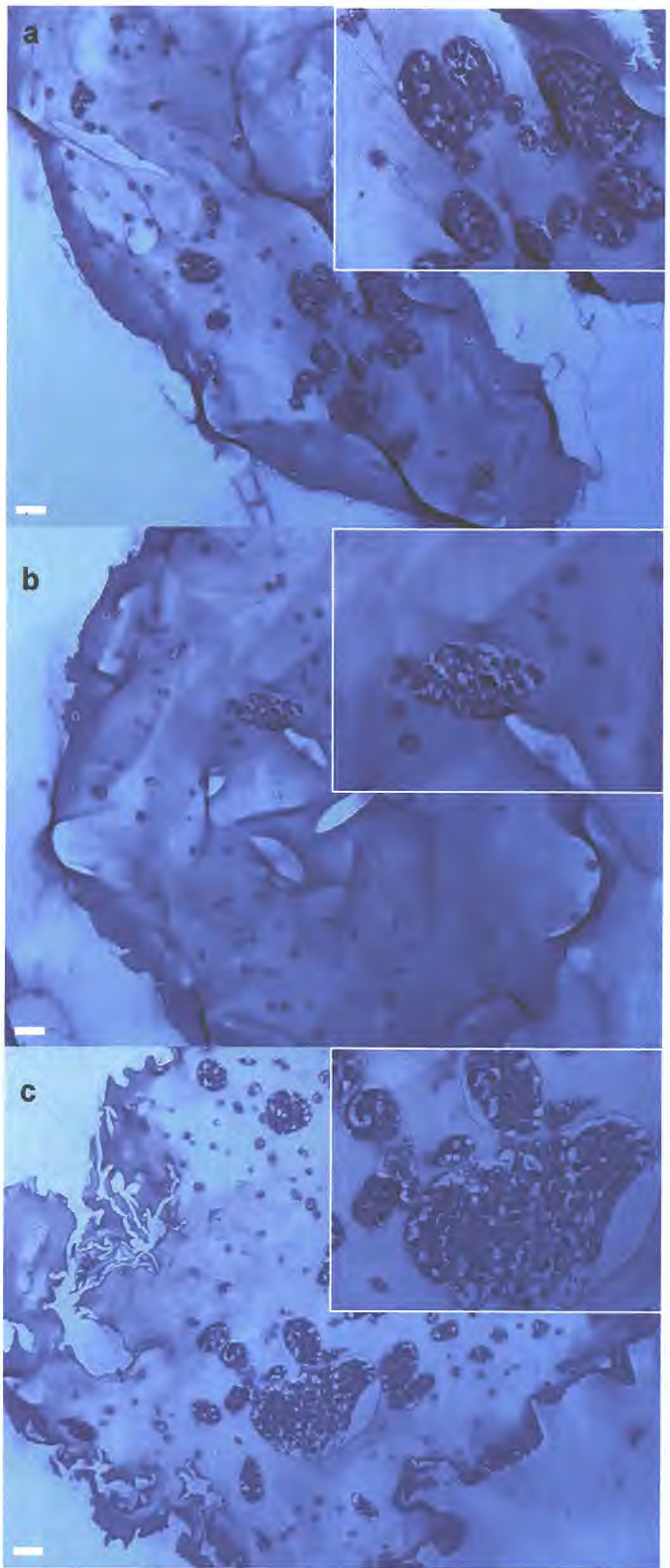


Figure 5.13. Day 8, paraffin embedded, sectioned, H&E stained alginate beads. a. 3D static. b. 3D stirred. c. 3D HARV. Scale bars = 100 µm. Inset high mag.

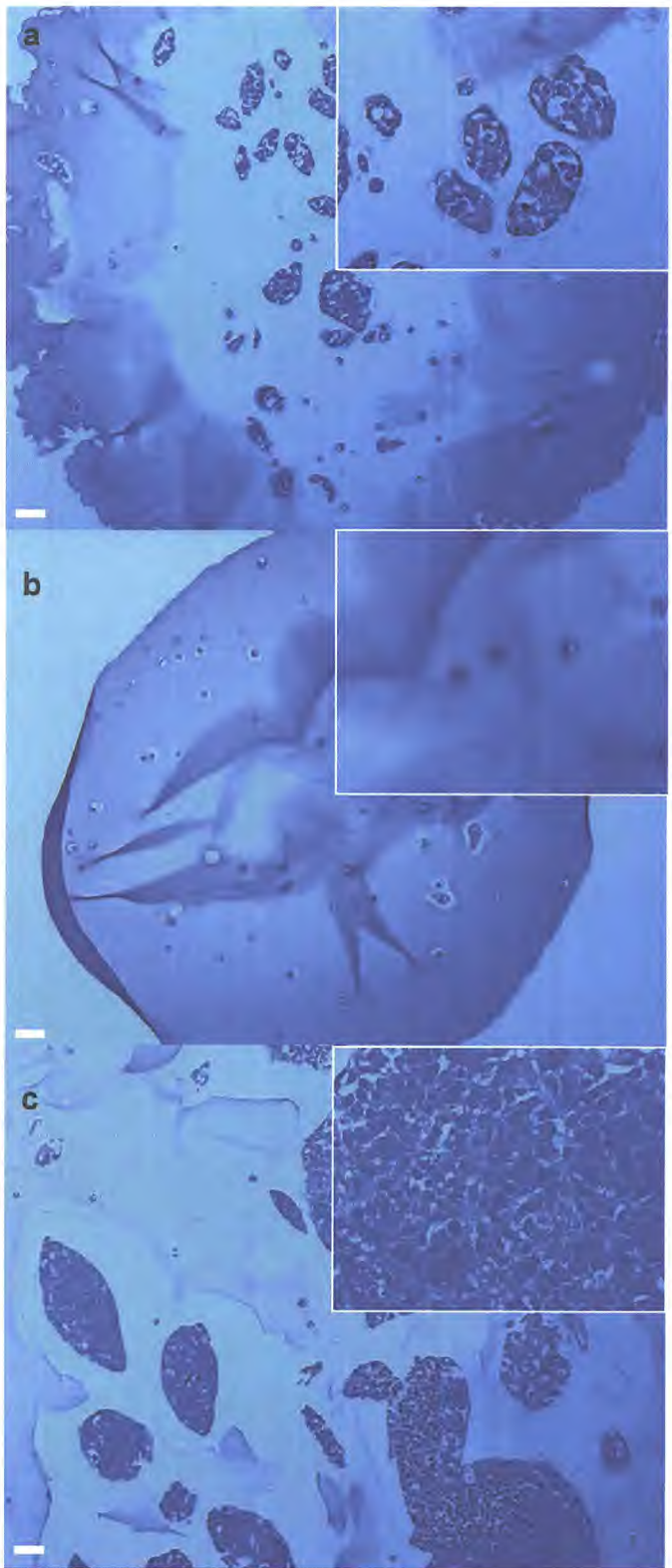


Figure 5.14. Day 15, paraffin embedded, sectioned, H&E stained alginate beads. a. 3D static. b. 3D stirred. c. 3D HARV. Scale bars = 100 µm. Inset high mag.

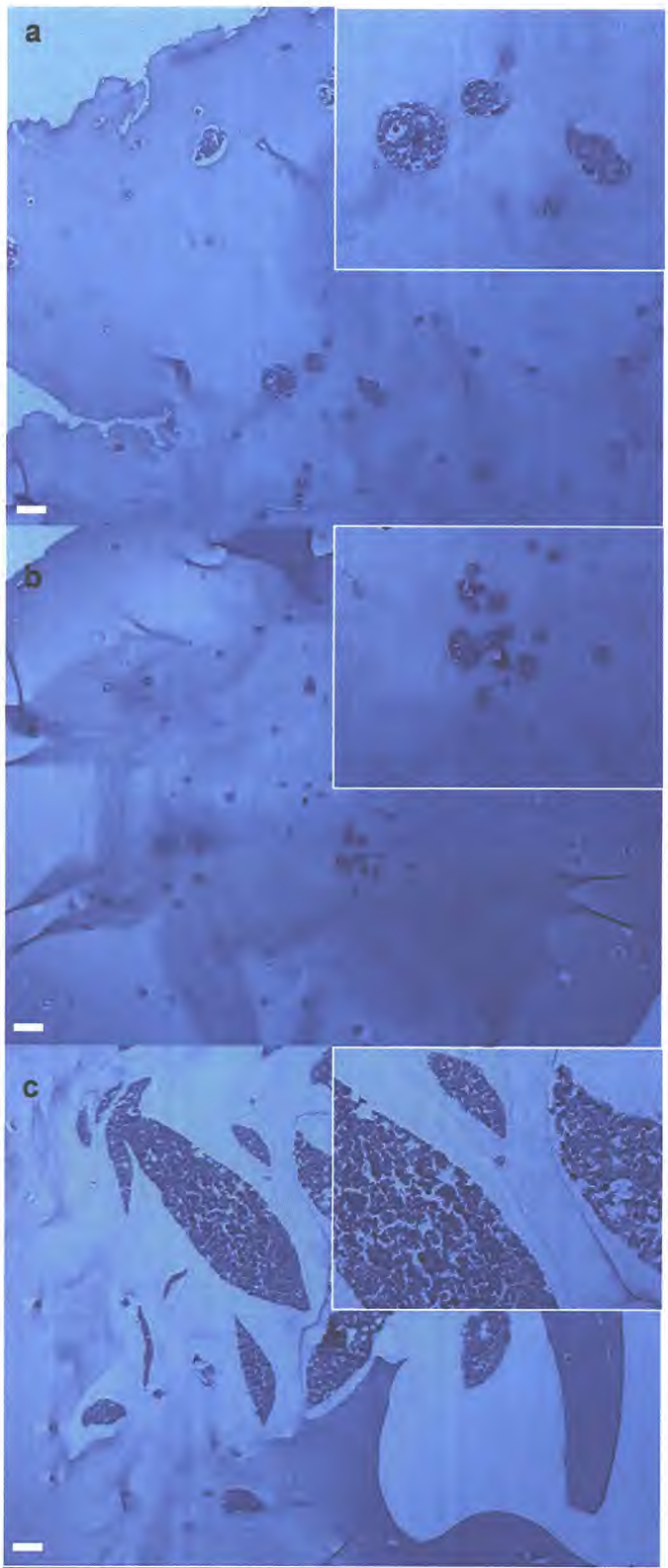


Figure 5.15. Day 22, paraffin embedded, sectioned, H&E stained alginate beads. a. 3D static. b. 3D stirred. c. 3D HARV. Scale bars = 100 µm. Inset high mag.

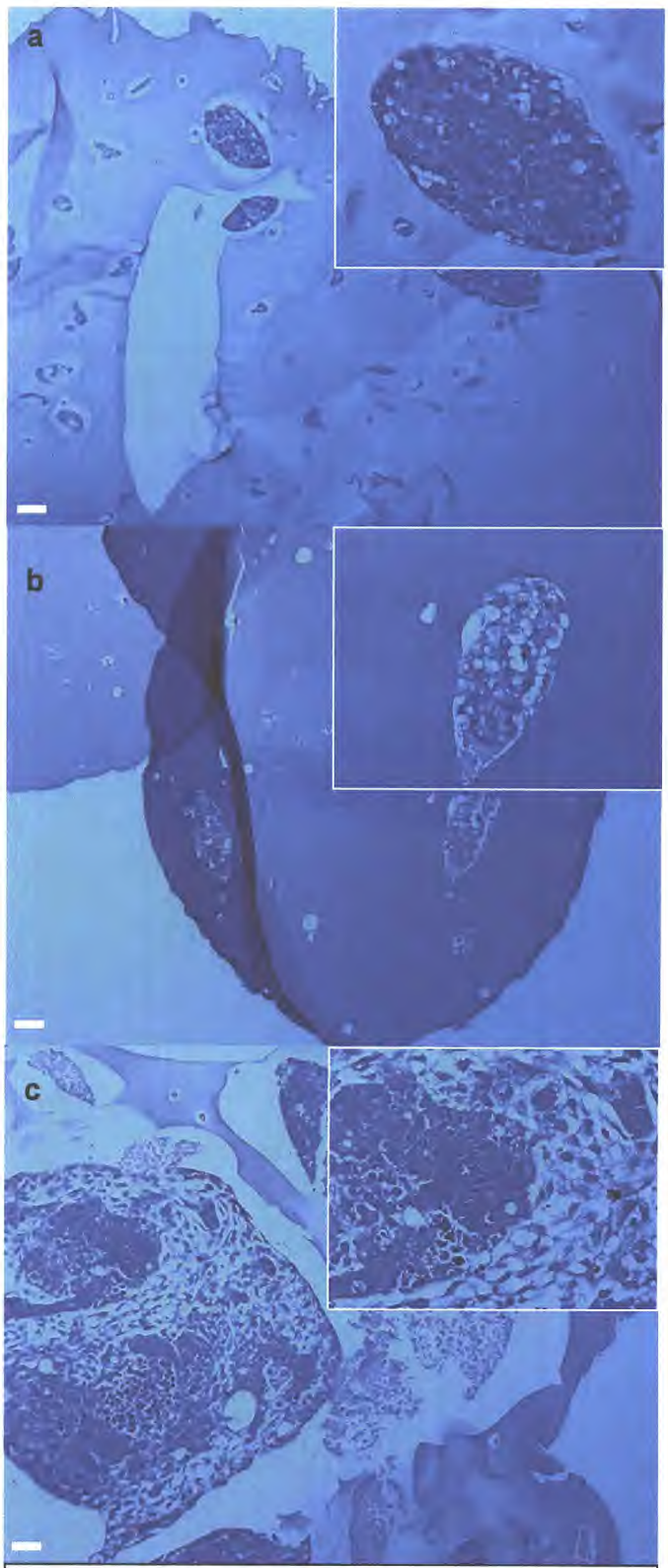


Figure 5.16. Day 29, paraffin embedded, sectioned, H&E stained alginate beads. a. 3D static. b. 3D stirred. c. 3D HARV. Scale bars = 100 µm. Inset high mag.

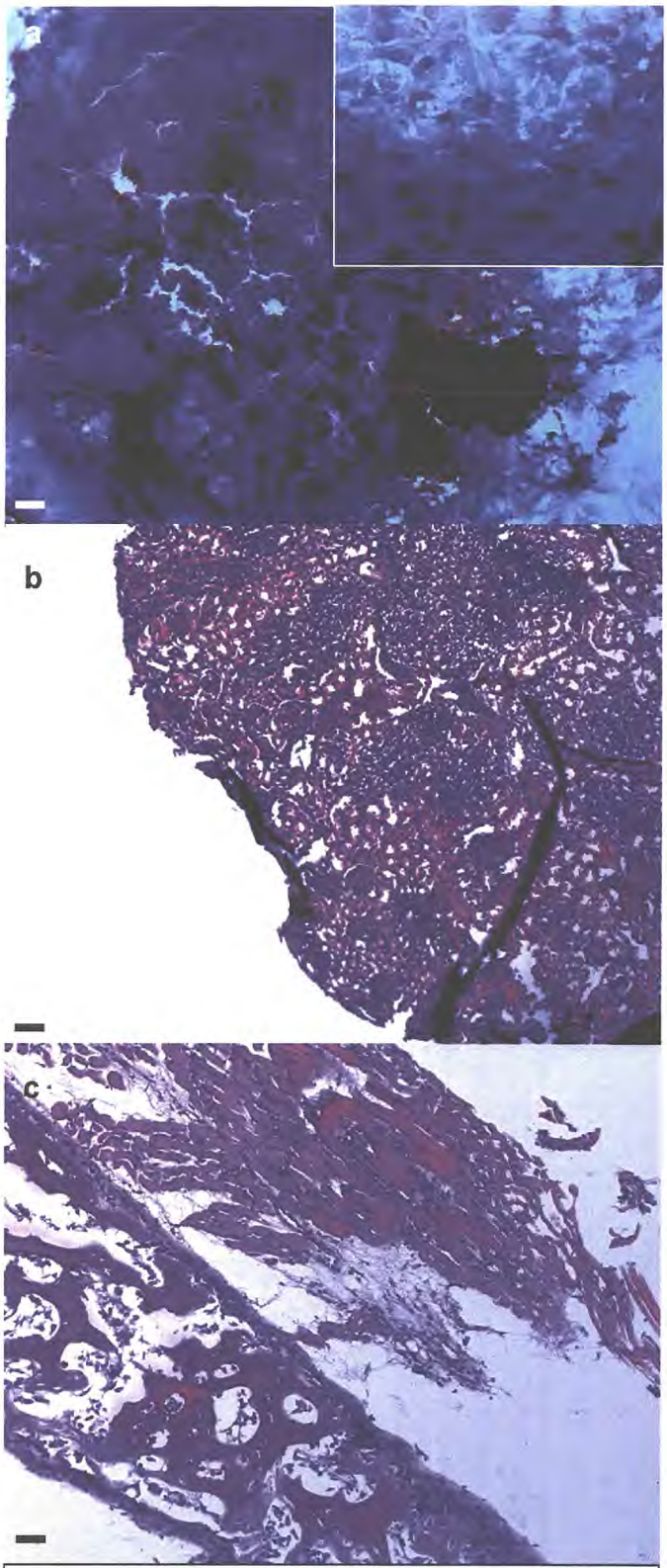


Figure 5.17. Day 29, paraffin embedded, sectioned, H&E stained controls. a. 2D static. b. mouse kidney. c. mouse bone/muscle. Scale bars = 100 µm. Inset high mag.

5.4.2.3. Alizarin Red S and von Kossa mineralisation staining

For convenience, the beads that were cultured in the 3D HARV bioreactor are shown in Figure 5.18 of H&E, ARS and von Kossa stains and a description of the 3D HARV culture follows. A comprehensive library of morphological and histological images of the other cultures: 2D static, 3D static and 3D stirred can be found following the description of the 3D HARV bioreactor for direct comparisons (Figures 5.20-24).

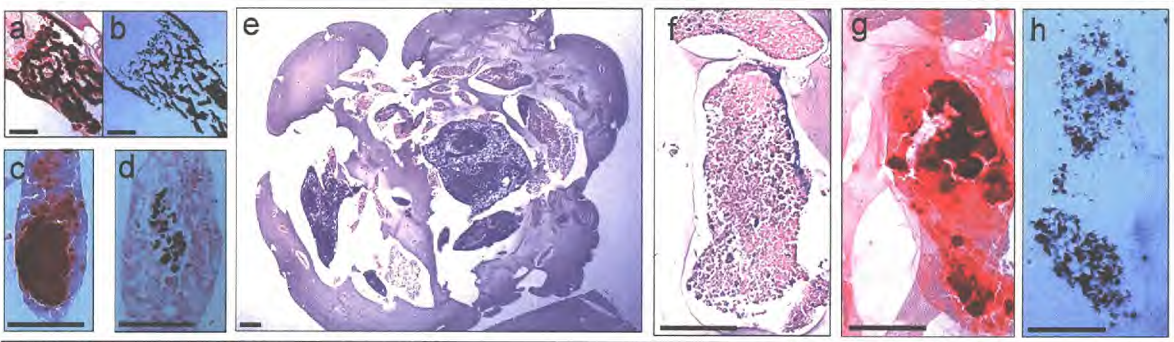


Figure 5.18. 3D HARV bone aggregate characterisation. a. Balb/c mouse bone ARS positive control b. Balb/c mouse bone vKossa positive control (LBD) c. Day 22, ARS (LBD) d. Day 22, vKossa and neutral red (LBD) e. Day 29 H&E f. Day 29 H&E g. Day 29 ARS (same section as f.) h. Day 29 vKossa, (same section as f.) Scale bars from a-f, 100 µm.

The 3D mineralised tissue formed in the 3D cultures from the mESCs was thoroughly characterised during the osteogenesis culture period. Serial sections were analysed to examine tissue formation throughout the alginate beads. Figure 5.18 demonstrates that 3D mineralised tissue was prominently formed at day 22 (Figure 5.18cd) and 29 (Figure 5.18gh) within the alginate beads, as shown by the Alizarin Red S and von Kossa staining. As is evident, the samples contained a large proportion of mineralised tissue that permeated the entire section. Variations in the intensity of staining were observed between day 22 and day 29 of culture. Specifically, the day 22 samples showed that

ARS stained tissue was uniformly red in colour but did not reach the red/black intensity found in the mouse bone positive controls (Figure 5.18ab). The day 22 samples usually contained tissue that ranged from 100 to 300 µm in diameter with the mineralised areas ranging from 50 to 100 µm in width. In contrast, at day 29 the alginate beads contained larger tissue aggregations, as evidenced by the haematoxylin/eosin staining (Figure 5.18ef); the largest tissue section having dimensions greater than 500 x 500 µm. Certain areas of the tissue formed appeared necrotic by staining pink as opposed to blue under the H&E stain, however the majority were uniformly viable, as shown by viability staining (Figure 5.3). The tissue that appeared necrotic was limited to the areas that contained mineralised tissue (Figure 5.18f) and is consistent with the entrapment of osteoblasts within matrix that subsequently mineralises. This may also be further evidence for the "disappearance" of viable colonies on day 22 of 3D HARV culture (Figure 5.3).

Furthermore, the tissue that was produced tended to occupy the centre of the beads and was highly ordered with columnar cell borders. At day 29, the tissue formed was more similar to the red/black ARS staining found in the positive controls (Figure 5.19gh). As an example, Figure 5.6 illustrates the amount of 2D bone nodules or 3D mineralised aggregates generated when stained with Alizarin Red S. This is for illustrative purposes only to give an idea of the amount of 3D mineralised tissue that forms in 2D and 3D HARV bioreactor culture.

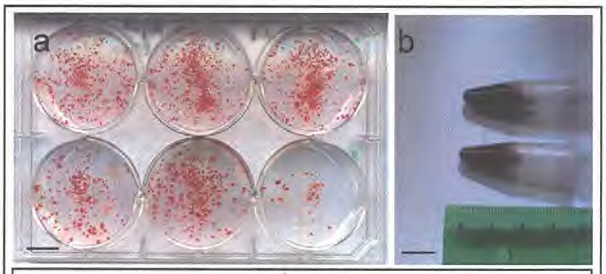


Figure 5.19. Macroscopic comparison of bone quantity from 2D and 3D HARV culture. a. Each 6 well plate well has an area of 10 cm^2 and day 5 EBs were disrupted and seeded at 50,000 cells per well. b. Each vial contains 3D tissue from between 50 and 100 beads seeded with 10,000 undifferentiated mESCs per bead. Scale bars = 100 µm.

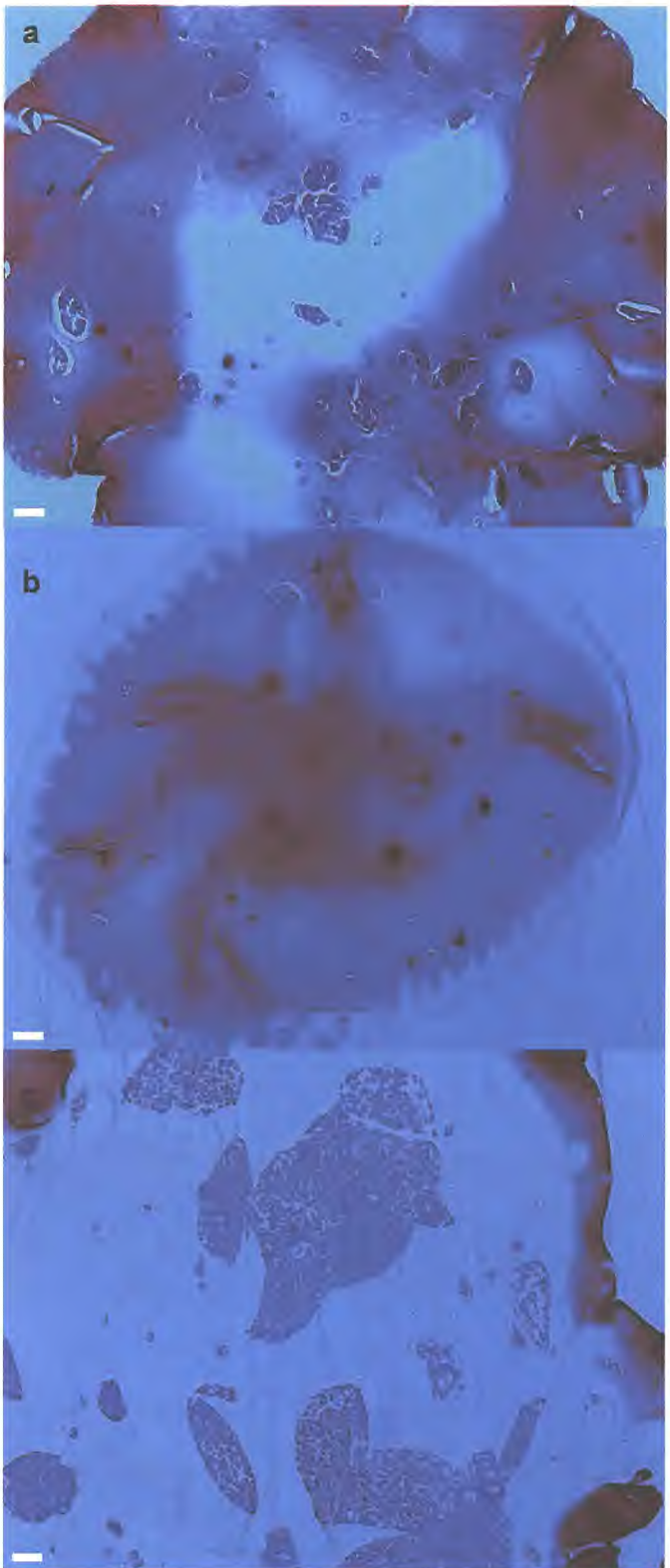


Figure 5.20. Day 15, paraffin embedded, sectioned, Alizarin Red S stained alginate beads. a. 3D static. b. 3D stirred. c. 3D HARV. Scale bars = 100 µm.

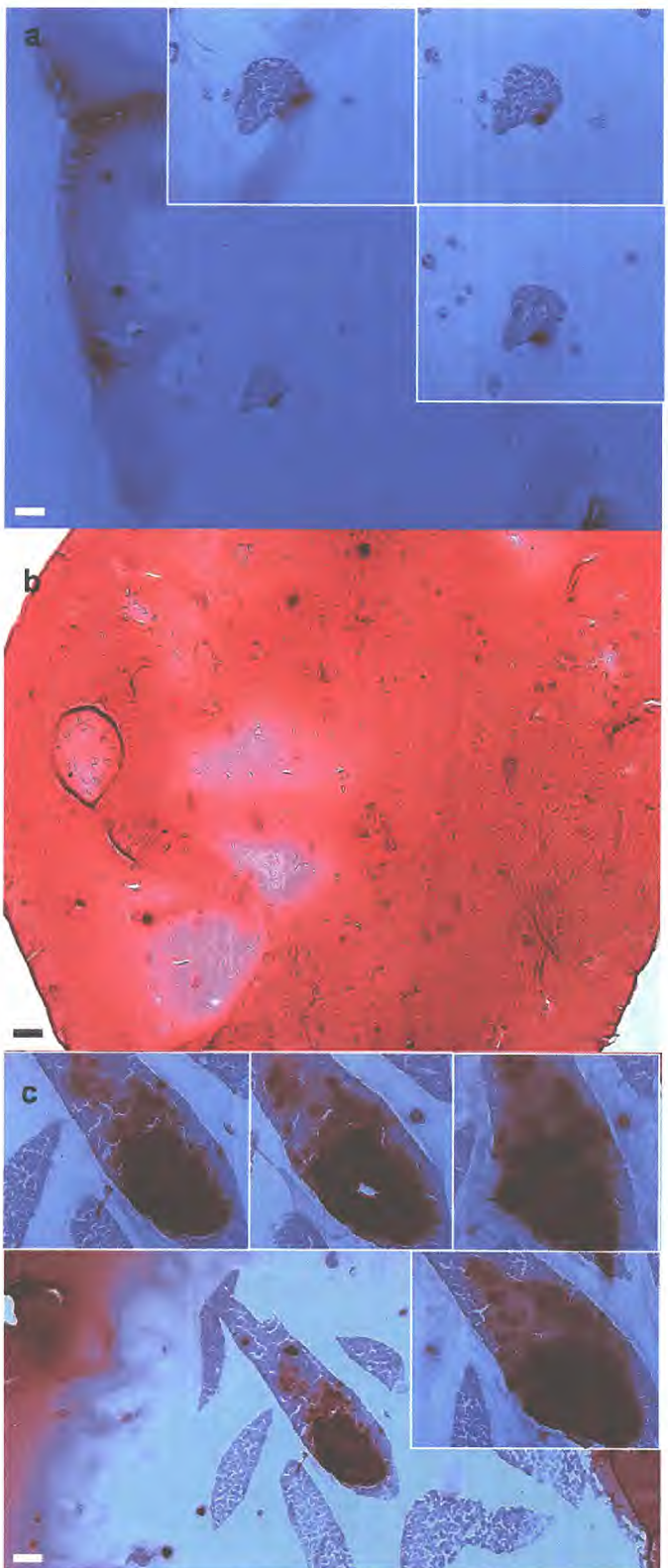


Figure 5.21. Day 22, paraffin embedded, sectioned, Alizarin Red S stained alginate beads. a. 3D static. b. 3D stirred. c. 3D HARV. Scale bars = 100 µm. Inset high mag serial sections.

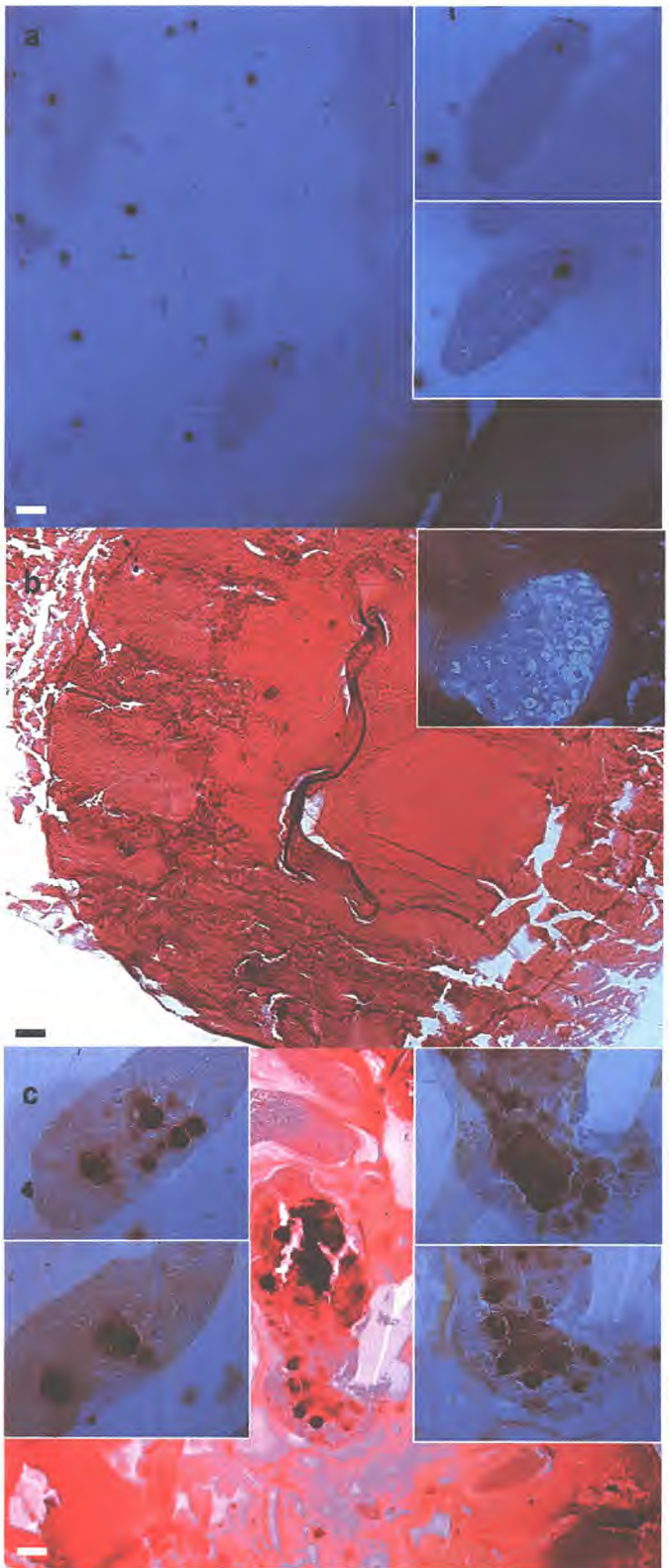


Figure 5.22. Day 29, paraffin embedded, sectioned, Alizarin Red S stained alginate beads. a. 3D static. b. 3D stirred. c. 3D HARV. Scale bars = 100 µm. Inset high mag serial sections.

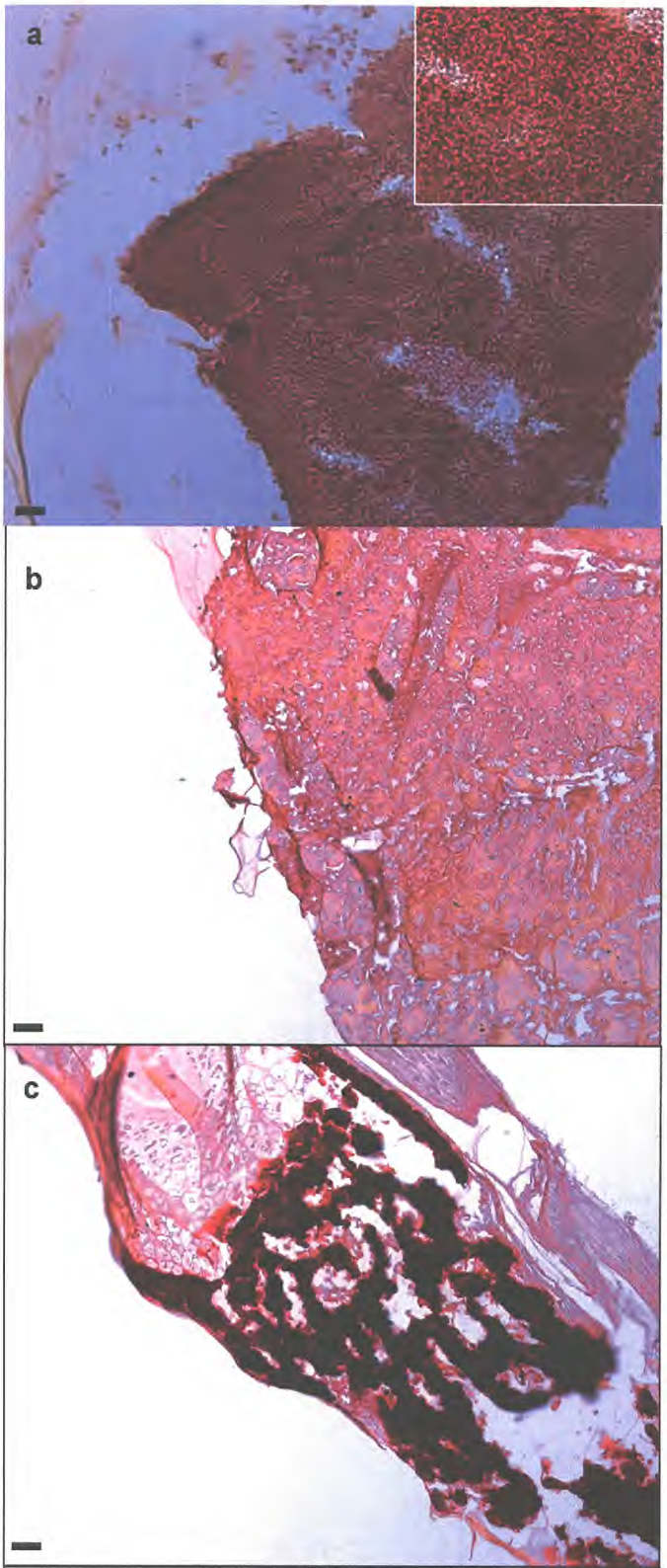


Figure 5.23. Day 29, paraffin embedded, sectioned, Alizarin Red S stained controls. a. 2D static. b. mouse kidney. c. mouse bone/muscle. Scale bars = 100 µm. Inset high mag serial sections.

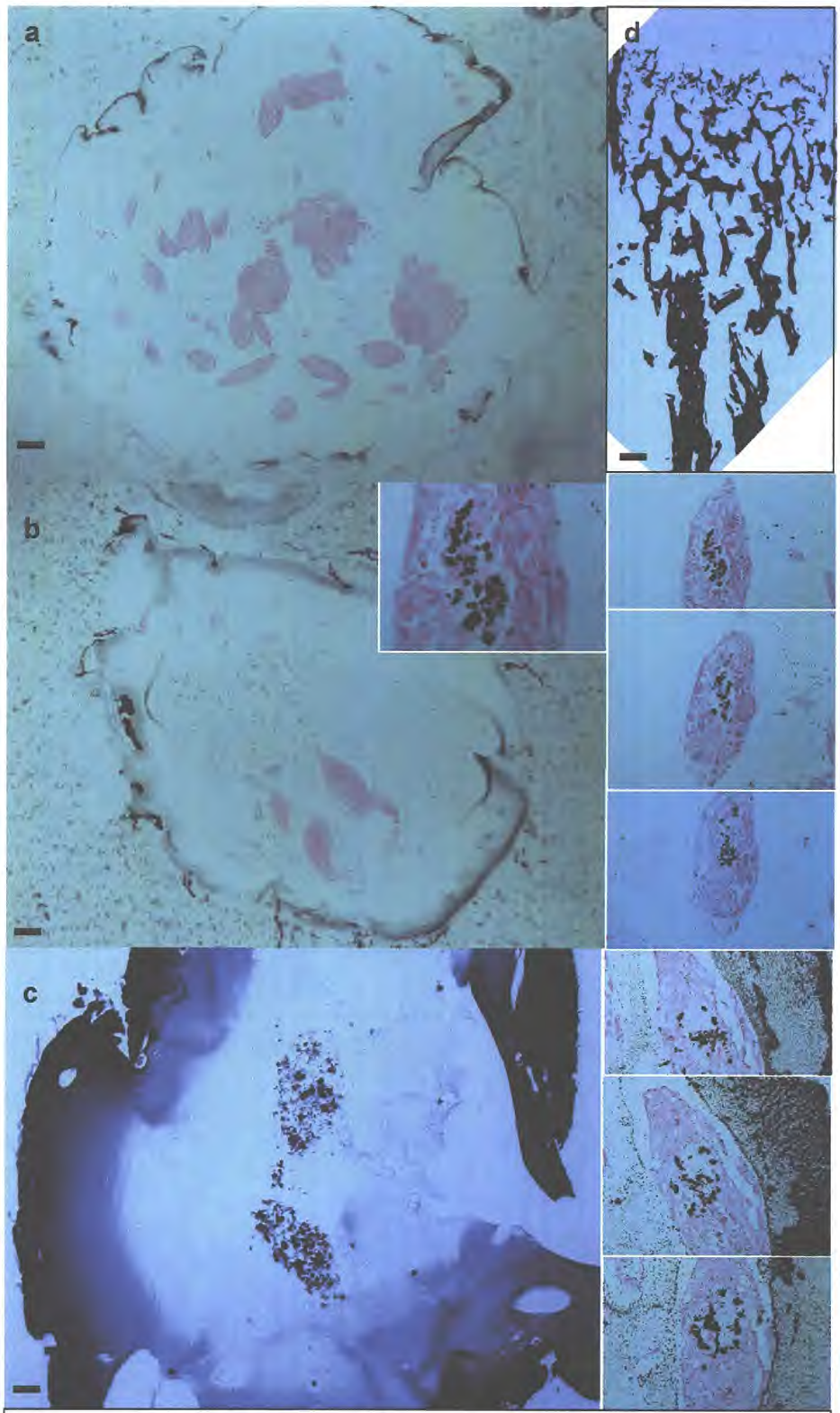


Figure 5.24. Day 15, 22 and 29, paraffin embedded, sectioned, von Kossa stained beads. a. 3D HARV day 15. b. 3D HARV day 22. c. 3D HARV day 29. d. Mouse bone control. Scale bars = 100 µm. Inset high mag serial sections.

5.4.2.4. Immunocytochemistry

Maintenance and EB formation stage

Immunostaining was performed on 2D, 3D static, 3D stirred and 3D HARV cultures but only the HARV cultures are shown with 2D or mouse bone controls. Some successful immunostaining from the 2D, 3D static and 3D stirred cultures is shown in Appendix 1.7&8 but most of the staining was discontinued due to poor tissue quality throughout the latter parts of osteogenic differentiation.

In Figure 5.25a-c, at day 3 the encapsulated mESCs cultured in the 3D HARV expressed Oct-4 (in the nuclei) and CD9 (on the surface), indicative of an undifferentiated phenotype. Furthermore at day 8, Flk-1 expression was present in the 3D culture (Figure 5.25d), which is indicative of mesodermal tissue formation.

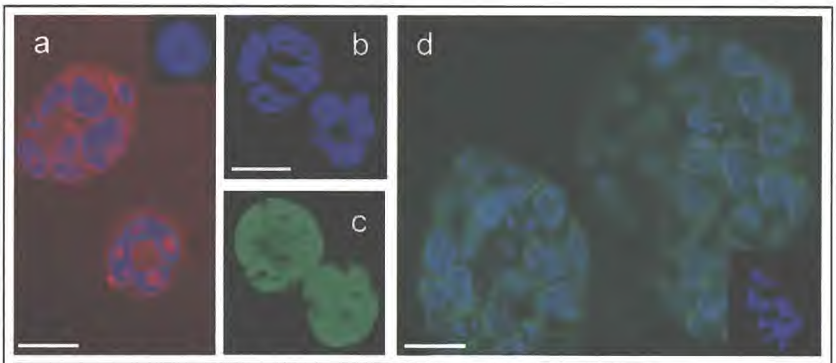


Figure 5.25. 3D tissue characterisation, day 3 to 8. Immunocytochemistry indicates pluripotent stem cells and mesodermal tissue. a. Day 3, DAPI (blue) and CD9 (red) b. Day 3, DAPI (blue) c. Day 3, Oct-4 (green) d. Day 8, DAPI (blue) and Flk-1 (green). Negative control images are inset and were from 2D mESCs cultured on tissue culture plastic. Scale bar, 20 µm.

Osteogenic differentiation stage

The 3D mineralised tissue formed in the alginate beads was further analysed by immunocytochemistry for the expression of bone tissue-specific markers, such as OB-cadherin, collagen type-I and osteocalcin. OB-cadherin, which identifies osteoblasts (277), was detected on days 15, 22 and 29 of culture (Figure

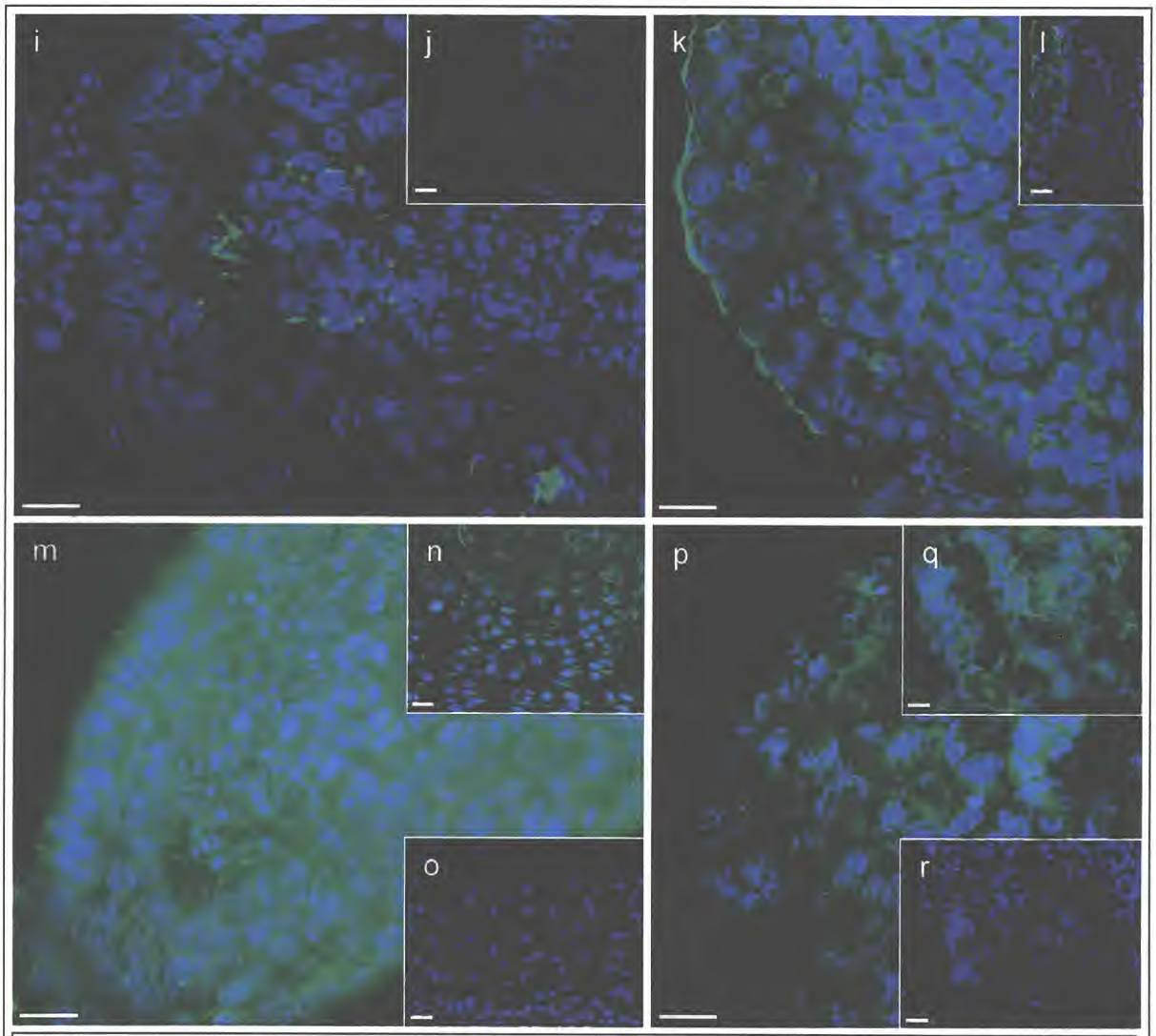


Figure 5.26. Bone aggregate immunocytochemical characterisation. Day 15 to 29 with positive and negative controls. i. Day 29 DAPI (blue) and Osteocalcin (green). j. Balb/c mouse bone negative control, DAPI (blue) and Osteocalcin (green) k. Day 29 DAPI, (blue) and Osteocalcin (green) l. Balb/c mouse bone positive control, DAPI (blue) and Osteocalcin (green) m. Day 29, DAPI (blue) and OB-cadherin (green) n. Balb/c mouse bone positive control, DAPI (blue) and OB-cadherin (green) o. Balb/c mouse bone negative control, DAPI (blue) and OB-cadherin (green) p. Day 29, DAPI (blue) and collagen-I (green) q. Balb/c mouse bone positive control DAPI (blue) and collagen-I (green) r. Balb/c mouse bone negative control, DAPI (blue) and collagen-I (green). Scale bars g-j " 20 µm.

5.26m) and was ubiquitously distributed throughout the large sections of tissue formed. Most of the staining was confined to the edges of the tissues where the cells were organised in a columnar fashion. Isolated occurrences of osteocalcin in mineralised regions were in "ring" formations (50 μm radius), at the centres of the tissues at both day 22 and 29 (Figure 5.26i). The nuclei in the centre of these rings were condensed, more compact and may well have been trapped osteocytes. Moreover, mineralisation also occurred on the edges of some tissues and diminished towards the centre of the tissue over a 50 μm distance which was similar to mouse femur controls (See Figure 5.26k). Osteocalcin staining was detected on the periphery of the mineralised sections on the same tissue samples staining positive for OB-cadherin (Figure 5.26k). Osteocalcin staining became less pronounced towards the centre of the tissue, similar to the edges of mouse femur positive controls. Finally, collagen type-I was also detected, albeit at lower levels, compared to the mouse bone positive controls and only visible on day 29 (Figure 5.26p).

5.4.2.5. DNA cell quantification

The number of metabolically active, undifferentiated cells in each bead on day 0 was confirmed by measuring the amount of DNA in a single bead and was found to be 10,287±228 cells per bead (mean ± SE; n=2 analysing 150 beads for each replicate). After 29 days of culture in the HARV bioreactor there were 859,716±13,492 (mean ± SE; n=6), based on the DNA quantity per bead, representing an 84-fold increase from encapsulation. Six million undifferentiated cells in 600 beads were cultured in this system and produced over 5×10^8 cells.

5.4.2.6. Biochemical characterisation

2D static analysis was performed and yielded results that were comparable to previously published work from the same laboratory (232) but 3D static and stirred cultures did not provide sufficient tissue qualities or quantities based on the sensitivity of the assays used. As a guide, the 3D HARV live/dead viability images have been incorporated within Figure 5.27.

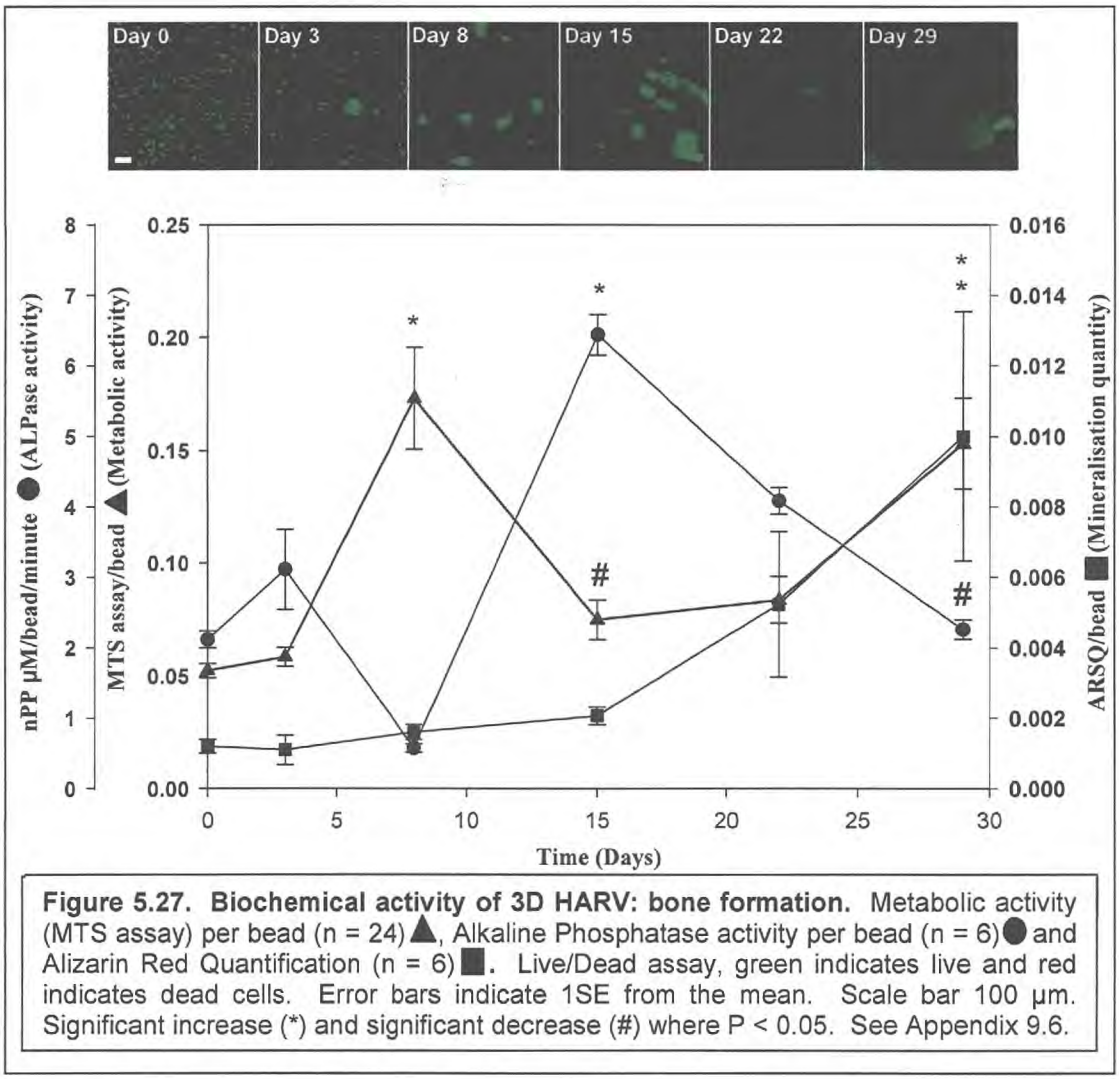


Figure 5.27. Biochemical activity of 3D HARV: bone formation. Metabolic activity (MTS assay) per bead (n = 24) ▲, Alkaline Phosphatase activity per bead (n = 6) ● and Alizarin Red Quantification (n = 6) ■. Live/Dead assay, green indicates live and red indicates dead cells. Error bars indicate 1SE from the mean. Scale bar 100 µm. Significant increase (*) and significant decrease (#) where $P < 0.05$. See Appendix 9.6.

Cell viability of the encapsulated mESCs did not prove to decrease with culture time as the colonies increased in size. At day 3, there was evidence of limited cell death, as indicated by the paucity of red cells (Figure 5.27); however the majority of cells began to form discrete, live colonies. Although colony size increased with culture time, colony numbers did not increase markedly during the first 3 weeks of culture, despite the fact that viability was very high (Figure 5.27). Finally, after 29 days of culture, live colonies were clearly visible in higher numbers than on day 22 and were also larger than they were earlier in culture.

The number of metabolically active, undifferentiated mESCs per bead on day 0, assessed by measuring the amount of DNA in a single bead, was found to be 10,287 ± 228 cells per bead (mean ± SE; n=2 analysing 150 beads for each replicate). After 29 days of culture in the HARV bioreactor there were 859,716 ± 13,492 cells per bead (mean ± SE; n=6), representing an 84-fold increase from the beginning of encapsulation. The changes in metabolic activity appeared to relate to the stage of culture, the type of medium used and the time of feeding. From day 0 to day 3, the beads were cultured in maintenance medium and only a small increase in metabolic activity per bead was registered (Figure 5.27). On day 3 the culture medium was changed from the maintenance medium to the EB formation medium and this resulted in a vast increase ($p < 0.05$) in metabolic activity per bead, as shown in Figure 2. At day 8, the differentiation medium was introduced and the metabolic activity dropped significantly by day 15 and only increased slightly by 22. From day 22 to 29 a further significant increase ($p < 0.05$) in metabolic activity per bead was also noticed (Figure 5.27). However, due to the 84-fold increase in the cell

number by day 29 of culture within the alginate beads, the metabolic activity per cell does not increase.

ALPase and the amount of mineralisation were used as indicators of osteogenic differentiation during the osteogenesis period (day 15 to day 29 of culture) but also measured from day 0. ALPase activity decreased significantly ($p < 0.05$) in a linear manner from 6.4 ± 0.29 to 2.26 ± 0.14 nPP µM/bead/minute (mean ± SE) between day 15 and day 29 (Figure 5.27). In contrast, the amount of mineralisation per bead (based on absorbance at 410 nm) increased linearly ($p < 0.05$) from 0.0021 ± 0.0003 on day 15 to 0.0999 ± 0.0035 (mean ± SE) on day 29, as shown in figure 5.27. The absorbance readings were normalised per bead but actual readings were taken using the mineralised contents of around 100 beads per reading.

5.4.2.7. Reverse Transcription-PCR

EB formation stage

The amount of RNA used for reverse transcription was always 1 µg and this can be seen in the uniformity of the *GapDH* bands after PCR amplification. RT-PCR is not quantitative or even semi-quantitative unless the reactions are performed in triplicate and the intensity of each band normalised to the housekeeping gene. However, one may infer that expression levels increase or decrease by the visual appearance of the bands but firm conclusions must only be drawn based on the presence or absence of any banding, not intensity.

Oct-4 is a transcriptional regulator found in early embryos and undifferentiated ESCs but diminishes with differentiation. In Figure 5.28, Oct-4

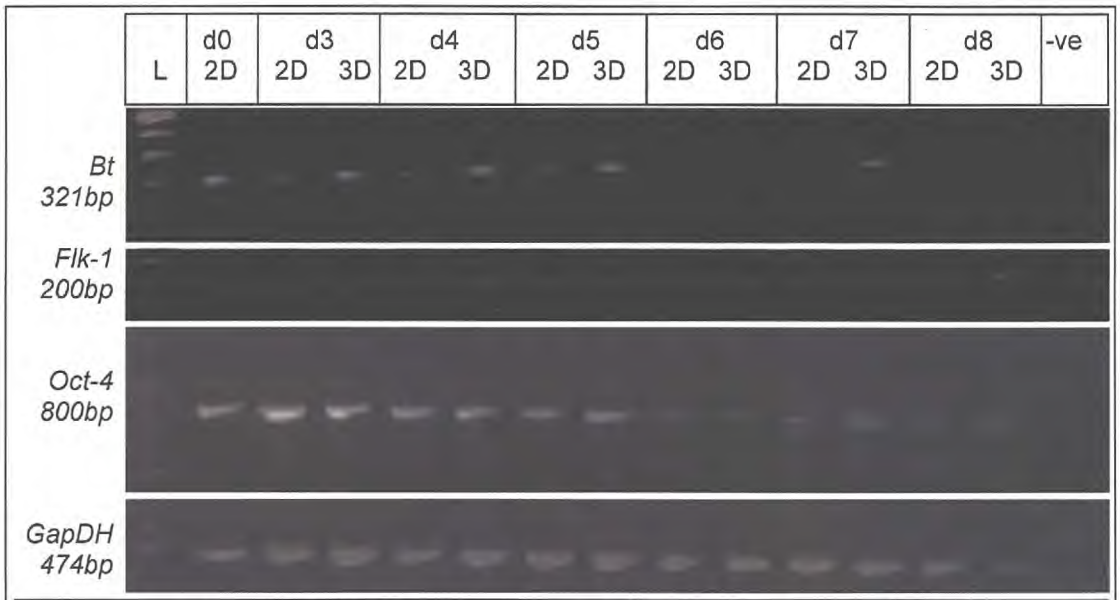


Figure 5.28. RT-PCR characterisation from day 0 to 8 in 2D and 3D HARV culture. mRNA expression in 2D and 3D HARV culture. L = 100bp DNA ladder. -ve = PCR water control with GapDH primers. GapDH = Glyceraldehyde-3-phosphate dehydrogenase, Bt = Brachyury T, Flk-1 = Foetal liver kinase-1 and Oct-4 = Octamer binding factor 3/4.

expression was present from day 0 to day 8 in both 2D and 3D cultures but there was an obvious decrease in expression throughout the time course based on visual band intensity, indicating differentiation. The appearance of Oct-4 expression found in this study in 2D EB formation is supported in the literature (140;148) by diminishing expression through differentiation.

Brachyury T is a requirement for normal mesodermal development in the mouse and is expressed during 2D EB formation at days 1, 2, 3, 4 and 5 (88;89;140;148;226) depending on the culture parameters used. It is clear that *Brachyury T* expression was present in the undifferentiated mESCs in both 2D and 3D which suggests a heterogeneous population of cells already exists in

these cell stocks. Prof. Peter Andrews' group has also identified *Brachyury T* expression in both human EC (278) and hESCs (279) that are undifferentiated, which confuses matters. It is also evident that expression, by visual inspection fluctuates until day 7 and diminishes at day 8 in both 2D and 3D. The fluctuations in expression could coincide with the feeding. In addition, Flk-1 an established mesodermal surface marker (87;247) only begins to be expressed in this study, in both 2D and 3D at day 4, diminishing on day 6 (coinciding with the feed day) and re-appearing on days 7 and 8.

Differences between the 2D and 3D cultures were not observed in terms of expression or lack of expression at specific time points. The only difference of potential importance that may be inferred is the intensity of the *Brachyury T* expression from day 3 to day 5 (day 0 to day 3 of EB formation).

Osteogenic differentiation stage

RT-PCR demonstrated (Figure 5.29) the expression of *Cbfa-1* and *collagen type-I* at days 15, 22 and 29 within the 3D beads. *Collagen type-IIA* (transient embryonic form) (208) and *osteocalcin* expression was found at days 15 and 22 and then at the same intensity as controls (MC-3T3-E1 cell line) on day 29.

RT-PCR analysis (Figure 5.29) further confirms the presence of

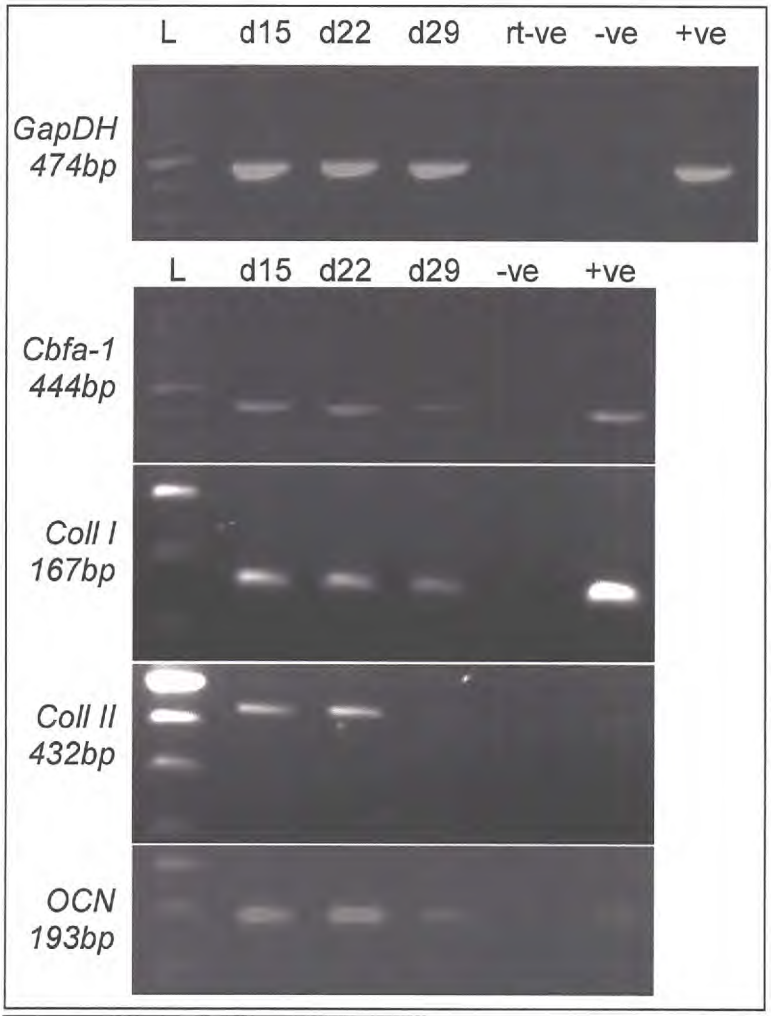


Figure 5.29. RT-PCR characterisation from day 15 to 29 in 3D HARV culture. mRNA expression in 3D HARV culture on days 15, 22 and 29. L = 100bp DNA ladder. RT-ve = no RT enzyme using day 29 HARV RNA with GapDH primers. -ve = PCR water control with *GapDH* primers. +ve = MC-3T3-E1 cells cultured for 10 days in osteogenic medium. *GapDH* = *Glyceraldehyde-3-phosphate dehydrogenase*, *Cbfa-1* = *core-binding factor alpha-1*, *Coll I* = *Collagen type-I*, *Coll* = *Collagen type-IIA* (432bp), *Collagen type-IIB* (225bp) and *OCN* = *Osteocalcin*.

terminally differentiated, 3D mineralised tissue that does not contain mature cartilage. Again, the definitive phenotype of the endpoint 3D tissue generated in this study appears to be mitotically active, mature osteoblasts which express *Cbfa-1*, *collagen type-I*, and *osteocalcin* (280;281). Embryonic *collagen type-IIA*

(splice variant A) expression is normal during mESC osteogenic differentiation (208;282) and similarly, *osteocalcin* expression has also been previously reported from days 7 to 21 of osteogenic differentiation (283), corresponding to days 15 to 29 in this study. The lack of any mature *collagen type-IIB* (splice variant B, 225bp) expression indicates that mature cartilage is not present and the 3D mineralised tissue primarily consists of collagen type-I.

5.4.2.8. Medium analysis

Media samples were taken from 2 separate HARV reactors, at the same time of day, for 29 days. Beads were not removed from the reactors from day 0 to 29. The media samples were frozen and stored immediately upon collection at -80 °C to preserve the characteristics until analysis. Control media, in duplicate were also analysed to provide medium benchmarks for maintenance, EB differentiation and osteogenic stages. Feed days were 0, 1, 2, 3, 6, 8, 11, 15, 18, 21, 22, 25 and 27. Table 5.2 gives an indication of "basal" levels in the 3 different media (n = 2) and all were warmed to 37 °C before freezing. Appendix 9.9 provides details of how the parameters were measured.

Table 5.2. Basal analyte values from fresh media samples.

Control medium MEANS	pH @ 37oC	PO2 @ 37oC mmHg	Na+ mmol/L	K+ mmol/L	Ca++ mmol/L	GLU mmol/L	Lac mmol/L	Gluc mmol/L	NH4+ mmol/L	AirSat %	Osm mOsm/kg
Maintenance	7.5405	258.4	144.1	5.35	1.425	0.225	1.15	28.4	0.6	175.8	428.5
SD	0.01	0.14	6.79	0.21	0.05	0.02	1.63	3.82	0.00	0.00	19.09
Differentiation	7.2555	240.05	137.45	5.65	1.39	0.86	2.5	5.9	0.5	163	395
SD	0.08	7.14	1.06	0.07	0.03	0.03	0.28	0.99	0.00	5.23	2.83
Differentiation + OS	7.327	229.2	143.1	5.55	1.24	0.665	2.55	6.55	0.5	155.6	402.5
SD	0.09	3.96	0.99	0.07	0.01	0.04	0.07	0.07	0.00	3.11	7.78

Maintenance medium, EB formation or differentiation medium and osteogenic differentiation medium samples were taken in duplicate from two separate batches, warmed to 37°C in an incubator and frozen immediately at -80°C prior to analysis at room temperature (21°C). OS = osteogenic supplements.

Calcium

Initial observations indicate that after just 1 day, calcium levels increase from 1.43 mmol/L in maintenance medium to 2.42 mmol/L and return almost immediately to a basal level on day 2 (1.63 mmol/L) (Figure 5.30). From days 3 to 8, iCa^{2+} levels remain constant just above 1 mmol/L which is slightly below the mean levels for differentiation medium suggesting some increased uptake during EB differentiation. However, upon change from differentiation to osteogenic medium, in which the iCa^{2+} levels are very similar in control samples, the cells within the culture system dramatically deplete the levels of iCa^{2+} to 0.5 mmol/L from day 9 to day 29. It is clear that in fresh osteogenic medium there is 1.24 ± 0.01 mmol/L iCa^{2+} (Mean±1SD) and as soon as the bioreactors are fed, the iCa^{2+} levels drop to half this level after 24 hours. Until the next feed day, further drops in iCa^{2+} are seen in a repeatable, controlled manner to levels as low as 0.245 mmol/L on day 15 (day 7 of osteogenic differentiation).

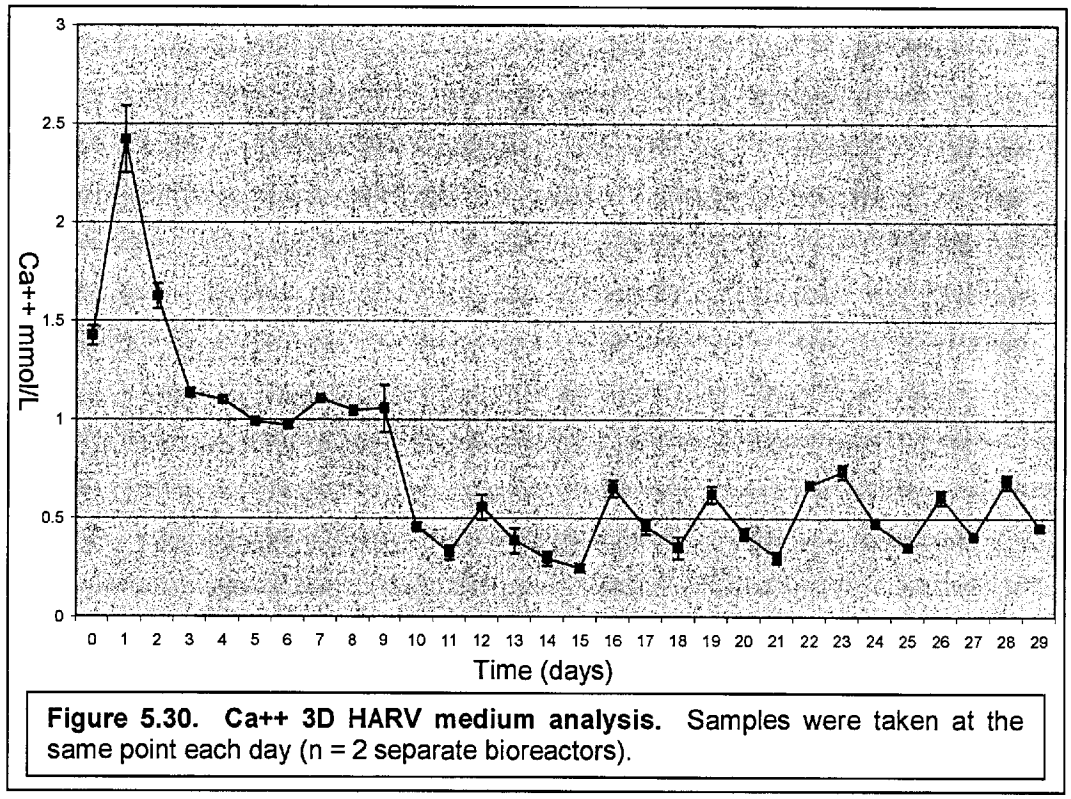


Figure 5.30. Ca++ 3D HARV medium analysis. Samples were taken at the same point each day (n = 2 separate bioreactors).

Potassium/Sodium

Potassium and sodium levels do not fluctuate to extremes around the mean basal levels and only show a basic trend of linear increase from the day of a feed followed by a drop back to basal levels (Figure 5.31&32).

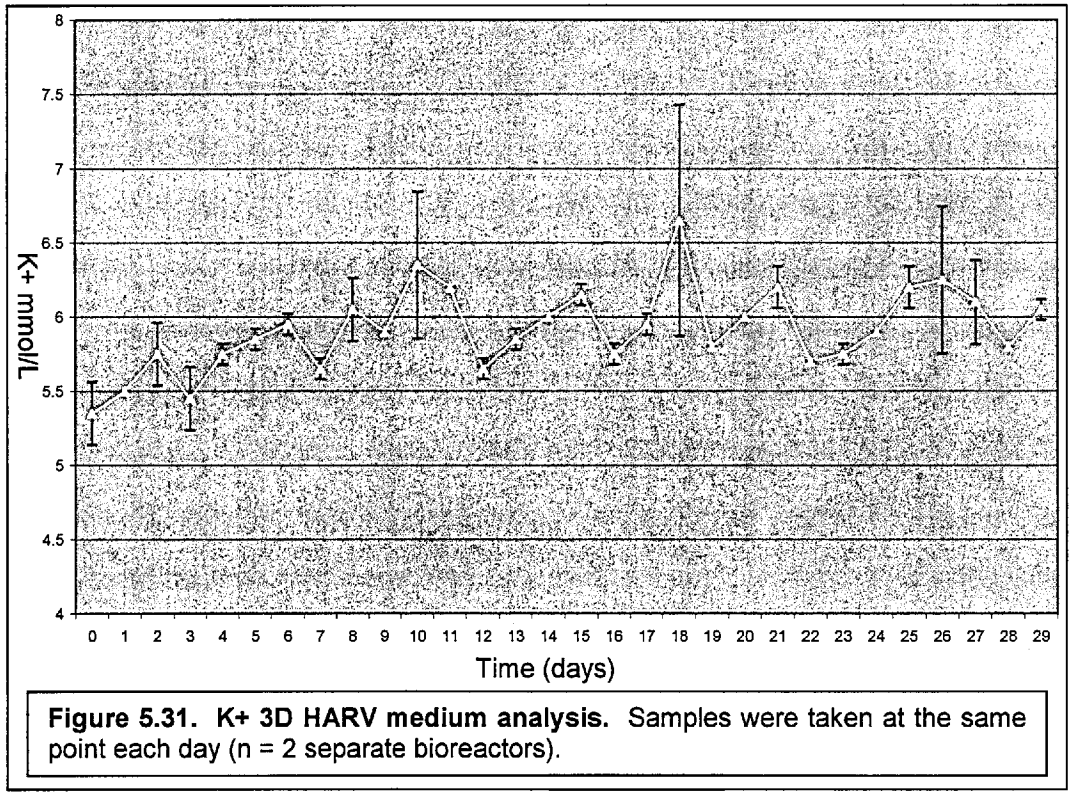


Figure 5.31. K+ 3D HARV medium analysis. Samples were taken at the same point each day (n = 2 separate bioreactors).

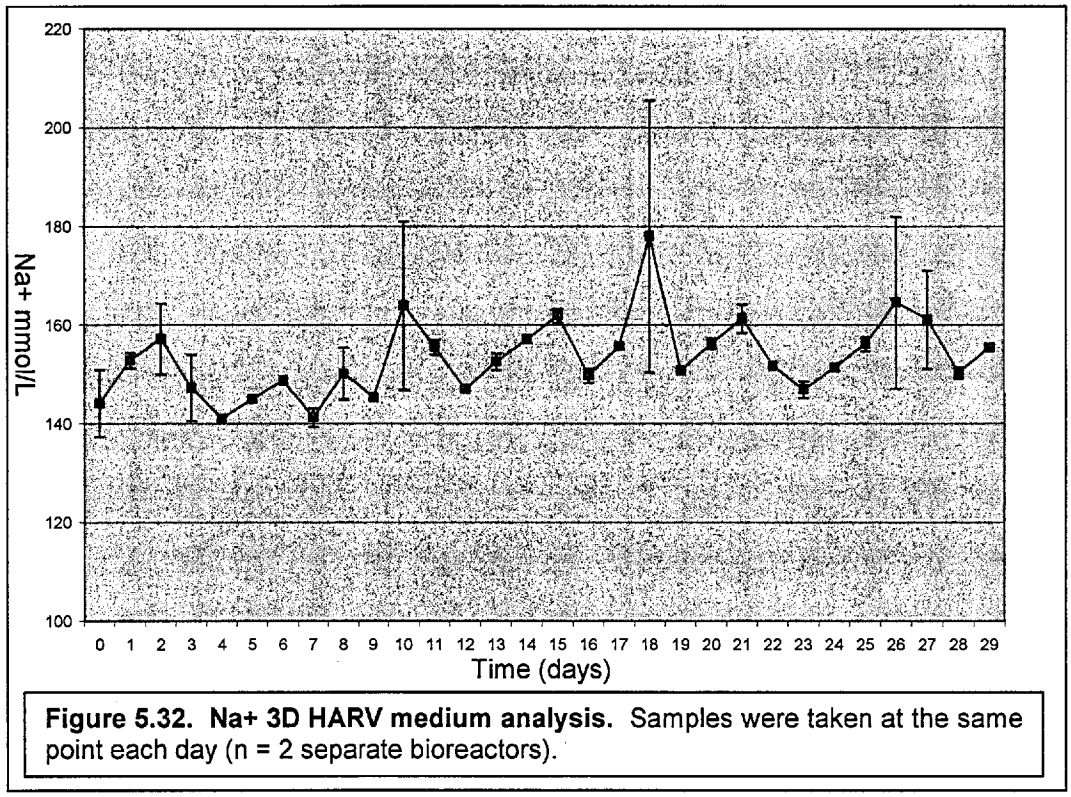


Figure 5.32. Na+ 3D HARV medium analysis. Samples were taken at the same point each day (n = 2 separate bioreactors).

Ammonium

The basal levels for ammonium (NH_4^+) are between 0.5 and 0.6 mmol/L (Figure 5.33). However, levels within this culture system increased rapidly in the first few days of culture and then increased to a higher level of around 2.25 mmol/L for the remaining culture period. The levels of ammonium increased from around 1.5 mmol/L, 24 hours after feeding in a linear fashion to around 3.25 mmol/L and subsequently dropped again after another feed. The fluctuations became less pronounced towards the end of the culture period suggesting a drop in overall metabolic activity.

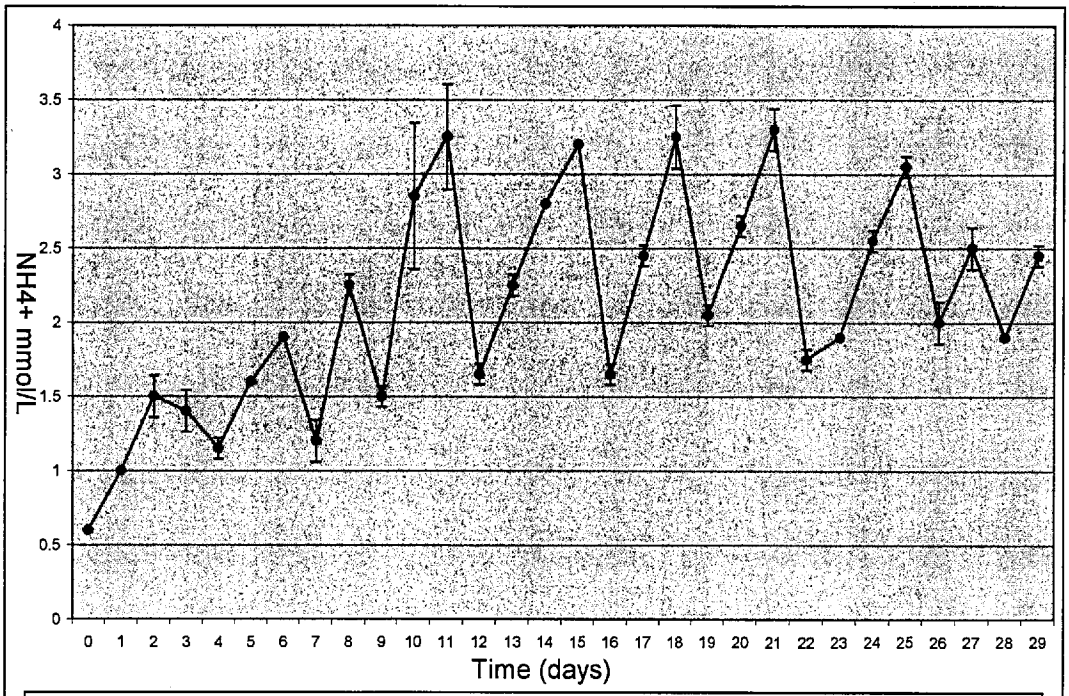


Figure 5.33. NH4+ 3D HARV medium analysis. Samples were taken at the same point each day (n = 2 separate bioreactors).

Glucose

Glucose levels in the form of D-Glucose (Dextrose) are provided in the media used in these experiments (Figure 5.34). In DMEM there is 25 mmol/L and in αMEM there is 5.56 mmol/L. Of course, these media are supplemented with 10% and 15% (v/v) FCS, thus altering the overall concentrations. The mean levels of glucose in maintenance, differentiation and osteogenic media were 28.4 ± 3.82, 5.9 ± 0.99 and 6.55 ± 0.07 mmol / L respectively indicating that the addition of serum provides a slight increase in molar glucose levels from the basal media. The maintenance medium (DMEM based) provides sufficient glucose for the cells in culture. However, the cells appear to require higher levels of glucose corresponding to an increase in metabolic activity (Figure 5.27) on day 3 and 4. Upon change from DMEM to αMEM based medium from day 3 onwards the amount of glucose in the media is clearly not high enough and the cells are metabolising the glucose (5.56 mmol/L) immediately.

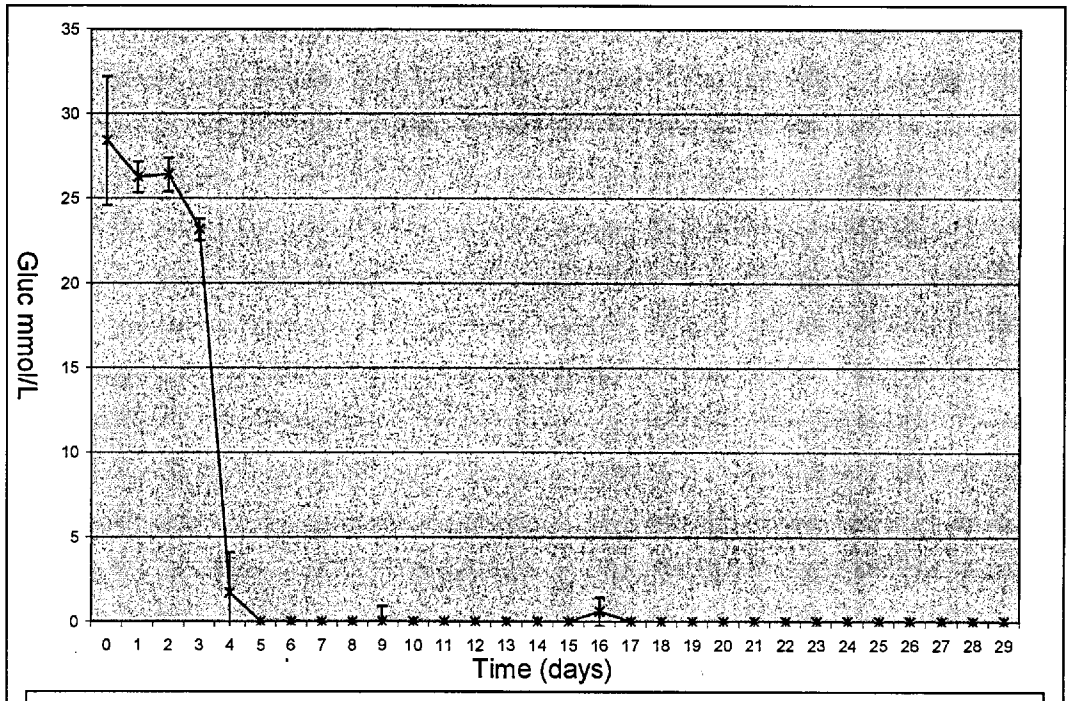


Figure 5.34. Glucose 3D HARV medium analysis. Samples were taken at the same point each day (n = 2 separate bioreactors).

Glutamate

In DMEM based medium there is 4 mmol/L of L-Glutamine and this is increased by supplementation to 6 mmol/L L-glutamine into maintenance media (Figure 5.35). In αMEM based media (differentiation and osteogenic medium) there is 2 mmol/L and no more is added. Glutamine is converted by cells via oxidative metabolism to glutamate and ammonium (NH_3) (by Glutaminase) when glucose is depleted. Glutamate is then converted by glutamate oxidase to ketoglutarate and ammonium (NH_3).

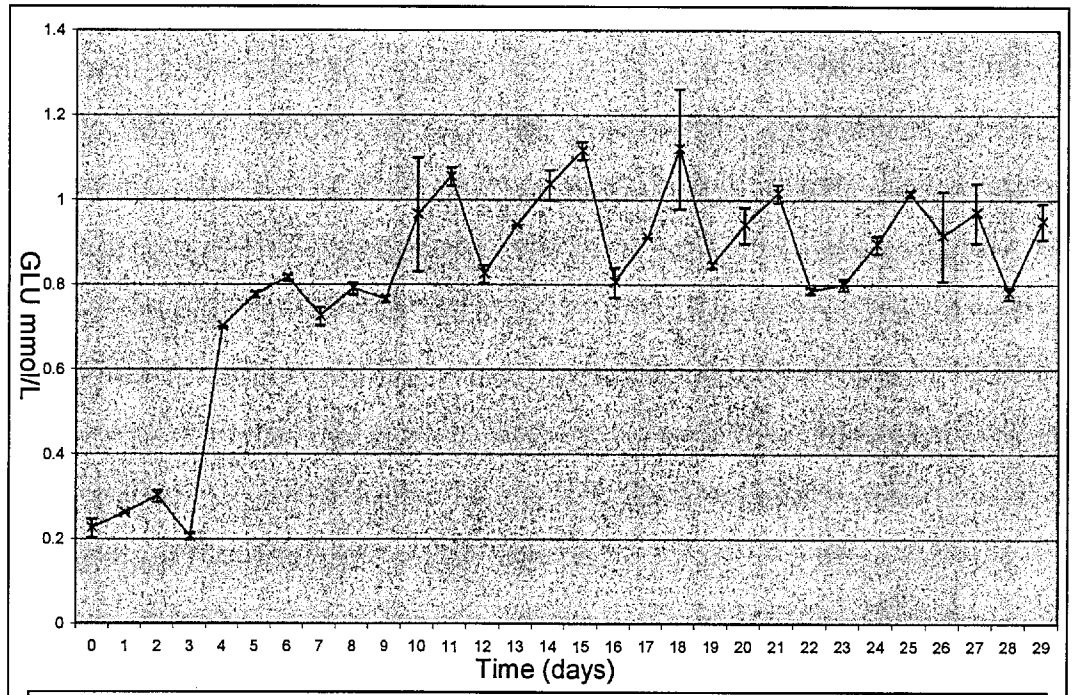


Figure 5.35. Glutamate 3D HARV medium analysis. Samples were taken at the same point each day (n = 2 separate bioreactors).

The drop in glucose available to the cells upon change from maintenance to differentiation medium corresponds with the increase in ammonium produced. Moreover, the switch from using glucose as the main energy source to glutamine is also noticeable with the increase in glutamate at the same time

(days 3 and 4). However, basal glutamate levels in maintenance (0.23 ± 0.02 mmol/L), differentiation (0.66 ± 0.03 mmol/L) and osteogenic differentiation medium (0.67 ± 0.04 mmol/L) are similar to those measured from the media samples. While L-glutamine is an essential component of most cell culture media, it is also the most unstable of the common medium components, decomposing spontaneously in aqueous, neutral solutions, forming ammonium.

Lactate

Lactate forms through lactic acid fermentation during anaerobic glycolysis in order to maintain an overall electron balance. Normally lactate is shunted around the body to respiring tissues where it is metabolised further or converted back to glucose (gluconeogenesis). However, if it is formed in high quantities it cannot be readily consumed. Animal cells can reduce limited amounts of pyruvate to lactate in a single step.

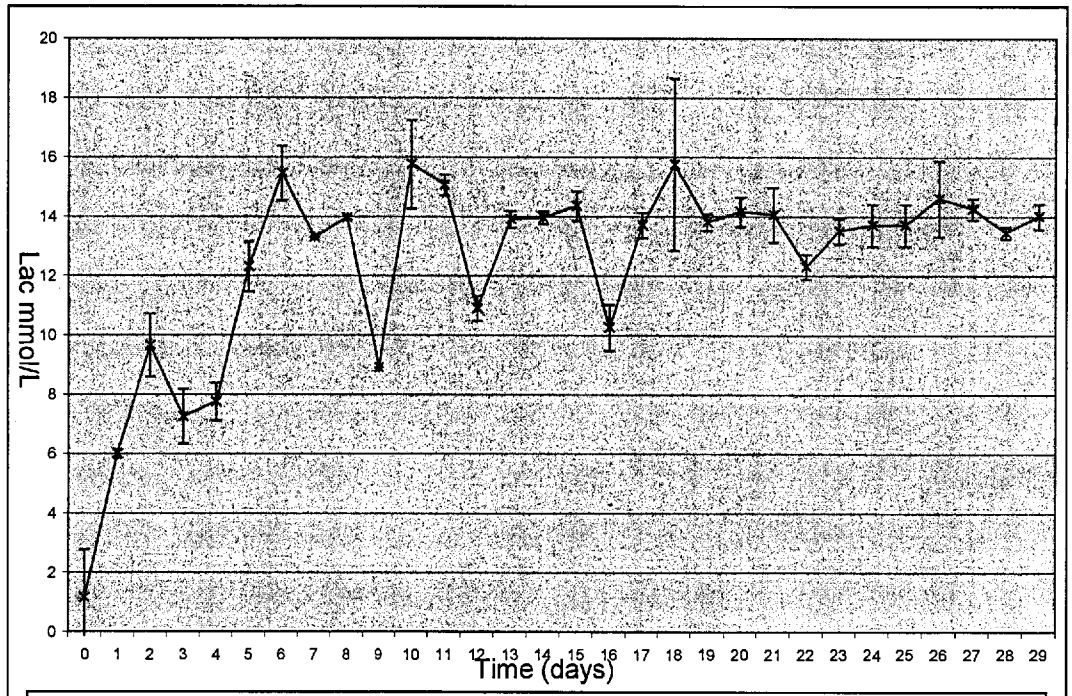


Figure 5.36. Lactate 3D HARV medium analysis. Samples were taken at the same point each day (n = 2 separate bioreactors).

The amount of lactate produced arises through the rapid consumption of glucose. It is clear that metabolism is incredibly high throughout the culture period but fluctuates around 13 mmol/L, probably due to the lack of glucose (Figure 5.36). The largest fluctuations occur between days 4 and 19 and the fluctuation intensity decreases until day 29, suggesting a drop in cell division but a regular turnover of the cells in existence.

pH

Although the pH data fluctuate in this study it must be noted that the media samples were frozen before analysis and this would have affected the readings. The pH of a solution is the concentration of hydrogen ions in the solution. The unusually high pH levels from day 0 (1 hour after beads in medium) to day 3 can be attributed to unused Ca^{2+} release from the alginate beads (Figure 5.37). This detachment from alginate molecules would cause a decrease in hydrogen

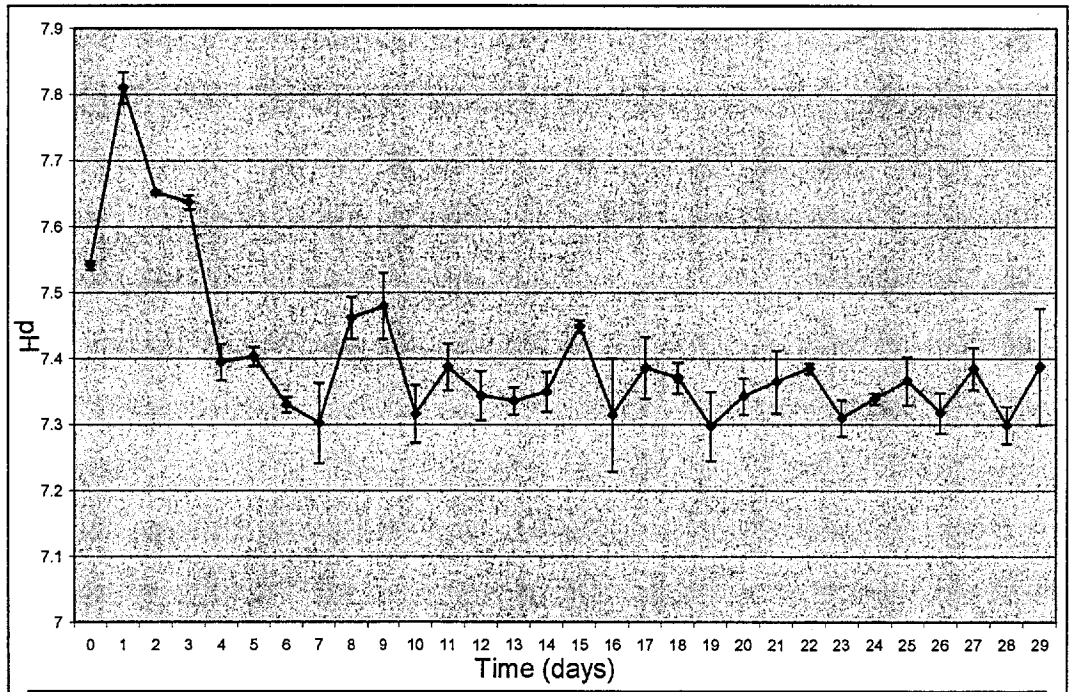


Figure 5.37. pH 3D HARV medium analysis. Samples were taken at the same point each day (n = 2 separate bioreactors).

ions in the medium and thus an increase in pH. The pH levels during EB differentiation and osteogenic differentiation do not fluctuate greatly which are attributed to the buffering capacity of the medium used.

Partial pressure of Oxygen (P O_2)

Although the P O_2 data fluctuate in this study it must be noted that the media samples were frozen before analysis and this would have affected the readings. The level of P O_2 never rose above 300 mmHg and more importantly, never dropped below 142 mmHg, which is the level produced by a conventional 5% CO_2 / 95% air incubator (Figure 5.38).

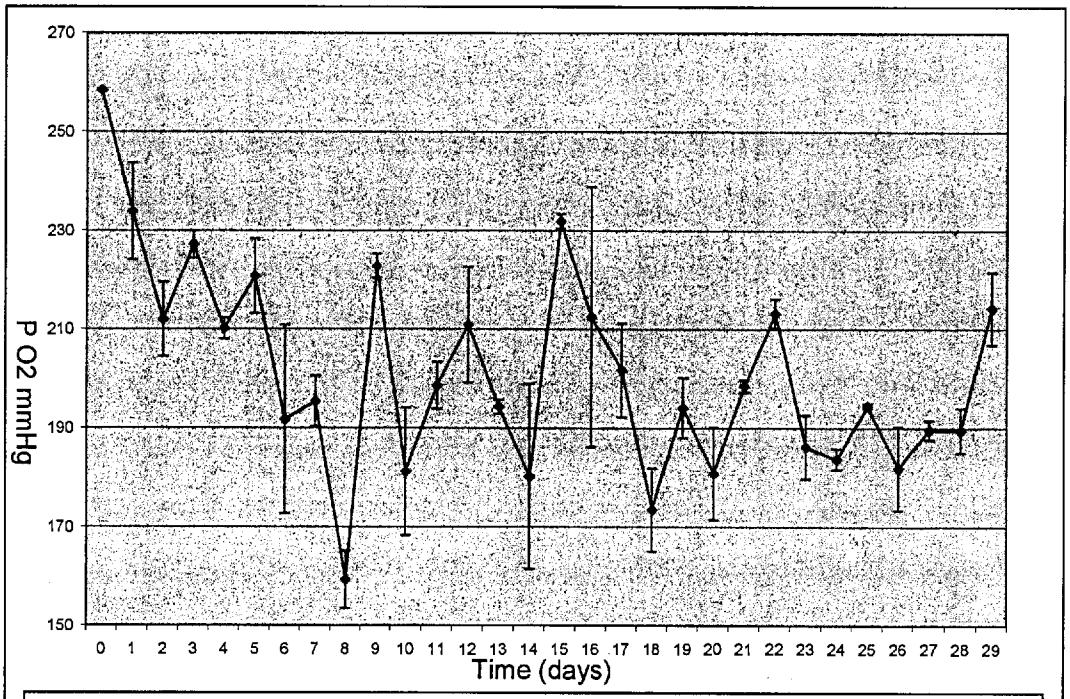


Figure 5.38. P O_2 @ 37°C 3D HARV medium analysis. Samples were taken at the same point each day (n = 2 separate bioreactors).

5.4.2.9. Micro-computed tomography (micro-CT) imaging

Micro-CT analysis of negative controls (beads without cells) produced images with very little contrast (Figure 5.39). In contrast, 3D mineralised tissue, formed within the alginate beads from the mESCs provided suitable contrast.

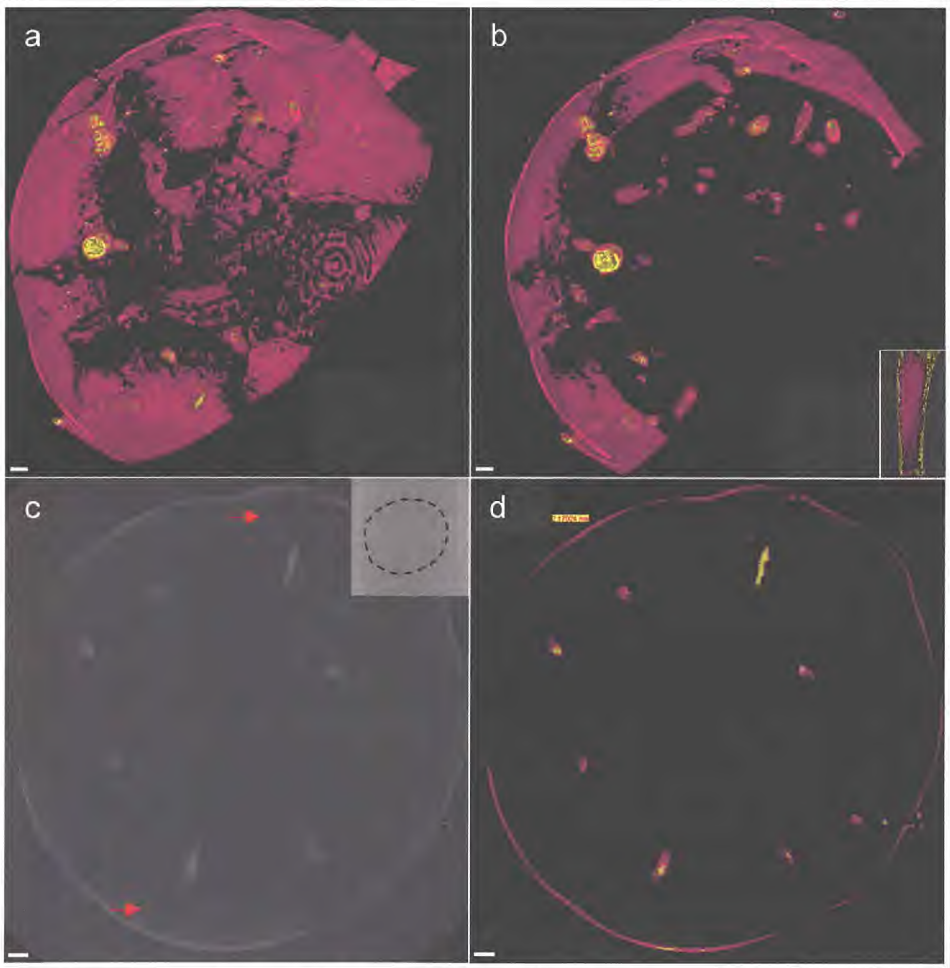


Figure 5.39. 3D HARV micro-computed tomography. Mineralised aggregate imaging on day 29 with positive and negative controls.
a. False colour, day 29 bone containing alginate bead, 3D sector reconstruction b. False colour, day 29 bone containing alginate bead, 3D segment reconstruction b inset. False colour image, Balb/c mouse femur positive control encapsulated, 2D cross section c. Greyscale transmission image, day 29 bone containing alginate bead, 2D cross section (red arrows indicate soft tissue surrounding mineralised aggregate) c inset. Greyscale transmission image negative control, alginate bead, 2D cross section, dotted line denotes bead border d. False colour, day 29 bone containing alginate bead, 2D cross section. Scale bars from a-d, 100μm. Colouration in false colour images indicates level of attenuation from highest (yellow), to purple and the lowest (black), indicating hard to soft tissue respectively.

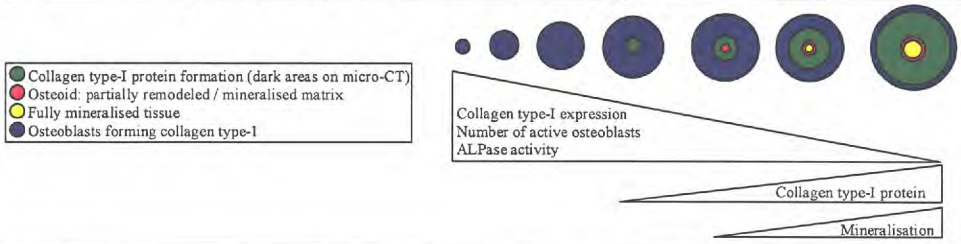
Besides the dense 3D mineralised aggregates, the superficial "crust" (purple) of the alginate beads was also detected by micro-CT outlining the periphery of the alginate beads (Figure 5.39) at days 15, 22 and 29. The 3D mineralised aggregates, within the bead itself (yellow), indicated high levels of attenuation in their centres with decreasing attenuation (purple) as distance from the core of the 3D mineralised aggregates increased. A positive control of mouse femur was imaged to compare the degree of mineralisation (Figure 5.39). Completely scanning a randomly selected alginate bead provided a 3D reconstruction of the mineralised aggregate sections within the alginate bead. On day 15, 3D mineralised aggregates were not visible, but by day 22, 14 small aggregates (<50 μm) were visible. However, on day 29 enumeration of these 3D mineralised aggregates within the bead revealed that 44 ± 7 (SE, n = 2) such aggregates were present, ranging in size from 50 to 250 μm (Figure 5.39). These 3D mineralised aggregates were surrounded by soft tissue (Figure 5.39c, red arrows) as darker regions. This system generates 859,716±13,492 (mean ± SE; n=6) cells per bead but the proportion of bone cells is unknown.

5.4.3. Development of mESCs to bone

This section brings together all the results and techniques of analysis and interprets them as a continous bioprocess from undifferentiated mESC on day 0 to 3D mineralised bone tissue on day 29.

Table 5.3. 3D HARV feeding, analysis and bone aggregate formation.

3D HARV Media changes	0	1	2	3	4	5	6	7	8	9	10	11	12	13	14	15	16	17	18	19	20	21	22	23	24	25	26	27	28	29
Maintenance	F	F	F																											
"EB" Formation				F				F																						
Osteogenic Differentiation									F			F				F			F			F	F			F		F		
Biochemical assays																														
MTS	X			X					X							X							X						X
ALPase	X			X					X							X							X						X
Alizarin quantification	X			X					X							X							X						X
Histochemistry																														
Immunostaining	X			X					X							X							X						X
Alizarin staining																X							X						X
von Kossa staining																X							X						X
Other																														
micro-CT																X							X						X
DNA quantification	X																													X
Live / Dead imaging	X			X					X							X							X						X
RT-PCR	X	X	X	X	X	X	X	X	X							X							X						X



Representation of biochemical, histochemical and other analysis in a chronological order. X indicates analysis performed on this day. F = feed day. Triangles indicate increase/decrease of expression/presence/activity.

Table 5.4. Phenotypic development of mESCs during 3D HARV culture.

Time (days)	0	3	4	5	6	7	8	15	22	29
Biochemical										
ALPase	+	+	-					+++	++	+
MTS	+	+					+++	+	+	+++
Live/Dead	++	++		++			++	++	+	++
ARSQ								+	++	+++
ARS								-	+	++
vKossa								-	+	+
micro-CT								-	+	++
RT-PCR										
Oct3/4	+++	+++	+++	+++	+	++	+			
Flk-1	-	-	+	+	-	+	+			
Brachyury T	++	++	++	++	+	++	-			
Cbfa1								+++	+++	++
Coll I								+++	+++	+++
Coll IIA								+++	+++	+
OCN								++	+++	+
ICC										
Oct3/4	+	+								
CD9	+	+								
Flk-1							+			
OB-Cadherin								+	+	+
Coll I								-	-	+
OCN								-	+	+

Schematic of biochemical, histochemical, immunocytochemical and gene expression from day 0 to day 29 in the 3D HARV. + = Intensity based on measured or visual expression, - = no band/background stain

5.4.3.1. Day 0 – 3 "Maintenance stage"

The undifferentiated mESCs were encapsulated in alginate beads on day 0 as a single cell suspension and were not affected by the encapsulation procedure in terms of viability or metabolic activity. After three days of culture in maintenance medium the cells formed small colonies and retained their phenotype, viability and metabolic activity levels. There were no obvious signs of differentiation.

5.4.3.2. Day 3 – 8 "EB formation stage"

The undifferentiated colonies of mESCs were placed in differentiation medium for 5 days in order to form the three germ layers and formed mesodermal tissue by day 8. The feeding regime changed from daily to once every two/three days and it was clear that the encapsulated cells were depleting the levels of glucose available to them well before the feed day. This was however only apparent retrospectively after media analysis.

In the ES/EB model system, mesoderm, as defined by expression of the T-box gene *Brachyury*, is induced within 48 hours of the onset of differentiation and persists until day 5 (284). The timing of *Brachyury T* expression in the mouse ES/EB model is dependent on the culture parameters used (88;89;140;148;226) and is also found in the undifferentiated population of some hESCs (279). In the mouse embryo, the T-box gene *Brachyury* is first detected in the developing primitive streak and the newly emerging mesoderm (285). Mesoderm is generated from the epiblast or embryonic ectoderm through the process of gastrulation that is initiated at approximately day 6.5 (3 days after ICM isolation or day 3 of EB formation) of gestation [reviewed by Tam and Behringer *et al.* (286)]. In this study mesoderm begins to develop

from day 0 of EB formation and is still present by day 8. Co-expression of *Flk-1* and *Brachyury T* exists on days 4, 5 and 7 in the 3D HARV and the lack of expression on day 6 was probably due to a lack of nutrients and gene down regulation, due to starvation (feed day was day 3 of EB formation). Therefore, in the 3D HARV, mesodermal tissue formation (not gene expression), is visible between day 4 and 8 (Flk-1 antigen expression on day 8) that relates to the presence of mesoderm during mouse gestation (initiated at approximately day 6.5 or 7) (287). It appears that expression of mesoderm at the gene level (*Brachyury T*; days 3→7) is then immediately followed by the appearance of mesodermal tissue at the protein level (Flk-1; days 4→8).

5.4.3.3. Day 8 – 15 "Osteogenic differentiation stage"

Following culture for 5 days in the EB formation medium, colony size in the alginate beads had increased dramatically, in some cases reaching 400 µm in diameter, without any significant decrease in viability. The colonies grew evenly in discrete "pockets" within the beads that have been reported to be more conducive to growth (2). Even though we encapsulated undifferentiated mESCs and did not form EBs using the traditional suspension method, expression of the Flk-1 antigen during days 3-8 in culture confirmed the development of mesoderm (211;288) (Table 5.4).

Expression of OB-cadherin early during osteogenesis (day 15) indicated the presence of osteoblasts in the 3D cultures (277) (Table 5.3 & 5.4). These osteoblasts were both alive (esterase activity) and metabolically active (dehydrogenase activity) at day 15. At the onset of osteogenic differentiation (day 8), metabolic activity per bead was high and reached a low at day 15, which correlated with ALPase activity being at its highest level whereas mineralisation was near its lowest. As osteogenesis proceeded (days 15 to 29),

a decrease in ALPase activity (per bead) and an increase in mineralisation was observed, as has been shown in other models of osteogenic differentiation and growth (289). ALPase activity in skeletal tissues is thought to increase the local inorganic phosphate levels, destroy inhibitors of hydroxyapaptite crystal growth, and aid in phosphate transport, amongst other functions (290). The latter part of osteogenesis may be the stage where osteoblasts become trapped within the secreted matrix and reduce their metabolic activity drastically in order to divert their resources to mineralisation. The drop in ALPase activity, the increase in mineralisation, and the low metabolic activity per cell at days 22 and 29 suggest that the cell phenotype during this period could be that of mature osteoblasts. This is further substantiated by the fact that by the end of osteogenesis (on day 29) osteocalcin, OB-cadherin and collagen type-I proteins were detected. Extrapolated figures from the 2D versus 3D experiments give us indications to the number of 2D or 3D bone nodules/aggregations that can form from undifferentiated mESCs where both the media treatment regimes were identical. Table 5.5 essentially indicates that 223 and 227 undifferentiated mESCs will differentiate into a single 2D bone nodule or a single 3D mineralised aggregate respectively.

Table 5.5. Efficiency of 2D versus 3D mESC osteogenic differentiation cultures.

	# of Day 0 Undifferentiated mESCs	Approximate # of Day 8 EB cells	Replating density	# of Day 29 bone nodules (2D) or bone aggregates (3D) formed	Minimum media volume required (L)	Efficiency of nodule/aggregate formation per mESC
2D	5×10^6	2×10^7	$2.5 \times 10^4/cm^2$ (or 400 x 6 well plate wells)	2.24×10^4 (estimated based on 56 ± 26 per six well plate well)	1.26	223:1
3D	6×10^6	Unknown	N/A	2.64×10^4 (44 ± 7 per bead)	0.6	227:1

Osteocalcin expression is transient in embryonic bone whereas it is one of the most abundant proteins in adult bone, binding to hydroxyapatite in a calcium-dependent manner (291;292). Woven bone is characterised by irregular bundles of collagen fibres, large and numerous osteocytes, and delayed, disorderly calcification that occurs in irregularly distributed patches (48). The presence of osteocalcin in rings and on the edges of the 3D tissue aggregates in this study, at both days 22 and 29, concurs with the micro-CT results. These observations suggest that the mineralised tissue in the alginate beads was formed by condensation of apatite crystals (bone development) and potentially at the leading edge of the osteoid front (adult lamellar bone). Our data infer that the cells, were mostly osteoblasts with proliferative capacity (281) and that hydroxyapatite had been deposited. It is accepted that differentiation from multipotent progenitors to mature osteocytes follows the proliferation, extracellular matrix development and mineralisation stages with some apoptosis being seen in mature nodules (93).

I would propose that the ossification centres are the locations that first begin to generate small amounts of collagen type-I (indicated by gene expression but not by immunocytochemistry) at day 15 (Table 5.3 and Table 5.4). As ossification continues and begins to remodel/replace the collagen

matrix with mineral from the centre outwards, the gene expression levels drop. However, the amount of collagen type-I protein was only detectable at day 29. I think what occurs is represented below in diagrammatic form. From what we have seen with the micro-CT there doesn't appear to be any mineralisation at all on day 15 but this occurs in a partially mineralised state on day 22 and then fully mineralises on day 29 with partially mineralised tissue surrounding it. I would also hypothesise, as we saw ring stuctures / OCN immunostaining that mineralisation proceedes from the foci outwards from day 22 to 29 and needs a collagen type-I matrix for it to actually remodel. This can be seen on the micro-CT as darker regions surrounding the mineralised aggregates. As the osteoblasts produce more and more collagen type-I they become trapped in matrix and mineralisation will therefore follow. In short, I would suggest that these results do not indicate that osteogenic differentiation exclusively begins at day 8 and ends at day 29 but more likely; initiates at day 8 in some populations, at ossification centres and then continues to initiate in three-dimensions, concomitantly, having different stages of differentiation at any one time, as one would find *in vivo*. The majority however co-incide and it would be useful to analyse both the types and quantities of each progenitor at any given time point.

5.4.4. Application of 3D HARV culture model

The 3D mineralised tissue formation model can now be used to revolutionise the way in which cell culture is performed and monitored.

5.4.4.1. HepG2 conditioned medium

A recent publication from the same laboratory indicated that treating mESCs with conditioned medium from a hepatocarcinoma cell line (HepG2) resulted in an increase in 2D bone nodule formation (232). Therefore, mESCs were

cultured in 2D as a control, in 3D HARV, as previously described, and also in 3D HARV but with the substitution of differentiation medium for HepG2 conditioned medium from day 4 until day 8. HepG2 (ATCC HB-8605) cells were seeded at 5 x 10^4 cells/cm^2 in maintenance medium minus 2-mercaptoethanol and LIF. The cells were cultured in three layered flasks producing greater volumes and the medium was collected after 4 days, filtered (0.2 µm filter) and stored at -20°C or +4°C for no longer than two weeks. This conditioned medium (CM) was then added 1:1 with conventional maintenance medium and used to culture the cells within the alginate beads for 5 days in the HARV bioreactor. Prior to this addition, the mESCs, as previously described, were cultured for 3 days in maintenance medium in order to form colonies of undifferentiated mESCs within the beads, effectively mimicking the experimental protocols described previously (232). The medium was then changed to osteogenic medium for a further 21 days culture as previously described.

Morphology

Colonies formed in 3D HARV, HepG2 conditioned medium were smaller (diameter = 100 µm) than conventional 3D HARV culture by day 7, which was expected as the amount of serum was 5% lower [10% (v/v)] than differentiation medium and half the medium was conditioned (used). Compared to day 8, 2D EBs that are typically cystic in their centres (inset Figure

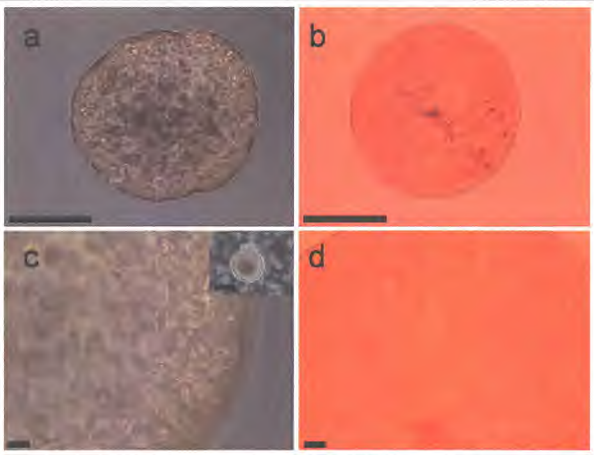


Figure 5.40. Morphological 3D HARV, 3D HepG2 HARV and 2D EBs. a. day 7 HARV (low mag.). b. day 7 HepG2 HARV (low mag.). c. day 7 HARV (high mag.), inset day 8 EB control (high mag.). d. day 7 HepG2 HARV (high mag.). Scale bars, ab = 1 mm, cd = 100 µm.

5.40c) both 3D HARV colonies are smaller. Germ layers are present in 2D EBs but are not immediately evident in 3D HARV culture when viewed with a colour camera at low magnification (Figure 5.40). There is evidence of germ layer formation in some high power colour images (Figure 5.7kmon; Day 7) and some high magnification images using a black and white CCD camera (Figure 5.44) but this is circumstantial and has not been confirmed with immunocytochemistry. It is known that the colonies on day 8 in 3D HARV culture do possess the mesodermal marker Flk-1 (Figure 5.25).

After 29 days of culture, both 3D HARV and 3D HARV HepG2 cultures yielded what appeared like deposits of mineralised tissue which is similar to what appears in 2D cultures (inset Figure 5.41a) and both cultures penetrated the outer surfaces of the beads. In addition, both 3D HARV and 3D HARV HepG2 cultures formed tissue that were naturally pigmented with a red colouration (Figure 5.41ce). Also, in 3D HARV HepG2 cultures, glandular like regions were formed that had discrete layers of tissue, distributed in a circular array (Figure 5.41e).

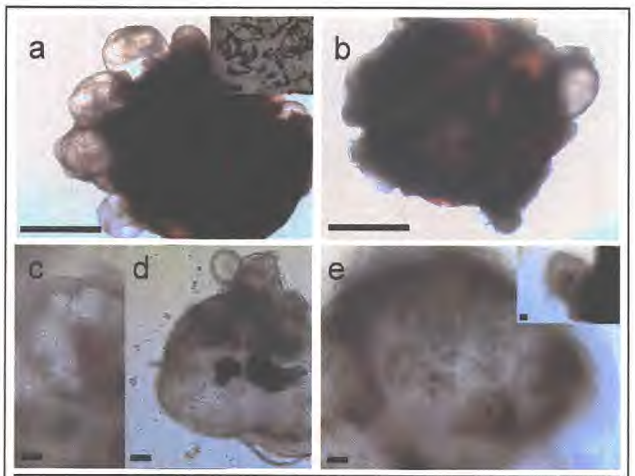


Figure 5.41. Morphological 3D HARV, 3D HepG2 HARV and 2D bone nodules day 29. a. day 29 HARV (low mag.). inset 2D bone nodules day 29 (low mag.) b. day 29 HepG2 HARV (low mag.). c. day 29 HARV (high mag.) erythrocytes. d. day 29 HARV (high mag.) bone aggregate. e. day 29 HepG2 HARV (high mag.) glandular formation. Inset day 29 HepG2 HARV (high mag.) bone aggregate. Scale bars, ab = 1 mm, bcd/insets = 100 µm.

Alizarin Red S and von Kossa staining in serial sections

At day 29, both 3D HARV and 3D HARV HepG2 cultures formed 3D mineralised aggregates, in serial sections, in all beads that were sectioned (Figure 5.42). Mineralised aggregates reached similar sizes in diameter (200 µm) and were present both within and external to the bead surface. Intensity of staining was similar to mouse bone positive controls as previously described (Figure 5.18). The mineralised aggregates were either in the centre of soft tissue or spanned the entire tissue diameter. Both ARS and von Kossa staining

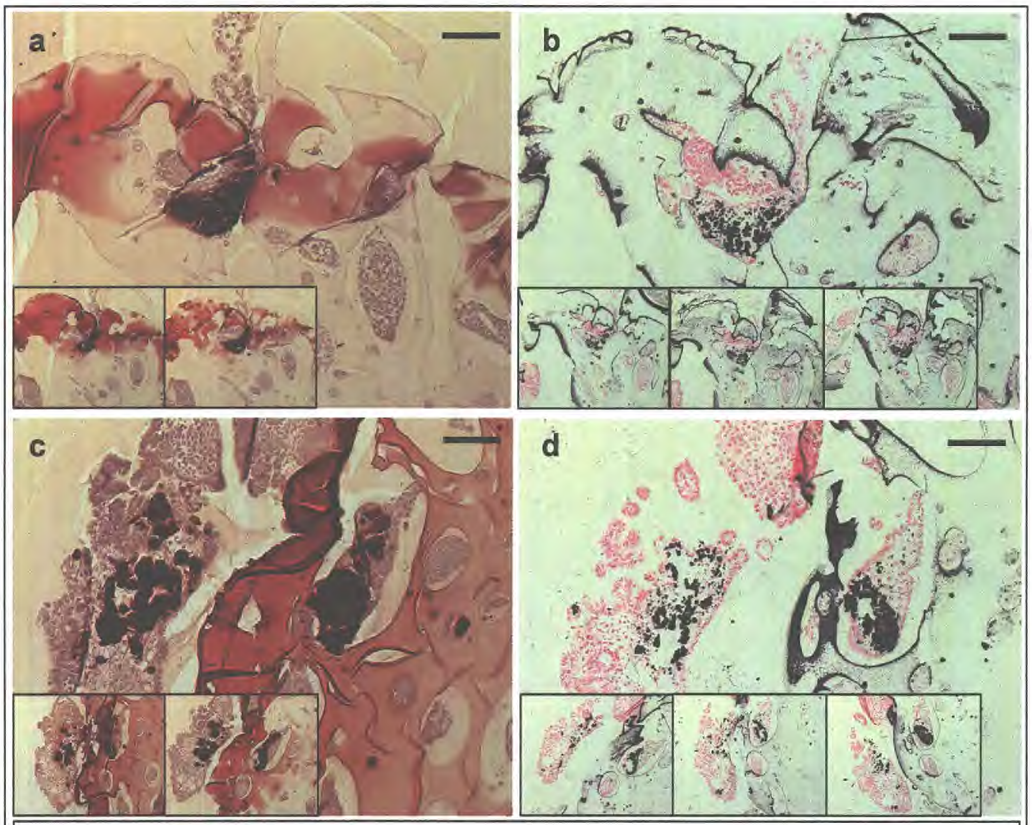


Figure 5.42. Alizarin Red S and von Kossa staining on 3D HARV and 3D HARV HepG2 cultures day 29. a. 3D HARV Alizarin Red S. b. 3D HARV von Kossa. c. 3D HARV HepG2 Alizarin Red S. d. 3D HARV HepG2 von Kossa. Insets = serial sections. Scale bars = 100 µm

revealed the presence of mineralised aggregates in serial sections from the same beads. It was also clear that mineralised aggregates tended to form predominantly in a region approximately 500 μm region beneath the outer surface of the bead. This region could be described as the interface between the strong and medium gelled zones (2), possibly in area's of weakness such as shafts or pockets, reportedly conducive to growth and unusual microenvironments but this has not been confirmed. These clusters or shafts are reported to contain on their inner surfaces, positive residual charges in the form of calcium ions and pockets of space within the alginate beads. The heterogeneity of calcium ion repartition presumably affects the wall-membrane permeability of confined cells, and then the morphological and physiological behaviour (2). It has been reported that excess calcium can inhibit cell growth as previously discussed, however, if the 3D mineralised aggregations are specifically forming within these regions then these pockets or shafts maybe a means by which to induce 3D mineralised tissue formation, at will and appear to be favourable to 3D mineralised aggregate formation.

Mineralisation quantification

In 2D culture, the use of HepG2 conditioned medium induced a 10-fold increase in 2D bone nodule formation by day 14 of osteogenic differentiation and a 21-fold increase by day 29 (232). In 3D HARV culture the quantity of 3D mineralised tissue formed after 22 days [day 14 in previous study (232)] was reported as 2.64-fold greater in 3D HARV HepG2 as opposed to 3D HARV

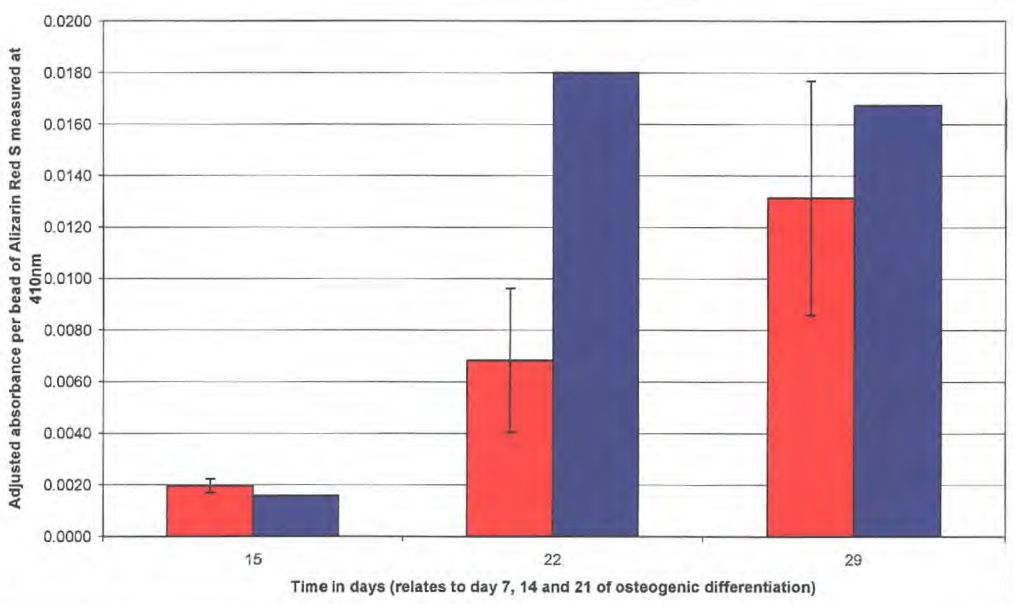


Figure 5.43. Alizarin Red S quantification, day 15 to day 29 comparing 3D HARV and 3D HARV HepG2 conditioned medium. Conventional medium (n = 2 x 2) and HepG2 conditioned medium (n = 1) and the error bars represent 1 standard error from the mean. 3D HARV■ & 3D HARV HepG2■

(Figure 5.43) whereas at day 29 the difference was reduced to 1.27-fold. Therefore, using the medium regime previously reported, the time taken to form the same amount of mineralised tissue per bead takes 1 week less in 3D HARV HepG2 than 3D HARV culture. It must also be noted that the osteogenic differentiation regime in Hwang, *et al.* (232) was optimised by the temporal addition of dexamethasone from day 14 to day 21 of 2D bone nodule formation

(day 22 to 29 in this study) and therefore the 3D HARV HepG2 culture could further enhance 3D mineralised tissue formation with simple modifications. The continuous addition of dexamethasone was originally chosen for reproducibility and simplicity.

5.4.4.2. Perfusion culture

The feeding regime for the perfusion reactor was different to the HARV cultures as the need to feed the cultures manually (batch fed) was not needed. The continual perfusion of medium allowed the medium storage bottle (500 mL capacity) to be filled with a larger volume compared to the actual reactor volume (50 mL). Therefore, on day 0, the entire system was perfused with 150 mL of maintenance medium which was enough to allow the 600 beads (6 x 10^6 cells) in the 50 mL reactor to remain undifferentiated for 3 days. After 3 days the entire reactor was flushed and replaced with 150 mL of differentiation medium until day 8. On days 8, 15 and 22 the medium was again flushed and replaced with 150 mL of osteogenic medium until day 29. The rotation rate was set at 25 RPM in order to maintain free-fall.

Perfusion analysis was limited to medium sampling, morphological images and micro-CT reconstruction as it became apparent that the conditions within the perfusion reactor were not conducive to growth and inhibited tissue growth. Medium analysis did not reveal real differences or indications to the problems within the culture system and the only difference was in the feed strategy, the reactor speed and the reactor dimensions.

Morphology

3D HARV cultures grew as normal and the CCD camera gave an indication morphologically that layers of tissue were forming within the alginate beads, as they normally do in 2D culture (Figure 5.44). In 3D Perfusion culture, cells formed low numbers of colonies that were only 100 µm in diameter by day 29.

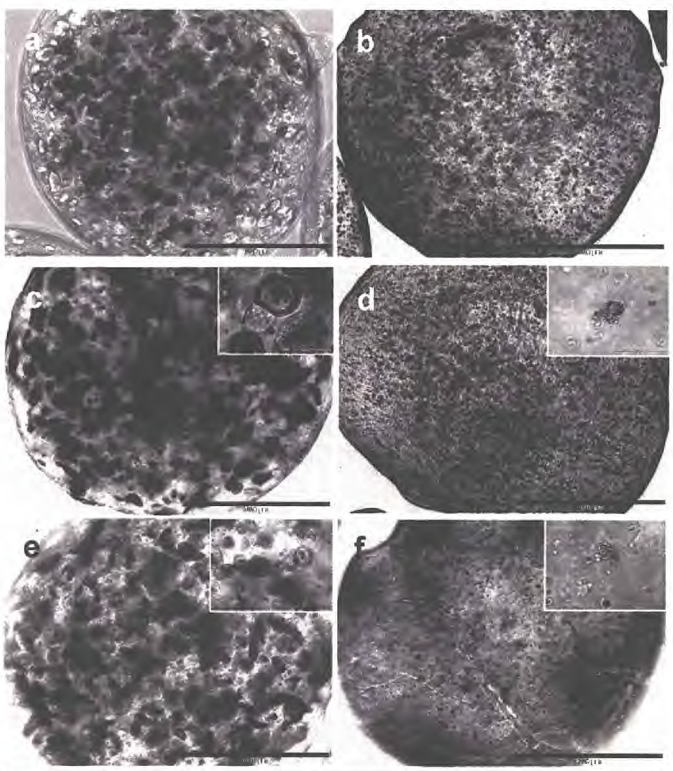


Figure 5.44. Morphological images of beads cultured in 3D HARV & 3D Perfusion cultured beads. a. day 8 HARV. b day 8 Perfusion. c. day 12 HARV. d. day 12 Perfusion. e. day 15 HARV. f. day 15 Perfusion. Insets (high mag). Scale bars = 1000 µm.

Micro-CT

Micro-CT imaging revealed that no mineralised tissue was formed at any time during 3D Perfusion culture (Figure 5.45). This study however, revealed that mineralised aggregates capable of attenuating x-rays formed as early as day 22 in 3D HARV culture, albeit smaller (<50 µm diameter) but no less abundant than at day 29.

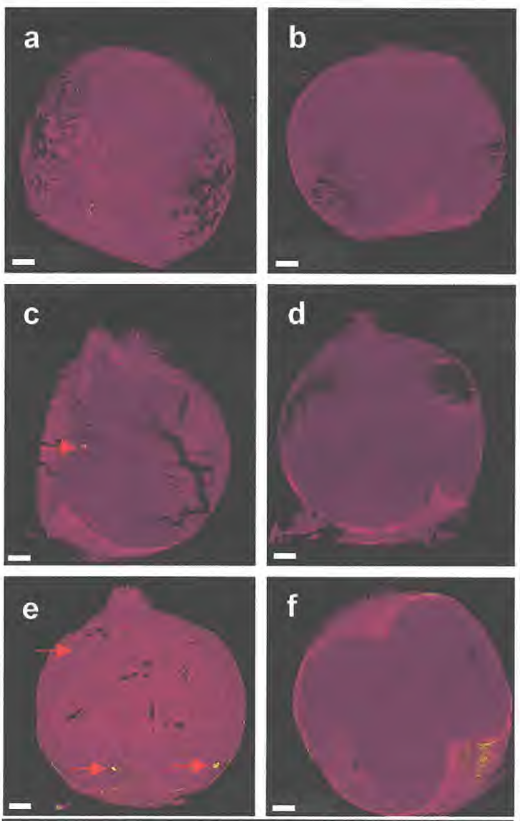


Figure 5.45. Micro-CT images of 3D HARV & 3D Perfusion cultured beads. a. day 15 HARV. b day 15 Perfusion. c. day 22 HARV. d. day 22 Perfusion. e. day 29 HARV. f. day 29 Perfusion. Scale bars = 250 µm. Purple indicates low attenuation & yellow indicates high attenuation. Red arrows indicate mineralised aggregates. NB some pixels of the superficial crusts were incorrectly coloured yellow due to contrast boundary limitations between the bead and the medium.

5.5. Discussion

In this work, we sought to develop an integrated, simplified, reproducible and easily automated process for the production of osteogenic cells from mESCs that would be amenable to scale-up for the generation of clinically relevant numbers of bone cells. In this single, integrated process, we maintained and differentiated mESCs, encapsulated in alginate hydrogels, in HARV bioreactors into osteogenic cells that were capable of producing 3D mineralised tissue. This was demonstrated by stained mineralised aggregates, micro-CT and presence of the OCN protein and other markers. This is the first report of undifferentiated mESCs forming 3D mineralised tissue in a 3D integrated process, without the need for cell culture manipulation. A recent publication from Sandstorms group highlighted the problems of traditional ESC culture and offered a simplified solution (247) for mESC expansion.

Cell viability was measured by live/dead staining as living cells hydrolyse membrane-permeant calcein AM through intracellular esterases to yield cytoplasmic green fluorescence (530 nm) or membrane-impermeant ethidium homodimer-1 labelling the nucleic acids with red fluorescence (585 nm). This gave a brief snapshot of the viability of cells at the moment of staining. It was clear that viability at the beginning and end of 3D HARV culture was maintained but the disappearance of cells at certain time points was perplexing at first. At day 22 for example, in 3D HARV culture, the visual drop in viable green cells was clearly significant but was not accompanied by red, dead cells. This was at first confusing as the cells had just disappeared, yet morphologically they were still within the bead. Closer examination of the MTS metabolic activity data also provides us with a clue that metabolic activity of the cells within the beads between days 15 and 22 dropped to a lower level. However, this level of

metabolic activity (MTS assay) was the same as the metabolic activity measured at days 0 and 3 where viable cells were detected with the live/dead assay. The MTS tetrazolium compound (Owens reagent) is bio reduced by cells into a coloured Formosan product that is soluble in tissue culture medium. This conversion is presumably accomplished by nicotinamide-adenine-dinucleotide-phosphate or nicotinamide adenine dinucleotide (NADPH or NADH) produced by dehydrogenase enzymes in metabolically active cells (293). Therefore, this tells us the exact timing of levels of metabolic activity at specific time points. In 3D HARV culture, intracellular esterase activity of the cells in the beads is high on days 0, 3, 8, 15 and 29 of culture but low at day 22. In contrast, dehydrogenase enzyme activity is at the same, low level between days 0 and 3 as well as days 15 and 22 whereas at days 8 and 29 it is much higher. In short, at day 22, we know that both dehydrogenase and esterase activity are low, presumably diverting resources towards mineralisation, but the cells themselves are still viable.

5.5.1. Maintenance and "EB formation" stages

Each batch of 600 beads was made by gelation in the calcium chloride solution for 6 to 10 minutes meaning the first bead to be dropped received 10 minutes of gelation and the last received 6 minutes. The gelation of alginate is a reaction-diffusion process, in which calcium and alginate diffuse towards each other over a constant constituting boundary to form a stable structure: the Ca-alginate gel network. It seams reasonable to assume that the superficial crust on the bead always forms (as all beads remained intact) and therefore beads with a shorter exposure to the calcium solution have less time to form a calcium-alginate gradient and have a larger weak gelled-zone from the centre of the bead (2).

During the maintenance phase of ESC culture it is imperative to maintain pluripotency and cell viability and it would be vital for LIF to penetrate the bead. The beads in this study could be considered as "semi-solid" and possess both heterogeneity in their calcium distribution and in the arrangement of polysaccharide blocks. Calcium and alginate gradients are found to exist that diminish from the superficial crust (highest concentration) to the bead centre (weak gelled zone) (2). This may be why colonies preferred to grow 500 μm from the crust of the bead although there may have also been an oxygen gradient for example. Beads, similar in manufacture were also found to possess pores of 68 kDa which would, for example easily allow the diffusion of LIF (256). Three days of maintenance culture was previously empirically determined in order to generate colonies of sufficient size that would sufficiently generate EBs, similar to the traditional ESC culture methodology.

After a further 5 days in differentiation medium, the complete lack of non-viable cells indicated that culture conditions were favourable on day 8 and the presence of the Flk-1 antigen (211;288) gave an indication that the tissue was capable of terminally differentiating to tissues of a mesodermal origin. In the mouse embryo, mesoderm is generated from the epiblast or embryonic ectoderm through the process of gastrulation that is initiated at approximately day 6.5 of gestation [see review (294)]. At the onset of gastrulation, the epiblast cells in the region that defines the posterior part of the embryo undergo an epithelial to mesenchymal transition and form a transient structure known as the primitive streak from which the mesoderm emerges. The newly formed mesoderm migrates away from the primitive streak, moves laterally and anteriorly and is patterned into various populations with distinct developmental fates. *Brachyury T* is expressed in all nascent mesoderm and downregulated

as these cells undergo patterning and specification into the derivative tissues (226). In addition, expression of *Flk-1*; a mesodermal marker (87), in the literature is normally later than *Brachyury T* at days 3, 4 and 5 of EB formation (87;148) and sometimes found in combination with *Brachyury T* (226) as reported in this study on days 1 to 4 of EB formation in both 2D and 3D. It appears that the undifferentiated mESCs (E14Tg2a), as found in some lines of hESCs and germ cells (278;279), express *Brachyury T* and this diminishes with time during differentiation.

5.5.2. Osteogenic differentiation stage

On day 8 of culture, in differentiation medium, the three osteogenic supplements (L-ascorbate-2-phosphate, β-glycerophosphate and dexamethasone) were added continuously until day 29. The immunostaining at day 15 revealed widespread positive staining for OB-cadherin indicating the presence of osteoblasts and they were both alive (esterase activity) and metabolically active (dehydrogenase activity). At the low point in metabolic activity per bead (Day 15), ALPase activity was at its highest level, whereas mineralisation was at its lowest. The decrease in ALPase activity and increase in mineralisation between days 15 and 29 can be explained by the fact that ALPase activity is generally known to increase prior to and then decrease once mineralisation is sufficiently progressed. ALPase activity in skeletal tissues is hypothesised to increase local inorganic phosphate levels (Pi), destroy inhibitors of hydroxyapatite crystal growth and aid in the transport of Pi, amongst other functions (290). The occurrences of mineralisation and osteocalcin expression, exclusively on day 22 and again on day 29 suggest that the cells that are metabolically active after day 22, were, in the majority,

osteoblasts that have proliferative capacity (281). It is accepted that differentiation from multipotent progenitors to mature osteocytes undergo proliferation, extracellular matrix development and mineralisation and some apoptosis is seen in mature nodules (93).

The significant decrease in metabolic activity per bead between day 8 and day 15 was followed by a decrease in ALPase activity between day 15 and 29 and an increase in mineralisation in the same time period. This was presumably the stage whereby the osteoblasts had become trapped within the secreted matrix and reduced their metabolic activity drastically in order to divert their resources to mineralisation. The drop in ALPase activity, the increase in mineralisation and significant increase in metabolic activity per bead between day 22 and 29 suggests that the cell phenotype between day 22 and day 29 may be that of mitotically active, mature osteoblasts. On day 29 osteocalcin, OB-cadherin and collagen type-I proteins were detected, suggesting that the endpoint cell type in this assay may again be a mature osteoblast. However, Shimko *et al.* (262) has provided evidence that mESCs induced to differentiate towards bone, without EB formation results in mineralisation that is not accepted as conventional osteogenesis. They reported that production of both osteocalcin and collagen type-I was delayed and that ALPase activity was not consistent with normal osteogenesis. In contrast, our data present evidence that 3D culture without conventional 2D EB formation, allows conventional osteogenesis to occur, indicated by decreasing levels of ALPase and the concomitant exhibition of bone specific proteins as early as day 15 for OB-cadherin.

Osteocalcin appears transiently in embryonic bone and is one of the most abundant proteins in adult bone where it binds to hydroxyapatite in a

calcium-dependent manner (291;292). The observance of osteocalcin in rings and on the edges of the 3D tissue aggregates in this study, at both day 22 and day 29 concurs with the micro-CT attenuations and infers that hydroxyapatite had been deposited in both places. Woven bone *in vivo* is characterised by irregular bundles of collagen fibres, large and numerous osteocytes, and delayed, disorderly calcification which occurs in irregularly distributed patches (48). These observations infer that 3D mineralised tissue has formed by both condensation of apatite crystals (woven bone during development) and at the leading edge of the osteoid front (lamellar bone in adults) (51).

RT-PCR analysis further confirms the presence of terminally differentiated, 3D mineralised tissue that does not contain mature cartilage. Again, the definitive phenotype of the endpoint 3D tissue generated in this study appears to be mature osteoblasts as they express *Cbfa-1*, *collagen type-I*, and *osteocalcin* (280;281). Embryonic *collagen type-II* (splice variant A) expression is normal during mESC osteogenic differentiation (208;282) and similarly, *osteocalcin* expression has also been previously reported from days 7 to 21 of osteogenic differentiation (283), corresponding to days 15 to 29 in this study. The lack of any mature *collagen type-II* (splice variant B, 225bp) expression indicates that cartilage is not present and the 3D mineralised tissue primarily consists of collagen type-I. The slight, but noticeable decrease in *collagen type-I* expression at day 29 is found in rat osteoblast cultures and signifies the end of the matrix maturation period and the finalisation of mineralisation (289). Although, the drop in expression was seen in all the bone specific markers and may signify the beginning of the onset of cellular senescence.

Accurate medium analysis/comparisons throughout 2D mESC culture was not possible as the methodology was fragmented, used varying medium

volumes and cell density altered drastically between operators and institutions. The 3D HARV integrated culture system is in one vessel throughout and allows accurate measurements of a spectrum of different medium characteristics. Making comparisons to 2D culture was difficult but the basal analyte values gave some indication to the consumption rates of the cells within the 3D HARV culture system. There are limited amounts of media analysis in the literature regarding 2D mESCs but this is limited to undifferentiated expansion in a mechanised process. The 2D mESCs were found to consume between 5 – 10 mmol/L glucose per day and produce between 10 – 20 mmol/L lactate per day (5 mmol/L in the first few days) (295). Another publication using hESCs in the slow turning lateral vessel (STLV) bioreactor reported that pH levels remaining between 7.2-3, P O_2 levels dropped below 142 mmHg (below normal incubator levels) and glucose consumption linearly increasing throughout differentiation (22 days) (192).

It is known that increased levels of calcium within cultures inhibits cellular growth (296) and the initial spike of calcium within the 3D HARV cultures above basal levels may inhibit cell growth. Ionised calcium (iCa^{2+}) is not bound to any proteins and gives an indication of the amount of calcium available for metabolic activity. The spike appears to be attributed to a leaching effect from the alginate beads within the reactor, whereby they release free iCa^{2+} trapped within the bead and increase the iCa^{2+} levels within the medium by almost 1 mmol/L. Conversely, when calcium reacts with phosphates and forms precipitates, this produces H^+ ions, lowering the pH, explaining the drop in medium calcium levels throughout osteogenic differentiation (such as hydroxyapatite). The reverse happens when these precipitates break which

would explain the initial increase in pH when Ca^{2+} ions break from alginate, sequestering H^+ ions and increasing the pH.

Energy use and metabolite production is complex throughout the 3D HARV culture. It appears that during the differentiation phases of culture the cells require higher levels of glucose than is provided and glucose levels drop to 0 mmol/L and therefore look for an alternative energy source. They appear to revert to glutamine as an alternative source for oxidative metabolism. Glutamine, as discussed earlier, is converted to glutamate and ammonium when glucose levels are depleted and glutamate is then converted to ketoglutarate and ammonium. The change in energy source can be indirectly inferred from the fluctuations in glutamate and ammonium levels. The only noticeable difference in glutamate from basal levels is from day 10 when levels fluctuate between approximately 0.8 and 1.2 mmol/L which is also supported by a rise in ammonium levels during this period of culture. The levels of glutamate and ammonium are clearly higher than basal levels in osteogenic differentiation medium and indicate a shift from glucose to glutamine as the main energy source. Lactate, a product of anaerobic glycolysis and rapid glucose consumption increases to levels far in excess of basal levels indicating a higher metabolic rate during the course of the culture period.

These P O_2 levels maintained during this study indicate levels that are permissive for growth of mESCs and their derivatives. A recent study provided some useful P O_2 data during the culture of mESCs. *In vivo*, prior to vascularisation, ESCs and their progeny exist in P O_2 less than 40 mmHg whereas most *in vitro* culture is performed at 5% CO_2 / 95% in an air incubator that produces gas phase P O_2 of 142 mmHg (297). In their study, they concluded that anaerobic metabolism accounted for 40% of the total ATP

produced at 286 and 142 mmHg, and 50, 70, and 100% at 36, 7, and 0 mmHg respectively. Maintaining a P O_2 of 40 mmHg or above is probably preferable to minimise lactate production, but the mESCs are not sensitive to either higher or lower P O_2 conditions. As long as glucose and other nutrients and growth factors are present and excessive amounts of wastes do not accumulate, mESCs are tolerant of any P O_2 less than 300 mmHg.

5.5.3. HepG2 conditioned medium

The use of HepG2 conditioned medium by reducing the EB formation period, has already been shown to enhance osteogenic differentiation and inhibit cardiogenic differentiation in 2D culture (232). The 3D HARV culture system is an ideal system for adaptation of medium regimes that are successful in 2D culture. It was clear that the 3D HARV HepG2 culture produced smaller colonies than 3D HARV culture during the first week of culture, which was expected. Attributable to lower levels of glucose, vitamins and minerals and higher levels of secondary metabolites for example. In 3D HARV culture the amount of mineralisation increases in a linear fashion from day 15 to day 29 and forms aggregations on day 22 that increase in size by day 29. In 3D HARV HepG2 culture (albeit n = 1) there was more mineralised tissue after 22 days then there was after 29 days of 3D HARV culture. What is not clear is the quality or degree of mineralisation at day 22 and 29 in both cultures. It would be beneficial to perform micro-CT analysis on 3D HARV HepG2 beads on both day 22 and 29 in order to compare this to the 3D HARV culture. If the mineralised aggregates produced by day 22 in 3D HARV HepG2 culture are of a similar size to 3D HARV aggregates on day 29 then this would be a significant

discovery, reducing the time taken to form large 3D mineralised aggregates by 7 days.

5.5.4. Perfusion bioreactor culture

It was clear that the 3D perfusion system employed in this study did not provide a suitable environment to culture mESCs. The medium analysis did not indicate any conditions that were not conducive to growth. The only difference between the HARV and Perfusion reactors were the physical dimensions (both were 50 mL capacity), the central perfusion bar, the rotation rates and the means by which the medium is oxygenated. The oxygenation levels in both reactors were within acceptable levels for growth and the rotation rates were both set to provide continual particle free-fall. Visually the beads did collide considerably with the central perfusion bar in the 3D perfused system. It is clear that the cells were not proliferating early on in the 3D perfusion reactor as well as the 3D HARV reactor, but there was some morphological evidence of colony size increase in the perfusion reactor. Therefore, the cells' growth within the perfusion reactor was stunted in some manner that is not clear with the information available. Further characterisation and reactor manipulation is needed before this perfusion system is able to reproducibly produce 3D mineralised aggregations.

5.5.5. Comparison to the literature and existing knowledge

There are two final points to address: i) how can the results of 3D mineralised tissue formation in this study be compared to other published literature and ii) what are the advantages of this approach and why does this provide a useful method to culture ESCs. The first report of 3D mineralised tissue formation, *in vitro* was using hMSCs cultured on mineralised collagen, induced to form bone.

However, the collagen matrix was already mineralised and they did not indicate whether mineralisation occurred from the MSCs themselves (298;299). Kihira *et al.* (2004) then showed that rMSCs grown in 2D culture formed "3D" bone nodules although this interpretation is not true 3D mineralised aggregation as it is limited, in space by the 2D culture vessel (300). In addition, Laino *et al.* (2005) also provided some more convincing evidence in terms of "3D" bone formation but again this was monolayer cultured to form 2D bone nodules. Finally, Chaudhury *et al.* (2004) did give an indication that 3D bone could form but did not distinctively provide evidence that 3D bone formation had occurred apart from that after 4 weeks of incubation of seeded scaffolds, small nodular patches of excreted extracellular matrix (bone nodule structures) could be seen. The mineralisation on the 3D scaffolds was confirmed by TEM and then with later subculture in 2D and von Kossa staining. The actual amount of 3D mineralised tissue produced was unclear from the number of osteoprogenitors. It must also be noted that the cells used in this study to form 3D mineralised tissue from mESCs were differentiated to form osteoprogenitors in a traditional 2D manner (approximately 32 days) and it then took a further 28 days to form 3D mineralised tissue; a total of 60 days. In contrast, our study shows that 3D mineralised tissue formation from undifferentiated mESCs is possible in 22 days (38 days less), without the need for an inductive scaffold Open-Cell Polylactic Acid (OPLA) and fragmented, laborious, static culture systems. The amount of 3D mineralised tissue actually formed in our 3D HARV system can be estimated; assuming the aggregations are all uniform in size and are spherical. On day 29 there were on average 44 mineralised aggregates and their diameters were around 150 μm. Therefore the amount of mineralised tissue generated per bead was around 7.8×10^{-5} cm^3 or 0.05 cm^3 of mineralised

tissue from 600 beads. This calculated amount only constitutes 3D mineralised tissue and is not indicative of the soft tissue formed around the mineralised aggregations.

5.6. Conclusion

A similar, fragmented culture process has been reported (301), by allowing both mouse and human undifferentiated ESCs to aggregate for 1 day in maintenance medium, then encapsulating in agarose. Similar fragmented methodologies (246), although useful are still constrained in terms of manufacturing potential. This alternative methodology discovered in this thesis provides an alternative to traditional ESC culture and removes the bottleneck from providing large scale, 3D mineralised tissue for clinical applications. It is simple, integrated, relies on minimal operator intervention, provides reproducible results and is amenable to scale-up and online monitoring. In addition, the 3D HARV system allows maintenance of mESCs, the formation of mesodermal tissue and osteogenic differentiation similar to that found *in vivo*.

For surgical operations such as Lumbar spondylolysis where a cancellous bone graft is required to repair a lysis of 0.3-4 cm (110), a single alginate bead (diameter = 2.3 mm) containing 44 ± 7 (SE, n = 2) 3D mineralised aggregates derived from 10,000 undifferentiated mESCs, provides a tangible amount of material to repair such a defect if this model could be directly adapted to hESCs. In addition, the mineralised tissue filled alginate capsules may be directly injected into the defect area (198;302;303) and provide some form of immunogenic protection from the hosts defences (201;260).

6. DISCUSSION AND CONCLUSIONS

6.1. Aims and objectives

The overall aim was to investigate ESCs as a source of material for bone tissue repair using mESCs as a model.

Goal	Aims and Objectives
DEFINED MEDIA	• To formulate novel, defined serum-free media that allow cell viability, proliferation and transition throughout mESC maintenance, EB formation and osteogenic differentiation. • To optimise and define the components of serum-free media that maximises the efficiency of osteogenic differentiation from mESCs.
3D CULTURE	• To form 3D tissue within characterised alginate beads suitable for scale-up and ultimately 3D bone formation. • The integration of traditional mESC culture through the encapsulation of undifferentiated mESCs and formation of 3D bone. • The production of clinically-relevant differentiated cells through culture in an integrated bioreactor culture system.

6.2. Summary of major findings from this thesis

The main derivative from exploring defined media formulation was that mESC culture could be artificially divided into three distinct phases: a) maintenance b) EB formation and c) osteogenic differentiation. The transition from serum containing medium to serum-free medium was achieved and bone nodules were formed, exclusively in serum-free media, without the need for osteogenic supplements. The components of the media were defined apart from knock out serum replacement (Invitrogen) which is a proprietary formulation. Optimisation of osteogenic differentiation was not achieved as time and resources were limiting factors. The purpose of defining media, free from animal products is

obvious when the ultimate goal of tissue engineering is to provide tissue for human repair. It would appear that although successful, time and resources should be spent upon media formulation using hESCs, with the mESC results as a model.

Looking at the media development results it was clear that traditional ESC culture is fragmented, time-consuming and laborious. Integrating these stages into one single step is the simplest and most parsimonious means by which to form terminally differentiated tissue that is amenable to scale-up. The vehicle or scaffold (alginate encapsulation) in which these cells would transit through the three stages of ESC to bone formation was defined and characterised. It was unknown whether mineralised tissue would form in 3D alginate encapsulated beads without traditional, suspension EB formation as previous studies indicated that EB formation was obligatory for bone formation similar to that found *in vivo* (262). However, it was clear that 3D mineralised tissue was able to form after 29 days, encapsulated in 3D alginate beads and cultured in a HARV bioreactor.

6.3. Future work and clinical implications

6.3.1. Defined media

There are a number of questions and directions this area of research could go but I would suggest they are undertaken by an appropriate grant application or joint public-private funded project. Future goals and questions to be answered:

- What are the key factors in serum that allow the survival and transition of cells from serum-containing to serum-free media?
- Pheno/Geno-typic analysis of stem cells populations that are capable of transition from serum-containing to serum-free medium – as

differentiation progresses, do the stem cells lose their mechanisms for repair / survival?

- Identification of the inhibitors as well as inducers of mesoderm differentiation and the elucidation of the cross talking mechanisms that allow mesodermal differentiation.
- What factors allow the induction of mesodermal differentiation and also the commitment of osteogenic differentiation – is there a point at which osteogenic differentiation is terminal?

Identifying the exact mechanisms of differentiation is not only helpful for developmental biology but needed in order to provide homogeneous tissues for clinical applications once the hESC model is investigated further. Single-cell encapsulation (Section 4.4.2.3) will be an invaluable tool in order to study developmental pathways in a high-throughput manner.

The defined media regime was heterogeneous and identifies the need for full control over the differentiation process in order to produce tissue suitable for the clinic. The presence of smooth muscle contraction was clearly identified in this exclusively serum-free culture system along with other unidentified cell types. In February 1997, the FDA published two documents entitled "A Proposed Approach to the Regulation of Cellular and Tissue-Based Products" and "Reinventing the Regulation of Human Tissues" that established the current framework for the regulation of cell- and tissue engineered products. The intention of this FDA act was to: a) control the spread of infectious disease; b) prevent handling that may damage tissue products; and c) ensure safety and efficacy of such products [for a full review see (170)]. Compliance with these FDA regulations implies that the following clause will be adhered to:

(iii) Assessment of product purity. Assaying for residual growth factors and serum proteins is critical to ensure that no toxic products are administered to the patient along with the cell-therapy product. In this respect, it is noteworthy that proteins derived from fetal bovine serum have been shown to combine with MHC class I cells and to trigger T-lymphocyte proliferation in mixed lymphocyte reactions (304). Antibodies against bovine 2 microglobulin have been found in mice to which syngeneic lymphoblasts cultured in medium containing foetal bovine serum were administrated (305). These data substantiate the need of well-designed compatibility procedures that assure complete elimination of foetal bovine serum in the final cell-containing tissue engineered product.

Both the references within this clause are pre 1990 and it has recently been found (2005) that the nonhuman sialic acid Neu5Gc can be incorporated by hESCs and EBs from both the murine feeder layer and medium (163) which, intensifies the need for a chemically defined medium.

6.3.2. 3D culture

Modelling and measuring the transfer of nutrients and oxygen gradients (306) is essential in an optimised culture system but this was beyond the scope of this thesis. The pore dimensions were not determined but it was found that similar pores have been measured in the literature and they are a maximum of 1 μm in diameter on the external surface (261). This would not allow cell entry or exit from the bead unless the beads were mechanically split or disrupted in some way. It was also clear that the beads were heterogeneous in their nature when

viewing the calcium distribution within the beads which was expected due to the reaction-diffusion kinetics (2).

It has also been reported that alginates harbour contaminants (Chris Mason – personal communication) depending on the source and purification procedure (307) and current American Society for Testing Materials (ASTM) standards fail to be specific about the necessary requirements for a biomedical grade alginate so that it can safely be used for encapsulation purposes (308-310). It would be extremely advisable to investigate further the sources of alginate and the purification mechanisms such as Pronova as a startng point.

The micro encapsulation techniques are certainly useful and provide some intriguing incite into ESC development. However, micro encapsulation and ESCs have not been widely explored and there are only rudimentary techniques (Protein secretion assay & Growth Assay) to monitor single cell kinetics (www.onecell.com). These areas would need to progress or be investigated concomitantly in order to have an accurate system for encapsulation and also analysis to prove useful. In spite of this, single cell encapsulation has been investigated using umbilical cord blood stem cells (311).

6.3.3. 3D bone formation

The results and findings in this thesis are extremely useful and remove another hurdle for stem cell tissue engineering to reach the clinic. There are a number of avenues to pursue before the results in this thesis can be applied confidently.

It is unclear whether the 3D mineralised aggregates have undergone endochondral or intramembranous ossification but the lack of any collagen type-IIB (adult) and the presence of collagen type-IIA (embryonic) suggest that

intramembranous ossification is more likely. Intramembranous ossification is characterised by mesenchymal cells differentiating into osteoblasts at ossification centres, forming complex extracellular matrices ossifying concomitantly (for a review see (93)). What is clear is that mineralised nucleation sites appear in distinct regions of the alginate bead and usually in the centre of soft tissue (Figure 5.22c). It is known that crystal formation is induced by nucleation i.e., provision of a surface on which crystal lattice formation can proceed readily, as the levels of serum P_i and Ca^{2+} are supersaturated. The normal, triple-stranded, quarter-staggered collagen serves as the nucleating agent for bone formation. This occurs in special areas or holes (~40 nm) resulting from the unique way in which the collagen molecules are packed (312). The formation of bone as a consequence of the structure and organisation of its organic matrix, with subsequent nucleation of crystallisation from a super-saturated medium appears to be occurring in the 3D HARV culture system. However, in order to achieve homogeneous bone formation then a collagen lattice must either be pre-fabricated with sufficiently large holes or formed directly (collagen type-I) during mESC development, using the alginate bead as a scaffold. This would require a revision of the alginate bead manufacture process.

In order to translate these research findings from the lab into the clinic then the procedures undertaken in this thesis need to be considered as a bioprocess and approached with GMP, European and American regulations in mind. The processes of encapsulation (upstream), bioreactor culture and harvesting of the cells (downstream) for further use can be seen as three separate processes. The entire process would need to be enclosed with a GMP facility or ideally in a modular boxed system to reduce costs and

portability. Having encapsulation, culture and harvesting modules that are easy to sterilise, contain dispoable consumable elements, on-line monitoring and also completely automated in order to remove the fragmented, subjective nature of human intervention into current cell culture practices.

The 3D perfusion system was clearly not optimised and was attempted as a proof of concept study to test whether the 3D HARV culture system was transferable between bioreactors. However, Martin *et al.* (2004) identify that optimal flow conditions of a bioreactor should not be determined through a trial-and-error approach, but rather should be supported by simulation methods. Computational fluid dynamic (CFD) software packages have been increasingly developed during the past decade and are a powerful tool to calculate flow fields, shear stresses and mass transport within and around 3D constructs. CFD models have been used to calculate the momentum and oxygen transport within a concentric cylinder bioreactor for cartilage tissue engineering and to design and characterise a scaled-up version (313).

6.4. Concluding Remarks

Bone healing *in vivo* is generally considered to be biologically optimal since the vast majority of defects in this tissue heal spontaneously with minimal treatment (170). However, around 450,000 fractures in the USA each year will require further treatment for compromised healing because of either improper fracture fixation, loss of bone, metabolic disturbances, impairment of blood supply and infection (170;314). Autologous bone harvested from donor sites such as the iliac crest is the preferred treatment. Grafts of this kind are osteoconductive (they provide a scaffold on which bone cells can proliferate), osteoinductive (they induce proliferation of undifferentiated cells and their differentiation into

osteoblasts), and osteogenic (they provide a reservoir of skeletal stem and progenitor cells that can form new bone) [for a full review see (170)].

Serum-free media development is a time consuming but worthwhile process that involves fore thought and probably a commercial goal in order to fund the preliminary research itself. Micro encapsulation (251) and single-cell high-throughput platforms (264;265) will vastly improve medium formulation using factorial design (315-317) (bottom-up) and proteomics (318;319) using HepG2 media for example (232;320;321) (top-down), will enable convergent formulations that are suitable for clinical applications.

As discussed in this excellent review (322), recent signaling results support an emerging perspective that hESCs, like mESCs (219) (and perhaps stem cells in general), maintain their undifferentiated state by inhibiting signaling (and gene expression) programs that lead to the development of specific cell types. At the signaling level, interactions between extracellular factors and crosstalk between signaling pathways may be an important part of this negative regulation. ESCs can be considered to be an unstable energy state (323) balanced in a high energy local minimum in the energy landscape, with a tendency upon perturbation to differentiate (to a lower energy state) along different lineages (322). It is not only critical to think along these lines for media formulation but to envisage the ball passing through a 3-dimensional simulation towards tissue specific endpoints.

From 2001 to 2005 the number of publications with bone and stem cells in the abstract/title has increased linearly: 477 in 2001, 621 in 2002, 758 in 2003, 884 in 2004 and 852 in 2005* (Total = 3592, Appendix 9.16). Of these publications, 26 of these contained the words alginate+stem cells. Within these selected populations there appears to be some seminal articles that have

shaped the direction of the 3D sections of this thesis. From the earliest article in 2001, the goal of integration was paramount but not taken up by the research community. These publications show the development of 3D stem cell culture for clinical applications over a 5 year period.

2001 J. P. Magyar, M. Nemir, E. Ehler, N. Suter, J. C. Perriard, and H. M. Eppenberger. Mass production of embryoid bodies in microbeads. Ann.N.Y.Acad.Sci. 944:135-143, 2001.

2003 H. L. Ma, S. C. Hung, S. Y. Lin, Y. L. Chen, and W. H. Lo. Chondrogenesis of human mesenchymal stem cells encapsulated in alginate beads. J.Biomed.Mater.Res. 64A (2):273-281, 2003.

2004 G. R. Chaudhry, D. Yao, A. Smith, and A. Hussain. Osteogenic Cells Derived From Embryonic Stem Cells Produced Bone Nodules in Three-Dimensional Scaffolds. J.Biomed.Biotechnol. 2004 (4):203-210, 2004.

2004 S. M. Dang and P. W. Zandstra. Scalable production of embryonic stem cell-derived cells. Methods Mol.Biol. 290:353-364, 2004.

2004 S. Gerecht-Nir, S. Cohen, A. Ziskind, and J. Itskovitz-Eldor. Three-dimensional porous alginate scaffolds provide a conducive environment for generation of well-vascularized embryoid bodies from human embryonic stem cells. Biotechnol.Bioeng. 88 (3):313-320, 2004.

2004 C. Selden and H. Hodgson. Cellular therapies for liver replacement. Transpl.Immunol. 12 (3-4):273-288, 2004.

2005 J. E. Barralet, L. Wang, M. Lawson, J. T. Triffitt, P. R. Cooper, and R. M. Shelton. Comparison of bone marrow cell growth on 2D and 3D alginate hydrogels. J.Mater.Sci.Mater.Med. 16 (6):515-519, 2005.

2005 C. Bauwens, T. Yin, S. Dang, R. Peerani, and P. W. Zandstra. Development of a perfusion fed bioreactor for embryonic stem cell-derived cardiomyocyte generation: Oxygen-mediated enhancement of cardiomyocyte output. Biotechnol.Bioeng. 90 (4):452-461, 2005.

2005 E. Y. Fok and P. W. Zandstra. Shear-Controlled Single-Step Mouse Embryonic Stem Cell Expansion and EB-Based Differentiation. Stem Cells, 2005.

2005 N. S. Hwang, M. S. Kim, S. Sampattavanich, J. H. Baek, Z. Zhang, and J. Elisseeff. The Effects of Three Dimensional Culture and Growth Factors on the Chondrogenic Differentiation of Murine Embryonic Stem Cells. Stem Cells, 2005.

2005 D. J. Park, B. H. Choi, S. J. Zhu, J. Y. Huh, B. Y. Kim, and S. H. Lee. Injectable bone using chitosan-alginate gel/mesenchymal stem cells/BMP-2 composites. J.Craniomaxillofac.Surg. 33 (1):50-54, 2005.

The results from this thesis effectively encapsulates the above articles by integrating and simplifying a field that required reproducibility and uniformity in order to effectively translate this research into commercially viable, clinical products. The formation of 3D, fully mineralised tissue from mESCs although novel, still needs to be continued in order to provide clinical products for humans. There are obviously many challenges still to be overcome before

bone tissue engineering from ESCs, reaches the clinic. To name a few: a) clinically acceptable hESC source verification b) homogeneous bone tissue production c) efficacy and safety trials within a mouse & human model d) serum-free media formulation / optimisation e) negation of the immune response f) ethical acceptance from the general public g) reproducible manufacture of clinical quantities of tissue.

7. REFERENCES

(1) Zimmerman AM, Vierck JL, O'Reilly BA, Dodson MV. Formulation of a defined medium to maintain cell health and viability in vitro. Methods Cell Sci 2000;22(1):43-9.

(2) Bienaime C, Barbotin JN, Nava-Saucedo JE. How to build an adapted and bioactive cell microenvironment? A chemical interaction study of the structure of Ca-alginate matrices and their repercussion on confined cells. J Biomed Mater Res 2003;67A(2):376-88.

(3) Simpson NE, Stabler CL, Simpson CP, Sambanis A, Constantinidis I. The role of the CaCl2-guluronic acid interaction on alginate encapsulated betaTC3 cells. Biomaterials 2004;25(13):2603-10.

(4) Hay P. Engineering Giant. London: Batsford; 1973.

(5) Stock UA, Vacanti JP. Tissue engineering: current state and prospects. Annu Rev Med 2001;52:443-51.

(6) Skalak R, Fox CF. Tissue Engineering. Ann Biomed Eng 1991;19:529-33.

(7) Bisceglie V. Über die antineoplastische Immunität; heterologe Einpflanzung von Tumoren in Hühner-Embryonen. Ztschr Krebsforsch 1933;40:122-40.

(8) Bell E, Ehrlich HP, Buttle DJ, Nakatsuji T. Living tissue formed in vitro and accepted as skin-equivalent tissue of full thickness. Science 1981;211(4486):1052-4.

(9) Burke JF, Yannas IV, Quinby WC, Jr., Bondoc CC, Jung WK. Successful use of a physiologically acceptable artificial skin in the treatment of extensive burn injury. Ann Surg 1981;194(4):413-28.

(10) Hench LL. Biomaterials. Science 1980;208(4446):826-31.

(11) Hench LL, Wilson J. Surface-active biomaterials. Science 1984;226(4675):630-6.

(12) Kirschstein R, Skirboll LR. Stem cells: Scientific Progress and Future Research Directions. Department of Health and Human Services; 2001.

(13) Zandstra PW, Nagy A. Stem cell bioengineering. Annu Rev Biomed Eng 2001;3:275-305.

(14) Horwitz EM, Prockop DJ, Fitzpatrick LA, Koo WW, Gordon PL, Neel M, Sussman M, Orchard P, Marx JC, Pyeritz RE, Brenner MK. Transplantability and therapeutic effects of bone marrow-derived mesenchymal cells in children with osteogenesis imperfecta. Nat Med 1999;5(3):309-13.

(15) D'Ippolito G, Schiller PC, Ricordi C, Roos BA, Howard GA. Age-related osteogenic potential of mesenchymal stromal stem cells from human vertebral bone marrow. J Bone Miner Res 1999;14(7):1115-22.

(16) Quarto R, Thomas D, Liang CT. Bone progenitor cell deficit and age-associated decline in bone repair capacity. Calcif Tissue Int 1995;56:123-9.

(17) McCulloch CA, Strugurescu M, Hughes F, Melcher AH, Aubin JE. Osteogenic progenitor cells in rat bone marrow stromal populations exhibit self-renewal in culture. Blood 1991;77(9):1906-11.

(18) Bishop AE, Buttery LD, Polak JM. Embryonic stem cells. J Pathol 2002;197(4):424-9.

(19) Toyooka Y, Tsunekawa N, Akasu R, Noce T. Embryonic stem cells can form germ cells in vitro. Proc Natl Acad Sci U S A 2003;100(20):11457-62.
(20) Bianco P. Marrow Stromal Stem Cells. The Journal of Clinical Investigation 2000;105(12):1663-8.
(21) Odorico JS, Kaufman DS, Thomson JA. Multilineage differentiation from human embryonic stem cell lines. Stem Cells 2001;19(3):193-204.
(22) Paul G, Li JY, Brundin P. Stem cells: hype or hope? Drug Discov Today 2002;7(5):295-302.
(23) Pera MF. Human pluripotent stem cells: a progress report. Curr Opin Genet Dev 2001;11(5):595-9.
(24) Watt FM, Hogan BL. Out of Eden: stem cells and their niches. Science 2000;287(5457):1427-30.
(25) Byers P, Bonadio J. The molecular basis of clinical heterogeneity of Osteogenesis Imperfecta: Mutations in type I collagen genes have different effects on collagen processing. In: Lloyd J, Scriver C, editors. Genetic and metabolic Diseases in Pediatrics.London: Butterworth; 1985. p. 56-90.
(26) Miller MD, Brinker MR. Review of Orthopaedics. 3rd ed. Philadelphia: W.B. Saunders Company; 2000.
(27) Bruder SP, Caplan AI. Bone Regeneration Through Cellular Engineering. In: Lanza RP, Langer R, Vacanti J, editors. Principles of Tissue Engineering. 2nd ed. London: Academic Press; 2000. p. 683-96.
(28) Hench LL, Splinter RJ, Allen WC, Greenlee TK. Bonding mechanisms at the interface of ceramic prosthetic materials. J Biomed Mater Res 1971;2:117-41.
(29) Bielby R, Pryce R, Hench LL, Polak JM. Enhanced Derivation of Osteogenic Cells from Embryonic Stem Cells by Treatment with Sol-Gel Bioactive Glass. Tissue Eng [6], 693. 2000.
Ref Type: Abstract
(30) Buttery LD, Bourne S, Xynos JD, Wood H, Hughes FJ, Hughes SP, Episkopou V, Polak JM. Differentiation of osteoblasts and in vitro bone formation from murine embryonic stem cells. Tissue Eng 2001;7(1):89-99.
(31) Phillips BW, Belmonte N, Vernochet C, Ailhaud G, Dani C. Compactin enhances osteogenesis in murine embryonic stem cells. Biochem Biophys Res Commun 2001;284(2):478-84.
(32) Bielby RC, Christodoulou IS, Pryce RS, Radford WJ, Hench LL, Polak JM. Time- and concentration-dependent effects of dissolution products of 58S sol-gel bioactive glass on proliferation and differentiation of murine and human osteoblasts. Tissue Eng 2004;10(7-8):1018-26.
(33) Sottile V, Thomson A, McWhir J. In vitro osteogenic differentiation of human ES cells. Cloning Stem Cells 2003;5(2):149-55.
(34) Oh SK, Kim HS, Park YB, Seol HW, Kim YY, Cho MS, Ku SY, Choi YM, Kim DW, Moon SY. Methods for expansion of human embryonic stem cells. Stem Cells 2005;23(5):605-9.
(35) Sikavitsas VI, Bancroft GN, Lemoine JJ, Liebschner MA, Dauner M, Mikos AG. Flow perfusion enhances the calcified matrix deposition of marrow stromal cells in biodegradable nonwoven fiber mesh scaffolds. Ann Biomed Eng 2005;33(1):63-70.
(36) Holtorf HL, Jansen JA, Mikos AG. Flow perfusion culture induces the osteoblastic differentiation of marrow stroma cell-scaffold constructs in

the absence of dexamethasone. J Biomed Mater Res A 2005;72(3):326-34.
(37) Bancroft GN, Sikavitsas VI, Mikos AG. Design of a flow perfusion bioreactor system for bone tissue-engineering applications. Tissue Eng 2003;9(3):549-54.
(38) Mueller SM, Mizuno S, Gerstenfeld LC, Glowacki J. Medium perfusion enhances osteogenesis by murine osteosarcoma cells in three-dimensional collagen sponges. J Bone Miner Res 1999;14(12):2118-26.
(39) Bancroft GN, Sikavitsas VI, van den DJ, Sheffield TL, Ambrose CG, Jansen JA, Mikos AG. Fluid flow increases mineralized matrix deposition in 3D perfusion culture of marrow stromal osteoblasts in a dose-dependent manner. Proc Natl Acad Sci U S A 2002;99(20):12600-5.
(40) Lim F, Moss RD. Microencapsulation of living cells and tissues. J Pharm Sci 1981;70(4):351-4.
(41) Magyar JP, Nemir M, Ehler E, Suter N, Perriard JC, Eppenberger HM. Mass production of embryoid bodies in microbeads. Ann N Y Acad Sci 2001;944:135-43.
(42) Majmudar G, Bole D, Goldstein SA, Bonadio J. Bone cell culture in a three-dimensional polymer bead stabilizes the differentiated phenotype and provides evidence that osteoblastic cells synthesize type III collagen and fibronectin. J Bone Miner Res 1991;6(8):869-81.
(43) Galilei G, Discorsi E. Dimostrazioni Matematiche intorna a due nuove Scienze. Translated by H. Crew and A. deSalvio, pp. 118-134.New York: Macmillan; 1638. p. 118-34.
(44) Weinmann JP, Sicher H. Bone and Bones. London: Mosby; 1955.
(45) Wolff J. Das gesetz der transformation der knochen. Berlin: A Hirschwald; 1891.
(46) Salter RB. Textbook of disorders and injuries of the musculoskeletal system. 1st ed. Baltimore: Williams and Wilkins; 1995.
(47) Karaplis AC. Embryonic Development of Bone and the Molecular Regulation of Intramembranous and Endochondral Bone Formation. In: Bilezikian JP, Raisz LG, Rodan GA, editors. Principles of Bone Biology (VOL I) . Second ed. London: Academic Press; 2002. p. 33-58.
(48) Baron R. Anatomy and ultrastructure of bone - histogenesis, growth and remodelling. WWW 2002 [cited 2005 Jun 28];Available from: URL: http://www.endotext.org/parathyroid/parathyroid1/parathyroidframe1.htm
(49) Marks SC, Odgren PR. Structure and Development of the Skeleton. In: Bilezikian JP, Raisz JP, Rodan GA, editors. Principles of Bone Biology. 2nd ed. California: Academic Press; 2002. p. 1-15.
(50) Weiner S, Traub W. Bone structure: from angstroms to microns. FASEB J 1992;6(3):879-85.
(51) Weiner S, Traub W, Wagner HD. Lamellar bone: structure-function relations. J Struct Biol 1999;126(3):241-55.
(52) Sommerfeldt DW, Rubin CT. Biology of bone and how it orchestrates the form and function of the skeleton. Eur Spine J 2001;10 Suppl 2:S86-S95.
(53) Lecanda F, Towler DA, Ziambaras K, Cheng SL, Koval M, Steinberg TH, Civitelli R. Gap junctional communication modulates gene expression in osteoblastic cells. Mol Biol Cell 1998;9(8):2249-58.
(54) Ferrari SL, Traianedes K, Thorne M, Lafage-Proust MH, Genever P, Cecchini MG, Behar V, Bisello A, Chorev M, Rosenblatt M, Suva LJ. A role for N-cadherin in the development of the differentiated osteoblastic phenotype. J Bone Miner Res 2000;15(2):198-208.

(55) Mosley JR. Osteoporosis and bone functional adaptation: mechanobiological regulation of bone architecture in growing and adult bone, a review. J Rehabil Res Dev 2000;37(2):189-99.
(56) Canalis E, Pash J, Gabbitas B, Rydziel S, Varghese S. Growth factors regulate the synthesis of insulin-like growth factor-I in bone cell cultures. Endocrinology 1993;133(1):33-8.
(57) Rydziel S, Shaikh S, Canalis E. Platelet-derived growth factor-AA and -BB (PDGF-AA and -BB) enhance the synthesis of PDGF-AA in bone cell cultures. Endocrinology 1994;134(6):2541-6.
(58) Globus RK, Plouet J, Gospodarowicz D. Cultured bovine bone cells synthesize basic fibroblast growth factor and store it in their extracellular matrix. Endocrinology 1989;124(3):1539-47.
(59) Canalis E, Pash J, Varghese S. Skeletal growth factors. Crit Rev Eukaryot Gene Expr 1993;3(3):155-66.
(60) Manolagas SC, Jilka RL. Bone marrow, cytokines, and bone remodeling. Emerging insights into the pathophysiology of osteoporosis. N Engl J Med 1995;332(5):305-11.
(61) Zhou H, Hammonds RG, Jr., Findlay DM, Fuller PJ, Martin TJ, Ng KW. Retinoic acid modulation of mRNA levels in malignant, nontransformed, and immortalized osteoblasts. J Bone Miner Res 1991;6(7):767-77.
(62) Rizzoli R, Poser J, Burgi U. Nuclear thyroid hormone receptors in cultured bone cells. Metabolism 1986;35(1):71-4.
(63) Barnard R, Ng KW, Martin TJ, Waters MJ. Growth hormone (GH) receptors in clonal osteoblast-like cells mediate a mitogenic response to GH. Endocrinology 1991;128(3):1459-64.
(64) Levy JR, Murray E, Manolagas S, Olefsky JM. Demonstration of insulin receptors and modulation of alkaline phosphatase activity by insulin in rat osteoblastic cells. Endocrinology 1986;119(4):1786-92.
(65) Wei LL, Leach MW, Miner RS, Demers LM. Evidence for progesterone receptors in human osteoblast-like cells. Biochem Biophys Res Commun 1993;195(2):525-32.
(66) Clement-Lacroix P, Ormandy C, Lepescheux L, Ammann P, Damotte D, Goffin V, Bouchard B, Amling M, Gaillard-Kelly M, Binart N, Baron R, Kelly PA. Osteoblasts are a new target for prolactin: analysis of bone formation in prolactin receptor knockout mice. Endocrinology 1999;140(1):96-105.
(67) Eriksen EF, Colvard DS, Berg NJ, Graham ML, Mann KG, Spelsberg TC, Riggs BL. Evidence of estrogen receptors in normal human osteoblast-like cells. Science 1988;241(4861):84-6.
(68) Komm BS, Terpening CM, Benz DJ, Graeme KA, Gallegos A, Korc M, Greene GL, O'Malley BW, Haussler MR. Estrogen binding, receptor mRNA, and biologic response in osteoblast-like osteosarcoma cells. Science 1988;241(4861):81-4.
(69) Colvard D, Spelsberg T, Eriksen E, Keeting P, Riggs BL. Evidence of steroid receptors in human osteoblast-like cells. Connect Tissue Res 1989;20(1-4):33-40.
(70) Darwish HM, DeLuca HF. Recent advances in the molecular biology of vitamin D action. Prog Nucleic Acid Res Mol Biol 1996;53:321-44.
(71) Kindmark A, Torma H, Johansson A, Ljunghall S, Melhus H. Reverse transcription-polymerase chain reaction assay demonstrates that the 9-cis retinoic acid receptor alpha is expressed in human osteoblasts. Biochem Biophys Res Commun 1993;192(3):1367-72.

(72) Ng KW, Partridge NC, Niall M, Martin TJ. Epidermal growth factor receptors in clonal lines of a rat osteogenic sarcoma and in osteoblast-rich rat bone cells. Calcif Tissue Int 1983;35(3):298-303.
(73) Mohan S, Linkhart T, Rosenfeld R, Baylink D. Characterization of the receptor for insulin-like growth factor II in bone cells. J Cell Physiol 1989;140(1):169-76.
(74) Bennett A, Chen T, Feldman D, Hintz RL, Rosenfeld RG. Characterization of insulin-like growth factor I receptors on cultured rat bone cells: regulation of receptor concentration by glucocorticoids. Endocrinology 1984;115(4):1577-83.
(75) Canalis E, Pash J, Varghese S. Skeletal growth factors. Crit Rev Eukaryot Gene Expr 1993;3(3):155-66.
(76) Kells AF, Schwartz HS, Bascom CC, Hoover RL. Identification and analysis of transforming growth factor beta receptors on primary osteoblast-enriched cultures derived from adult human bone. Connect Tissue Res 1992;27(4):197-209.
(77) Lacey DL, Erdmann JM, Tan HL, Ohara J. Murine osteoblast interleukin 4 receptor expression: upregulation by 1,25 dihydroxyvitamin D3. J Cell Biochem 1993;53(2):122-34.
(78) Shelly JA, Laborde AL. Interleukin-1 binding, internalization, and processing in a murine osteoblastic cell line, MC3T3.E1. Eur Cytokine Netw 1992;3(5):469-75.
(79) Debiais F, Hott M, Graulet AM, Marie PJ. The effects of fibroblast growth factor-2 on human neonatal calvaria osteoblastic cells are differentiation stage specific. J Bone Miner Res 1998;13(4):645-54.
(80) Koenig BB, Cook JS, Wolsing DH, Ting J, Tiesman JP, Correa PE, Olson CA, Pecquet AL, Ventura F, Grant RA, . Characterization and cloning of a receptor for BMP-2 and BMP-4 from NIH 3T3 cells. Mol Cell Biol 1994;14(9):5961-74.
(81) Clover J, Oates J, Edwards C. Anti-cytokeratin 5/6: a positive marker for epithelioid mesothelioma. Histopathology 1997;31(2):140-3.
(82) Lanyon LE. Osteocytes, strain detection, bone modeling and remodeling. Calcif Tissue Int 1993;53 Suppl 1:S102-S106.
(83) Ajubi NE, Klein-Nulend J, Alblas MJ, Burger EH, Nijweide PJ. Signal transduction pathways involved in fluid flow-induced PGE2 production by cultured osteocytes. Am J Physiol 1999;276(1 Pt 1):E171-E178.
(84) Teitelbaum SL. Bone resorption by osteoclasts. Science 2000;289(5484):1504-8.
(85) Albright J, Skinner H. Bone: structural organization and remodelling dynamics. In: Albright J, Brand R, editors. The scientific basis of orthopaedics. 2nd ed. East Norwalk: Appleton and Lange; 1987. p. 161-98.
(86) Rubinacci A, Villa I, Dondi BF, Borgo E, Ferretti M, Palumbo C, Marotti G. Osteocyte-bone lining cell system at the origin of steady ionic current in damaged amphibian bone. Calcif Tissue Int 1998;63(4):331-9.
(87) Nakayama N, Duryea D, Manoukian R, Chow G, Han CY. Macroscopic cartilage formation with embryonic stem-cell-derived mesodermal progenitor cells. J Cell Sci 2003;116(Pt 10):2015-28.
(88) Johansson BM, Wiles MV. Evidence for involvement of activin A and bone morphogenetic protein 4 in mammalian mesoderm and hematopoietic development. Mol Cell Biol 1995;15(1):141-51.

(89) Wiles MV, Johansson BM. Embryonic Stem Cell Development in a Chemically Defined Medium. ExpCell Res 1999;247(1):241-8.
(90) Olsen BJ. Bone morphogenesis and enbryonic development. In: Favus MJ, editor. Primer on the metabolic bone diseases and disorders of mineral metabolism. 4th ed. Philadelphia: Lippincott, Williams and Wilkins; 1999. p. 11-4.
(91) Luo G, Ducy P, McKee MD, Pinero GJ, Loyer E, Behringer RR, Karsenty G. Spontaneous calcification of arteries and cartilage in mice lacking matrix GLA protein. Nature 1997;386(6620):78-81.
(92) Anderson HC. Molecular biology of matrix vesicles. Clin Orthop Relat Res 1995;(314):266-80.
(93) Aubin JE, Triffitt JT. Mesenchymal Stem Cells and Osteoblast Differentiation. In: Bilezikian JP, Raisz LG, Rodan GA, editors. Principles of Bone Biology (VOL I) . Second ed. London: Academic Press; 2002. p. 59-81.
(94) Ducy P, Schinke T, Karsenty G. The osteoblast: a sophisticated fibroblast under central surveillance. Science 2000;289(5484):1501-4.
(95) Ducy P. Cbfa1: a molecular switch in osteoblast biology. Dev Dyn 2000;219(4):461-71.
(96) Heng BC, Cao T, Stanton LW, Robson P, Olsen B. Strategies for directing the differentiation of stem cells into the osteogenic lineage in vitro. J Bone Miner Res 2004;19(9):1379-94.
(97) Ducy P, Zhang R, Geoffroy V, Ridall AL, Karsenty G. Osf2/Cbfa1: a transcriptional activator of osteoblast differentiation. Cell 1997;89(5):747-54.
(98) Kim IS, Otto F, Zabel B, Mundlos S. Regulation of chondrocyte differentiation by Cbfa1. Mech Dev 1999;80(2):159-70.
(99) Nakashima K, Zhou X, Kunkel G, Zhang Z, Deng JM, Behringer RR, de Crombrugghe B. The novel zinc finger-containing transcription factor osterix is required for osteoblast differentiation and bone formation. Cell 2002;108(1):17-29.
(100) Jheon AH, Suzuki N, Nishiyama T, Cheifetz S, Sodek J, Ganss B. Characterization of the 5'-flanking region of the rat AJ18 gene. Gene 2003;310:203-13.
(101) Aubin JE. Bone stem cells. J Cell Biochem Suppl 1998;30-31:73-82.
(102) Bellows CG, Aubin JE, Heersche JN, Antosz ME. Mineralized bone nodules formed in vitro from enzymatically released rat calvaria cell populations. Calcif Tissue Int 1986;38(3):143-54.
(103) Maeda T, Kawane T, Horiuchi N. Statins augment vascular endothelial growth factor expression in osteoblastic cells via inhibition of protein prenylation. Endocrinology 2003;144(2):681-92.
(104) Hwang R, Lee EJ, Kim MH, Li SZ, Jin YJ, Rhee Y, Kim YM, Lim SK. Calcyclin, a Ca2+ ion-binding protein, contributes to the anabolic effects of simvastatin on bone. J Biol Chem 2004;279(20):21239-47.
(105) Beresford JN, Graves SE, Smoothy CA. Formation of mineralized nodules by bone derived cells in vitro: a model of bone formation? Am J Med Genet 1993;45(2):163-78.
(106) Fredrickson BE, Baker D, McHolick WJ, Yuan HA, Lubicky JP. The natural history of spondylolysis and spondylolisthesis. J Bone Joint Surg Am 1984;66(5):699-707.
(107) Rowe GG, Roche MB. The etiology of separate neural arch. J Bone Joint Surg Am 1953;35-A(1):102-10.

(108) Stasinopoulos D. Treatment of spondylolysis with external electrical stimulation in young athletes: a critical literature review. Br J Sports Med 2004;38(3):352-4.
(109) Standaert CJ, Herring SA. Spondylolysis: a critical review. Br J Sports Med 2000;34(6):415-22.
(110) Debnath UK, Freeman BJ, Gregory P, de la HD, Kerslake RW, Webb JK. Clinical outcome and return to sport after the surgical treatment of spondylolysis in young athletes. J Bone Joint Surg Br 2003;85(2):244-9.
(111) Gregory PL, Batt ME, Kerslake RW. Comparing spondylolysis in cricketers and soccer players. Br J Sports Med 2004;38(6):737-42.
(112) Yaszemski MJ, Payne RG, Hayes WC, Langer R, Mikos AG. Evolution of bone transplantation: molecular, cellular and tissue strategies to engineer human bone. Biomaterials 1996;17(2):175-85.
(113) Boskey AL. Musculoskeletal disorders and orthopedic conditions. JAMA 2001;285(5):619-23.
(114) Wilson EB. The cell in development and inheritance. New York: Macmillan; 1896.
(115) Stem Cell Biology. New York: Cold Spring Harbour Labratory Press; 2001.
(116) Zwaka TP, Thomson JA. Differentiation of human embryonic stem cells occurs through symmetric cell division. Stem Cells 2005;23(2):146-9.
(117) Matsui Y, Toksoz D, Nishikawa S, Nishikawa S, Williams D, Zsebo K, Hogan BL. Effect of Steel factor and leukaemia inhibitory factor on murine primordial germ cells in culture. Nature 1991;353(6346):750-2.
(118) Smith AG. Embryonic Stem Cells. In: Marshak DR, Gardner RL, Gottlieb D, editors. Stem Cell Biology. 1st ed. New York: Cold Spring Harbour Labratory Press; 2001. p. 205-30.
(119) Stevens LC. Studies on transplantable testicular teratomas of strain 129 mice. J Natl Cancer Inst 1958;20:1257-70.
(120) Smith A. Embryonic stem cells. In: Marshak DR, Gardner RL, Gottlieb D, editors. Stem cell biology. 1 ed. Cold Spring Harbor: Cold Spring Harbor Laboratory Press; 2001. p. 205-30.
(121) Andrews PW, Przyborski SA. Embryonal Carcinoma Cells As Embryonic Stem Cells. In: Marshak DR, Gardner RL, Gottlieb D, editors. Stem Cell Biology. 1st ed. New York: Cold Spring Harbour Labratory Press; 2001. p. 231-65.
(122) Evans MJ, Kaufman MH. Establishment in culture of pluripotential cells from mouse embryos. Nature 1981;292:154-6.
(123) Martin GR. Isolation of a pluripotent cell line from early mouse embryos cultured in medium conditioned by teratocarcinoma stem cells. Proc Natl Acad Sci U S A 1981;78(12):7634-8.
(124) Thomson JA, Marshall VS. Primate embryonic stem cells. Curr Top Dev Biol 1998;38:133-65.
(125) Thomson JA, Itskovitz-Eldor J, Shapiro SS, Waknitz MA, Swiergiel JJ, Marshall VS, Jones JM. Embryonic stem cell lines derived from human blastocysts. Science 1998;282(5391):1145-7.
(126) Senior K. Cord blood: from waste product to valuable resource. Trends Mol Med 2001;7(1):3-4.
(127) Thesleff I, Tummers M. Stem cells and tissue engineering: prospects for regenerating tissues in dental practice. Med Princ Pract 2003;12 Suppl 1:43-50.

(128) Liu Y, Rao MS. Transdifferentiation-fact or artifact. J Cell Biochem 2003;88(1):29-40.
(129) Hoffman LM, Hall L, Batten JL, Young H, Pardasani D, Baetge EE, Lawrence J, Carpenter MK. X-Inactivation Varies in hESC Lines. Stem Cells 2005.
(130) Suda Y, Suzuki M, Ikawa Y, Aizawa S. Mouse embryonic stem cells exhibit indefinite proliferative potential. J Cell Physiol 1987;133(1):197-201.
(131) Rugg-Gunn PJ, Ferguson-Smith AC, Pedersen RA. Epigenetic status of human embryonic stem cells. Nat Genet 2005;37(6):585-7.
(132) Maitra A, Arking DE, Shivapurkar N, Ikeda M, Stastny V, Kassauei K, Sui G, Cutler DJ, Liu Y, Brimble SN, Noaksson K, Hyllner J, Schulz TC, Zeng X, Freed WJ, Crook J, Abraham S, Colman A, Sartipy P, Matsui SI, Carpenter M, Gazdar AF, Rao M, Chakravarti A. Genomic alterations in cultured human embryonic stem cells. Nat Genet 2005.
(133) Andrews PW, Benvenisty N, McKay R, Pera MF, Rossant J, Semb H, Stacey GN. The International Stem Cell Initiative: toward benchmarks for human embryonic stem cell research. Nat Biotechnol 2005;23(7):795-7.
(134) Pesce M, Gross MK, Scholer HR. In line with our ancestors: Oct-4 and the mammalian germ. Bioessays 1998;20(9):722-32.
(135) Nichols J, Zevnik B, Anastassiadis K, Niwa H, Klewe-Nebenius D, Chambers I, Scholer H, Smith A. Formation of pluripotent stem cells in the mammalian embryo depends on the POU transcription factor Oct4. Cell 1998;95(3):379-91.
(136) Niwa H, Miyazaki J, Smith AG. Quantitative expression of Oct-3/4 defines differentiation, dedifferentiation or self-renewal of ES cells. Nat Genet 2000;24(4):372-6.
(137) Chambers I, Colby D, Robertson M, Nichols J, Lee S, Tweedie S, Smith A. Functional expression cloning of Nanog, a pluripotency sustaining factor in embryonic stem cells. Cell 2003;113(5):643-55.
(138) Mitsui K, Tokuzawa Y, Itoh H, Segawa K, Murakami M, Takahashi K, Maruyama M, Maeda M, Yamanaka S. The homeoprotein Nanog is required for maintenance of pluripotency in mouse epiblast and ES cells. Cell 2003;113(5):631-42.
(139) Kanatsu-Shinohara M, Toyokuni S, Shinohara T. CD9 Is a Surface Marker on Mouse and Rat Male Germline Stem Cells. Biol Reprod 2004;70(1):70-5.
(140) Oka M, Tagoku K, Russell TL, Nakáno Y, Hamazaki T, Meyer EM, Yokota T, Terada N. CD9 is associated with leukemia inhibitory factor-mediated maintenance of embryonic stem cells. Mol Biol Cell 2002;13(4):1274-81.
(141) Smith TA, Hooper ML. Medium conditioned by feeder cells inhibits the differentiation of embryonal carcinoma cultures. Exp Cell Res 1983;145(2):458-62.
(142) Smith AG, Hooper ML. Buffalo rat liver cells produce a diffusible activity which inhibits the differentiation of murine embryonal carcinoma and embryonic stem cells. Dev Biol 1987;121(1):1-9.
(143) Smith AG, Heath JK, Donaldson DD, Wong GG, Moreau J, Stahl M, Rogers D. Inhibition of pluripotential embryonic stem cell differentiation by purified polypeptides. Nature 1988;336(6200):688-90.
(144) Yamane T, Dylla SJ, Muijtjens M, Weissman IL. Enforced Bcl-2 expression overrides serum and feeder cell requirements for mouse

embryonic stem cell self-renewal. Proc Natl Acad Sci U S A 2005;102(9):3312-7.
(145) Chambers I, Smith A. Self-renewal of teratocarcinoma and embryonic stem cells. Oncogene 2004;23(43):7150-60.
(146) Martin GR, Evans MJ. Differentiation of clonal lines of teratocarcinoma cells: formation of embryoid bodies in vitro. Proc Natl Acad Sci U S A 1975;72(4):1441-5.
(147) Desbaillets I. Embryoid Bodies: an in vitro model of mouse embryogenesis. Experimental Physiology 2000.
(148) Leahy A, Xiong JW, Kuhnert F, Stuhlmann H. Use of developmental marker genes to define temporal and spatial patterns of differentiation during embryoid body formation. J Exp Zool 1999;284(1):67-81.
(149) Bongso A, Fong CY, Ng SC, Ratnam S. Isolation and culture of inner cell mass cells from human blastocysts. Hum Reprod 1994;9(11):2110-7.
(150) Xu C, Inokuma MS, Denham J, Golds K, Kundu P, Gold JD, Carpenter MK. Feeder-free growth of undifferentiated human embryonic stem cells. Nat Biotechnol 2001;19(10):971-4.
(151) Amit M, Carpenter MK, Inokuma MS, Chiu CP, Harris CP, Waknitz MA, Itskovitz-Eldor J, Thomson JA. Clonally Derived Human Embryonic Stem Cell Lines Maintain Pluripotency and Proliferative Potential for Prolonged Periods of Culture. Developmental Biology 2000;227(2):271-8.
(152) Reubinoff BE, Pera MF, Fong CY, Trounson A, Bongso A. Embryonic stem cell lines from human blastocysts: somatic differentiation in vitro. Nat Biotechnol 2000;18(4):399-404.
(153) Itskovitz-Eldor J, Schuldiner M, Karsenti D, Eden A, Yanuka O, Amit M, Soreq H, Benvenisty N. Differentiation of human embryonic stem cells into embryoid bodies compromising the three embryonic germ layers. Mol Med 2000;6(2):88-95.
(154) Chadwick K, Wang L, Li L, Menendez P, Murdoch B, Rouleau A, Bhatia M. Cytokines and BMP-4 promote hematopoietic differentiation of human embryonic stem cells. Blood 2003.
(155) Kehat I, Kenyagin-Karsenti D, Snir M, Segev H, Amit M, Gepstein A, Livne E, Binah O, Itskovitz-Eldor J, Gepstein L. Human embryonic stem cells can differentiate into myocytes with structural and functional properties of cardiomyocytes. J Clin Invest 2001;108(3):407-14.
(156) Assady S, Maor G, Amit M, Itskovitz-Eldor J, Skorecki KL, Tzukerman M. Insulin production by human embryonic stem cells. Diabetes 2001;50(8):1691-7.
(157) Levenberg S, Golub JS, Amit M, Itskovitz-Eldor J, Langer R. Endothelial cells derived from human embryonic stem cells. Proc Natl Acad Sci U S A 2002;99(7):4391-6.
(158) Doble BW, Woodgett JR. GSK-3: tricks of the trade for a multi-tasking kinase. J Cell Sci 2003;116(Pt 7):1175-86.
(159) Martinez A, Castro A, Dorronsoro I, Alonso M. Glycogen synthase kinase 3 (GSK-3) inhibitors as new promising drugs for diabetes, neurodegeneration, cancer, and inflammation. Med Res Rev 2002;22(4):373-84.
(160) Nakashima K, Colamarino S, Gage FH. Embryonic stem cells: staying plastic on plastic. Nat Med 2004;10(1):23-4.
(161) Sato N, Meijer L, Skaltsounis L, Greengard P, Brivanlou AH. Maintenance of pluripotency in human and mouse embryonic stem cells

through activation of Wnt signaling by a pharmacological GSK-3-specific inhibitor. Nat Med 2004;10(1):55-63.

(162) Xu RH, Peck RM, Li DS, Feng X, Ludwig T, Thomson JA. Basic FGF and suppression of BMP signaling sustain undifferentiated proliferation of human ES cells. Nat Methods 2005;2(3):185-90.

(163) Martin MJ, Muotri A, Gage F, Varki A. Human embryonic stem cells express an immunogenic nonhuman sialic acid. Nat Med 2005;11(2):228-32.

(164) Polak JM, Bishop AE. Stem cells and tissue engineering. NYAS 2006;1068:-352.

(165) Wakayama T, Tabar V, Rodriguez I, Perry AC, Studer L, Mombaerts P. Differentiation of embryonic stem cell lines generated from adult somatic cells by nuclear transfer. Science 2001;292(5517):740-3.

(166) Hwang WS, Roh SI, Lee BC, Kang SK, Kwon DK, Kim S, Kim SJ, Park SW, Kwon HS, Lee CK, Lee JB, Kim JM, Ahn C, Paek SH, Chang SS, Koo JJ, Yoon HS, Hwang JH, Hwang YY, Park YS, Oh SK, Kim HS, Park JH, Moon SY, Schatten G. Patient-Specific Embryonic Stem Cells Derived from Human SCNT Blastocysts. Science 2005.

(167) Heng BC, Cao T, Stanton LW, Robson P, Olsen B. Strategies for directing the differentiation of stem cells into the osteogenic lineage in vitro. J Bone Miner Res 2004;19(9):1379-94.

(168) Randle WL, Fagg R, George E. Establishment of an In Vitro Clonogenic Human Cord Blood (hCB) Assay for the Assessment of Haematotoxicity. Comparative Clinical Pathology 11[2], 129. 2002.
Ref Type: Abstract

(169) Petit-Zeman S. Regenerative medicine. Nat Biotechnol 2001;19(3):201-6.

(170) Logeart-Avramoglou D, Anagnostou F, Bizios R, Petite H. Engineering bone: challenges and obstacles. J Cell Mol Med 2005;9(1):72-84.

(171) Vacanti CA, Bonassar LJ, Vacanti MP, Shufflebarger J. Replacement of an avulsed phalanx with tissue-engineered bone. N Engl J Med 2001;344(20):1511-4.

(172) Barnes D, Sato G. Serum-free cell culture: a unifying approach. Cell 1980;22(3):649-55.

(173) Barnes D, Sato G. Methods for growth of cultured cells in serum-free medium. Anal Biochem 1980;102(2):255-70.

(174) Dartsch PC, Weiss HD, Betz E. Human vascular smooth muscle cells in culture: growth characteristics and protein pattern by use of serum-free media supplements. Eur J Cell Biol 1990;51(2):285-94.

(175) Ham RG, McKeehan WL. Media and growth requirements. Methods Enzymol 1979;58:44-93.

(176) Lennon DP, Haynesworth SE, Young RG, Dennis JE, Caplan AI. A chemically defined medium supports in vitro proliferation and maintains the osteochondral potential of rat marrow-derived mesenchymal stem cells. Exp Cell Res 1995;219(1):211-22.

(177) Goldsborough MD, Tilkins ML, Price PJ, Lobo-Alfonso J, Morrison JR, Stevens ME, Meneses J, Pedersen R, Koller B, Iatour A. Serum-free culture of murine embryonic stem cells. Focus 1998;20(1):8-12.

(178) Wiles MV, Johansson BM. Analysis of factors controlling primary germ layer formation and early hematopoiesis using embryonic stem cell in vitro differentiation. Leukemia 1997;11 Suppl 3:454-6.

(179) Furue M, Okamoto T, Hayashi Y, Okochi H, Fujimoto M, Myoishi Y, Abe T, Ohnuma K, Sato GH, Asashima M, Sato JD. Luekemia inhibitory factor as an anti-apoptotic mitogen for pluripotent mouse embryonic stem cells in a serum-free medium without feeder cells. In Vitro Cell Dev Biol Anim 2005;41(1):19-28.
(180) Wong M, Tuan RS. Nuserum, a synthetic serum replacement, supports chondrogenesis of embryonic chick limb bud mesenchymal cells in micromass culture. In Vitro Cell Dev Biol Anim 1993;29A(12):917-22.
(181) Abbott A. Cell culture: biology's new dimension. Nature 2003;424(6951):870-2.
(182) Nielson LK. Bioreactors for Hematopoietic Cell Culture. Annual Review of Biomedical Engineering 1999;1:129-52.
(183) Martin I, Wendt D, Heberer M. The role of bioreactors in tissue engineering. Trends Biotechnol 2004;22(2):80-6.
(184) Vunjak-Novakovic G, Martin I, Obradovic B, Treppo S, Grodzinsky AJ, Langer R, Freed LE. Bioreactor cultivation conditions modulate the composition and mechanical properties of tissue-engineered cartilage. J Orthop Res 1999;17(1):130-8.
(185) Vunjak-Novakovic G. The fundamentals of tissue engineering: scaffolds and bioreactors. Novartis Found Symp 2003;249:34-46.
(186) Jeevarajan AS, Vani S, Taylor TD, Anderson MM. Continuous pH monitoring in a perfused bioreactor system using an optical pH sensor. Biotechnol Bioeng 2002;78(4):467-72.
(187) Sutherland RM, Sordat B, Bamat J, Gabbert H, Bourrat B, Mueller-Klieser W. Oxygenation and differentiation in multicellular spheroids of human colon carcinoma. Cancer Res 1986;46(10):5320-9.
(188) Sikavitsas VI, Temenoff JS, Mikos AG. Biomaterials and bone mechanotransduction. Biomaterials 2001;22(19):2581-93.
(189) Hillsley MV, Frangos JA. Bone tissue engineering: the role of interstitial fluid flow. Biotechnol Bioeng 1994;43(7):573-81.
(190) Davisson T, Sah RL, Ratcliffe A. Perfusion increases cell content and matrix synthesis in chondrocyte three-dimensional cultures. Tissue Eng 2002;8(5):807-16.
(191) Yamada KM, Clark K. Cell biology: survival in three dimensions. Nature 2002;419(6909):790-1.
(192) Gerecht-Nir S, Cohen S, Itskovitz-Eldor J. Bioreactor cultivation enhances the efficiency of human embryoid body (hEB) formation and differentiation. Biotechnol Bioeng 2004;86(5):493-502.
(193) Botchwey EA, Pollack SR, Levine EM, Johnston ED, Laurencin CT. Quantitative analysis of three-dimensional fluid flow in rotating bioreactors for tissue engineering. J Biomed Mater Res 2004;69A(2):205-15.
(194) Wiesmann HP, Joos U, Meyer U. Biological and biophysical principles in extracorporal bone tissue engineering. Part II. Int J Oral Maxillofac Surg 2004;33(6):523-30.
(195) Yu X, Botchwey EA, Levine EM, Pollack SR, Laurencin CT. Bioreactor-based bone tissue engineering: the influence of dynamic flow on osteoblast phenotypic expression and matrix mineralization. Proc Natl Acad Sci U S A 2004;101(31):11203-8.
(196) Grant GT, Morris ER, Rees DA, Smith PJC, Thom D. BiologicalInteractions Between Polysaccharides and Divalent Cations: The Egg-Box Model. FEBS Lett 1973;32:195-8.

(197) Gutowska A, Jeong B, Jasionowski M. Injectable gels for tissue engineering. Anat Rec 2001;263(4):342-9.
(198) Park DJ, Choi BH, Zhu SJ, Huh JY, Kim BY, Lee SH. Injectable bone using chitosan-alginate gel/mesenchymal stem cells/BMP-2 composites. J Craniomaxillofac Surg 2005;33(1):50-4.
(199) Stevens MM, Qanadilo HF, Langer R, Prasad S, V. A rapid-curing alginate gel system: utility in periosteum-derived cartilage tissue engineering. Biomaterials 2004;25(5):887-94.
(200) Koch S, Schwinger C, Kressler J, Heinzen C, Rainov NG. Alginate encapsulation of genetically engineered mammalian cells: comparison of production devices, methods and microcapsule characteristics. J Microencapsul 2003;20(3):303-16.
(201) Lanza RP, Kuhtreiber WM, Ecker D, Staruk JE, Chick WL. Xenotransplantation of porcine and bovine islets without immunosuppression using uncoated alginate microspheres. Transplantation 1995;59(10):1377-84.
(202) Stabler CL, Sambanis A, Constantinidis I. Effects of alginate composition on the growth and overall metabolic activity of betaTC3 cells. Ann N Y Acad Sci 2002;961:130-3.
(203) Stabler C, Wilks K, Sambanis A, Constantinidis I. The effects of alginate composition on encapsulated betaTC3 cells. Biomaterials 2001;22(11):1301-10.
(204) Constantinidis I, Rask I, Long RC, Jr., Sambanis A. Effects of alginate composition on the metabolic, secretory, and growth characteristics of entrapped beta TC3 mouse insulinoma cells. Biomaterials 1999;20(21):2019-27.
(205) Chang TM. SEMIPERMEABLE MICROCAPSULES. Science 1964;146:524-5.
(206) Ma HL, Hung SC, Lin SY, Chen YL, Lo WH. Chondrogenesis of human mesenchymal stem cells encapsulated in alginate beads. J Biomed Mater Res 2003;64A(2):273-81.
(207) Awad HA, Quinn WM, Leddy HA, Gimble JM, Guilak F. Chondrogenic differentiation of adipose-derived adult stem cells in agarose, alginate, and gelatin scaffolds. Biomaterials 2004;25(16):3211-22.
(208) Tanaka H, Murphy CL, Murphy C, Kimura M, Kawai S, Polak JM. Chondrogenic differentiation of murine embryonic stem cells: Effects of culture conditions and dexamethasone. J Cell Biochem 2004;93(3):454.
(209) Mironov V, Boland T, Trusk T, Forgacs G, Markwald RR. Organ printing: computer-aided jet-based 3D tissue engineering. Trends Biotechnol 2003;21(4):157-61.
(210) Loebel DA, Watson CM, De Young RA, Tam PP. Lineage choice and differentiation in mouse embryos and embryonic stem cells. Dev Biol 2003;264(1):1-14.
(211) Dang SM, Kyba M, Perlingeiro R, Daley GQ, Zandstra PW. Efficiency of embryoid body formation and hematopoietic development from embryonic stem cells in different culture systems. Biotechnol Bioeng 2002;78(4):442-53.
(212) Smith AG. Culture and Differentiation of Embryonic Stem Cells. Journal of Tissue Culture Methods 1991;13:89-94.
(213) Hooper M, Hardy K, Handyside A, Hunter S, Monk M. HPRT-deficient (Lesch-Nyhan) mouse embryos derived from germline colonization by cultured cells. Nature 1987;326(6110):292-5.

(214) Wong G, Cohn DV. Separation of parathyroid hormone and calcitonin-sensitive cells from non-responsive bone cells. Nature 1974;252(5485):713-5.
(215) Gregory CA, Gunn WG, Peister A, Prockop DJ. An Alizarin red-based assay of mineralization by adherent cells in culture: comparison with cetylpyridinium chloride extraction. Anal Biochem 2004;329(1):77-84.
(216) Li Y, Powell S, Brunette E, Lebkowski J, Mandalam R. Expansion of human embryonic stem cells in defined serum-free medium devoid of animal-derived products. Biotechnol Bioeng 2005.
(217) Scholer HR, Ruppert S, Suzuki N, Chowdhury K, Gruss P. New type of POU domain in germ line-specific protein Oct-4. Nature 1990;344(6265):435-9.
(218) Ying QL, Smith AG. Defined conditions for neural commitment and differentiation. Methods Enzymol 2003;365:327-41.
(219) Ying QL, Nichols J, Chambers I, Smith A. BMP induction of Id proteins suppresses differentiation and sustains embryonic stem cell self-renewal in collaboration with STAT3. Cell 2003;115(3):281-92.
(220) Temple S. Embryonic stem cell self-renewal, analyzed. Cell 2003;115(3):247-8.
(221) Arsenian S, Weinhold B, Oelgeschlager M, Ruther U, Nordheim A. Serum response factor is essential for mesoderm formation during mouse embryogenesis. EMBO J 1998;17(21):6289-99.
(222) Weinman EJ, Lakkis J, Akom M, Wali RK, Drachenberg CB, Coleman RA, Wade JB. Expression of NHERF-1, NHERF-2, PDGFR-alpha, and PDGFR-beta in normal human kidneys and in renal transplant rejection. Pathobiology 2002;70(6):314-23.
(223) Soriano P. The PDGF alpha receptor is required for neural crest cell development and for normal patterning of the somites. Development 1997;124(14):2691-700.
(224) Ward CM, Barrow KM, Stern PL. Significant variations in differentiation properties between independent mouse ES cell lines cultured under defined conditions. Exp Cell Res 2004;293(2):229-38.
(225) Czyz J, Wobus A. Embryonic stem cell differentiation: the role of extracellular factors. Differentiation 2001;68(4-5):167-74.
(226) Fehling HJ, Lacaud G, Kubo A, Kennedy M, Robertson S, Keller G, Kouskoff V. Tracking mesoderm induction and its specification to the hemangioblast during embryonic stem cell differentiation. Development 2003;130(17):4217-27.
(227) Zhao GQ. Consequences of knocking out BMP signaling in the mouse. Genesis 2003;35(1):43-56.
(228) Canalis E, Economides AN, Gazzerro E. Bone morphogenetic proteins, their antagonists, and the skeleton. Endocr Rev 2003;24(2):218-35.
(229) Cheng H, Jiang W, Phillips FM, Haydon RC, Peng Y, Zhou L, Luu HH, An N, Breyer B, Vanichakarn P, Szatkowski JP, Park JY, He TC. Osteogenic activity of the fourteen types of human bone morphogenetic proteins (BMPs). J Bone Joint Surg Am 2003;85-A(8):1544-52.
(230) Cheng SL, Lecanda F, Davidson MK, Warlow PM, Zhang SF, Zhang L, Suzuki S, St John T, Civitelli R. Human osteoblasts express a repertoire of cadherins, which are critical for BMP-2-induced osteogenic differentiation. J Bone Miner Res 1998;13(4):633-44.
(231) Marie PJ. Fibroblast growth factor signaling controlling osteoblast differentiation. Gene 2003;316:23-32.

(232) Hwang YS, Randle WL, Bielby RC, Polak JM, Mantalaris A. Enhanced Derivation of Osteogenic Cells from Murine Embryonic Stem Cells After Treatment with HepG2- Conditioned Medium and Modulation of the Embryoid Body Formation Period: Application to Skeletal Tissue Engineering. Tissue Eng 2006;12(6):1381-92.
(233) Julka S, Regnier FE. Recent advancements in differential proteomics based on stable isotope coding. Brief Funct Genomic Proteomic 2005;4(2):158-77.
(234) Putz S, Reinders J, Reinders Y, Sickmann A. Mass spectrometry-based peptide quantification: applications and limitations. Expert Rev Proteomics 2005;2(3):381-92.
(235) Havre SL, Singhal M, Payne DA, Lipton MS, Webb-Robertson BJ. Enabling proteomics discovery through visual analysis. The peptide permutation and protein prediction tool. IEEE Eng Med Biol Mag 2005;24(3):50-7.
(236) Monteoliva L, Albar JP. Differential proteomics: an overview of gel and non-gel based approaches. Brief Funct Genomic Proteomic 2004;3(3):220-39.
(237) Honore B, Ostergaard M, Vorum H. Functional genomics studied by proteomics. Bioessays 2004;26(8):901-15.
(238) Lightfoot EN. Transport phenomena and living systems. New York: John Wiley; 1974.
(239) Ratcliffe A, Niklason LE. Bioreactors and bioprocessing for tissue engineering. Ann N Y Acad Sci 2002;961:210-5.
(240) Chang TM. Semipermeable microcapsules. Science 1964;146:524-5.
(241) Grant GT, Morris ER, Rees DA, Smith PJC, Thom D. Biological Interactions Between Polysaccharides and Divalent Cations: The Egg-Box Model. FEBS Lett 1973;32:195-8.
(242) Chen SS, Revoltella RP, Papini S, Michelini M, Fitzgerald W, Zimmerberg J, Margolis L. Multilineage differentiation of rhesus monkey embryonic stem cells in three-dimensional culture systems. Stem Cells 2003;21(3):281-95.
(243) Gerecht-Nir S, Cohen S, Ziskind A, Itskovitz-Eldor J. Three-dimensional porous alginate scaffolds provide a conducive environment for generation of well-vascularized embryoid bodies from human embryonic stem cells. Biotechnol Bioeng 2004;88(3):313-20.
(244) Levenberg S, Huang NF, Lavik E, Rogers AB, Itskovitz-Eldor J, Langer R. Differentiation of human embryonic stem cells on three-dimensional polymer scaffolds. Proc Natl Acad Sci U S A 2003.
(245) Chaudhry GR, Yao D, Smith A, Hussain A. Osteogenic Cells Derived From Embryonic Stem Cells Produced Bone Nodules in Three-Dimensional Scaffolds. J Biomed Biotechnol 2004;2004(4):203-10.
(246) Hwang NS, Kim MS, Sampattavanich S, Baek JH, Zhang Z, Elisseeff J. The Effects of Three Dimensional Culture and Growth Factors on the Chondrogenic Differentiation of Murine Embryonic Stem Cells. Stem Cells 2005.
(247) Fok EY, Zandstra PW. Shear-Controlled Single-Step Mouse Embryonic Stem Cell Expansion and EB-Based Differentiation. Stem Cells 2005.
(248) Balakrishnan B, Jayakrishnan A. Self-cross-linking biopolymers as injectable in situ forming biodegradable scaffolds. Biomaterials 2005;26(18):3941-51.

(249) Sambrook J, Russel DW. Molecular Cloning: A Laboratory Manual. Third ed. New York: Cold Spring Harbor Laboratory Press; 2001.
(250) Fundueanu G, Nastruzzi C, Carpov A, Desbrieres J, Rinaudo M. Physico-chemical characterization of Ca-alginate microparticles produced with different methods. Biomaterials 1999;20(15):1427-35.
(251) Evans ND, Randle WL, Hwang YS, Polak JM, Mantalaris A. Single alginate-encapsulated mouse embryonic stem cells divide to form undifferentiated colonies: potential for high thoughput screening of embryonic stem cell differentiation. 2005 Jun 24; ISSCR, San Francisco 2005.
(252) Murphy CL, Sambanis A. Effect of oxygen tension and alginate encapsulation on restoration of the differentiated phenotype of passaged chondrocytes. Tissue Eng 2001;7(6):791-803.
(253) Sugiura S, Oda T, Izumida Y, Aoyagi Y, Satake M, Ochiai A, Ohkohchi N, Nakajima M. Size control of calcium alginate beads containing living cells using micro-nozzle array. Biomaterials 2005;26(16):3327-31.
(254) Serp D, Cantana E, Heinzen C, von Stockar U, Marison IW. Characterization of an encapsulation device for the production of monodisperse alginate beads for cell immobilization. Biotechnol Bioeng 2000;70(1):41-53.
(255) Mason BJ, Jayaratne OW, Woods JD. An improved vibrating capillary device for producing uniform water droplets of 15 to 500μm radius. J Sci Instrum 1963;40:247-9.
(256) Guo JF, Jourdian GW, MacCallum DK. Culture and growth characteristics of chondrocytes encapsulated in alginate beads. Connect Tissue Res 1989;19(2-4):277-97.
(257) Gascan H, Godard A, Ferenz C, Naulet J, Praloran V, Peyrat MA, Hewick R, Jacques Y, Moreau JF, Soulillou JP. Characterization and NH2-terminal amino acid sequence of natural human interleukin for DA cells: leukemia inhibitory factor. Differentiation inhibitory activity secreted by a T lymphoma cell line. J Biol Chem 1989;264(36):21509-15.
(258) Hilton DJ, Nicola NA, Metcalf D. Specific binding of murine leukemia inhibitory factor to normal and leukemic monocytic cells. Proc Natl Acad Sci U S A 1988;85(16):5971-5.
(259) Diem K, Lentner C. Scientific Tables. New York: Ardsley, Geigy Pharmaceuticals; 1975.
(260) Aoki T, Umehara Y, Ferraresso C, Sugiyama N, Middleton Y, Avital I, Inderbitzin D, Demetriou AA, Rozga J. Intrasplenic transplantation of encapsulated cells: a novel approach to cell therapy. Cell Transplant 2002;11(6):553-61.
(261) McConell K, Jarman-Smith M, Stewart K, Chaudhuri JB. Culture of Meniscal Chondrocytes on alginate hydrogel matrices. Food and Bioproducts Processing 2004;82(C2):126-32.
(262) Shimko DA, Burks CA, Dee KC, Nauman EA. Comparison of in vitro mineralization by murine embryonic and adult stem cells cultured in an osteogenic medium. Tissue Eng 2004;10(9-10):1386-98.
(263) ISPCORP. The Algin/Calcium Reaction. 2005 Sep 15. Report No.: http://www.ispcorp.com/products/food/content/brochure/alginates/.
(264) Braschler T, Johann R, Heule M, Metref L, Renaud P. Gentle cell trapping and release on a microfluidic chip by in situ alginate hydrogel formation. Lab Chip 2005;5(5):553-9.

(265) He M, Edgar JS, Jeffries GD, Lorenz RM, Shelby JP, Chiu DT. Selective encapsulation of single cells and subcellular organelles into picoliter- and femtoliter-volume droplets. Anal Chem 2005;77(6):1539-44.
(266) Ragozzino E, Faggioli F, Barba M. Development of a one tube-one step RT-PCR protocol for the detection of seven viroids in four genera: Apscaviroid, Hostuviroid, Pelamoviroid and Pospiviroid. J Virol Methods 2004;121(1):25-9.
(267) Reimer T, Koczan D, Briese V, Friese K, Richter D, Thiesen HJ, Jeschke U. Absolute quantification of human chorionic gonadotropin-beta mRNA with TaqMan detection. 4. Mol Biotechnol 2000;14(1):47-57.
(268) Cao Y, Wilcox KS, Martin CE, Rachinsky TL, Eberwine J, Dichter MA. Presence of mRNA for glutamic acid decarboxylase in both excitatory and inhibitory neurons. Proc Natl Acad Sci U S A 1996;93(18):9844-9.
(269) Zabzdyr JL, Lillard SJ. Measurement of single-cell gene expression using capillary electrophoresis. Anal Chem 2001;73(23):5771-5.
(270) Chen G, Ewing AG. Chemical analysis of single cells and exocytosis. Crit Rev Neurobiol 1997;11(1):59-90.
(271) Pollack SR, Meaney DF, Levine EM, Litt M, Johnston ED. Numerical model and experimental validation of microcarrier motion in a rotating bioreactor. Tissue Eng 2000;6(5):519-30.
(272) Wolf DA, Schwarz RP. Experimental measurement of the orbital paths of particles sedimenting within a rotating viscous fluid as influenced by gravity. NASA Technical paper; 1992. Report No.: 3200.
(273) Chaudhry GR, Yao D, Smith A, Hussain A. Osteogenic Cells Derived From Embryonic Stem Cells Produced Bone Nodules in Three-Dimensional Scaffolds. J Biomed Biotechnol 2004;2004(4):203-10.
(274) Botchwey EA, Pollack SR, El Amin S, Levine EM, Tuan RS, Laurencin CT. Human osteoblast-like cells in three-dimensional culture with fluid flow. Biorheology 2003;40(1-3):299-306.
(275) Rucci N, Migliaccio S, Zani BM, Taranta A, Teti A. Characterization of the osteoblast-like cell phenotype under microgravity conditions in the NASA-approved Rotating Wall Vessel bioreactor (RWV). J Cell Biochem 2002;85(1):167-79.
(276) Douglas JF, Gasiorek JM, Swaffield JA. Some Properties of Common Fluids. Fluid Mechanics.Harlow: Prentice Hall; 2001. p. 896.
(277) Okazaki M, Takeshita S, Kawai S, Kikuno R, Tsujimura A, Kudo A, Amann E. Molecular cloning and characterization of OB-cadherin, a new member of cadherin family expressed in osteoblasts. J Biol Chem 1994;269(16):12092-8.
(278) Gokhale PJ, Giesberts AM, Andrews PW. Brachyury is expressed by human teratocarcinoma cells in the absence of mesodermal differentiation. Cell Growth Differ 2000;11(3):157-62.
(279) Draper JS, Moore HD, Ruban LN, Gokhale PJ, Andrews PW. Culture and characterization of human embryonic stem cells. Stem Cells Dev 2004;13(4):325-36.
(280) Zur Nieden NI, Kempka G, Ahr HJ. In vitro differentiation of embryonic stem cells into mineralized osteoblasts. Differentiation 2003;71(1):18-27.
(281) Komori T, Kishimoto T. Cbfa1 in bone development. Curr Opin Genet Dev 1998;8(4):494-9.
(282) Hegert C, Kramer J, Hargus G, Muller J, Guan K, Wobus AM, Muller PK, Rohwedel J. Differentiation plasticity of chondrocytes derived from mouse embryonic stem cells. J Cell Sci 2002;115(Pt 23):4617-28.

(283) Tai G, Polak JM, Bishop AE, Christodoulou I, Buttery LD. Differentiation of osteoblasts from murine embryonic stem cells by overexpression of the transcriptional factor osterix. Tissue Eng 2004;10(9-10):1456-66.
(284) Robertson SM, Kennedy M, Shannon JM, Keller G. A transitional stage in the commitment of mesoderm to hematopoiesis requiring the transcription factor SCL/tal-1. Development 2000;127(11):2447-59.
(285) Wilkinson DG, Bhatt S, Herrmann BG. Expression pattern of the mouse T gene and its role in mesoderm formation. Nature 1990;343(6259):657-9.
(286) Tam PP, Behringer RR. Mouse gastrulation: the formation of a mammalian body plan. Mech Dev 1997;68(1-2):3-25.
(287) Rossant J, Tam PP. Emerging asymmetry and embryonic patterning in early mouse development. Dev Cell 2004;7(2):155-64.
(288) Kataoka H, Takakura N, Nishikawa S, Tsuchida K, Kodama H, Kunisada T, Risau W, Kita T, Nishikawa SI. Expressions of PDGF receptor alpha, c-Kit and Flk1 genes clustering in mouse chromosome 5 define distinct subsets of nascent mesodermal cells. Dev Growth Differ 1997;39(6):729-40.
(289) Siggelkow H, Rebenstorff K, Kurre W, Niedhart C, Engel I, Schulz H, Atkinson MJ, Hufner M. Development of the osteoblast phenotype in primary human osteoblasts in culture: comparison with rat calvarial cells in osteoblast differentiation. J Cell Biochem 1999;75(1):22-35.
(290) Whyte MP. Hypophosphatasi. In: Bilezikian JP, Raisz LG, Rodan GA, editors. Principles of Bone Biology. 2nd ed. London: Academic Press; 2002. p. 1229-48.
(291) Benayahu D, Shamay A, Wientroub S. Osteocalcin (BGP), gene expression, and protein production by marrow stromal adipocytes. Biochem Biophys Res Commun 1997;231(2):442-6.
(292) Raymond MH, Schutte BC, Torner JC, Burns TL, Willing MC. Osteocalcin: genetic and physical mapping of the human gene BGLAP and its potential role in postmenopausal osteoporosis. Genomics 1999;60(2):210-7.
(293) Berridge MV, Tan AS. Characterization of the cellular reduction of 3-(4,5-dimethylthiazol-2-yl)-2,5-diphenyltetrazolium bromide (MTT): subcellular localization, substrate dependence, and involvement of mitochondrial electron transport in MTT reduction. Arch Biochem Biophys 1993;303(2):474-82.
(294) Tam PP, Behringer RR. Mouse gastrulation: the formation of a mammalian body plan. Mech Dev 1997;68(1-2):3-25.
(295) Terstegge S, Laufenberg I, Pochert J, Brustle O. An automated system for embryonic stem cells culture. Hamilton Life Science Robotics; 2005.
(296) Sank A, Chi M, Shima T, Reich R, Martin GR. Increased calcium levels alter cellular and molecular events in wound healing. Surgery 1989;106(6):1141-7.
(297) Powers DA, Huang RB, Colton CK. Effects of oxygen on murine embryonic stem cell energetics and growth. Stem Cell Engineering Annual Meeting, Cincinnati, OH: American Institute of Chemical Engineers; 2005.
(298) Niemeyer P, Krause U, Punzel M, Fellenberg J, Simank HG. [Mesenchymal stem cells for tissue engineering of bone: 3D-cultivation and osteogenic differentiation on mineralized collagen]. Z Orthop Ihre Grenzgeb 2003;141(6):712-7.

(299) Niemeyer P, Krause U, Fellenberg J, Kasten P, Seckinger A, Ho AD, Simank HG. Evaluation of mineralized collagen and alpha-tricalcium phosphate as scaffolds for tissue engineering of bone using human mesenchymal stem cells. Cells Tissues Organs 2004;177(2):68-78.
(300) Kihara T, Oshima A, Hirose M, Ohgushi H. Three-dimensional visualization analysis of in vitro cultured bone fabricated by rat marrow mesenchymal stem cells. Biochem Biophys Res Commun 2004;316(3):943-8.
(301) Dang SM, Gerecht-Nir S, Chen J, Itskovitz-Eldor J, Zandstra PW. Controlled, scalable embryonic stem cell differentiation culture. Stem Cells 2004;22(3):275-82.
(302) Yang WD, Cao Q, Qian QC, Tang LH, Yang LJ, Mao TQ. [A study of injectable autogenous tissue-engineered bone]. Zhonghua Kou Qiang Yi Xue Za Zhi 2003;38(5):393-5.
(303) Leblond FA, Simard G, Henley N, Rocheleau B, Huet PM, Halle JP. Studies on smaller (approximately 315 microM) microcapsules: IV. Feasibility and safety of intrahepatic implantations of small alginate poly-L-lysine microcapsules. Cell Transplant 1999;8(3):327-37.
(304) MacDermott RP, Bragdon MJ. Fetal calf serum augmentation during cell separation procedures accounts for the majority of human autologous mixed leukocyte reactivity. Behring Inst Mitt 1983;(72):122-8.
(305) Kievits F, Boerenkamp WJ, Ivanyi P. H-2-dependent binding of xenogeneic beta 2-microglobulin from culture media. J Immunol 1988;140(12):4253-5.
(306) Chen K, Ng CE, Zweier JL, Kuppusamy P, Glickson JD, Swartz HM. Measurement of the intracellular concentration of oxygen in a cell perfusion system. Magn Reson Med 1994;31(6):668-72.
(307) Tam SK, Dusseault J, Polizu S, Menard M, Halle JP, Yahia L. Impact of residual contamination on the biofunctional properties of purified alginates used for cell encapsulation. Biomaterials 2005.
(308) ASTM International. Standard Classification for Tissue Engineered Medical Products(TEMPs). West Conshohocken, PA, USA: ASTM International; 2004. Report No.: F2211-04.
(309) ASTM International. Standard Guide for Characterization and Testing of

(315) Moreau JE, Chen J, Bramono DS, Volloch V, Chernoff H, Vunjak-Novakovic G, Richmond JC, Kaplan DL, Altman GH. Growth factor induced fibroblast differentiation from human bone marrow stromal cells in vitro. J Orthop Res 2005;23(1):164-74.
(316) Damgaard B, Sanfeliu A, Cairo JJ, Casas C, Sola C, Godia F. Substitution of transferrin by FeCl3 in the development of a low foetal calf serum concentration medium for KB-26.5 hybridoma cell line. Cytotechnology 1993;13(2):133-41.
(317) Kane MT. Variability in different lots of commercial bovine serum albumin affects cell multiplication and hatching of rabbit blastocysts in culture. J Reprod Fertil 1983;69(2):555-8.
(318) Julka S, Regnier FE. Recent advancements in differential proteomics based on stable isotope coding. Brief Funct Genomic Proteomic 2005;4(2):158-77.
(319) Lim JW, Bodnar A. Proteome analysis of conditioned medium from mouse embryonic fibroblast feeder layers which support the growth of human embryonic stem cells. Proteomics 2002;2(9):1187-203.
(320) Rathjen J, Rathjen PD. Mouse ES cells: experimental exploitation of pluripotent differentiation potential. Curr Opin Genet Dev 2001;11(5):587-94.
(321) Rathjen J, Dunn S, Bettess MD, Rathjen PD. Lineage specific differentiation of pluripotent cells in vitro: a role for extraembryonic cell types. Reprod Fertil Dev 2001;13(1):15-22.
(322) Rao B, Zandstra P. Culture development for human embryonic stem cell propagation: molecular aspects and challenges. Curr Opin Biotechnol 2005.
(323) Waddington CH, Robertson E. Selection for developmental canalisation. Genet Res 1966;7(3):303-12.
(324) Koh JS, Lieberthal W, Heydrick S, Levine JS. Lysophosphatidic acid is a major serum noncytokine survival factor for murine macrophages which acts via the phosphatidylinositol 3-kinase signaling pathway. J Clin Invest 1998;102(4):716-27.
(325) McIntyre TM, Pontsler AV, Silva AR, St Hilaire A, Xu Y, Hinshaw JC, Zimmerman GA, Hama K, Aoki J, Arai H, Prestwich GD. Identification of an intracellular receptor for lysophosphatidic acid (LPA): LPA is a transcellular PPARgamma agonist. Proc Natl Acad Sci U S A 2003;100(1):131-6.
(326) Schratt G. Serum response factor is crucial for actin cytoskeletal organization and focal adhesion assembly in embryonic stem cells. The Journal of Cell Biology 2002.
(327) Kane MT. Minimal nutrient requirements for culture of one-cell rabbit embryos. Biol Reprod 1987;37(4):775-8.
(328) Biggers JD, Summers MC, McGinnis LK. Polyvinyl alcohol and amino acids as substitutes for bovine serum albumin in culture media for mouse preimplantation embryos. Hum Reprod Update 1997;3(2):125-35.

8. DERIVATIONS FROM THIS THESIS

Publications, presentations, posters, patents and awards generated during this thesis.

1. Abstract accepted at American Institute of Chemical Engineers conference 2006.
   J.M.Cha, W.L.Randle, M.R.Placzek, Y.S.Hwang, A.E.Bishop, J.M.Polak and A.Mantalaris.
   Integrated 3D Expansion and Osteogenic Differentiation of Murine Embryonic Stem Cells in a Simulated Microgravity Bioreactor.
2. W.L.Randle, Y.S.Hwang, J.M.Polak and A.Mantalaris. Integrated 3D expansion and osteogenic differentiation of murine embryonic stem cells. (Submitted to Stem Cells).
3. Patent application (UK/USA). Culture Methods. Mr. Wesley Randle, Prof. Dame J. Polak, and Dr. A. Mantalaris.
4. Poster at International Society for Stem Cell Research Conference 2005.
   Integrated expansion and differentiation of mouse ES cells in alginate beads cultured in bioreactors for bone tissue engineering applications.
   Athanassios Mantalaris, Wesley L. Randle, Yu-shik Hwang, Nicholas D. Evans and Julia M. Polak.
5. Poster at International Society for Stem Cell Research Conference 2005.
   Single alginate-encapsulated mouse embryonic stem cells divide to form undifferentiated colonies: potential for high throughput screening of embryonic stem cell differentiation
   Nicholas D. Evans, Athanassios Mantalaris, Wesley L. Randle, Yu-shik Hwang and Julia M. Polak.
6. Poster at International Society for Stem Cell Research Conference 2005.
   Controlling mesodermal development of murine embryonic stem cells results in enhanced osteogenic differentiation: applications for skeletal tissue engineering.
   Robert Bielby, Athanassios Mantalaris, Yu-shik Hwang, Wesley L. Randle, Nicholas D. Evans and Julia M. Polak.
7. Enhanced derivation of osteogenic cells from murine embryonic stem cells following treatment with HepG2 conditioned medium and modulation of the embryoid body formation period: application to skeletal tissue engineering
   Yu-Shik Hwang, M.Sc; Wesley L. Randle, B.Sc; Robert C. Bielby, Ph.D; Julia M. Polak, MD, and Athanasios Mantalaris, Ph.D (accepted for publication in tissue engineering)
8. Imperial College "Ideas Challenge" 2nd Prize for novel idea related to cartilage tissue engineering and a viable business plan (2004). Y.S.Hwang and W.L.Randle.
9. Imperial College "Business Challenge" Finalist Prize for novel idea related to sports tissue engineering and an in depth business plan (2004). W.L.Randle, I.Bassi, K.E.Hall, O.Tsigkou, A.Mantalaris and A.Vats.
10. Imperial College "Ideas Challenge" First Prize for novel idea related to sports tissue engineering and a viable business plan (2003). W.L.Randle and K.E.Hall
11. Ioan Notingher, Isabelle Bisson, Anne E Bishop, Wesley L. Randle, Julia M. P. Polak, Larry L. Hench. In-Situ Spectral Monitoring of mRNA Translation in Embryonic Stem Cells during Differentiation In-Vitro. Anal Chem. 2004 Jun 1;76(11):3185-93.
12. Poster at Tissue Engineering Society International Conference.
    Osteogenic Differentiation of Mouse Embryonic Stem Cells in Serum Free Culture Medium and Scalable Production for Bone Repair.
    Randle, Wesley.L., Mantalaris, Athanassios., Buttery, Lee.D.K. & Polak, Julia.M. (2003)
13. Poster at Stem Cells: Shaping the Future Conference.
    Osteogenic Differentiation of Mouse Embryonic Stem Cells in Serum Free Culture Medium
    Randle, Wesley.L., Mantalaris, Athanassios., Buttery, Lee.D.K. & Polak, Julia.M. (2003)
14. Best poster award in the PhD student category at TESI (2003).
15. Julia Polak Research Trust award travel bursary (2003).

9. APPENDICES

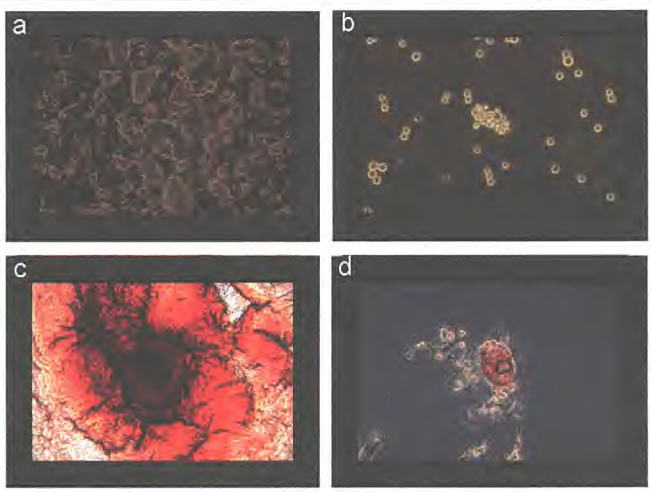
9.1. Serum-free experiments

Experiment 1	MAINTENANCE	EB FORMATION	DIFFERENTIATION
Media selection	Maintenance (serum)	Differentiation (serum)	Osteogenic (serum)
	Maintenance (serum)	Differentiation (serum)	Lennon (serum-free)
	Maintenance (serum)	Differentiation (serum-free*)	Osteogenic (serum)
	Maintenance (serum)	Differentiation (serum-free*)	Lennon (serum-free)
Cells	mESC	EBs	Disrupted EBs (dEBs) and Whole EBs (EBs)
Methods	EBs either left intact (EBs) or disrupted (dEB) and then plated into either serum control (Buttery) or serum-free (Lennon) media with or without gelatin-coated dishes. Control (osteogenic-serum) experiments adhered and proliferated and formed bone nodules as previously described. After 3 days in culture on both gelatin and tissue plastic, EBs in Lennon's media adhered and proliferated in a monolayer. On day 4 after the first medium change the edges of these monolayers began to detach and after 21 days all cells were non-viable (a small amount of serum was transferred to the cultures when isolating the EBs whereas dEBs were first washed with PBS). Various other surfaces were used such as tissue culture plastic, gelatin and fibronectin but similar results were obtained. * The use of knock out serum replacement (Invitrogen, UK) to culture EBs and then plated in maintenance (serum) or Lennon's (serum-free) media was unsuccessful.		
Conclusions	Small amounts of serum when transferring EBs to maintenance (serum-free) medium allowed adherence and proliferation until the first medium change. dEBs preferred method to differentiate ESCs as this would enable FACS sorting and CFU-assays.		
Experiment 2			

Lennon's (serum-free) medium was verified using low passage (<p5) mouse osteoblasts. Cells were initially cultured in differentiation medium (serum), washed and then passaged into differentiation medium (serum) or Lennon's media (serum-free) on fibronectin (25 μg/mL) coated tissue culture plastic. The morphological images identified similar results to that in the literature using rat MSCs (176) which indicated that Lennon's media (serum-free) was correctly formulated.			
Experiment 3	MAINTENANCE	EB FORMATION	DIFFERENTIATION
Media selection	Maintenance (serum)	Differentiation (serum)	Osteogenic (serum)
	Maintenance (serum)	Differentiation (serum)	Lennon's+LP A (serum-free)
Cells	mESCs	EBs	Disrupted EBs
Methods	The small amount of serum transfer from the first set of experiments indicated trace amounts of soluble (rather than attachment factors) factor(s) may allow cell adhesion, survival and / or proliferation when added to M3 medium. A literature search identified serum response factor (SRF), which is present in serum at small concentrations that fitted the criteria. Lysophosphatidic acid (LPA) activates the SRF cascade (221;324-326) and was added to M3 medium in a suitable range. The dEBs were then plated on either tissue culture plastic or gelatin coated tissue culture plastic. Controls adhered and proliferated in Buttery medium but very few cells (five or six) cells adhered (no proliferation) when LPA was added at 10μM to M3 medium.		
Conclusions	The day five EB stage after light trypsinisation to a single cell suspension appears to be a very sensitive stage when initiating mES cell differentiation.		
Experiment 4	MAINTENANCE	EB FORMATION	DIFFERENTIATION
Media selection	Maintenance (serum) then Maintenance (serum-free) for 1 passage.	Differentiation (serum) or Wiles' (serum-free without BMP4)	Not applicable
Cells	mESCs	EBs	Not applicable

Methods	Wiles *et al.* (89) indicated a protocol and protein free-chemically defined medium (P-CDM) to maintain and form EBs using mESCs. The protocols were followed exactly apart from maintaining the mESCs in maintenance medium (serum-containing). The quality and quantity of EB formation was poor. The EB formation procedure differed from previously established methods and this was thought to be the reason for a drop in EB formation. Wiles estimated that 450-600 EBs would form per dish but in reality, numbers were low and of poor quality. Wiles' protocol specified enumeration and specific cell densities (single cell suspension needed for enumeration) for EB seeding whereas previously established methods rely on "clumps" of cells to allow EB formation, which would not enable enumeration.		
Conclusions	The Wiles protocol for EB formation was estimated to be the cause of low quality and quantity EBs.		
Media selection	Maintenance (serum) then Maintenance (serum-free) for 1 passage.	Wiles medium (serum-free without BMP4)	Wiles medium with a range of additions.
Cells	mESCs	EBs	dEBs
Methods/Observations	EBs were formed with double the recommended cell numbers but yielded similar results to the previous experiment. They were disrupted and plated but no adherence or proliferation occurred.		
Conclusions	The protocol established by Wiles was obviously not working using this cell type and techniques. The previously established methods were considered to be the most fruitful way forward.		
Using Zimmermans (1) advice, the well established protocols were used for EB formation (Buttery *et al.* 2001) and also culture conditions under which ESCs would be able survive and adhere after disruption on day five were defined. After consultation with Dr Wiles and Prof Slack the osteogenic medium was formulated and the protocols that would allow survival, adherence and proliferation after disruption were established.			
Experiment 5	MAINTENANCE	EB FORMATION	DIFFERENTIATION
Media selection	Maintenance (serum) then Maintenance (serum-free) for 1 passage.	Wiles (serum-free without BMP4) or Differentiation (serum)	LWR1.1 medium See Appendix 9.2 and differentiation medium control (serum)
Cells	mESCs	EBs	dEBs

Methods	The EBs were trypsinised, and plated into LWR1.1 medium. 2.66 x 10^4 cells from dEBs were resuspended in 1mL of media and plated in duplicate in a 12 well plate (~5200 cells/cm^2) which is equivalent to the normal seeding density as previously used (30). The cells were also plated into 5 differently coated wells (coated for 30 minutes at h37/5): 100% FCS, 100% KOSR, 0.1% gelatin, 100µg/mL Poly-L-lysine (PLL) and tissue culture plastic control for 6 days (1 media change). Differentiation media (serum) grown EBs were also plated into Differentiation media (serum) on tissue culture plastic which resulted in extensive adherence, survival and proliferation. The most promising surface appeared to be FBS coated wells followed by just tissue culture plastic using LWR1.1 medium (See Appendix 9.3).		
Conclusions	LWR1.1 allowed adherence, survival and proliferation on tissue culture plastic.		
Experiment 6	**MAINTENANCE**	**EB FORMATION**	**DIFFERENTIATION**
Media selection	Maintenance (serum) then Maintenance (serum-free) for 1 passage.	Wiles (serum-free without BMP4) (serum)	LWR1.2 medium (See Appendix 9.4) and Differentiation medium (serum) control ± osteogenic supplements
Cells	mESCs	EBs	dEBs

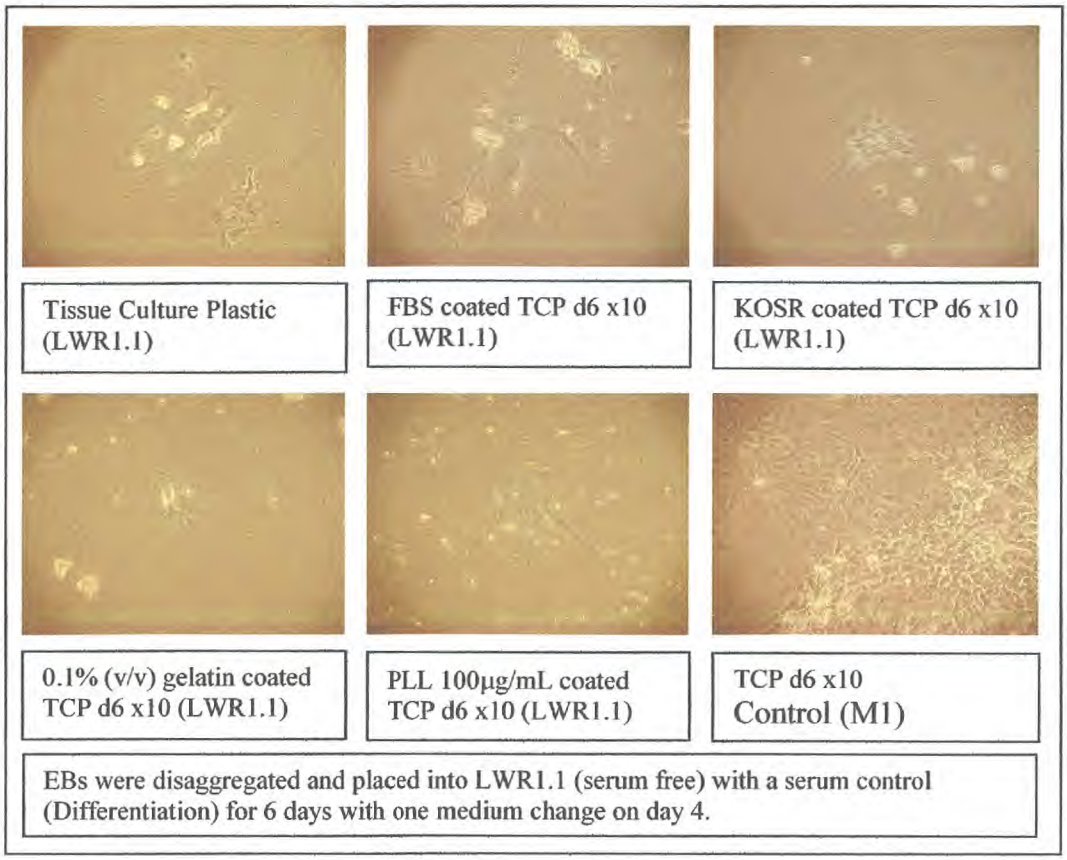
Methods	The protocols to maintain mESCs, form EBs and disrupt them for differentiation had now been established and were robust. Optimisation of the differentiation media (LWR1.1) was basic. Simply by removal of LPA and LIF and either the addition or removal of 15% (v/v) knock out serum replacement. EBs were formed by addition of BMP4 to Wiles medium at 2ng/mL to induce mesoderm formation. EBs were then disrupted and placed into various medium cocktails. Unfortunately some of the cultures were infected with fungal contamination (no antibiotics were used from EB stage onwards) probably due to the high amount of manipulation of each medium/culture. The EBs that did not have BMP4 supplementation were not contaminated and identified that only bone nodules would form when plated into Buttery (serum) medium. Some EBs that did have BMP4 supplementation were contaminated. However, the cultures that were not infected did indicate that the addition of the 15% knock out serum replacement supplement to LWR1.2 (serum-free) was essential to allow cell adherence, survival, proliferation and possible osteoblast differentiation.
Conclusions Ideal osteogenic serum-free media parameters/components (Appendix 9.5)	15% knock out serum replacement is essential for cell adherence, survival, proliferation and osteoblast differentiation in a completely serum-free medium (LWR1.2) when BMP4 was used to induce mesoderm formation in EBs (Figure 16).  **a.** undifferentiated mESCs, day 3 in Maintenance (serum-free) medium), x4. **b.** undifferentiated mES cells, day 0 of EB formation "clumps" of 15-20 cells, x20. **c.** Bone nodule stained with Alizarin red S. EBs were formed in Wiles (serum- free) medium, disrupted and plated for 21 days in Buttery (serum) suggesting arrested development during the EB stage. **d.** Bone nodule "like" tissue stained with Alizarin red S. EBs were formed in Wiles (serum-free) with BMP4, disrupted and plated for 21 days in osteogenic medium (serum) x10.

9.2. LWR1.1 serum-free medium

Component	Justification
50% DMEM-LG	(176)
33% MCDB-201 + phenol red	(176)
15% KOSR	WiCell 2000 hESC medium
2 mM L-Glutamine	ESC maintenance
1% NEAA	WiCell 2000 hESC medium
1% CDL	(89)
0.1% w/v PVA	(327)
450 µM 1-monothioglycerol	(89)
6 µg/mL Insulin	(89;176)
10 ng/mL PDGF- ββ	(176)
1 ng/mL bFGF	(176)
150 µg/mL apo-Transferrin	(89) and confirmation from Dr Michael Wiles
10 µM LPA	Personal experience
1 U/mL LIF	(89)

(328)

9.3. Serum-free medium surface coatings



9.4. LWR1.2 serum-free medium

Component	Justification
60% DMEM-LG	(176)
40% MCDB-201 + phenol red	(176)
±15% Knock out serum replacement	WiCell 2000 hESC medium
2 mM L-Glutamine	ESC maintenance
1% NEAA	WiCell 2000 hESC medium
1% CDL	(89)
0.1% w/v PVA	(327)
450 μM 1-monothioglycerol	(89)
6 μg/mL Insulin	(89;176)
10 ng/mL PDGF-ββ	(176)
1 ng/mL bFGF	(176)
150 μg/mL apo-Transferrin (328)	(89) and confirmation from Dr Michael Wiles

9.5. Desirable parameters for serum-free culture

1. High cell density to decrease stress and increase cell-cell contact
2. 10X less or no antibiotics.
3. High nutrient content basal medium favourable for bone formation.
4. Similar osmolarity / pH favoured by ES cells (by addition of 15% KOSR).
5. HEPES buffered media to ensure no pH extremes (low protein media increases stress upon cells).
6. Glutamine source.
7. Survival factors such as LIF/LPA optional (LIF may inhibit differentiation pathways by activation of STAT3 pathways).
8. Insulin at 6 μg/mL taken from Lennon (5 μg/mL) and Wiles (7 μg/mL).
9. 1-monothioglycerol as an antioxidant and reducing agent.
10. Amino acid source (328) and used in hESC culture.
11. Transferrin source 150 μg/mL (typographical error in (88) but confirmed by Michael Wiles in person) – iron chelating component.
12. pH = 7.2→7.4
13. Sterile filtered (0.2 μM).
14. Medium change every 2/3 days.

9.6. Statistics

The statistics below are based on small biological data sets. Normality tests identified that the data sets were not normally distributed but discussions with statisticians highlighted that the normality tests may not be accurate with such a small sample. Therefore, the ANOVA would be suitable to use in these circumstances as long as the major limitations of ANOVA are noted and that the significance should be high and not border line to be able to make a firm conclusion. Small p-values indicate that it is unlikely to have occurred purely by chance. P-values below 0.05 indicate statistically significant effects at the 5% significance level. Significant differences are highlighted in red. All statistics from MINITAB.

mESCs seeding densities and cell growth
(Appendix 9.6 - Page 258, Main body – Page 92).
Raw data (in triplicate on 1 occasion)

Cell Densityx10^5	Media	Passage	D3 Photo	TB count in three wells x 10^5			Mean	SD	SEM
				1	2	3			
1.5	M5	p22	X	2.2	3.4	6.6	4.1	2.3	1.1
2	M5	p22	X	3.4	6.4	2.4	4.1	2.1	0.8
2.5	M5	p22	X	11.6	3.8	5.6	7.0	4.1	1.4
3	M5	p22	X	11.6	9	11.4	10.7	1.4	0.4
3.5	M5	p22	X	7.2	16.6	9.8	11.2	4.9	3.2
1.5	M2	p22	X	2.6	2.8	2.4	2.6	0.2	0.1
2	M2	p22	X	3.6	6.2	2	3.9	2.1	0.8
2.5	M2	p22	X	3.8	6.8	2	4.2	2.4	0.8
3	M2	p22	X	2.8	6.8	11.8	7.1	4.5	1.3
3.5	M2	p22	X	13.2	10.2	6	9.8	3.6	2.4

(C1 = mean cell number after 3 days in culture, C2 = seeding density x 105/well (6WP) & C3 = Media)

C1	C2	C3
4.1	1.5	M5
4.1	2.0	M5
7.0	2.5	M5
10.7	3.0	M5
11.2	3.5	M5
2.6	1.5	M2
3.9	2.0	M2
4.2	2.5	M2
7.1	3.0	M2
9.8	3.5	M2

Two-way ANOVA: C1 versus C2, C3

```
Analysis of Variance for C1
Source        DF        SS        MS         F        P
C2             4    77.476    19.369     22.14    0.005
C3             1     9.025     9.025     10.31    0.033
Error          4     3.500     0.875
Total          9    90.001

                          Individual 95% CI
C2              Mean      -----+---------+---------+---------+------
1.5             3.35      (-----*-----)
2.0             4.00        (-----*-----)
2.5             5.60              (-----*-----)
3.0             8.90                        (-----*-----)
3.5            10.50                              (-----*-----)
                          -----+---------+---------+---------+------
                            3.00      6.00      9.00     12.00

                          Individual 95% CI
C3              Mean      ----+---------+---------+---------+-------
M5              7.42                    (---------*---------)
M2              5.52      (---------*---------)
                          ----+---------+---------+---------+-------
                           4.80      6.00      7.20      8.40
```

Media optimisation data

(Appendix 9.6 - Page 259, Main body – Page 99)

Raw data (in duplicate on two separate occasions).

EB formation	Differentiation		Experiment number				Bone nodule counts		
Media	Media		11	12	21	22	Total	Mean	SD
A	1	A1	4	2	1	0	7	2	2
	2	A2	0	0	18	26	44	11	13
	3	A3	1	5	0	0	6	2	2
	4	A4	33	31	76	74	214	54	25
B	1	B1	0	0	0	0	0	0	0
	2	B2	0	0	9	14	23	6	7
	3	B3	0	0	0	0	0	0	0
	4	B4	inf	inf	53	33	86	43	14
C	1	C1	0	0	0	0	0	0	0
	2	C2	15	8	26	18	67	17	7
	3	C3	0	0	0	0	0	0	0
	4	C4	80	41	75	27	223	56	26

(C6 = bone nodule counts, C7 = EB media & C8 = osteogenic media). The anomaly in B4 has been taken out on these statistical tests.

C6	C7	C8
2	A	1
11	A	2
2	A	3
54	A	4
0	B	1
6	B	2
0	B	3
43	B	4
0	C	1
17	C	2
0	C	3
56	C	4

Two-way ANOVA: C6 versus C7, C8

```
Analysis of Variance for C6
Source        DF        SS        MS        F        P
C7             2      82.7      41.3     3.05    0.122
C8             3    5150.9    1717.0   126.66    0.000
Error          6      81.3      13.6
Total         11    5314.9

                        Individual 95% CI
C7              Mean    -+---------+---------+---------+---------+
A               17.3                  (----------*----------)
B               12.3    (-----------*----------)
C               18.3                    (----------*----------)
                        -+---------+---------+---------+---------+
                       8.0       12.0      16.0      20.0      24.0

                        Individual 95% CI
C8              Mean    ----+---------+---------+---------+-------
1                0.7     (--*---)
2               11.3           (---*--)
3                0.7     (--*---)
4               51.0                                     (--*--)
                        ----+---------+---------+---------+-------
                          0.0       15.0      30.0      45.0
```

One-way ANOVA: C6 versus C7

```
Analysis of Variance for C6
Source     DF        SS        MS        F        P
C7          2        83        41     0.07    0.932
Error       9      5232       581
Total      11      5315

                                    Individual 95% CIs For Mean
                                    Based on Pooled StDev
Level       N      Mean     StDev  --------+---------+---------+--------
A           4     17.25     24.86     (-------------*------------)
B           4     12.25     20.69  (-------------*-------------)
C           4     18.25     26.41     (-------------*-------------)
                                    --------+---------+---------+--------
Pooled StDev =    24.11               0        20        40
```

One-way ANOVA: C6 versus C8

```
Analysis of Variance for C6
Source     DF        SS        MS        F        P
C8          3    5150.9    1717.0    83.75    0.000
Error       8     164.0      20.5
Total      11    5314.9

                                    Individual 95% CIs For Mean
                                    Based on Pooled StDev
Level       N      Mean     StDev  ---+---------+---------+---------+---
1           3     0.667     1.155  (--*--)
2           3    11.333     5.508        (--*--)
3           3     0.667     1.155  (--*--)
4           3    51.000     7.000                          (---*--)
                                    ---+---------+---------+---------+---
Pooled StDev =     4.528            0        20        40        60
```

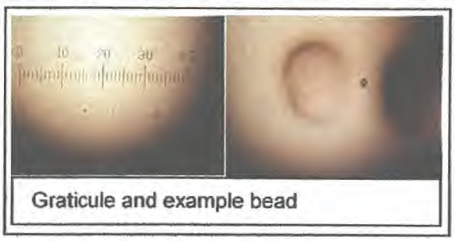
1.1% alginate bead measurements before and after culture (No cells – varying needle size)
(Appendix 9.6 - Page 261, Main body – Page 123)
Raw data

	Before	Horz. Distance	Vert. Distance	H/V	After	Horz. Distance	Vert. Distance	H/V	Change after 7 days in DMEM		
Needle Size	Sample	µm	µm			µm	µm		µm		
18G	1	3072	3199	0.96		3504	3466	1.01			
	2	2893	3374	0.86		3536	3223	1.10			
	3	3192	3216	0.99		3708	3244	1.14			
	4	3156	3160	1.00		3286	3301	1.00			
	5	3206	3153	1.02		3311	3392	0.98			
			Mean H/V	0.97			Mean H/V	1.04			
	Mean Diam	3104	3220	3162	Mean Diam	3469	3325	3397	235		
21G	1	2875	2721	1.06		2875	2924	0.98			
	2	2756	2875	0.96		2812	3076	0.91			
	3	2858	2735	1.04		3090	2840	1.09			
	4	2822	2710	1.04		2844	2858	1.00			
	5	2886	2851	1.01		2851	3005	0.95			
			Mean H/V	1.02			Mean H/V	0.99			
	Mean Diam	2839	2778	2809	Mean Diam	2894	2941	2917	109		
23G	1	2654	2671	0.99		2594	2323	1.12			
	2	2678	2439	1.10		2334	2503	0.93			
	3	2573	2573	1.00		2633	2432	1.08			
	4	2453	2633	0.93		2418	2467	0.98			
	5	2538	2854	0.89		2443	2510	0.97			
			Mean H/V	0.98			Mean H/V	1.02			
	Mean Diam	2579	2634	2607	Mean Diam	2484	2447	2466	-141		
25G	1	2411	2478	0.97		2467	2467	1.00			
	2	2351	2260	1.04		2492	2559	0.97			
	3	2309	2559	0.90		2394	2503	0.96			
	4	2299	2531	0.91		2302	2320	0.99			
	5	2467	2359	1.05		2401	2510	0.96			
			Mean H/V	0.97			Mean H/V	0.98			
	Mean Diam	2368	2437	2402	Mean Diam	2411	2472	2441	39		

	AlgD0			AlgD4			AlgGd0			AlgGd4		
	Horz. Distance	Vert. Distance	H/V	Horz. Distance	Vert. Distance	H/V	Horz. Distance	Vert. Distance	H/V	Horz. Distance	Vert. Distance	H/V
	µm	µm		µm	µm		µm	µm		µm	µm	
1000	2430	2360	1.03	2519	2283	1.10	2250	2310	0.97	2286	2604	0.88
	2259	2522	0.90	2532	2345	1.08	2224	2338	0.95	2330	2473	0.94
	2563	2430	1.05	2417	2319	1.04	2360	2326	1.01	2440	2153	1.13
	2329	2550	0.91	2435	2327	1.05	2262	2319	0.98	2440	2394	1.02
	2506	2452	1.02	2260	2430	0.93	2348	2237	1.05	2276	2491	0.91
	2496	2541	0.98	2522	2237	1.13	2275	2345	0.97	2324	2466	0.94
	2462	2481	0.99	2381	2445	0.97	2379	2250	1.06	2409	2389	1.01
	2490	2569	0.97	2468	2335	1.06	2338	2329	1.00	2422	2381	1.02
	2683	2278	1.18	2227	2432	0.92	2335	2126	1.10	2409	2458	0.98
	2481	2591	0.96	2476	2471	1.00	2250	2452	0.92	2330	2404	0.97
Mean	2470	2477		2424	2362		2302	2303		2366	2421	
100	2534	2392	1.06	2468	2237	1.10	2177	2383	0.91	2245	2476	0.91
	2383	2462	0.97	2322	2486	0.93	2316	2288	1.01	2589	2253	1.15
	2452	2493	0.98	2473	2312	1.07	2338	2389	0.98	2317	2337	0.99
	2506	2496	1.00	2401	2501	0.96	2196	2417	0.91	2489	2283	1.09
	2417	2392	1.01	2409	2432	0.99	2284	2329	0.98	2337	2401	0.97
	2386	2398	0.99	2381	2422	0.98	2253	2218	1.02	2386	2530	0.94
	2503	2411	1.04	2409	2381	1.01	2129	2164	0.98	2355	2442	0.96
	2503	2452	1.02	2519	2381	1.06	2493	2228	1.12	2430	2394	1.02
	2487	2427	1.02	2427	2299	1.06	2455	2275	1.08	2430	2296	1.06
	2541	2389	1.06	2568	2353	1.09	2417	2240	1.08	2201	2560	0.86
Mean	2471	2431		2438	2380		2306	2293		2378	2397	
10	2383	2462	0.97	2281	2476	0.92	2332	2243	1.04	2424	2409	1.01
	2433	2531	0.96	2281	2409	0.95	2338	2250	1.04	2278	2517	0.91
	2462	2465	1.00	2199	2532	0.87	2319	2237	1.04	2273	2560	0.89
	2515	2379	1.06	2450	2373	1.03	2427	2218	1.09	2430	2394	1.02
	2345	2515	0.93	2265	2555	0.89	2152	2427	0.89	2489	2332	1.07
	2322	2433	0.95	2304	2340	0.98	2288	2275	1.01	2360	2332	1.01
	2452	2354	1.04	2499	2353	1.06	2354	2234	1.05	2235	2437	0.92
	2525	2383	1.06	2263	2560	0.88	2348	2177	1.08	2378	2486	0.96
	2433	2446	0.99	2301	2435	0.95	2335	2319	1.01	2373	2545	0.93
	2645	2373	1.11	2214	2514	0.88	2291	2367	0.97	2324	2553	0.91
Mean	2452	2434		2306	2455		2318	2275		2356	2457	

Cells/bead	AlgD0		AlgD4		AlgGd0		AlgGd4	
	Mean Diam	SD	Mean Diam	SD	Mean Diam	SD	Mean Diam	SD
1000	2474	106	2393	96	2303	70	2394	95
100	2451	54	2438	81	2299	102	2388	107
10	2443	95	2380	117	2296	74	2406	97

Cells/bead	AlgD0		AlgD4		AlgGd0		AlgGd4	
	Mean H/V	SD	Mean H/V	SD	Mean H/V	SD	Mean H/V	SD
1000	1.00	0.08	1.03	0.07	1.00	0.05	0.98	0.07
100	1.02	0.03	1.03	0.06	1.01	0.07	1.00	0.09
10	1.01	0.06	0.94	0.07	1.02	0.06	0.96	0.06



Graticule and example bead

1.1% alginate bead sizes before and after culture (With cells – 25G needle)

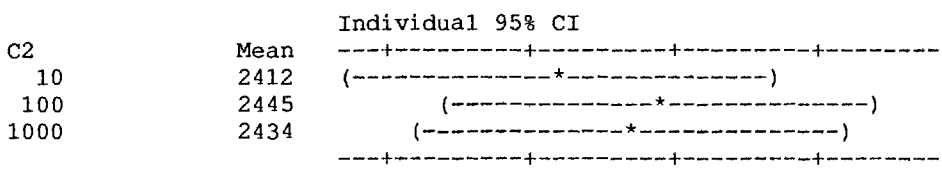
(C1 = Mean bead diameter, C2 = number of cells encapsulated & C3 = Before (B) or After (A) culture).

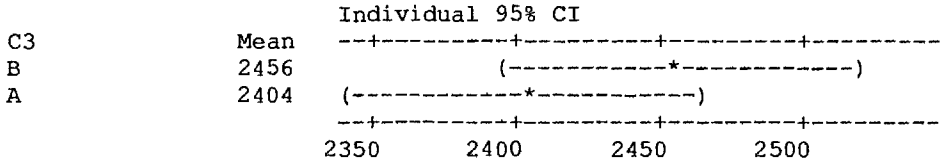
C1	C2	C3
2474	1000	B
2451	100	B
2443	10	B
2393	1000	A
2438	100	A
2380	10	A

Two-way ANOVA: C1 versus C2, C3

Analysis of Variance for C1

Source	DF	SS	MS	F	P
C2	2	1129	565	0.91	0.524
C3	1	4108	4108	6.62	0.124
Error	2	1241	621		
Total	5	6479			





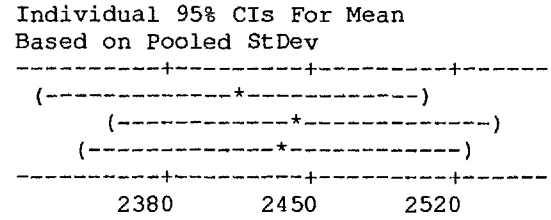
One-way ANOVA: C1 versus C2

Analysis of Variance for C1

Source	DF	SS	MS	F	P
C2	2	1129	565	0.32	0.750
Error	3	5350	1783		
Total	5	6479			

Level	N	Mean	StDev
10	2	2411.5	44.5
100	2	2444.5	9.2
1000	2	2433.5	57.3

Pooled StDev = 42.2



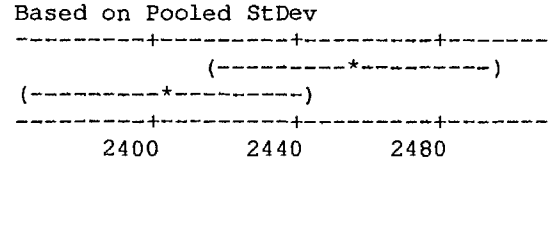
One-way ANOVA: C1 versus C3

Analysis of Variance for C1

Source	DF	SS	MS	F	P
C3	1	4108	4108	6.93	0.058
Error	4	2371	593		
Total	5	6479			

Level	N	Mean	StDev
B	3	2456.0	16.1
A	3	2403.7	30.4

Pooled StDev = 24.3



1.1% alginate + 0.1% gelatin bead sizes before and after culture (With cells – 25G needle)
(Appendix 9.6 - Page 263, Main body – Page 124)
(C1 = Mean bead diameter, C2 = number of cells encapsulated & C3 = Before (B) or After (A) culture).

C5	C6	C7
2303	1000	B
2299	100	B
2296	10	B
2394	1000	A
2388	100	A
2406	10	A

Two-way ANOVA: C5 versus C6, C7

```
Analysis of Variance for C5
Source        DF        SS        MS        F        P
C6             2      58.3      29.2     0.43    0.697
C7             1  14016.7   14016.7   208.68    0.005
Error          2     134.3      67.2
Total          5  14209.3

                        Individual 95% CI
C6              Mean    -----+---------+---------+---------+------
  10          2351.0          (---------------*---------------)
 100          2343.5     (---------------*---------------)
1000          2348.5        (---------------*---------------)
                        -----+---------+---------+---------+------
                        2325.0    2340.0    2355.0    2370.0

                        Individual 95% CI
C7              Mean    ---------+---------+---------+---------+--
B             2299.3    (-----*-----)
A             2396.0                                (-----*----)
                        ---------+---------+---------+---------+--
                            2310.0    2345.0    2380.0    2415.0
```

One-way ANOVA: C5 versus C6

```
Analysis of Variance for C5
Source     DF        SS        MS        F        P
C6          2        58        29     0.01    0.994
Error       3     14151      4717
Total       5     14209

                                  Individual 95% CIs For Mean
                                  Based on Pooled StDev
Level       N      Mean     StDev  --+---------+---------+---------+----
  10        2    2351.0      77.8    (-------------*-------------)
 100        2    2343.5      62.9   (-------------*-------------)
1000        2    2348.5      64.3   (-------------*-------------)
                                  --+---------+---------+---------+----
Pooled StDev =     68.7          2200      2300      2400      2500
```

One-way ANOVA: C5 versus C7

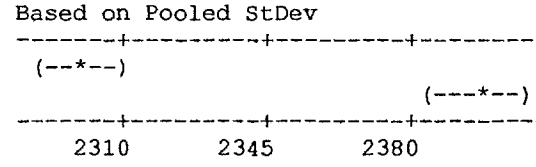
Analysis of Variance for C5

Source	DF	SS	MS	F	P
C7	1	14016.7	14016.7	291.00	0.000
Error	4	192.7	48.2		
Total	5	14209.3			

Level	N	Mean	StDev
B	3	2299.33	3.51
A	3	2396.00	9.17

Pooled StDev = 6.94

Individual 95% CIs For Mean
Based on Pooled StDev



3D HARV biochemical analysis (Days 0-8 performed by Yu-shik Hwang.)

ARSQ

(Appendix 9.6 - Page 265, Main body – Page 178)

Raw data (In duplicate on 3 separate occasions).

Reading	Day
0.0012000	0
0.0009000	0
0.0014000	0
0.0012000	0
0.0014000	0
0.0010000	0
0.0008000	3
0.0006000	3
0.0012000	3
0.0018000	3
0.0012000	3
0.0010000	3
0.0013000	8
0.0014000	8
0.0015000	8
0.0019000	8
0.0016000	8
0.0017000	8
0.0022641	15
0.0025956	15
0.0010618	15
0.0019379	15
0.0027191	15
0.0018314	15
0.0021465	22
0.0018259	22
0.0124917	22
0.0108078	22
0.0033857	22
0.0007487	22
0.0062823	29
0.0042367	29
0.0193651	29
0.0226458	29
0.0047970	29
0.0026659	29

Blank	1	2	3	Mean	SD
3D1	0.159	0.164	0.159	0.160667	0.002887
3D2	0.147	0.148	0.147	0.147333	0.000577
3D3	0.15	0.151	0.15	0.150333	0.000577
			Mean	0.152778	0.006241

3D1 Day	1	2	Mean	SD
15	0.335	0.319	0.327	0.011314
22	0.356	0.325	0.3405	0.02192
29	0.858	0.453	0.6555	0.286378

3D2 Day	1	2	Mean	SD
15	0.279	0.345	0.312	0.046669
22	1.409	1.066	1.2375	0.242538
29	1.774	1.959	1.8665	0.130815

3D3 Day	1	2	Mean	SD
15	0.358	0.617	0.4875	0.183141
22	0.515	0.605	0.56	0.06364
29	0.514	0.842	0.678	0.231931

Adjusted per bead

3D1					Bead Number	
Day	1	2	Mean	SD	1	2
15	0.002264	0.002596	0.00243	0.000234	77	61
22	0.002147	0.001826	0.001986	0.000227	91	90
29	0.006282	0.004237	0.005259	0.001446	111	69

3D2					Bead Number	
Day	1	2	Mean	SD	1	2
15	0.001062	0.001938	0.0015	0.000619	124	102
22	0.012492	0.010808	0.01165	0.001191	101	85
29	0.019365	0.022646	0.021005	0.00232	84	80

3D3					Bead Number	
Day	1	2	Mean	SD	1	2
15	0.002719	0.001831	0.002275	0.000628	124	100
22	0.003386	0.000749	0.002067	0.001865	121	85
29	0.004797	0.002666	0.003731	0.001507	110	87

ARSQ days 0 and 15

One-way ANOVA: C22 versus C23

```
Source  DF         SS         MS      F      P
C23      1  0.0000023  0.0000023  11.55  0.007
Error   10  0.0000020  0.0000002
Total   11  0.0000044

S = 0.0004510   R-Sq = 53.60%   R-Sq(adj) = 48.95%


                                  Individual 95% CIs For Mean Based on
                                  Pooled StDev
Level  N       Mean      StDev  -----+---------+---------+---------+----
 0     6  0.0011833  0.0002041  (--------*-------)
15     6  0.0020683  0.0006043                   (-------*--------)
                                  -----+---------+---------+---------+----
                                     0.00100   0.00150   0.00200   0.00250

Pooled StDev = 0.0004510
```

ARSQ days 15 and 29

One-way ANOVA: C25 versus C26

```
Source  DF         SS         MS     F      P
C26      1  0.0001887  0.0001887  5.00  0.049
Error   10  0.0003773  0.0000377
Total   11  0.0005660

S = 0.006143   R-Sq = 33.33%   R-Sq(adj) = 26.67%


                                  Individual 95% CIs For Mean Based on
                                  Pooled StDev
Level  N       Mean      StDev  -------+---------+---------+---------+--
15     6  0.002068  0.000604  (----------*----------)
29     6  0.009999  0.008666                (----------*----------)
                                  -------+---------+---------+---------+--
                                       0.0000    0.0050    0.0100    0.0150

Pooled StDev = 0.006143
```

MTS (Appendix 9.6 - Page 267, Main body – Page 178)

Raw data (In duplicate on 3 separate occasions)

32X(1.6)							Duplicate 1				Duplicate 2										Total number of cells in 3 beads			Cells per bead
Time	Standard1	Standard2	Standard3	Standard4	Mean	SD	Test1	Test2	Test3	Test4	Mean	SD	Test1	Test2	Test3	Test4	Mean	TMean	SD	Adjusted				
0	0.372	0.333	0.336	0.336	0.34778	0.0210772	0.431	0.465	0.456	0.438	0.4597	0.0247	0.497	0.472	0.424	0.411	0.418	0.4054	0.02436	0.044	13433			4478
3	0.321	0.335	0.479	0.468	0.46073	0.0643183	0.585	0.59	0.607	0.548	0.583	0.0267	0.685	0.627	0.645	0.628	0.6325	0.6115	0.02681	0.211	37597			12532
6	0.3	0.287	0.288	0.3	0.2963	0.0067124	0.297	0.298	0.302	0.288	0.2967	0.0064	0.305	0.298	0.295	0.288	0.2965	0.2955	0.00645	0.283	58598			19533
15	0.413	0.387	0.397	0.405	0.4003	0.0070564	0.409	0.403	0.405	0.384	0.4003	0.0113	0.407	0.385	0.407	0.403	0.4005	0.4005	0.00707	0.353	83030			27677
22	0.348	0.365	0.397	0.374	0.3681	0.0108264	0.359	0.348	0.392	0.377	0.3693	0.0108	0.359	0.348	0.392	0.377	0.3693	0.3693	0.01083	0.068	9899			3233
29	0.375	0.365	0.397	0.402	0.4148	0.0157136	0.723	0.666	0.677	0.667	0.6833	0.0289	0.707	0.667	0.677	0.667	0.6795	0.6795	0.02887	0.165	26770			8923
32X(1.6)							Duplicate 1				Duplicate 2										Total number of cells in 3 beads			Cells per bead
Time	Standard1	Standard2	Standard3	Standard4	Mean	SD	Test1	Test2	Test3	Test4	Mean	SD	Test1	Test2	Test3	Test4	Mean	TMean	SD	Adjusted				
0	0.403	0.404	0.403	0.418	0.4085	0.0063509	0.503	0.508	0.509	0.509	0.50725	0.576	0.568	0.568	0.609	0.633	0.6033	0.6038	0.01685	0.200	34838			11613
3	0.354	0.348	0.348	0.36	0.3625	0.0057446	0.601	0.57	0.564	0.539	0.5685	0.586	0.636	0.518	0.502	0.502	0.5025	0.5465	0.03177	0.197	34096			11365
6	0.307	0.325	0.325	0.321	0.32	0.0000195	1.363	1.23	1.332	1.357	1.328	1.228	1.122	1.067	1.041	1.041	1.11975	1.223375	0.13173	0.823	424977			141992
15	0.83	0.348	0.348	0.511	0.5295	0.017253	0.775	0.7	0.729	0.684	0.717	0.777	0.735	0.735	0.784	0.784	0.75775	0.737375	0.03586	0.412	73549			12930
22	0.348	0.365	0.365	0.351	0.358	0.007874	0.744	0.734	0.744	0.785	0.75175	0.723	0.633	0.678	0.739	0.823	0.69275	0.72225	0.03586	0.359	82548			28615
29	0.365	0.365	0.373	0.388	0.3818	0.0101525	1.015	1.088	1.107	1.026	1.06075	0.872	1.148	1.148	1.148	0.823	0.97425	1.0173	0.10619	0.550	239935			79982
32X(1.6)							Duplicate 1				Duplicate 2										Total number of cells in 3 beads			Cells per bead
Time	Standard1	Standard2	Standard3	Standard4	Mean	SD	Test1	Test2	Test3	Test4	Mean	SD	Test1	Test2	Test3	Test4	Mean	TMean	SD	Adjusted				
0	0.403	0.404	0.403	0.418	0.4085	0.0063509	0.503	0.508	0.509	0.509	0.50725	0.576	0.568	0.568	0.609	0.633	0.6033	0.6038	0.01685	0.200	34838			11613
3	0.354	0.348	0.348	0.36	0.3625	0.0057446	0.601	0.57	0.564	0.539	0.5685	0.586	0.636	0.518	0.502	0.502	0.5025	0.5465	0.03177	0.197	34096			11365
6	0.307	0.325	0.325	0.321	0.32	0.0000195	1.363	1.23	1.332	1.357	1.328	1.228	1.122	1.067	1.041	1.041	1.11975	1.223375	0.13173	0.823	424977			141992
15	0.83	0.348	0.348	0.511	0.5295	0.017253	0.775	0.7	0.729	0.684	0.717	0.777	0.735	0.735	0.784	0.784	0.75775	0.737375	0.03586	0.412	73549			12930
22	0.348	0.365	0.365	0.351	0.358	0.007874	0.744	0.734	0.744	0.785	0.75175	0.723	0.633	0.678	0.739	0.823	0.69275	0.72225	0.03586	0.359	82548			28615
29	0.365	0.365	0.373	0.388	0.3818	0.0101525	1.015	1.088	1.107	1.026	1.06075	0.872	1.148	1.148	1.148	0.823	0.97425	1.0173	0.10619	0.550	239935			79982
32X(1.6)							Duplicate 1				Duplicate 2										Total number of cells in 3 beads			Cells per bead
Time	Standard1	Standard2	Standard3	Standard4	Mean	SD	Test1	Test2	Test3	Test4	Mean	SD	Test1	Test2	Test3	Test4	Mean	TMean	SD	Adjusted				
0	0.403	0.404	0.403	0.418	0.4085	0.0063509	0.592	0.585	0.582	0.582	0.58375	0.587	0.564	0.571	0.571	0.577	0.5777	0.5813	0.01041	0.178	28868			9622
3	0.354	0.348	0.348	0.36	0.3625	0.0057446	0.51	0.508	0.541	0.539	0.5245	0.454	0.443	0.4	0.403	0.394	0.4135	0.6725	0.35581	0.287	59978			19992
6	0.307	0.325	0.325	0.321	0.32	0.0000195	0.744	0.729	0.729	0.729	0.7328	0.497	0.534	0.444	0.463	0.463	0.4845	0.615375	0.17439	0.090	12541			4180
15	0.83	0.348	0.348	0.511	0.5295	0.017253	0.744	0.729	0.729	0.729	0.7328	0.673	0.751	0.711	0.581	0.581	0.8515	0.88225	0.04124	0.328	73307			24462
22	0.348	0.365	0.365	0.351	0.358	0.007874	0.89	0.844	0.883	0.673	0.8233	0.751	1.061	1.007	0.900	0.900	0.96128	0.958	0.08133	0.580	186571			86224
29	0.365	0.365	0.373	0.388	0.3818	0.0101525	1.049	8.88	0.891	0.989	0.95478	0.851												

MTS days 3 and 8

One-way ANOVA: C28 versus C29

```
Source  DF      SS      MS      F      P
C29      1  1.4180  1.4180  25.02  0.000
Error   46  2.6070  0.0567
Total   47  4.0250

S = 0.2381   R-Sq = 35.23%   R-Sq(adj) = 33.82%


                              Individual 95% CIs For Mean Based on
                              Pooled StDev
Level   N    Mean   StDev  -----+---------+---------+---------+----
3      24  0.1755  0.0593  (------*-----)
8      24  0.5192  0.3314                          (------*-----)
                           -----+---------+---------+---------+----
                              0.15      0.30      0.45      0.60

Pooled StDev = 0.2381
```

MTS days 8 and 15

One-way ANOVA: C31 versus C32

```
Source  DF      SS      MS      F      P
C32      1  1.0414  1.0414  16.47  0.000
Error   46  2.9093  0.0632
Total   47  3.9506

S = 0.2515   R-Sq = 26.36%   R-Sq(adj) = 24.76%


                              Individual 95% CIs For Mean Based on
                              Pooled StDev
Level   N    Mean   StDev  --+---------+---------+---------+-------
 8     24  0.5192  0.3314                        (------*------)
15     24  0.2246  0.1291  (------*------)
                           --+---------+---------+---------+-------
                           0.15      0.30      0.45      0.60

Pooled StDev = 0.2515
```

MTS days 22 and 29

One-way ANOVA: C34 versus C35

```
Source  DF      SS      MS     F      P
C35      1  0.5177  0.5177  9.38  0.004
Error   46  2.5390  0.0552
Total   47  3.0567

S = 0.2349   R-Sq = 16.94%   R-Sq(adj) = 15.13%


                              Individual 95% CIs For Mean Based on
                              Pooled StDev
Level   N    Mean   StDev  -------+---------+---------+---------+--
22     24  0.2514  0.1515  (-------*-------)
29     24  0.4591  0.2957                  (-------*-------)
                           -------+---------+---------+---------+--
                                0.24      0.36      0.48      0.60

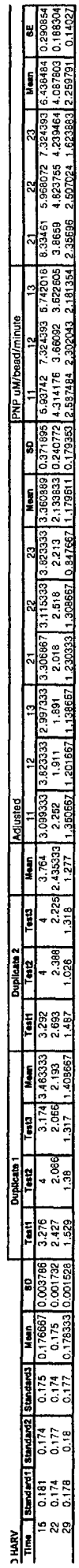
Pooled StDev = 0.2349
```

ALPase

Appendix 9.6 - Page 269, Main body – Page 178)

Raw data (In duplicate on 3 separate occasions)

Day					
0	**3**	**8**	**15**	**22**	**29**
2.082	**2.077**	**0.517**	**5.937**	**4.314**	**2.587**
1.966	**3.402**	**0.550**	**7.324**	**3.661**	**2.302**
2.052	**3.494**	**0.607**	**5.742**	**3.623**	**2.181**
2.086	**3.038**	**0.538**	**6.335**	**3.866**	**2.357**
2.207	**3.655**	**0.557**	**5.968**	**4.824**	**2.507**
2.307	**3.008**	**0.676**	**7.324**	**4.239**	**1.624**



HARV																															
						Duplicate 1				Duplicate 2				Adjusted						PNP uM/bead/minute											
Time	Standard1	Standard2	Standard3	Mean	SD	Test1	Test2	Test3	Mean	Test1	Test2	Test3	Mean	11	12	13	21	22	23	Mean	SD	11	12	13	21	22	23	Mean	SE
15	0.181	0.174	0.175	0.176667	0.003786	3.276	4	3.174	3.483333	3.292	4	4	3.764	3.099333	3.823333	2.997333	3.306667	3.115333	3.823333	3.360889	0.371695	5.90742	7.324393	5.742016	8.33461	5.968072	7.324393	6.436484	0.290854
22	0.174	0.177	0.174	0.175	0.001732	2.427	2.086	2.056	2.193	2.693	2.388	2.226	2.435333	2.252	1.911	1.891	2.016	2.518	2.213	2.133833	0.240772	4.314176	3.66092	3.822605	3.8659	4.823755	4.233464	4.087803	0.186304
29	0.178	0.18	0.177	0.178333	0.001528	1.529	1.38	1.317	1.409667	1.487	1.028	1.318	1.277	1.360667	1.201667	1.138667	1.230333	1.308667	0.847667	1.179611	0.179353	2.597484	2.302043	2.181354	2.35696	2.507024	1.623883	2.259791	0.14027

ALPase days 0 and 15

One-way ANOVA: C37 versus C38

```
Source  DF      SS      MS       F      P
C38      1  56.034  56.034  214.58  0.000
Error   10   2.611   0.261
Total   11  58.646

S = 0.5110   R-Sq = 95.55%   R-Sq(adj) = 95.10%

                                Individual 95% CIs For Mean Based on
                                Pooled StDev
Level  N    Mean   StDev  ---------+---------+---------+---------+
 0     6  2.1167  0.1212  (--*--)
15     6  6.4385  0.7124                              (--*--)
                          ---------+---------+---------+---------+
                                 3.0       4.5       6.0       7.5

Pooled StDev = 0.5110
```

ALPase days 15 and 29

One-way ANOVA: C40 versus C41

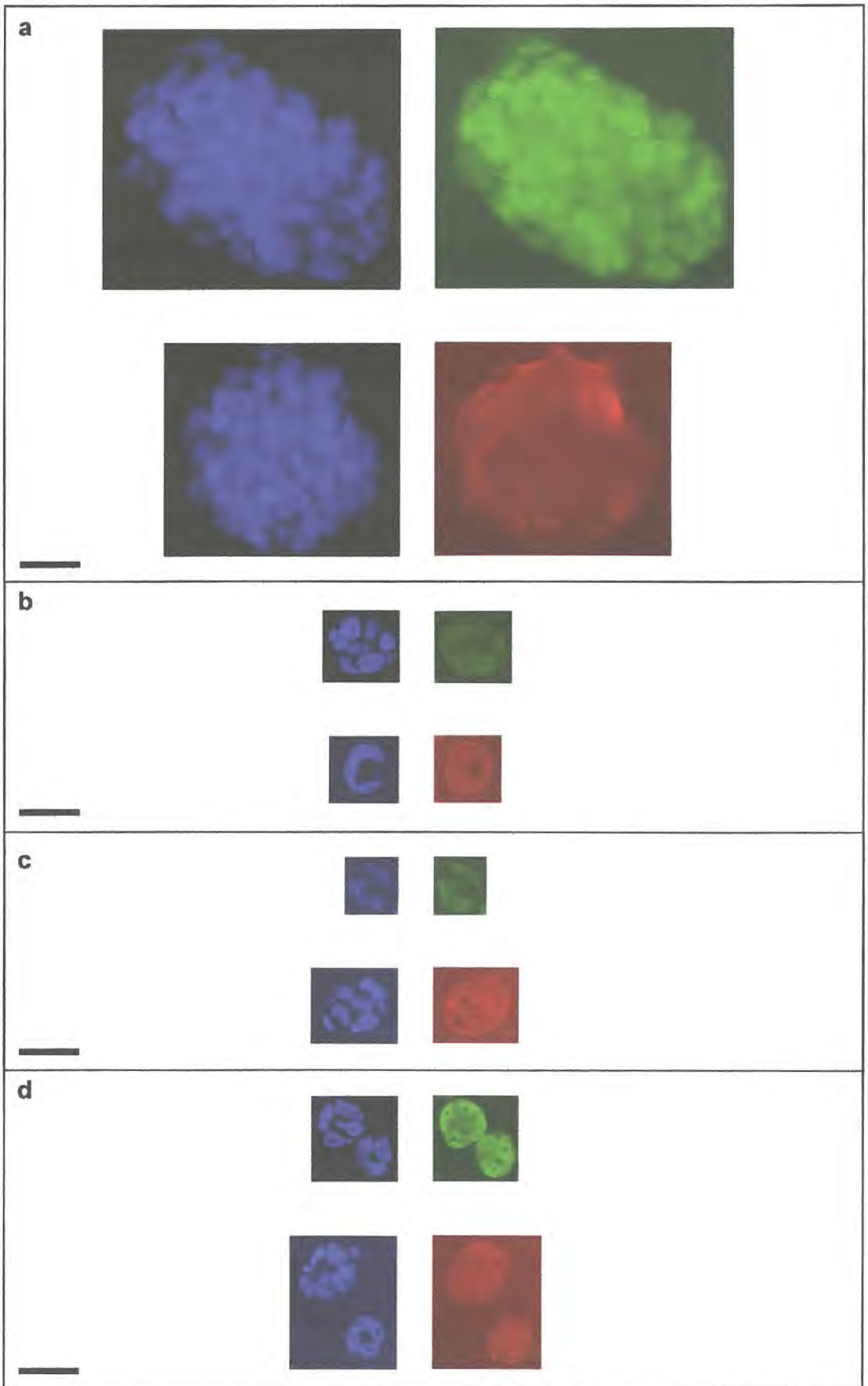
```
Source  DF      SS      MS       F      P
C41      1  52.384  52.384  167.46  0.000
Error   10   3.128   0.313
Total   11  55.513

S = 0.5593   R-Sq = 94.36%   R-Sq(adj) = 93.80%

                                Individual 95% CIs For Mean Based on
                                Pooled StDev
Level  N    Mean   StDev  --------+---------+---------+---------+-
15     6  6.4385  0.7124                              (--*--)
29     6  2.2598  0.3436  (--*--)
                          --------+---------+---------+---------+-
                                3.0       4.5       6.0       7.5

Pooled StDev = 0.5593
```

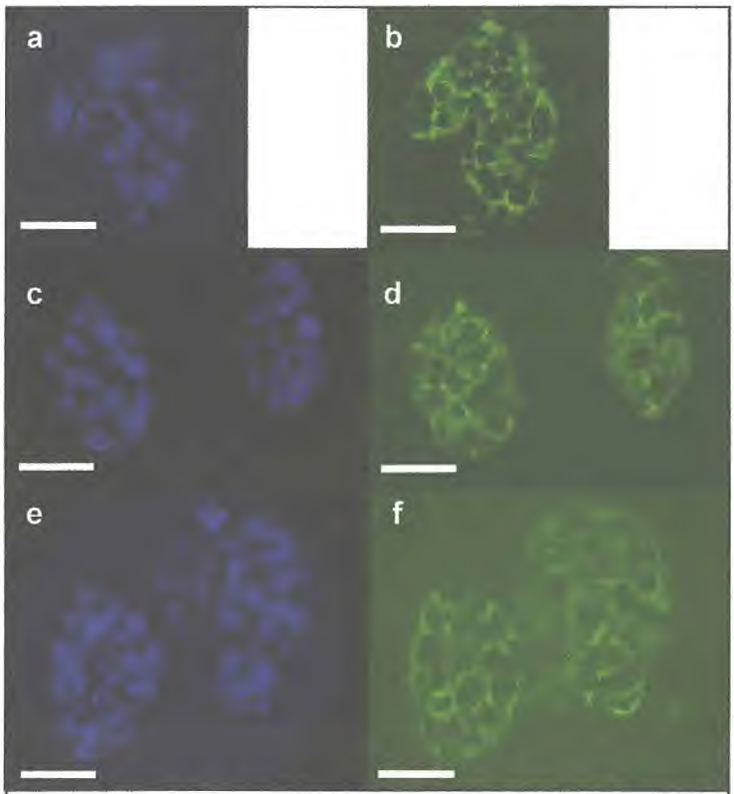
9.7. Day 3, bioreactor immunostaining



Day 3 pluripotency immunostaining. a. 2D static. b. 3D static. c. 3D stirred. d. 3D HARV. DAPI = blue, Oct-4 = FITC and CD9 = Rhodamine.1 = DAPI, 2 = Oct4, 3 = DAPI & 4 = CD9. Scale bar = 25 µm.

1	2
3	4

9.8. Day 8, bioreactor immunostaining



Day 8 mesoderm staining. a. 3D static DAPI. b. 3D static Flk-1. c. 3D stirred DAPI. d. 3D stirred Flk-1. e. 3D HARV DAPI. F. 3D HARV Flk-1. Scale bar = 25 μm.

9.9. Nova BioProfile 200

Raw data (in duplicate on one separate occasion)

Sample ID	Day	Measured Test Sample	pH @ 37oC	PO2 @ 37oC mmHg	Na+ mmol/L	K+ mmol/L	Ca++ mmol/L	GLU mmol/L	Lac mmol/L	Gluc mmol/L	NH4+ mmol/L	AirSat %	Osm mOsm/kg
25	0	H2	7.536	256.5	139.9	5.3	1.39	0.21	0	29.7	0.6	175.8	415
26	0	H3	7.545	256.3	148.9	5.5	1.46	0.24	2.5	31.1	0.6	178.6	442
27	1	H2	7.703	240.7	151.7	5.5	2.54	0.35	6.1	28.9	1	183.8	447
28	1	H3	7.627	226.9	153.9	5.8	2.3	0.26	5.9	25.6	1	154.4	450
29	1	P	7.318	301.5	151.5	5.5	2.67	0.23	4.5	23.9	0.8	137.1	442
30	2	H2	7.649	217.3	152.1	5.6	1.55	0.29	8.9	25.7	1.4	147.9	450
31	2	H3	7.653	206.6	152.2	5.9	1.57	0.31	10.4	27.1	1.6	149.8	472
32	2	P	7.543	193.9	154.1	5.6	1.22	0.36	4.4	30	1.4	139.9	454
33	3	H2	7.644	225.2	142.5	5.3	1.72	0.21	6.5	22.7	1.3	153.3	428
34	3	H3	7.629	228.1	152	5.9	1.15	0.2	7.9	23.6	1.5	148.9	447
35	3	P	7.403	169.6	154.5	5.8	1.2	0.22	4.3	27.5	1.5	135.9	453
36	4	H2	7.375	211.6	140.7	5.7	1.1	0.7	8.2	3.4	1.2	144	406
37	4	H3	7.414	208.6	141.2	5.8	1.1	0.7	7.3	0	1.1	141.9	402
38	4	P	7.405	211.9	150.1	6.1	1.32	0.7	2.8	1.8	0.7	144.2	416
39	5	H2	7.413	215.4	145.4	5.9	1	0.77	11.7	0	1.6	146.6	415
40	5	H3	7.393	226.1	144.6	5.8	0.98	0.78	12.9	0	1.6	153.9	415
41	5	P	7.453	240.4	141.6	5.8	1.13	0.72	3	0	1.1	163.6	399
42	6	H2	7.338	205.2	145	6	0.95	0.81	14.8	0	1.9	139.6	426
43	6	H3	7.322	178.22	146.4	5.9	0.96	0.82	16.1	0	1.9	121.5	426
44	6	P	7.491	260.5	140.7	5.8	1.08	0.74	3.2	0	1.3	157.8	402
45	7	H2	7.259	181.8	139.9	5.6	1.11	0.71	13.3	0	1.1	130.5	405
46	7	H3	7.345	199	142.6	5.7	1.1	0.74	13.3	0	1.3	135.4	411
47	7	P	7.42	224.3	168.1	6.6	1.19	0.87	3.8	5.3	1.6	152.6	457
48	8	H2	7.439	155.2	149.4	5.9	1.03	0.78	13.9	0	2.2	105.6	421
49	8	H3	7.434	163.4	153.6	6.2	1.06	0.8	14	0	2.3	111.1	426
50	8	P	7.531	234.7	151.7	6.1	1.03	0.83	3.6	4.2	1.7	159.5	425
51	9	H2	7.444	200.9	148.5	5.8	0.84	0.77	14.3	2.8	1.9	136.6	427
52	9	H3	7.515	204.4	148.9	5.8	0.87	0.78	14.3	4.1	2	139.1	429
53	9	P	7.397	219.1	145.6	5.6	1.11	0.67	2.5	8.4	0.7	149	413
54	10	H2	7.285	172	151.8	6	0.47	0.87	14.7	0	2.5	117	432
55	10	H3	7.347	180.3	175.9	6.7	0.44	1.06	16.8	0	3.2	129.4	481
56	10	P	7.4	223	178.7	6.6	1.23	0.85	3.9	5.8	0.9	151.7	476
57	11	H2	7.362	195.2	156.5	6.2	0.35	1.04	15.3	0	3	132.8	449
58	11	H3	7.412	201.9	154.4	6.2	0.3	1.07	14.6	0	3.5	137.4	459
59	11	P	7.467	230.1	159	6.7	1	0.78	3.3	4.2	1	160.6	416
60	12	H2	7.317	202.6	146.8	5.6	0.8	0.81	10.6	0	1.6	137.8	416
61	12	H3	7.37	219.2	147.2	5.7	0.51	0.84	11.2	0	1.7	149.1	418
62	12	P	7.481	227.9	154.1	5.8	0.99	0.8	3.6	4.7	1.1	155	428
63	13	H2	7.321	195.3	151.3	5.8	0.43	0.94	14.1	0	2.2	132.8	429
64	13	H3	7.35	193.3	153.7	5.9	0.34	0.94	13.7	0	2.3	131.5	434
65	13	P	7.4	232.3	158.9	6	0.98	0.76	3.1	9.7	1.2	158	436
66	14	H2	7.328	167	156.5	6	0.32	1.01	14.1	0	2.8	113.6	441
67	14	H3	7.371	193.5	157.6	6	0.27	1.06	13.8	0	2.8	131.6	443
68	14	P	7.414	206.8	163.2	6.2	0.92	0.83	3.6	5.9	1.4	140.7	447
69	15	H2	7.442	232.9	162.8	6.2	0.35	1.1	14.3	0	3.3	135.4	454
70	15	H3	7.405	220.8	160.8	6.1	0.23	1.13	14	0	3.2	167	450
71	15	P	7.468	239	165.5	6.2	0.87	0.87	3.8	5.9	1.4	158.5	452
72	16	H2	7.254	193.9	150.7	5.7	0.68	0.76	10.8	1.2	1.6	131.9	425
73	16	H3	7.375	231.1	148.7	5.8	0.62	0.83	9.7	0	1.7	156.7	420
74	16	P	7.377	237	148.2	5.8	1.2	0.69	2.6	7.3	0.8	161.2	418
75	17	H2	7.419	208.4	156	6	0.48	0.91	14	0	2.5	141.7	439
76	17	H3	7.353	195	155.3	5.9	0.43	0.91	13.4	0	2.4	132.6	437
77	17	P	7.38	228.3	151.9	5.9	1.12	0.75	3.1	3.3	0.9	155.2	421
78	18	H2	7.364	167.5	167.4	7.2	0.28	1.22	17.6	0	3.4	113.9	524
79	18	H3	7.367	178.4	168.5	6.1	0.31	1.02	13.7	0	3.1	122	445
80	18	P	7.468	234.4	173.4	6.7	1.2	0.88	4.2	4.5	1	158.9	475
81	19	H2	7.26	189.8	150.9	5.8	0.65	0.84	14	0	2	129.1	428
82	19	H3	7.334	198.4	150.5	5.8	0.59	0.85	13.6	0	2.1	134.9	428
83	19	P	7.382	227.2	156.4	6	1	0.83	3.5	3	1.2	154.5	431
84	20	H2	7.323	174.2	155.5	6	0.44	0.97	14.5	0	2.6	118.5	439
85	20	H3	7.362	187.4	156.9	6	0.4	0.91	13.8	0	2.7	127.4	441
86	20	P	7.359	202.2	163.6	6.3	1.01	0.8	3.5	8.8	1.1	137.5	451
87	21	H2	7.331	167.6	165.3	6.3	0.33	1.13	14.7	0	3.2	134.4	455
88	21	H3	7.368	169.3	159.2	6.1	0.28	1	13.4	0	3.4	135.5	448
89	21	P	7.377	222.6	200.8	7.5	1.07	1.06	5.3	8.2	1.4	151.3	524
90	22	H2	7.379	215.2	154.1	5.7	0.68	0.76	12	0	1.7	146.2	436
91	22	H3	7.39	211.1	152.2	5.7	0.65	0.79	12.6	0	1.8	143.6	439
92	22	P	7.462	232.9	160.2	6.4	0.97	0.92	4.8	4.8	1.6	159.4	459
93	23	H2	7.29	190.7	148.1	5.8	0.76	0.81	13.8	0	1.9	129.6	423
94	23	H3	7.329	181.6	145.7	5.7	0.71	0.79	13.2	0	1.9	123.5	417
95	23	P	7.398	217.1	146.8	5.6	1.11	0.67	3	4.8	0.7	147.6	412
96	24	H2	7.333	182.2	151.7	5.9	0.48	0.91	14.2	0	2.5	123.9	431
97	24	H3	7.345	185.2	150.9	5.9	0.46	0.88	13.2	0	2.6	125.9	429
98	24	P	7.402	215.8	185.6	6.6	1.33	0.89	3.6	10.9	0.8	146.7	494
99	25	H2	7.34	194.6	157.1	6.3	0.38	1.01	14.2	0	3	132.4	448
100	25	H3	7.392	194.2	155.1	6.1	0.34	1.02	13.8	0	3.1	132	458
101	25	P	7.454	217.9	164.9	6.2	1.08	0.82	3.8	3.6	1	146.1	447
102	26	H2	7.298	187.8	152.2	5.9	0.58	0.84	13.7	0	1.9	127.7	430
103	26	H3	7.339	175.8	176.8	6.6	0.63	0.99	15.5	0	2.1	119.5	480
104	26	P	7.377	221.3	167.9	6.4	1.05	0.85	4.1	3.1	1	150.4	453
105	27	H2	7.352	191	154	5.8	0.4	0.92	14	0	2.4	129.9	435
106	27	H3	7.407	186.2	165.1	6.3	0.41	1.02	14.5	0	2.6	127.9	463
107	27	P	7.375	209.6	156.6	6	0.95	0.84	4.1	2.3	1.1	142.4	451
108	28	H2	7.279	192.7	149.5	5.8	0.71	0.79	13.6	0	1.9	131	425
109	28	H3	7.319	186.3	151	5.8	0.66	0.77	13.3	0	1.9	126.7	426
110	28	P	7.355	203.5	160.6	6.1	0.93	0.83	4.4	9.2	1.2	138.4	445
111	29	H2	7.45	219.4	155.4	6	0.46	0.98	14.3	0	2.4	148.8	436
112	29	H3	7.325	209	155.3	6.1	0.44	0.92	13.7	0	2.5	141.7	436
113	29	P	7.461	223.8	163.9	6.3	0.92	0.91	4.8	6.1	1.3	151.7	449
998	NA	M1 Fresh 1	7.198	245.1	138.2	5.6	1.37	0.64	2.7	6.6	0.5	166.7	397
666	NA	M1 Fresh 2	7.313	235	136.7	5.7	1.41	0.68	2.3	5.2	0.5	159.3	393
999	NA	M1 + OS Fresh 1	7.26	232	143.8	5.5	1.23	0.64	2.6	6.6	0.5	157.8	406
777	NA	M1 + OS Fresh 2	7.394	226.4	142.4	5.6	1.25	0.69	2.5	6.5	0.5	153.4	397
25	0	H2	7.536	256.5	139.9	5.3	1.39	0.21	0	29.7	0.6	175.8	415
26	0	H3	7.545	256.3	148.9	5.5	1.46	0.24	2.5	31.1	0.6	178.6	442

HARV	Measured Test	pH @ 37oC	PO2 @ 37oC	Na+	K+	Ca++	GLU	Lac	Gluc	NH4+	AirSat	Osm
Mean	Day		mmHg	mmol/L	mmol/L	mmol/L	mmol/L	mmol/L	mmol/L	mmol/L	%	mOsm/kg
	0	7.5405	258.4	144.1	5.35	1.425	0.225	1.15	28.4	0.6	175.8	428.5
	1	7.81	253.8	152.8	5.5	2.42	0.26	8	26.25	1	159.1	448.5
	2	7.651	211.85	157.15	5.75	1.625	0.3	9.85	26.4	1.5	144.25	461
	3	7.6365	227.15	147.25	5.45	1.135	0.205	7.25	23.15	1.4	154.6	436.8
	4	7.3945	210.1	140.95	5.75	1.1	0.7	7.75	1.7	1.15	142.95	404
	5	7.403	220.75	145	5.85	0.99	0.775	12.3	0	1.6	150.25	415
	6	7.33	191.71	148.7	5.95	0.97	0.815	15.45	0	1.9	130.55	426
	7	7.302	195.4	141.25	5.65	1.105	0.725	13.3	0	1.2	132.95	408
	8	7.4615	159.3	150.1	6.05	1.045	0.79	13.95	0	2.25	108.35	428
	9	7.4795	222.8	145.3	5.9	1.055	0.765	8.9	0	1.5	151.6	412.5
	10	7.316	181.15	163.85	6.35	0.455	0.985	15.75	0	2.85	123.2	456.5
	11	7.387	198.55	155.45	6.2	0.325	1.055	15.05	0	3.25	135.1	441
	12	7.3435	210.9	147	5.65	0.555	0.825	10.9	0	1.65	143.45	417
	13	7.3355	194.3	152.5	5.85	0.385	0.94	13.9	0	2.25	132.15	431.5
	14	7.3495	180.25	157.05	6	0.295	1.035	13.95	0	2.8	122.6	442
	15	7.4485	231.85	161.8	6.15	0.245	1.115	14.35	0	3.2	157.7	452
	16	7.3145	212.5	149.7	5.75	0.65	0.805	10.25	0.6	1.65	144.3	422.5
	17	7.386	201.7	155.65	5.95	0.455	0.91	13.7	0	2.45	137.15	438
	18	7.3705	173.45	177.95	6.65	0.35	1.12	15.75	0	3.25	117.95	484.5
	19	7.297	184.1	150.7	5.8	0.62	0.845	13.8	0	2.05	132	428
	20	7.3425	180.8	156.2	6	0.42	0.94	14.15	0	2.65	122.95	440
	21	7.3845	198.45	161.25	6.2	0.3	1.015	14.05	0	3.3	134.95	450.5
	22	7.3845	213.15	151.65	5.7	0.665	0.785	12.3	0	1.75	144.95	427.5
	23	7.3095	186.15	146.9	5.75	0.735	0.8	13.5	0	1.9	126.55	420
	24	7.339	183.7	151.3	5.9	0.47	0.895	13.7	0	2.55	124.9	430
	25	7.396	194.5	156.1	6.2	0.36	1.015	13.7	0	3.05	132.2	440.5
	26	7.3175	181.8	164.5	6.25	0.605	0.915	14.6	0	2	123.6	455
	27	7.3845	189.6	161.05	6.1	0.405	0.97	14.25	0	2.5	128.9	449
	28	7.299	189.5	150.25	5.8	0.685	0.78	13.45	0	1.9	128.85	426.5
	29	7.3875	214.2	155.35	6.05	0.45	0.95	14	0	2.45	145.25	436

PERFUSION	Measured Test	pH @ 37oC	PO2 @ 37oC	Na+	K+	Ca++	GLU	Lac	Gluc	NH4+	AirSat	Osm
Single	Day		mmHg	mmol/L	mmol/L	mmol/L	mmol/L	mmol/L	mmol/L	mmol/L	%	mOsm/kg
	0	7.5405	258.4	144.1	5.35	1.425	0.225	1.15	28.4	0.6	175.8	428.5
	1	7.318	201.5	151.5	5.5	2.07	0.23	4.8	23.9	0.9	137.1	442
	2	7.543	193.9	154.1	5.8	1.26	0.28	4.4	30	1.4	131.9	454
	3	7.452	199.6	154.5	5.8	1.2	0.22	4.3	27.5	1.8	135.9	453
	4	7.408	211.9	150.1	6.1	1.32	0.7	2.8	1.8	0.7	144.2	416
	5	7.463	240.4	141.8	5.8	1.13	0.72	3	0	1.1	163.6	389
	6	7.431	202.5	142.7	5.6	1.08	0.74	3.2	0	1.3	137.8	402
	7	7.42	224.3	168.1	6.6	1.19	0.87	3.8	5.3	1.6	152.6	457
	8	7.531	224.1	151.7	6.1	1.03	0.83	3.6	4.5	1.7	152.8	425
	9	7.397	219.1	145.6	5.6	1.11	0.67	2.5	8.4	0.7	149	413
	10	7.4	223	178.7	6.6	1.23	0.85	3.9	5.8	0.9	151.7	476
	11	7.487	236.1	150	5.7	1	0.76	3.3	4.2	1	160.6	419
	12	7.481	227.9	154.1	5.8	0.99	0.8	3.6	4.7	1.1	155	428
	13	7.4	232.3	156.9	6	0.98	0.76	3.1	9.7	1.2	158	438
	14	7.414	206.8	163.2	6.2	0.92	0.83	3.6	5.9	1.4	140.7	447
	15	7.659	230	165.5	6.2	0.87	0.87	3.8	5.9	1.4	156.5	452
	16	7.377	237	148.2	5.8	1.2	0.69	2.6	7.3	0.8	161.2	418
	17	7.38	228.3	151.9	5.9	1.12	0.75	3.1	3.3	0.9	155.2	421
	18	7.388	204.4	178.4	6.7	1.2	0.89	4.2	4.5	1	138.9	475
	19	7.382	227.2	156.4	6	1	0.83	3.5	3	1.2	154.5	431
	20	7.359	202.2	163.6	6.3	1.01	0.8	3.5	9.8	1.1	137.5	451
	21	7.377	222.5	202.6	7.3	1.07	1.08	5.3	6.2	1.4	151.3	524
	22	7.492	232.9	169.2	6.4	0.87	0.92	4.8	4.6	1.4	158.4	458
	23	7.396	217.1	146.8	5.6	1.11	0.67	3	4.8	0.7	147.6	412
	24	7.402	215.6	185.6	6.8	1.33	0.88	3.8	10.9	0.8	146.7	494
	25	7.464	217.9	184.9	6.2	1.09	0.83	3.6	3.8	1	148.1	447
	26	7.377	221.3	167.9	6.4	1.05	0.85	4.1	3.1	1	150.4	453
	27	7.375	209.6	156.8	6	0.95	0.84	4.1	2.3	1.1	142.4	431
	28	7.355	203.5	160.6	6.1	0.93	0.83	4.4	9.2	1.2	138.4	445
	29	7.461	223.8	163.9	6.3	0.92	0.91	4.8	6.1	1.3	151.7	449

9.9.1. Measurement range

Measurement Range	
Na^+	40 -220 mmol/L
K^+	1.0 - 25.0 mmol/L
iCa	0.2 - 10 mmol/L
NH_4^+	0.2 - 25 mmol/L
pH	5.00 - 8.00
PO_2	0 - 800 mmHg
Glucose	0.2 - 15.0 g/L
Lactate	0.2 - 5.0 g/L
Glutamine	0.2 - 6.0 mmol/L

9.9.2. Principles of Measurement

9.9.2.1. Sodium, Potassium, Ionised Calcium and Ammonium

The electrolyte electrodes require a sensing (ion selective) membrane, a reference electrode, and an internal filling solution. Internal filling solution provides a fixed concentration of the ion and the sample provides a second ion concentration.

A suitable electrode membrane is selectively permeable to a single ion of interest in the sample. This selective electrode membrane establishes an electrical potential as the charge associated with the ion leaves its counter-ion behind in solution. The magnitude of this electrical potential is determined by the concentration difference between the 2 sides of the membrane.

9.9.2.2. pH Electrode

pH is measured using a hydrogen ion selective glass membrane. One side of the glass is in contact with a solution of constant pH. The other side is in contact with a solution of unknown pH. A change in potential develops which is

proportional to the pH difference of these solutions. This change in potential is measured against a reference electrode of constant potential. The magnitude of the potential difference is a measure, then, of the pH of the unknown solution.

9.9.2.3. Partial Pressure of Oxygen (PO_2)

The partial pressure (tension) of oxygen in solution is defined as the partial pressure of oxygen in the gas phase in equilibrium with the sample. PO_2 provides an indication of the availability of oxygen in inspired air.

PO_2 is measured amperometrically by the generation of a current at the electrode surface. As oxygen diffuses through a gas permeable membrane, the oxygen molecules are reduced at the cathode, consuming 4 electrons for every molecule of oxygen reduced. This flow of electrons is then measured by the electrode and is directly proportional to the partial pressure of oxygen.

9.9.2.4. Glucose

Glucose measurement is based on the level of H_2O_2 produced during the enzymatic reaction between glucose and oxygen molecules in the presence of the glucose oxidase enzyme.

9.9.2.5. Lactate

Lactate measurement is based on the level of H_2O_2 produced during the enzymatic reaction between lactate and oxygen molecules in the presence of the lactate oxidase enzyme.

9.9.2.6. Glutamine and Glutamate

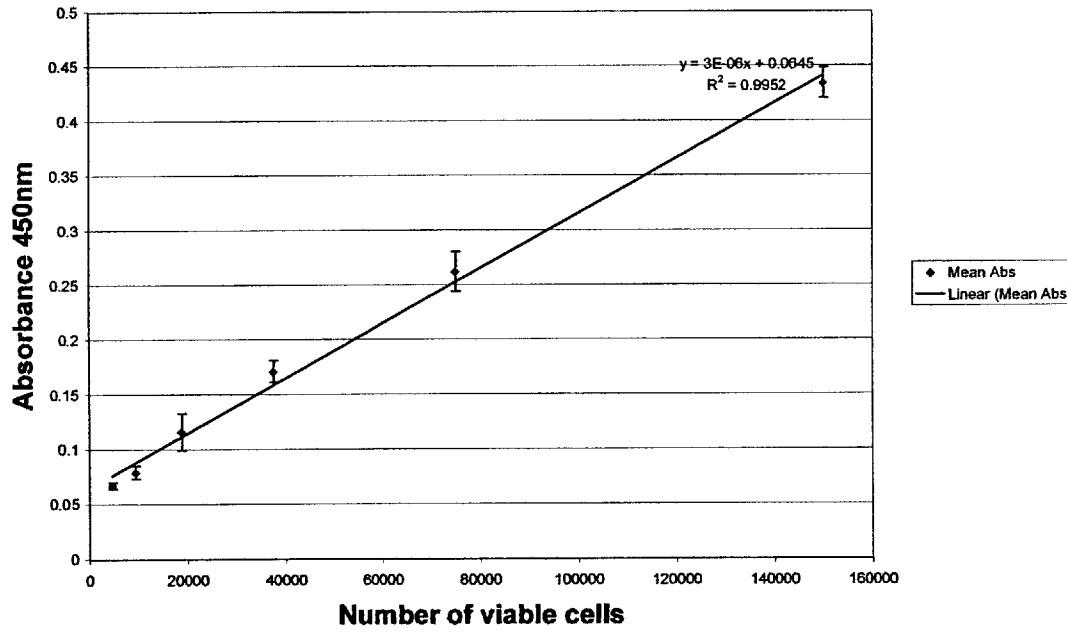
Glutamine measurement is based on the level of glutamate produced during the enzymatic reaction between glutamine and water molecules in the presence of the glutaminase enzyme. Then glutamate measurement is based on the level of H_2O_2 produced during the enzymatic reaction between glutamate and oxygen molecules in the presence of the glutamate oxidase enzyme.

9.10. Microbead cell morphology

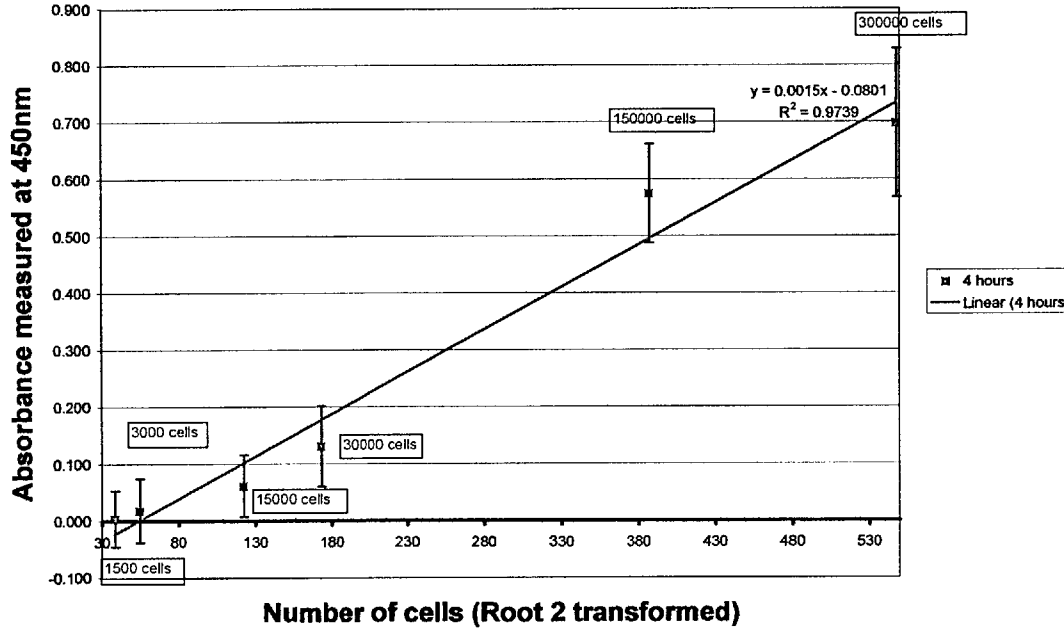


9.11. Calibration Curves

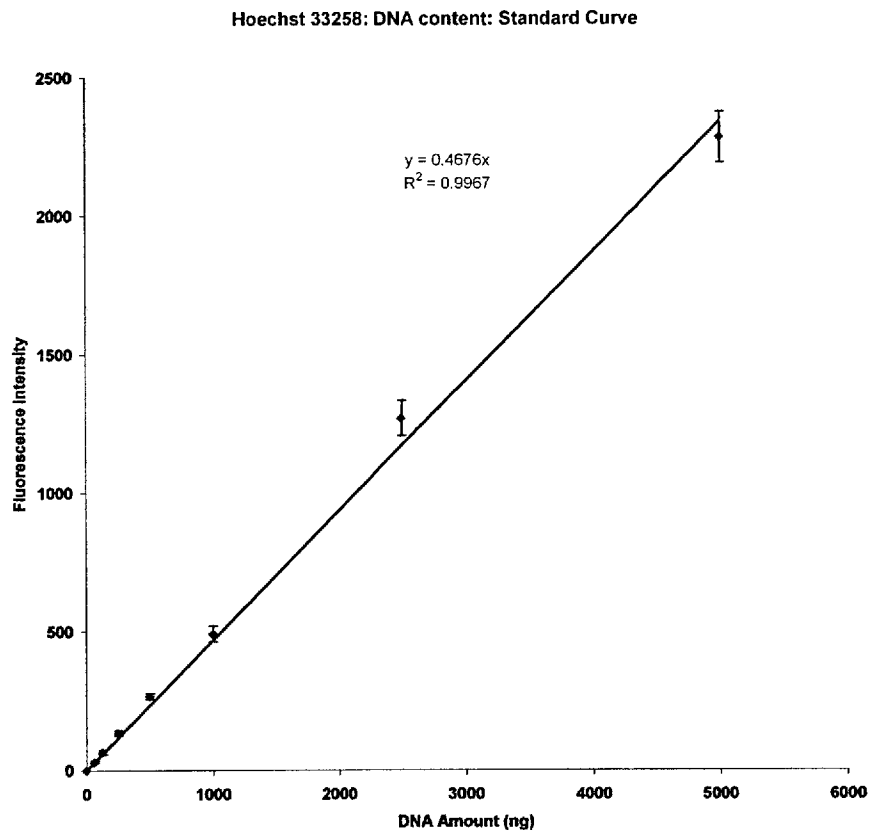
9.12. MTS assay 2D



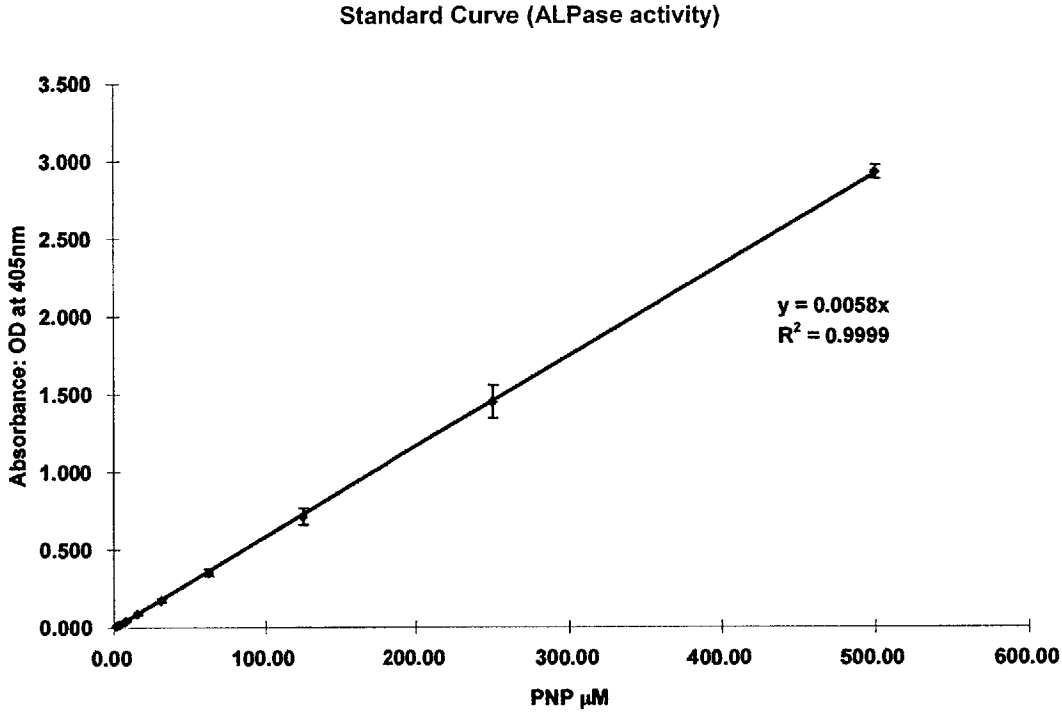
9.13. MTS assay 3D



9.14. DNA Hoescht



9.15. Alkaline Phosphatase activity



9.16. Pubmed Searches

Keyword 1	Keyword 2	Keyword 3	Year	# of Refs
Alginate			2001	307
	Bone		2001	13600
		Stem Cells	2001	1667
Alginate	Bone		2001	12
Alginate		Stem Cells	2001	3
	Bone	Stem Cells	2001	477
Alginate	Bone	Stem Cells	2001	2
Alginate			2002	283
	Bone		2002	14405
		Stem Cells	2002	2172
Alginate	Bone		2002	16
Alginate		Stem Cells	2002	3
	Bone	Stem Cells	2002	621
Alginate	Bone	Stem Cells	2002	1
Alginate			2003	324
	Bone		2003	15598
		Stem Cells	2003	2504
Alginate	Bone		2003	18
Alginate		Stem Cells	2003	4
	Bone	Stem Cells	2003	758
Alginate	Bone	Stem Cells	2003	3
Alginate			2004	333
	Bone		2004	16219
		Stem Cells	2004	3092
Alginate	Bone		2004	17
Alginate		Stem Cells	2004	9
	Bone	Stem Cells	2004	884
Alginate	Bone	Stem Cells	2004	0
Alginate			2005	320
	Bone		2005	13534
		Stem Cells	2005	2750
Alginate	Bone		2005	19
Alginate		Stem Cells	2005	7
	Bone	Stem Cells	2005	852
Alginate	Bone	Stem Cells	2005	4

Searches conducted on the 2nd October 2005 using Reference Manager v11's internet search function with the keywords in the abstract / title.
* 2005 publications only include Jan → Sep as the year still has 3 months to run before 2006 begins.